



**BANGLADESH NETWORK  
OFFICE FOR URBAN SAFETY**

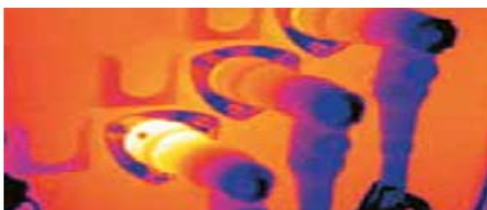


# **BNUS ANNUAL REPORT-2016**

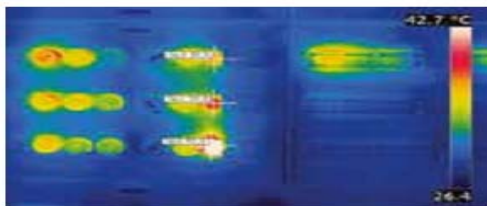
## **B**ANGLADESH **N**ETWORK OFFICE FOR **U**RBAN **S**AFETY **BUET, DHAKA, BANGLADESH**

**Edited By:**

**Mehedi Ahmed Ansary**



*Overheated connection*



**April 2017**





## CONTENTS

<b>PART-I: CYCLONE ROANU, 21 MAY 2016</b>	3
<b>PART-II: FIRE FROM ELEVATOR CRASH IN AT ALAUDDIN MARKET IN UTTARA OF DHAKA, 24 JUNE 2016</b>	17
<b>PART-III: FIRE IN INCIDENT IN TAMPACO FOILS LTD AT BSCIC INDUSTRIAL AREA, TONGI, GAZIPUR ON 10 SEPTEMBER, 2016</b>	20
<b>PART-IV: MEASUREMENT OF ELECTRICAL RESISTIVITY WITHIN A POWER PLANT AREA</b>	26
<b>PART-V: ASSESSMENT OF UNDERLYING CAUSES OF FIRE RISK IN OLD DHAKA: A CASE STUDY OF ISLAMBAG AREA IN WARD NO. 65, DHAKA SOUTH CITY CORPORATION</b>	36
<b>PART-VI: SEISMIC MICROZONATION OF COX'S BAZAR MUNICIPAL AREA BANGLADESH</b>	50
<b>PART-VII: EARTHQUAKE RELATED RESEARCH AND ACTIVITIES IN BANGLADESH DURING THE LAST SIX YEARS (2010-2016)</b>	64
<b>PART-VIII: USE OF JET GROUTING IN RETROFITTING OF A RMG FACTORY BUILDING IN CHITTAGONG, BANGLADESH</b>	79
<b>PART-IX: AMBIENT VIBRATION ANALYSIS OF HERITAGE UNREINFORCED MASONRY BUILDINGS IN BANGLADESH</b>	92
<b>PART-X: EFFECTS OF RELATIVE DENSITY AND EFFECTIVE CONFINING PRESSURE ON LIQUEFACTION RESISTANCE OF SANDS</b>	108
<b>PART-XI: EVALUATION OF LIQUEFACTION POTENTIAL FROM SPT AND CPT: A COMPARATIVE ANALYSIS</b>	117
<b>PART-XII: CPT-SPT BASED CORRELATIONS FOR COHESIONLESS SOIL FOR UTTARA 3RD PHASE, DHAKA</b>	125
<b>PART-XIII: THE UTILIZATION OF CPT AND SPT TO OBTAIN SOIL PARAMETERS FOR C- <math>\phi</math> SOIL AT UTTARA 3RD PHASE, DHAKA, BANGLADES</b>	155
<b>PART-XIII: EARTHQUAKE IN TRIPURA, 3 JANUARY 2017</b>	199



**BANGLADESH NETWORK  
OFFICE FOR URBAN SAFETY**



## **PART-I**

# **CYCLONE ROANU, 21 MAY 2016**

**BANGLADESH NETWORK OFFICE FOR URBAN  
SAFETY (BNUS), BUET, DHAKA**

**Prepared By: Uttama Barua**

**Mehedi Ahmed Ansary**

## 1. Introduction

The naming of tropical cyclones is a recent phenomenon. The process of naming cyclones involves several countries in the region and is done under the aegis of the World Meteorological Organisation. According to Hurricane Research Division, tropical cyclones are named to provide ease of communication between forecasters and the general public regarding forecasts, watches, and warnings. Since the storms can often last a week or longer and that more than one can be occurring in the same basin at the same time, names can reduce the confusion about what storm is being described. Eight countries in the region - Bangladesh, India, Maldives, Myanmar, Oman, Pakistan, Sri Lanka and Thailand - all contributed a set of names which are assigned sequentially whenever a cyclonic storm develops over the Arabian Sea and Bay of Bengal. Every time a cyclone occurs, a name is picked in the order of the names submitted by these countries. The cyclonic storm Roanu has been named by Maldives which means “coir rope” in Maldivian (Dhivehi) (Daily Star, 21 May 2016).

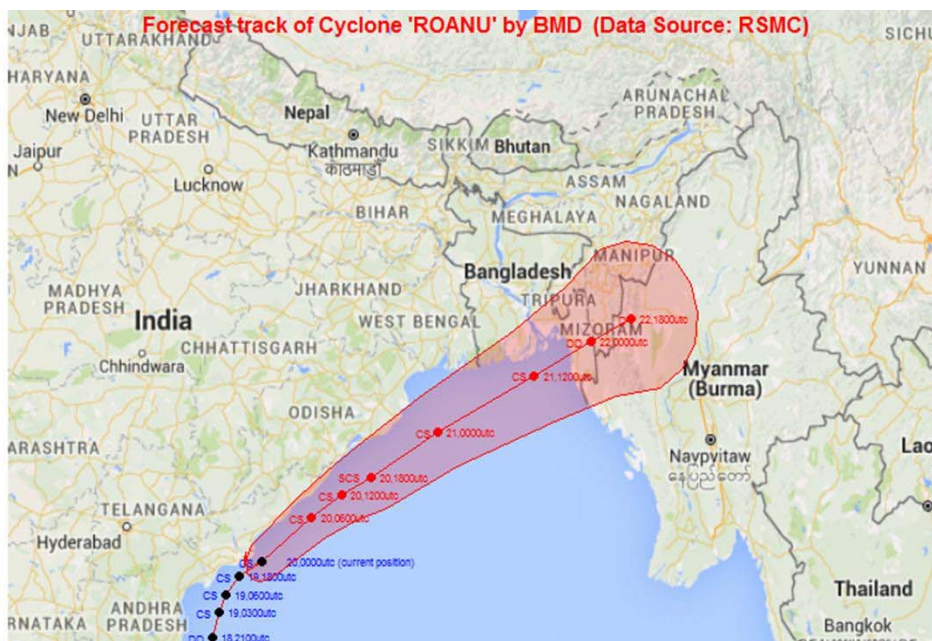


Figure 1: Projected track of cyclone Roanu

## 2. Meteorological History

Under the influence of a trough, a low pressure area formed over the Bay of Bengal on 14 May. It slowly consolidated as it paralleled the east coast of Sri Lanka, prompting the India Meteorological Department (IMD) to classify it as a depression on 17 May. On 19 May, the IMD reported that the storm had reached cyclonic storm intensity, and assigned it the name Roanu. In the late hours of that day, Roanu showed a weakening trend after most of the convection covering the LLCC was sheared

off. Roanu re-intensified as it accelerated east-northeastwards towards the coast of Bangladesh, and reached its peak intensity with winds of 85 km/h (50 mph) (Dhaka Tribune, 19 May 2016). On 21 May, around 1pm local time, Tropical Cyclone Roanu made landfall along the Barisal-Khulna-Chittagong coastal region of Bangladesh, bringing heavy rain, winds of up to 88km/h, and storm surges of up to 2m. While crossing the coastline, the storm had a speed of 60-80 kilometre per hour while heading east-northeastwards. It took 4-5 hours to cross the coast (Daily Star, 21 May 2016; Daily Sun, 21 May 2016). Some areas, including the offshore islands and chars, experienced tidal surges 4 to 5 feet above the normal tide. Continuing to accelerate inland, Roanu steadily weakened and degenerated into a remnant low the next day. As of 22 May, Cyclone Roanu had moved on to Myanmar (Dhaka Tribune, 22 May 2016).

### **3. Preparedness and Response**

On May 19 Bangladesh Meteorological Department advised maritime ports of Chittagong, Cox's Bazar, Mongla and Payra to hoist local warning signal No. 4. All fishing boats and trawlers along the northern part of the Bay and deep sea were asked to stay close to the coast and move with caution until further notice. Vessels were also advised not to venture into deep sea. In the evening after the deep depression transformed into a cyclonic storm, the Disaster Ministry held a special preparatory meeting with concern authorities for taking precautionary steps ahead of the Cyclone Roanu. After that the government started to prepare for a massive evacuation in 18 coastal districts Bangladesh. All the cyclone shelters in these districts were kept ready. District administrations in coastlines were also asked to mobilize nearly 60,000 volunteers trained under the Cyclone Preparedness Programme (CPP) and chart out detailed plans to face the impending disaster by holding emergency coordination meetings. The weekend holidays of civil servants of the 18 districts were cancelled as well. Preparations were underway to keep the damage to a minimum, and volunteers and officials were sent out with megaphones to issue alerts.

On May 20 with cyclone Roanu approaching closer, Chittagong port and coastal districts of Chittagong, Noakhali, Laxmipur, Feni, Chandpur, and their offshore islands and chars were put under danger signal number 7, Cox's Bazar port and coastal district of Cox's Bazar and its offshore islands and chars have been put under danger signal number 6, and Mongla and Payra ports and coastal districts of Bhola, Borguna, Patuakhali, Barisal, Pirozpur, Jhalokathi, Bagherhat, Khulna, Satkhira have been put under danger signal number 7. Since 5.10 pm on May 20, authorities suspended water transport through the country until further notice. Alongside, the government scrapped all leaves and holidays of officials and staff of Roads and Highways Department in the country's coastal areas as part of its preparation for the cyclone. All staff and officials were asked to

remain alert to keep uninterrupted road communication in the coastal areas. BMD was issuing regular special weather bulletins on the storm. Department of Disaster Management directed all the coastal district authorities to evacuate people from their homes and send them to cyclone shelters. Volunteers launched campaigns in the coastal areas to alert people to evacuate to safe zones and cyclone shelters that have been prepared. The government's Cyclone Preparedness Programme and Bangladesh Red Crescent Society were directing the evacuation process.



(a) Water transports harbored at the banks of Karnaphuli River in Chittagong on May 20 2016



(b) Fishermen shelving their boats in Firingibazar area of Karnaphuli river in Chittagong on May 20, 2016

Figure 2: Restriction on water transport

In Chittagong, control rooms were set up in coastal areas to facilitate evacuation of the marginalized people to safety shelters. The district administration set up control rooms in every upazila to monitor overall situation. A hotline - was opened to keep people in touch with updates in the district. All cyclone shelters in the coastal districts were kept open to people. Awareness campaign was started through loud speakers since afternoon and the relief workers were ready to combat any situation. Following a meeting of the Chittagong Port Authority, it asked all mother vessels to go to safer places and lighter vessels to move upstream. It stopped activities in the outer anchorage. At around 7:30pm on that day, the port authority ordered 19 vassals anchored in the port to depart jetty before the storm struck. In Cox's Bazar, the members of army, Border Guard Bangladesh, police and civil surgeon were deployed at different strategic points in the district as safety measures. Control room was set up to oversee the overall situation in the district. Around 516 cyclone shelters with accommodation capacity of around 5.15 lakh people were kept prepared including adequate amount of dry foods to ensure relief work.

The coastal districts of Chittagong, Noakhali, Laxmipur, Feni, Chandpur, Bhola, Borguna, Patuakhali, Barisal, Pirojpur, Jhalakati, Bagherhat, Khulna, Satkhira and their offshore islands and chars remained under the danger signal number seven on May 21. The Shah Amanat International

Airport, Chittagong suspended all of its flight operations due to Cyclonic storm Roanu. Meanwhile, goods loading and unloading from all ships remained suspended by Bangladesh Inland Water Transport Authority at Chittagong seaport since the morning as Cyclone Roanu nears the Barisal-Chittagong coast. In Chittagong, issues were ordered to ensure power supply, sanitation, medical assistance and enough dry food at the shelters. There were around 2,500 shelters in the cyclone-prone areas and 55,000 volunteers at work. Each shelter can hold around 1,500 people. The authorities were using megaphones in coastal areas to urge people to move to the shelters. Apprehending mudslides, the Chittagong district administration also asked people living in the foothills to move out.



Figure 3: A ship got stranded at Patenga sea beach during the cyclone Roanu



Figure 4: Sea water overflowing *beri badh* at Patenga sea beach, Chittagong as Cyclone Roanu made landfall

As part of addressing the risk of cyclone Roanu, eight community radio stations in the coastal region of Bangladesh broadcasted programmes for 348 hours for three days continuously from 19 May 2016. The community radio stations broadcasted their programmes round the clock to keep communities alert during and after the cyclone Roanu that hit country's coastal belt on 21 May 2016. A total of 116 community broadcasters --female 37, male 79 -- volunteers and members from 175 listeners clubs worked throughout the whole service. As the storm weakened, the cautionary signal was lowered to 3 at all the Maritime ports but goods handling remains suspended at Chittagong port after the cyclone landfall on May 21.

More than 538,000 people were moved into 3,554 temporary cyclone shelters. Despite such preparedness at the cyclone shelters in Sitakunda upazilla under Chittagong district, most of the shelters remained vacant as locals termed Roanu a usual natural phenomenon. Three shelters in the upazila were completely vacant on May 21 as people paid no heed to the repeated warnings of local Red Crescent volunteers. They saw such disasters many times in the past. Besides, cyclone shelters can ensure accommodation only for them but not for their domestic animals. These animals are part of their life and they just cannot leave them in a situation where they might die or get injured.



(a) Villagers going to cyclone shelter



(b) Cyclone shelter at Mirapara Cyclone Shelter in Patenga, Chittagong

Figure 5: Cyclone shelter

#### 4. Impact of the Cyclone

##### 4.1 Secondary hazards

Under the influence of the cyclonic storm, heavy Rain and thunder showers accompanied by temporary gusty and squally wind was continuing at most places over Dhaka, Khulna, Barisal, Chittagong and Sylhet divisions and at many places over Rajshahi and Rangpur divisions since early morning on May 21. Rains, caused by cyclone 'Roanu', swamped many parts of the capital, leaving the city life in disarray. Most of the low-lying areas in the city also went under rainwater. Roads in Kakrail, Mouchak, Malibagh, Mirpur, Kazipara, Shewrapara, Motijheel, Shantinagar, Razarbagh, Arambagh, Merul Badda, Elephant Road, Dhanmondi and Paltan areas were submerged, as the city's clogged drains failed to absorb the rainwater.



(a) Heavy rainfall in Dhaka



(b) Water logging due to heavy rainfall

Figure 6: Heavy rainfall resulted due to Cyclone Roanu

Commuters experienced immense sufferings for lack of transports, and many of them had to wade through the water-logged streets. They complained that rickshaws and CNG-run auto-rickshaw drivers charged them excessive fares, taking advantage of the inclement weather. The BMD,

meanwhile, recorded 43 mm of rain in 24 hours till 9:00am on May 21. Meanwhile, most of the low-lying areas of the district, including Chittagong, Noakhali, Lakshmipur, Feni, Chandpur, Bhola, Barguna, Patuakhali, Barisal, Pirojpur, Jhalakati, Bagerhat, Khulna and Satkhira, were inundated by the tidal surge. Banshkhali upazila in Chittagong is among the worst affected areas as several unions remained inundated with seawater rushing into the storm-battered villages till May 23.

#### **4.2 Human Casualty**

The cyclone caused at least 26 deaths and 100 injuries in seven districts across the country. Among them 12 were in Chittagong, 3 each in Noakhali, Cox's Bazar, and Bhola; 1 each in Feni, Patuakhali and Lakshmipur. Most of them died due to houses or trees collapsing on them in the storm or by waves sweeping them away. At least 20 people were admitted to Chittagong Medical College Hospital alone. At least 41 people were injured as Roanu uprooted trees and flattened homes in Cox's Bazar's Moheshkhali, Kutubdia and Ramu upazilas. At least forty people are also missing in these areas. In Feni, four people were reported missing. In Bhola, a cargo vessel with four crew members went missing in the Meghna. Around 4.83 lakh people in 104 unions of different upazilas in Chittagong were affected by the cyclone. Some 103,000 families were affected by it, of them, around 19,437 were affected severely and 83,660 partially. Around 50 thousand people in Cox's Bazar have been affected in the cyclone. Over 80 villages in Patuakhali and Barguna were flooded as a dam broke forcing people to move out.



Figure 7: Village in Banshkhali faded away due to cyclone Roanu

#### **4.3 Impact on Shelter**

Around one lakh houses were damaged and about 150,000 families were affected by the cyclone in the three districts. According to primary estimate of the district administration in Chittagong, around 2.5 lakh houses were damaged in the cyclone. In Cox's Bazar, at least 29,000 houses were damaged and 22,128 families were affected in the 71 unions of eight upazilas. In Bhola, several hundred houses were damaged by the storm as cyclone Roanu was getting closer to the coastal areas of Bangladesh. Over 100 houses were damaged in Patuakhali.



Figure 8: Impact on Shelters: Damages homes in Tajumuddin upazila of Bhola

#### 4.4 Impact on Agriculture

In Chittagong Division, seedbeds of aush paddy on around 400 hectares of land were under water. The cyclone ruined crops on 154 acres of land completely and that on 2,541 acres of land partially in Chittagong. Besides, 360 betel leaf orchards and vegetables on 3,100 hectares of land were damaged by the storm, according to the Department of Agricultural Extension (DAE). According to primary estimate of the district administration in Chittagong, the cyclone washed away domestic animals of some Tk 100 crore, and cropland worth around Tk 50 crore were damaged in the cyclone. At least 15,000 cattle were washed away in Sandwip alone. The storm dealt a heavy blow to shrimp farming as a tidal surge ravaged 2,117 shrimp enclosures in seven upazilas, causing a loss of around Tk 13 crore in Cox's Bazar. Over 2,000 livestock and 40,000 ducks and hens were swept away and 500 acres of grain field were ruined in the cyclone in Kutubdia of Cox's Bazar. Financially, the total damages would amount to about Tk 200 crore. Fish worth several lakh taka were washed away in Bhola. In Patuakhali, the farmers of all eight upazilas have to count losses as their standing crops were flooded by tidal surge and heavy rainfall. Besides, crops on 3,451 hectares of land were badly damaged in the eight upazilas, according to Patuakhali Agriculture Extension Department.



(a) Damaged local shops in Boubazar area of Rangabali upazila, Patuakhali

(b) Devastated shops at Patenga Sea beach, Chittagong

Figure 9: Impact on properties

#### 4.5 Impact on Properties

Damage to properties was extensive. Several hundred shops of Jhinuk Market in Patenga of Chittagong were swept away. Around 75 shops have been destroyed by the tides in the naval area, informed locals. In Patenga beach area around 300 shops were completely washed away, said Shamshul Alam, general secretary of Patenga Sea Beach Shop Owners Co-operative Association. In Chittagong, property and goods worth of more than Taka 100 crore have been damaged in the Reazuddin Bazar, Khatun-ganj, Boxirhat, Terrybazar, Chaktai, and Chittagong Shopping Complex due to cyclonic storm. Around 500 shacks were damaged in Banshkahli. Sea water entered the shops and warehouses in Khatungaj, Chaktai, Asadganj and Korbaniganj areas in Chittagong city during the storm. In Kutubdia of Cox's Bazar, about 167 educational and religious institutions were either fully or partially damaged.



(a) Damaged coastal embankment at Banshbari union in Sitakundu upazila



(b) Damaged dam at Nalchiraghat of Hatiya, Noakhali



(c) Damaged Airport road, Chittagong



(d) Damaged road in Kuakata sea beach



(e) Damaged road in Kutubdia, Cox's Bazar

Figure 10: Impact on infrastructure

#### **4.6 Impact on Infrastructure**

Rain triggered by the cyclone flooded embankments in the three upazilas and damaged many roads, which will worsen the condition of roads as the rainy season is going to begin soon. A 30-kilometre stretch of the 130km long embankment in Banshkhali upazila in Chittagong was damaged, while 20 kilometer in Sandwip and 10 kilometer in Anwara. The villagers are now in constant fear that the damaged part would collapse any moment, allowing seawater to swamp their houses and fields. Eighteen kilometres of embankment was washed away while 157 kilometres of road link suffered damage in Kutubdia of Cox's Bazar. A chill of fear swept over around 20,000 people in Sitakunda's Banshbari union as high tidal surges hit the dilapidated embankment in the area. The barrage, which was built to protect the homes and crops of locals, has fallen into disrepair over the last six years as the local administration took no measures to renovate the 3km structure. They said they had apprehensions that the embankment might collapse anytime after tidal surges lashed it.

Along with damaging Naval Academy road, cyclone Roanu has inflicted massive damage on the Chittagong city protection embankment. The four-kilometer naval road facilitates movement from airport. It's a famous tourist destination for its location along the estuary of Karnaphuli River and the Bay of Bengal. It is owned by Chittagong Port Authority. The mayor had already informed them and they said they would start repairing soon. People living in the coastal areas of Patenga and South Haliahahar are in fear whether it will be able to stand the high tide during the rainy season when the sea condition will be rough. If the embankment could not stand the tidal surge, then around three

lakh people would suffer. Moreover if the trees had not been cut down, it would not have happened. They were cut a few months ago for implementing the Outer Ring Road project. Some CDA officials were seen repairing the most damaged parts of the embankment by filling sand around 12:00 noon on May 23.

Cyclone Roanu has done so much damage to the Kuakata beach that it is difficult to even take a walk on it now. A portion of a connecting road from zero point to the beach was washed away as tidal surges hit the beach on Saturday. Rubble of structures, roads and stumps of uprooted trees laid scattered along the beach from Lembur Char to Gangamoti. Trees of the coconut garden, Tamarisk garden and Gangamoti reserve forest were badly damaged in the cyclone. The storm also destroyed over 25 temporary shops.

#### **4.7 Impact on Power Supply and Telecommunication**

Power supply was cut in all seven upazilas of Patuakhali since May 20. There were power cuts in Barisal and in Pirojpur. The power distribution system was seriously disrupted on May 21. So the power supply was suspended immediately after the cyclonic Roanu hit the Barisal-Chittagong coast near Chittagong at noon. The cyclone disrupted telecom services in the coastal areas, particularly cellular services, as many of the transmission centers of mobile operators were down due to a power crisis. However, many subscribers got back services by May 23 evening. Operators also took preparatory measures to minimize the expected disruption before the storm hit. Subscribers of Chittagong area were severely affected by Roanu while those from Noakhali and a greater part of Comilla region also suffered. Some parts of Barisal, Bhola and Cox's Bazar were also affected, and cellular services of all operators suffered due to power cuts.



Figure 11: People trying to salvage belongings from their ruined houses at Premashia in Banshkhali upazila of Chittagong

#### 4.7 Impact on Human Life

Upon their return home from cyclone shelters, many found their houses razed to the ground, belongings gone, crops ruined and fish farms washed away. The affected people were passing their days without food and pure drinking water since May 21, after losing everything to the cyclone. According to Chittagong District Relief and Rehabilitation Office (DRRO) homeless people of the two upazilas were living at the cyclone shelters as it is too tough for them to rebuild houses immediately. In Bhola, around 10,000 people of Tazumuddin Upazila were running short of food after the cyclone destroyed their homes. Even 48 hours after the cyclone, many people in the storm-hit villages complained of getting no aid from the government. Around 500 students including 50 examinees of the ongoing Higher Secondary Certificate examination have plunged into a deep crisis as they lost their text books and other school accessories in the cyclone in the Tajumuddin *upazila* of Bhola.



Figure 12: Rescue operation in Patenga Sea beach, Chittagong

#### 5. Relief Works

The affected people were in urgent need of relief in terms of rice, oil, salt, sugar, safe water and medicine to survive until starting life anew. The Disaster Management and Relief Minister visited Banskhali and Anwara upazilas on May 23 and assured the affected people of providing with tin sheets and money for constructing their houses. He gave Tk 20,000 each to the families of 12 victims in Khankhanbad union of the upazila and ordered the local administration to arrange adequate relief, food and water for the affected people. As of May 24 the local administration distributed Tk 3.30 lakh, 87 tonnes of rice, 80 sacks of puffed rice and molasses among the cyclone-hit people in the district.



Figure 13: Relief operation by Bangladesh Navy in association with local administration

Bangladesh Navy took the initiatives to hand out relief materials to the victims of cyclone Roanu when cyclone affected people were put in a severe crisis due to a shortage of food, drinking water and medicine, the release added. As part of the efforts, around 500 navy personnel along with six ships and high-speed boats were deployed in the coastal areas to rescue and provide relief to the victims of the cyclone Roanu. The navy in association with local administration is providing security and relief to Roanu victims in Kutubdia and Maheshkhali areas. The relief materials include food items, hygienic water, saline and medicines have already been taken to the affected areas. Besides, navy teams are continuing search operations in the deep sea.

## 6. Lessons Learned

Bangladesh is vulnerable to cyclones because of its location at the triangular shaped head of the Bay of Bengal, the sea-level geography of its coastal area and its high population density. In recent years, Bangladesh has developed tremendously in the area of disaster management, which is well ahead of many countries. This is why the country is considered a role model in managing natural disasters. The two deadliest cyclones occurred in 1970 and 1991 had claimed some 500,000 and almost 140,000 lives respectively. But during the past 20 years, the country managed to reduce deaths and injuries from cyclones while the most recent severe cyclone Sidr of 2007 caused an estimated 4234 deaths, a nearly 50-fold reduction compared with the devastating 1970 cyclone. Cyclone Roanu caused twenty four deaths with 88 kilometres wind speed per hour, while another such tropical tidal storm Aila of 2009 with identical intensity had claimed 200 lives when it ravaged the coastlines. Thus, in terms of casualty figures the loss of lives caused by the Roanu was nearly 10 times less than that of Aila of 2009. It is a testament to the country's cyclone response and disaster preparedness systems that despite its intensity, the storm caused far fewer deaths than many previous cyclones of this scale in past decades.

The disaster management ministry, fire brigade and meteorological department worked together to keep the impact of Roanu to a minimum. This included a massive evacuation campaign, mobilisation of medical aid and the readiness of a large number of volunteers as well as cancellation of weekly holidays of government officials in 18 coastal districts. Apart from prompt alerts to the people, including fishermen and trawler operators regarding the advancing cyclone, operations of water vessels were suspended and the airport in Chittagong was closed, for safety reasons. The strength and attributes of the disaster management strategies include community resilience, volunteerism, the Early Warning System, community based decision making process, government commitment, a vibrant NGO sector and an appreciable legal and institutional framework. Early warnings, preparedness, proactive measures, and evacuation of certain areas by government, the communities themselves, and volunteers, illustrated how death and destruction during a natural disaster can be drastically limited. But the storm has left several thousand people homeless, hungry and utterly devastated, apart from doing damage to the infrastructure. It is important now to ensure timely relief and rehabilitation is provided to the many thousands of people who saw houses, crops, and livestock destroyed in the cyclone so that they can rebuild their homes and their lives.

Lessons must also be learned about how to further improve cyclone preparedness. Roanu also offers important lessons in recovery compared to previous disasters. Most of the areas hit by the cyclone were also affected by cyclone Komen, and two floods, in 2015. Arguably, inadequate investment in recovery after the 2015 disasters, combined with a limited investment in measures to reduce disaster impacts, including in infrastructure, resulted in Roanu having greater impact in those vulnerable areas. Once again, inclusion of short and long-term risk in infrastructure development has emerged as a major priority for a resilient Bangladesh. Emphasis should be given on other infrastructure improvements as well, such as disaster-resilient roads and bridges, paved trading areas, integrated water supply systems, efficient power supply systems, and proper drainage and sanitation facilities. These infrastructure improvements are vital both to prevent loss of life, and to improve people's standard of living and make them more resilient to extreme weather events.



**BANGLADESH NETWORK  
OFFICE FOR URBAN SAFETY**



## **PART-II**

# **FIRE FROM ELEVATOR CRASH IN AT ALAUDDIN MARKET IN UTTARA OF DHAKA, 24 JUNE 2016**

**BANGLADESH NETWORK OFFICE FOR URBAN  
SAFETY (BNUS), BUET, DHAKA**

**Prepared By: Uttama Barua**

**Mehedi Ahmed Ansary**

On 24 June 2016, a fire initiated with an explosion at 17-storied Tropical Alauddin Tower Shopping Complex in Uttara of Dhaka around 6:15pm. The fire originated at one of the three basements of 15-storey Tropical Alauddin Tower Shopping Complex after a lift full of passengers fell in its shaft with a loud bang. The fire quickly spread in the mall. After initiation of fire, smoke was seen coming out from the third, fourth and fifth floors. The explosion ripped apart the market's basement and shattered the window panes. The fire did not spread to any of the upper floors of the building, which mostly house shops, but the ceiling of the ground floor came off, damaging shops, doors and windows. After getting informed, a total of 13 fire fighting units of Fire Service and Civil Defense (FSCD) were deployed to bring the fire under control. The fire was brought under control within one and half hour.

Over 100 people were injured in the incident including some people with severe burn injuries. Three victims including 10-year-old girl, an eight-month-old boy and their father were apparently in critical condition and were sent to Uttara campus of Bangladesh Medical College Hospital. Later, considering their critical condition they were transferred and admitted in the burn unit of the Dhaka Medical College Hospital. On the next day, one of the victims died at Dhaka Medical College Hospital taking the death toll in the incident to seven. Most of the injured were pedestrians, including children, who sustained wounds as pieces of glass and other fittings fell on them from different floors.

Meanwhile, the fire service and civil defence formed a four-member probe committee, headed by its deputy director Zahurul Haque to investigate the incident. After forming the committee, they were investigating the accidents and restricted public entry to the basements of the building for proper investigation. Moreover, they had sent letters to Rajuk, Dhaka North City Corporation and Bangladesh University of Engineering and Technology to investigate the matter and teams of those institutions had already visited the spot.

From investigation it was found that an elevator snapped and crashed in the basement and started the fire. In primary investigation it was found that the electro-mechanical maintenance of the shopping mall was poor. So the building, considering the electro-mechanical maintenance, might be called risky. This resulted in the crash of the lift and eventually the explosion at the basement initiated the fire. Additionally, under the impact of the lift crash, building glasses — from the 5th floor to the ground floor — smashed and their broken pieces fell on the people staying on different floors, leaving many injured.



Figure 1: Tropical Alauddin Tower Shopping Complex in Uttara after fire explosion



Figure 2: Fire fighting



Figure 3: Rescue operation



## **PART-III**

# **FIRE IN INCIDENT IN TAMPACO FOILS LTD AT BSCIC INDUSTRIAL AREA, TONGI, GAZIPUR ON 10 SEPTEMBER, 2016**

**BANGLADESH NETWORK OFFICE FOR URBAN  
SAFETY (BNUS), BUET, DHAKA**

**Prepared By: Uttama Barua**

**Mehedi Ahmed Ansary**

## 1. The Incident

On 10 September, 2016 at 5:00 am an incident of explosion occurred at the factory building of Tampaco Foils Ltd in BSCIC industrial area, Tongi, Gazipur, some 20km north of capital Dhaka. The company manufactures paper backed foils, plugs wrap paper, cigarette paper, filter tipping paper and printed, metalised and laminated films for different local industrial units as well as multinational organisations.



Figure 1: Black plumes of smoke from the building

The explosion triggered a massive fire and led to the partial collapse of the four-storey factory building. The raging blaze reduced the factory to ruins as parts of the upper floors of the four-storey building caved in. Black plumes of smoke from the building spiralled upward, engulfing the area in the initial hours of the incident. The explosion at the factory was so strong that it caused large chunks of debris to fly in all directions. Even some windowpanes at a few nearby buildings were broken off due to the impact of the blast. The factory blaze also engulfed an adjoining five-storey building. A BUET expert team that visited the site in the afternoon said that the five-storey building too might collapse and warned the firefighters against attempting to enter it. Both the buildings are owned by Tampaco and situated on one compound.



Figure 2: Collapsed building of Tampaco Foils Ltd

## **2. Fire extinguishing**

The fire could not be extinguished till 11 September, 2016 because the explosion was huge and the fire triggered by the blast spread quickly because flammable chemicals and oil drums were stored at the factory. About 150 firefighters of 25 units and around 50 volunteers worked since morning to douse the blaze, but they had to struggle from outside of the building as they could not enter it due to the chemical containers in the factory. They tried to move into the interior of the building. But the attempt was frustrated by thick smoke and broken chunks of concrete. A fresh fire broke out in the building's western part around 11:00am, forcing rescuers and volunteers to get out of the building. Additionally, there was no access to the buildings for an effective fire fighting as the compound with only one entry is surrounded by industrial and residential structures. The buildings were very long in shape and both had deposits of chemicals making fire fighting difficult. They were doing defensive fire fighting to ensure that the fire did not engulf any other adjoining buildings and structures. Fire fighters put out the blaze around 5:00 pm on 11 September 2016, nearly 36 hours after the factory was engulfed in flames – what authorities blamed on a boiler explosion in the factory.



Figure 3: Fire extinguishing operation



Figure 4: Fire extinguishing operation including local and fire service personnel

### 3. Rescue operation

After dousing the fire, rescue operation was started on 12 September 2016 in the morning. A team of 14 independent engineering brigades joined the rescue operations led by Brigadier General A SM Mahmud Hasan with heavy equipment on the site. They were assisted by Gazipur City Corporation, the fire service, Gazipur administration and local police. The rescue operators said that, it may take

up to two months to remove all the rubble from the Tampaco site because the rubble is even more than the Rana Plaza debris and there were some drums containing ethyl there too. The operators lacked the experience in handling such chemicals.



Figure: Initial rescue operation by local people



Figure 5: Rescue operation including local and fire service personnel



Figure 6: Rescue operation



Figure 7: Rescuer operation including army and fire service personnel

#### 4. Casualties

Established in 1978, the factory has around 350 workers working in three shifts. About 100 people were working in the morning shift, who were already in a holiday mood as it was their last working day before the weeklong Eid vacation. But it turned out to be a devastated day in their lives. Local people started the rescue operation, thus they could rescue some 30 to 40 people alive before the

arrival of the firefighters at the spot. But, the locals could not save those trapped inside because of the extreme heat of the inferno. Many of the workers were trapped inside the building and begging for help.

More than 100 people were injured, who were admitted to Tongi 50-bed hospital. Some of them in critical conditions were sent to Dhaka Medical College hospital. Till 11 September, 2016, at least 30 people were killed and another 10 people were still missing. 21 died at the scene and the rest succumbed to their wounds at Dhaka Medical College Hospital (DMCH) and other health facilities including Tongi Government Hospital, Uttara Adhunik Medical College Hospital and Kurmitola Medical College Hospital. Parts of the debris fell on the road in front of the structure killing three rickshaw passengers instantly. The rescuers recovered more bodies from the spot as the rescue operation went on. By 27 September 2016, the death toll rose to 39 and another 10 people were still missing.

Ministry for Labour and Employment declared to give Tk 2 lakh to each family of the deceased and also promised to give Tk 1 lakh each injured worker to ensure proper medical treatment for them.

### **5. Investigation of the incident**

Separate probe committees were formed to investigate the incident. The Fire Service and Civil Defence Department formed a five-member probe body with its Deputy Director as the head to file a report within 10 working days. The BSCIC formed a three-member committee with its regional director of Dhaka to submit its report within seven days. Meanwhile, Gazipur district administration also formed a five-member probe committee to submit its report within 15 working days. The Department of Inspection for Factories and Establishments (DIFE) also formed a three-member body to find out the cause of the incident within seven days.

The factory was risky since it was housed in a 40-year-old building. Initially it was assumed that the fire was triggered by a boiler explosion. The Office of the Chief Inspector of Boilers initially ruled out the possibility of the fire being caused by a boiler explosion. But the inspection at the factory site revealed that there was no damage to the two boilers of the packaging factory. Thus, the authority dismissed reports that the fire at Tampaco Foils was caused by a boiler explosion. In contrary, the survivors from the disaster claimed that it was an explosion during gas leak that brought the factory down. A survivor claimed that he could hear gas leaking and smelled its odour on the fateful day. On 24 September 2016, the Titas Gas Transmission and Distribution Committee concluded after assessment that, did not find faults in gas pipeline responsible for the incident because the pipeline was found unharmed. They assumed that the explosion was resulted due to chemical explosion. Moreover gas supply to the factory was suspended within half an hour of the incident, although they

found evidence of gas use beyond the approved limit. The factory was consuming gas at least twice the permitted amount at the time of the incident.



## **PART-IV**

# **MEASUREMENT OF ELECTRICAL RESISTIVITY WITHIN A POWER PLANT AREA**

**BANGLADESH NETWORK OFFICE FOR URBAN  
SAFETY (BNUS), BUET, DHAKA**

**Prepared By: Pushpendue Biswas**

**Mehedi Ahmed Ansary**

**Test Point 01:**

The electrode spacing was 2 m. Resistivity tomography for Test point 01 was measured with Wenner array. The validity of Wenner ERT section of Test point 01 is supported by good low RMS error of 1.38% for the 3<sup>rd</sup> iteration. The depth of the investigation was found of about 7.0 m. The resistivity's along the profile span a range of 0.226-20 Ω m. The soil profile is shown in the Table 1. This profile exists two soil layers. The top layer exist clayey filling sand from 0 to 3.0 m which was saturated during the test by rain water (the resistivity pseudosection shows water in the resistivity model on the surface level). The second layer exist clay and sand mixture from 3.0 to 7.0 m almost. Figure 1 shows the model resistivity of ERT at Test point 01.

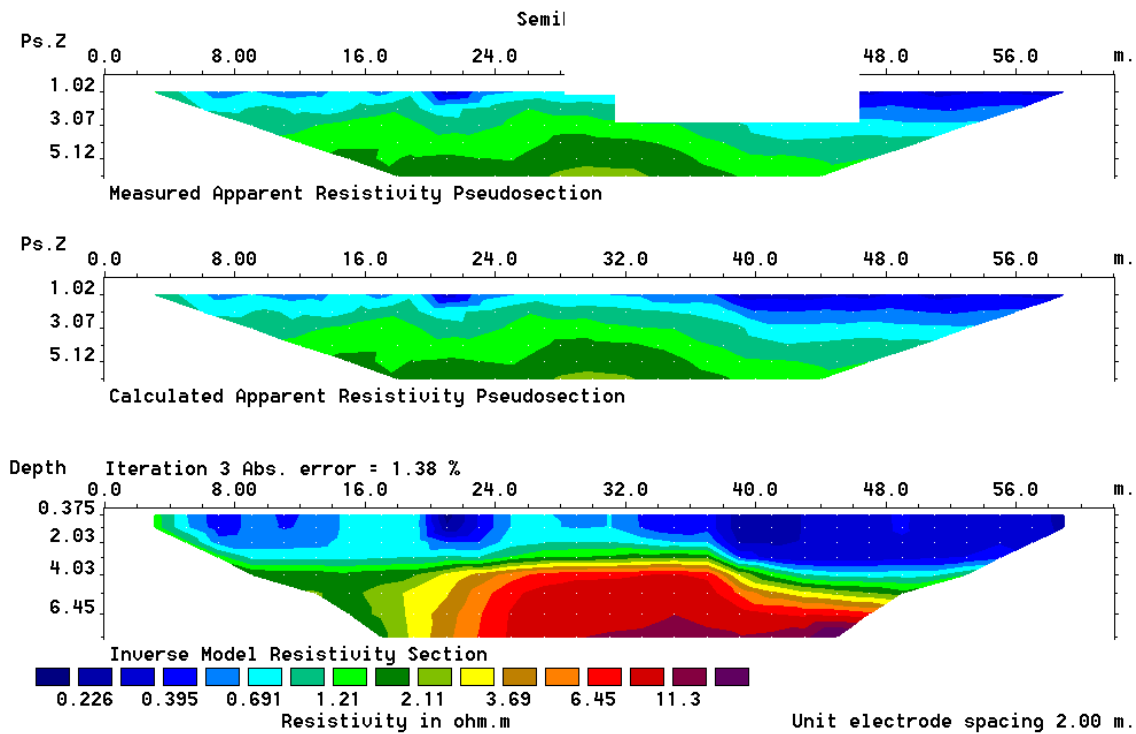


Figure 1: Model resistivity of ERT at **Test point 01**

Table 1: Electrical Resistivity Tomography (ERT) result at **Test point 01**

Depth (meter)	Soil Type	Resistivity Range (Ω m)
0 to 3.0	Clayey filling Sand	0.226-3.69
3.0 to 7.0	Clay and Sand mixture	3.69-20

**Test Point 02:**

The electrode spacing was 2 m. Resistivity tomography for Test point 02 was measured with Wenner array. The validity of Wenner ERT section of Test point 02 is supported by good RMS error of 37.8% for the 3<sup>rd</sup> iteration. The depth of the investigation was found of about 7.0 m. The resistivity's along the profile span a range of 0.25-12 Ω m. The soil profile is shown in the Table 2. This profile exist mixed soil layers. It could be defined as one layer of combination of clay and sand mix. Figure 2 shows the model resistivity of ERT at Test point 02.

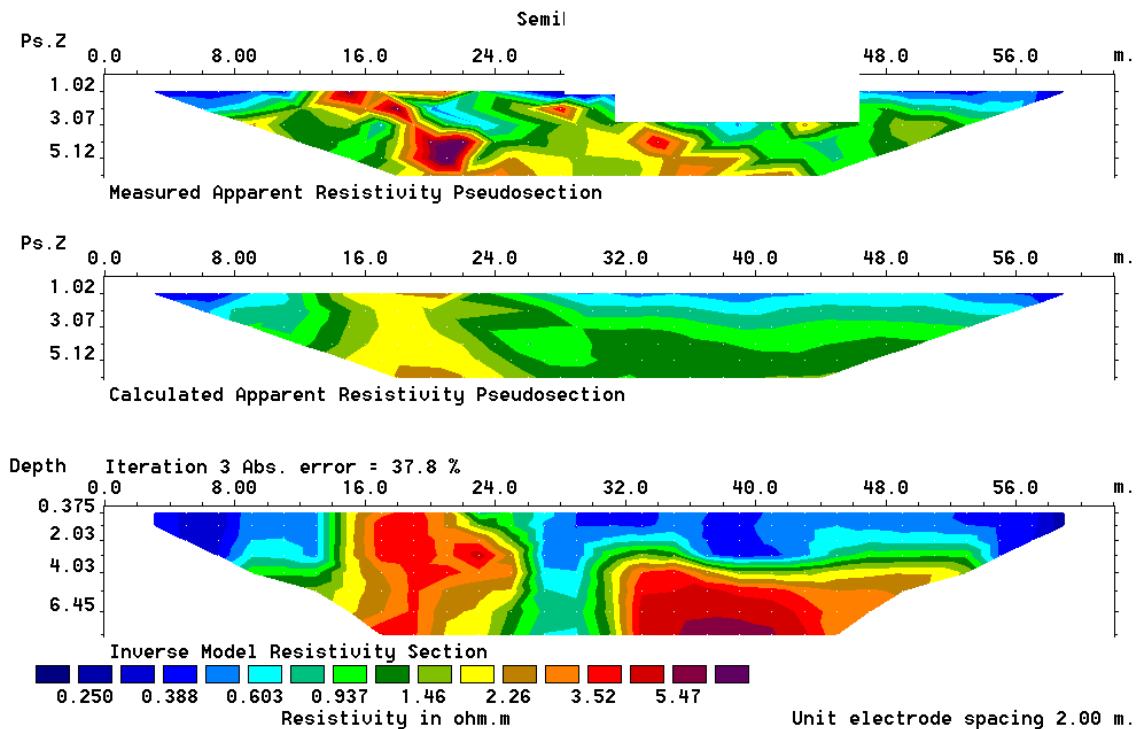


Figure 2: Model resistivity of ERT at **Test point 02**

Table 2: Electrical Resistivity Tomography (ERT) result at **Test point 02**

Depth (meter)	Soil Type	Resistivity Range (Ω m)
0 to 7.0	Clay and Sand mixture	0.25-12

**Test Point 03:**

The electrode spacing was 2 m. Resistivity tomography for Test point 03 was measured with Wenner array. The validity of Wenner ERT section of Test point 03 is supported by good low RMS error of 1.13% for the 3<sup>rd</sup> iteration. The depth of the investigation was found of about 7.0 m. The resistivity's along the profile span a range of 3.41-494 Ω m. The soil profile is shown in the Table 3. This profile exists two soil layers. The top layer exist clay and sand mixture from 0 to 3.0 m almost. The second layer exist clay from 3.0 to 7.0 m almost. Figure 3 shows the model resistivity of ERT at Test point 03.

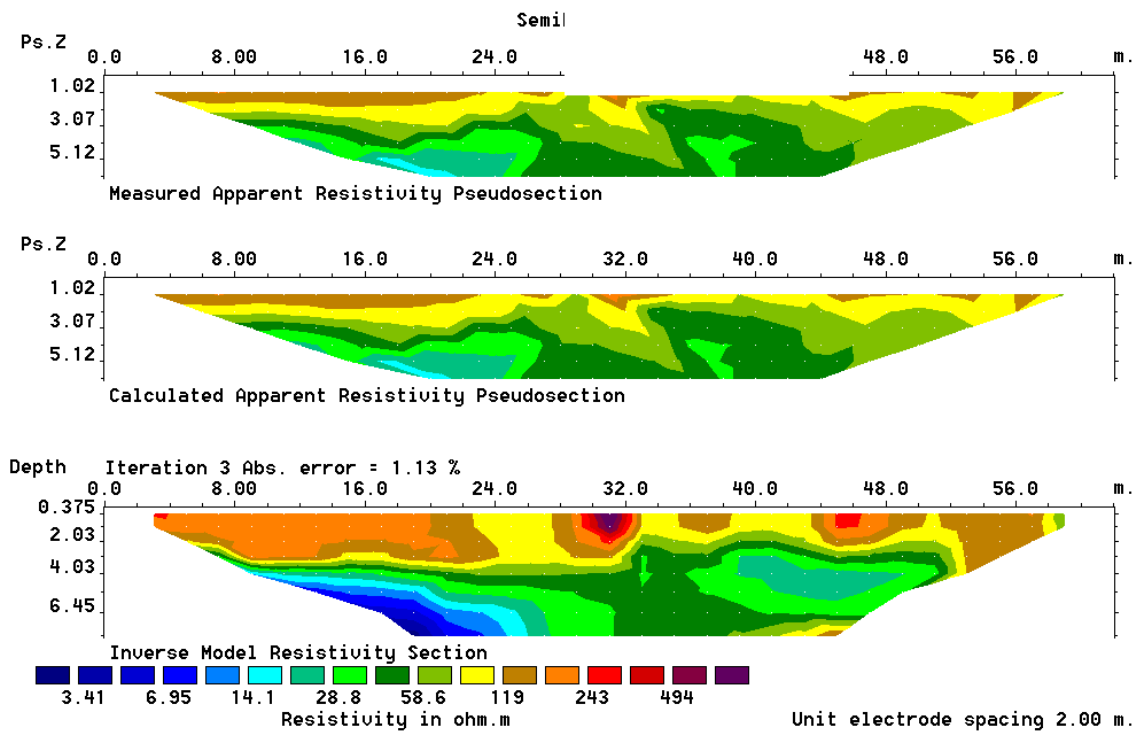


Figure 3: Model resistivity of ERT at **Test point 03**

Table 3: Electrical Resistivity Tomography (ERT) result at **Test point 03**

Depth (meter)	Soil Type	Resistivity Range (Ω m)
0 to 3.0	Clay and Sand mixture	3.41-250
3.0 to 7.0	Clay	8.0-58.6

**Test Point 04:**

The electrode spacing was 2 m. Resistivity tomography for Test point 04 was measured with Wenner array. The validity of Wenner ERT section of Test point 04 is supported by good low RMS error of 9.6% for the 3<sup>rd</sup> iteration. The depth of the investigation was found of about 7.0 m. The resistivity's along the profile span a range of 2.45-778 Ω m. The soil profile is shown in the Table 4. This profile exists two soil layers. The top layer exist clay and sand mixture from 0 to 3.0 m almost with **water saturation**. The second layer exist clay from 3.0 to 7.0 m almost. Figure 4 shows the model resistivity of ERT at Test point 04.

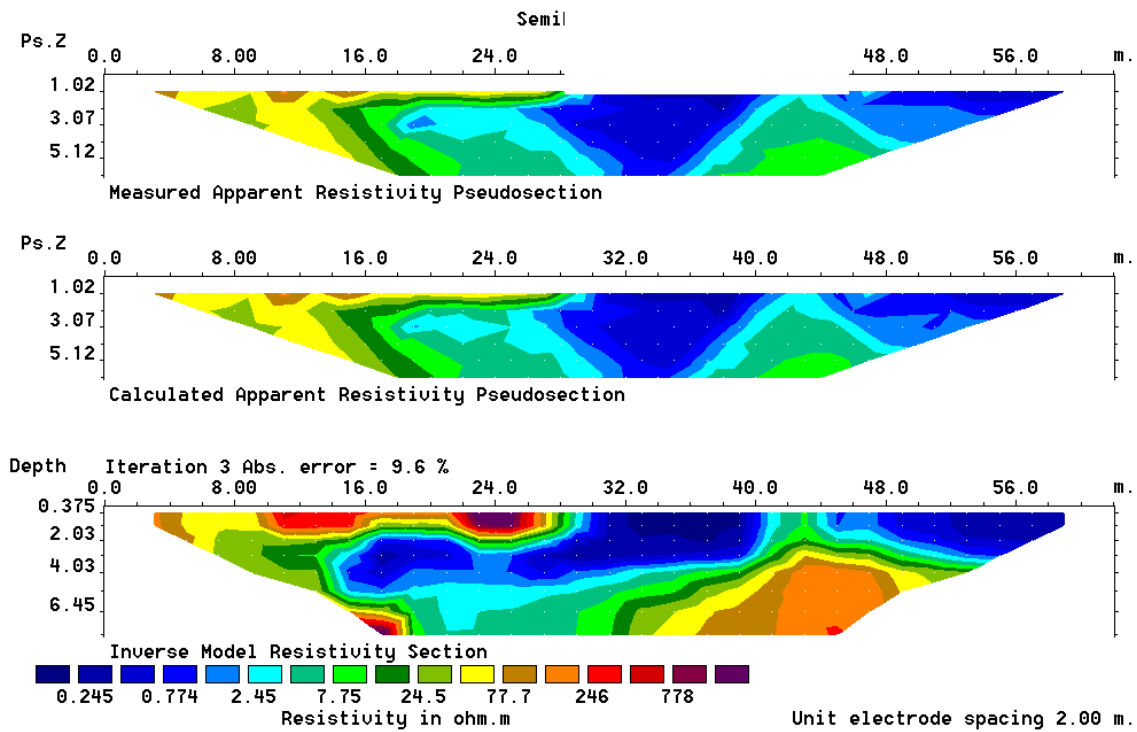


Figure 4: Model resistivity of ERT at **Test point 04**

Table 4: Electrical Resistivity Tomography (ERT) result at **Test point 04**

Depth (meter)	Soil Type	Resistivity Range (Ω m)
0 to 3.0	Clay and Sand mixture	3.41-250
3.0 to 7.0	Clay	8.0-100

**Test Point 05:**

The electrode spacing was 2 m. Resistivity tomography for Test point 05 was measured with Wenner array. The validity of Wenner ERT section of Test point 05 is supported by good low RMS error of 29.2% for the 3<sup>rd</sup> iteration. The depth of the investigation was found of about 7.0 m. The resistivity's along the profile span a range of .316-50 Ω m. The soil profile is shown in the Table 5. This profile exists two soil layers. The top layer exist clay and sand mixture from 0 to 3.5 m almost with **very high water saturation**. The second layer exist clay from 3.5 to 7.0 m almost. Figure 5 shows the model resistivity of ERT at Test point 05.

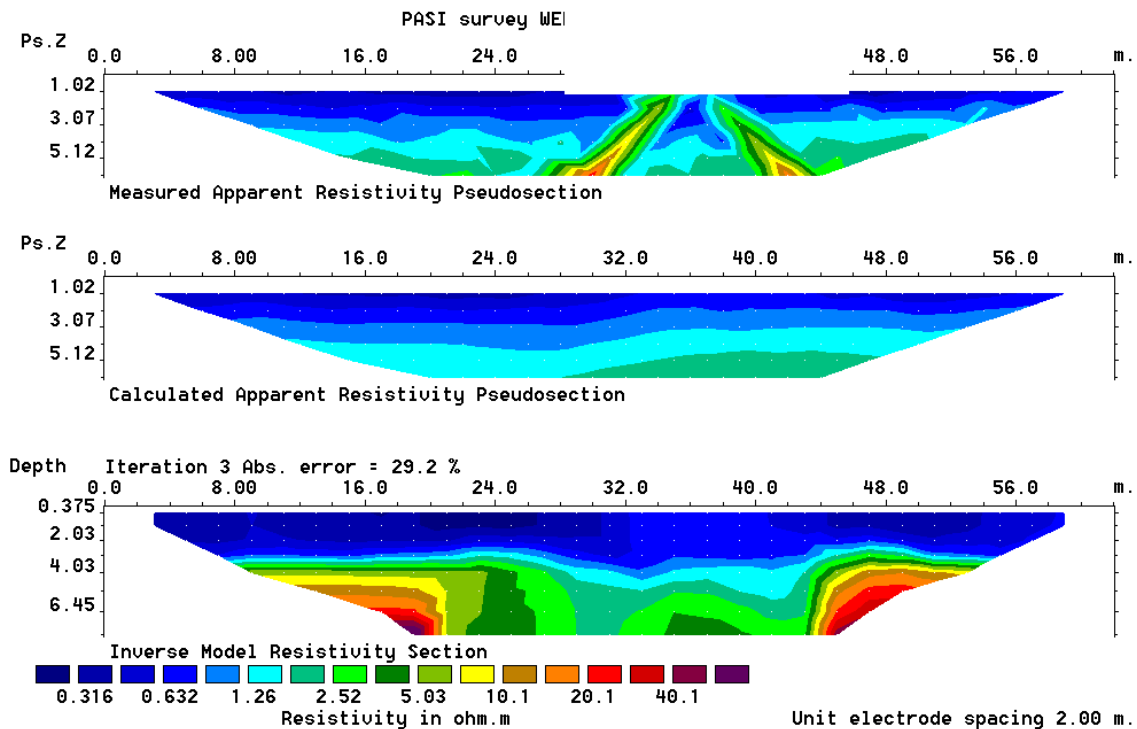


Figure 5: Model resistivity of ERT at **Test point 05**

Table 5: Electrical Resistivity Tomography (ERT) result at **Test point 05**

Depth (meter)	Soil Type	Resistivity Range (Ω m)
0 to 3.5	Clay and Sand mixture	1.0-6.0
3.5 to 7.0	Clay	1.0-40

**Test Point 06:**

The electrode spacing was 2 m. Resistivity tomography for Test point 06 was measured with Wenner array. The validity of Wenner ERT section of Test point 06 is supported by good low RMS error of 15.2% for the 3<sup>rd</sup> iteration. The depth of the investigation was found of about 7.0 m. The resistivity's along the profile span a range of .28-40 Ω m. The soil profile is shown in the Table 6. This profile exists two soil layers. The top layer exist clay and sand mixture from 0 to 3.5 m almost with **very high water saturation**. The second layer exist clay from 3.5 to 7.0 m almost. Figure 6 shows the model resistivity of ERT at Test point 06.

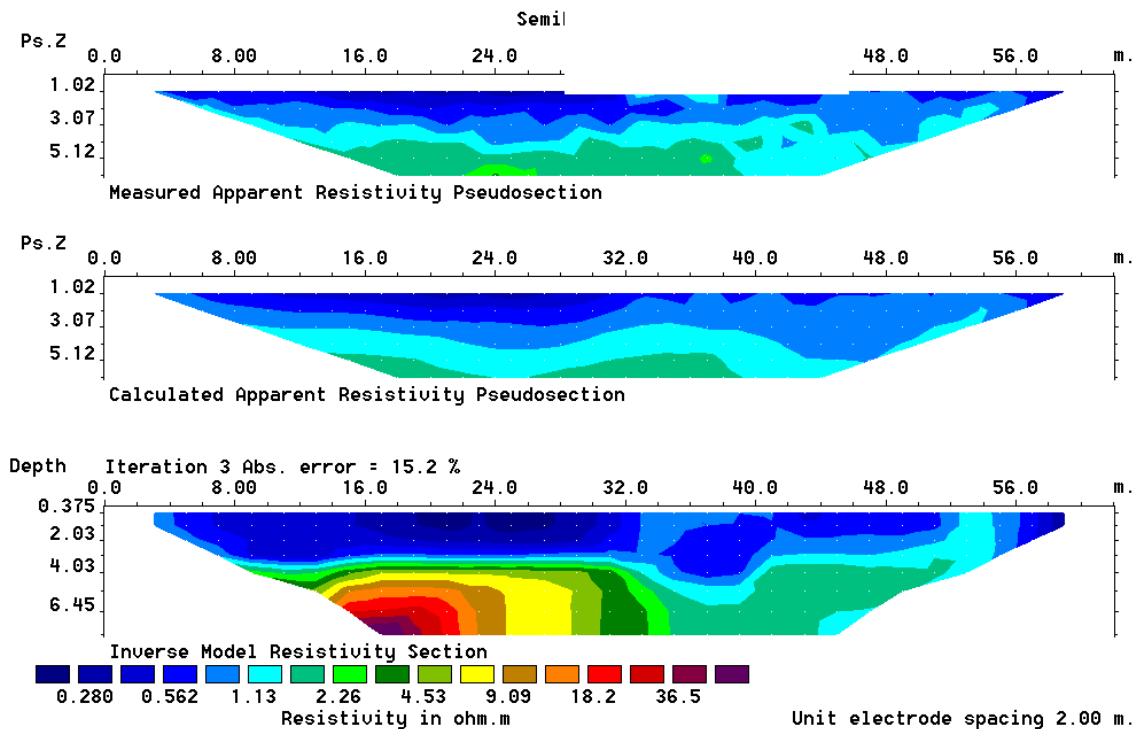


Figure 6: Model resistivity of ERT at **Test point 06**

Table 6: Electrical Resistivity Tomography (ERT) result at **Test point 06**

Depth (meter)	Soil Type	Resistivity Range (Ω m)
0 to 3.5	Clay and Sand mixture	1.0-8.0
3.5 to 7.0	Clay	10-40

**Test Point 07:**

The electrode spacing was 2 m. Resistivity tomography for Test point 07 was measured with Wenner array. The validity of Wenner ERT section of Test point 07 is supported by good low RMS error of 15.2% for the 3<sup>rd</sup> iteration. The depth of the investigation was found of about 7.0 m. The resistivity's along the profile span a range of 2.35-520 Ω m. The soil profile is shown in the Table 7. This profile exists two soil layers. The top layer exist filling sand from 0 to 3.5 m almost. The second layer exist clay from 3.5 to 7.0 m almost. Figure 7 shows the model resistivity of ERT at Test point 07.

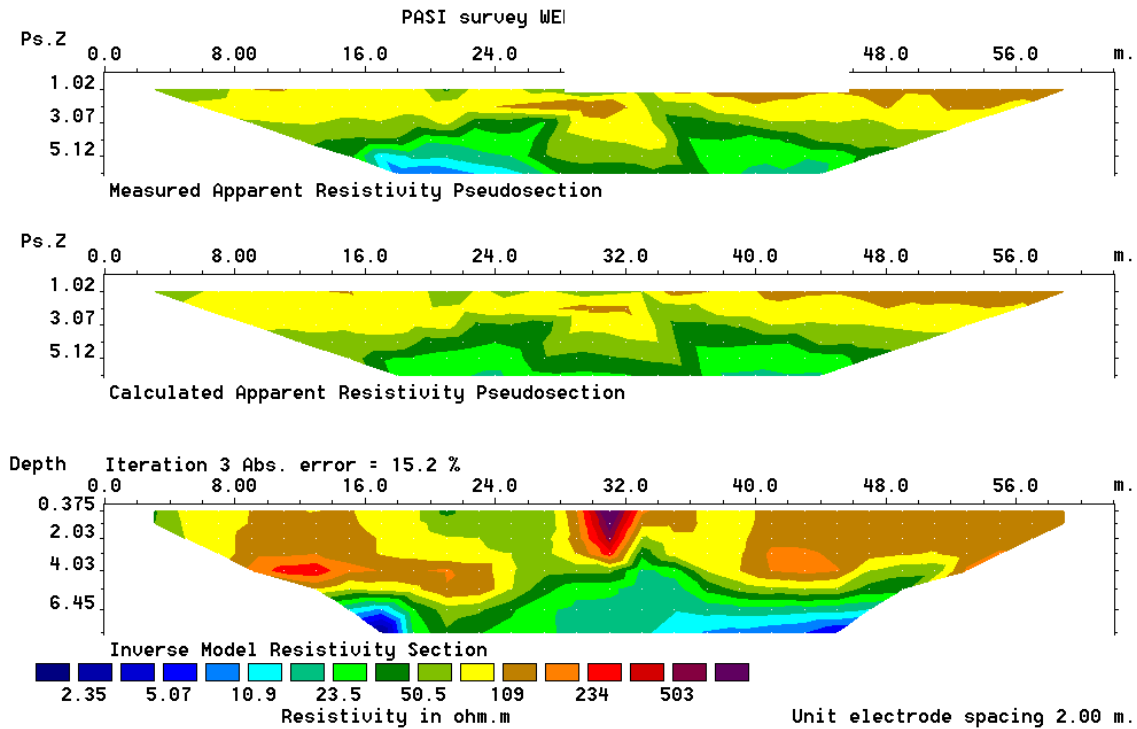


Figure 7: Model resistivity of ERT at **Test point 07**

Table 7: Electrical Resistivity Tomography (ERT) result at **Test point 07**

Depth (meter)	Soil Type	Resistivity Range (Ω m)
0 to 3.5	Filling Sand	100-250
3.5 to 7.0	Clay	5.07-70

**Test Point 08:**

The electrode spacing was 2 m. Resistivity tomography for Test point 08 was measured with Wenner array. The validity of Wenner ERT section of Test point 08 is supported by good low RMS error of 7.8% for the 3<sup>rd</sup> iteration. The depth of the investigation was found of about 7.0 m. The resistivity's along the profile span a range of 0.56-200 Ω m. The soil profile is shown in the Table 8. This profile exists two soil layers. The top layer exist clay from 0 to 3.5 m almost with **very high water saturation**. The second layer exist clay and sand mix from 3.5 to 7.0 m almost. Figure 8 shows the model resistivity of ERT at Test point 08.

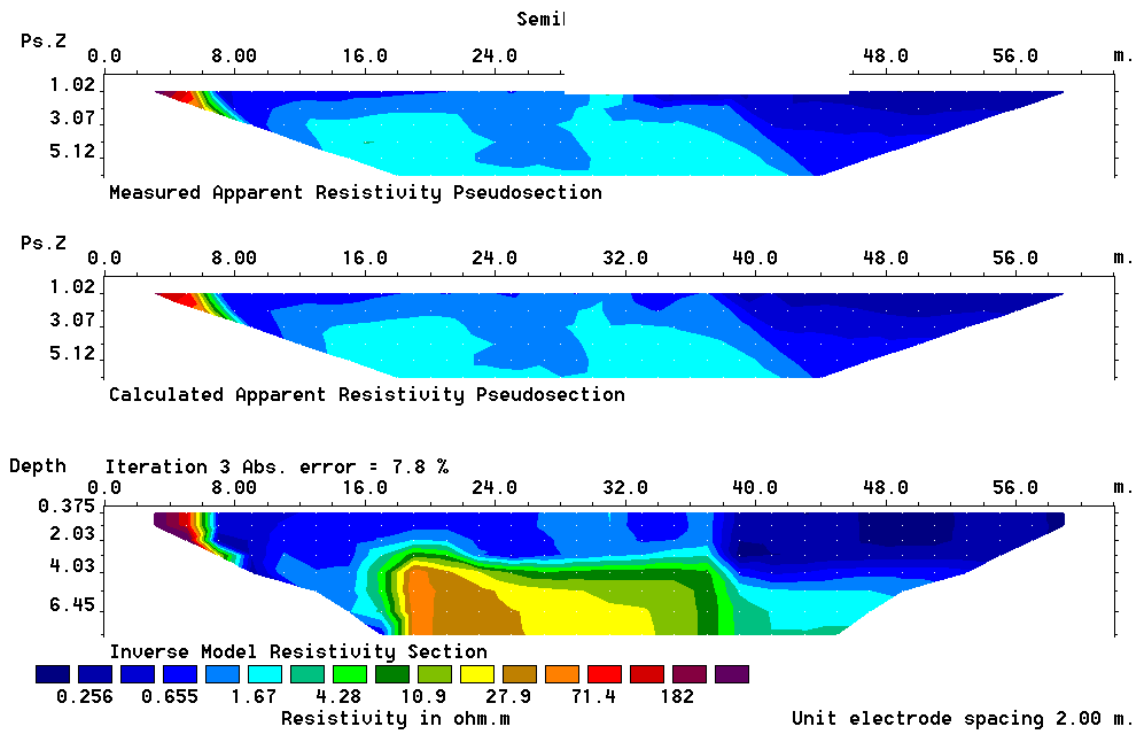


Figure 8: Model resistivity of ERT at **Test point 08**

Table 8: Electrical Resistivity Tomography (ERT) result at **Test point 08**

Depth (meter)	Soil Type	Resistivity Range (Ω m)
0 to 3.5	Clay	1.0-12
3.5 to 7.0	Clay and sand mix	13-170



## **PART-V**

# **ASSESSMENT OF UNDERLYING CAUSES OF FIRE RISK IN OLD DHAKA: A CASE STUDY OF ISLAMBAG AREA IN WARD NO. 65, DHAKA SOUTH CITY CORPORATION**

**BANGLADESH NETWORK OFFICE FOR URBAN  
SAFETY (BNUS), BUET, DHAKA**

**Prepared By: Uttama Barua**

**Mehedi Ahmed Ansary**

## 1. INTRODUCTION

Incident of fire is hazardous when it results in loss of human life and economy. In urban areas the effect of fire hazard is much more in comparison to other areas because of the development pattern and land use. In Dhaka, the capital city of Bangladesh, fire hazards cause huge life and economic loss every year (BSFCD). The causes behind such large scale fire hazards in the city are: violation of building codes and non-compliance with the Firefighting and Extinguishing Law, dense building concentrations, lack of safety measures, narrow roads, flammable building materials and electrical system as well as the lack of resources to raise awareness and response skills (BFSCD, 2003). Particularly in Old Dhaka, incidents of fire hazards are more frequent than any other part of the city. In this area, most of the buildings are of mixed use, where the ground floor and/or the first floor are used for small factories like chemical, plastic, rubber etc., mechanical shop, welding shops, warehouse and food shops, etc. Rests of the floors of the buildings are used for residential purpose mainly for the workers of the factories and shops. Thus, fire hazard vulnerability of Old Dhaka is very high.

In case of fire incidents in Dhaka city, firefighting is a very important job, but fire prevention is more crucial to prevent an actual fire accident from happening. In general, fire protection equipments and the use of firefighting tools are given more emphasis, neglecting the importance of practicing fire preventive measures. The purpose of fire prevention plan is to eliminate the causes of fire and to prevent loss of life and property by fire (OSHCON, 2006), for which a clear understanding of underlying cause of fire are required to be identified to take initiatives thereby. Bangladesh, as a developing country, cannot afford the huge amount of loss caused by fire accidents every year in Dhaka city, particularly in Old Dhaka. So, this study aims at assessment of the reasons of fire risk in Old Dhaka to pave the way for the preparation of a fire prevention plan for Old Dhaka. In this study, Islambag area of Ward No. 65 (Figure 1) of Old Dhaka was selected for the assessment. The causes are that, fire incidents are very common phenomenon in this area and this area is one of most vulnerable areas to fire hazard because of its traditional land use and population density. Thus in this study, assessment of fire risk was done to find out potential underlying causes behind fire hazard in Islambag area of Ward 65 of Old Dhaka.

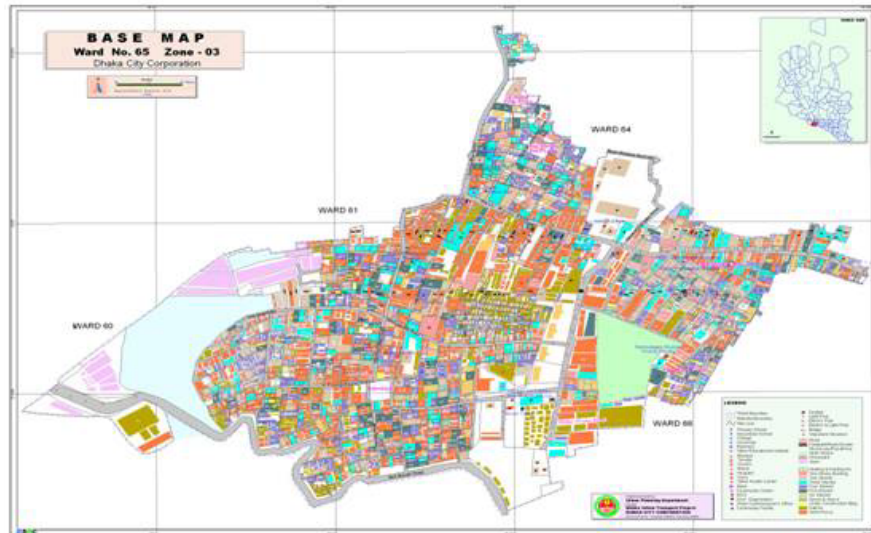


Figure 1: Study Area (Ward No. 65 of Dhaka city) (Source: Dhaka City Corporation)

The main reasons for any fire hazard are the sources of fire hazard and other factors accelerating the incident. Fires require fuel, an adequate oxygen supply, and an ignition source, i.e., the Fire Triangle, which when brought together, cause fires (Figure 2). Fire prevention can be accomplished by maintaining control over one or more of these three required elements (UoC, 2005).

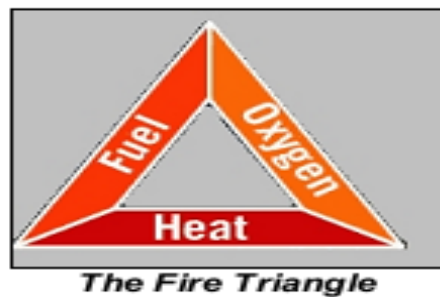


Figure 2: Fire triangle (Source: UoC, 2005)

An ignition source is something that can cause an accelerant or flammable material to ignite, e. g. unsafe electrical conditions, machines and equipments, hot work, careless smoking etc. (Margentino, & Malinowski, 1992). The ignition sources can pose a fire hazard if they are placed near the combustible materials (EHSS, 2011).

- Unsafe Electrical Conditions
- Machines and equipment
- Hot work
- Careless Smoking

Anything that can burn is potential fuel for a fire or, in some cases, an explosion (Margentino, & Malinowski, 1992). Certain types of substances can ignite at relatively low temperatures or pose a risk of catastrophic explosion if ignited (OSHCON, 2006)

- Combustible Materials
- Flammable Materials
- Accelerants (OSHCON, 2006; EHSS, 2011, Margentino, & Malinowski, 1992).

The main source of oxygen for a fire or explosion is in the general body of air. There are also other sources of oxygen, such as bottled oxygen, compressed air distribution systems and chemicals that release oxygen when heated (oxidizing agents) such as hydrogen peroxide etc. (HSE, 2012).

Beyond the main sources of fire, there are other factors which are not responsible for ignition of a fire, but fire protection and ease of firefighting to reduce loss depend on these factors.

- Structural condition
- Safety measures

In this study, thermal image captured by thermal imaging camera has been used for identification of ignition sources of fire in the factories located in the study area. A thermal imaging camera is a unique and non-contact tool utilizing infrared thermography which is the art of transforming an infrared image into a radiometric one allowing temperature values to be read from the image. Thus the tool produces thermal image indicating the exact location of energy losses through scanning and visualizing the temperature distribution of entire surfaces quickly and accurately providing precise and convincing argumentation (FLIR, 2011a & 2011b).

Thermal imaging cameras are powerful and noninvasive tools for monitoring and diagnosing these conditions, identifying problems early, allowing them to be documented and corrected before becoming more serious and more costly to repair (FLIR, 2011a).

Electrical devices are usually rated in power indicating the maximum amount of energy the device can consume without being damaged (Taib, Jadin, & Kabir, 2012). If an electrical equipment is operated above its specifications, this results in lower efficiency of the device, causing the energy to be spent in generating heat (FLIR, 2011b, Haidar, Asiegbu, Hawari, & Ibrahim, 2012, and Taib, Jadin, & Kabir, 2012). Faulty connections and wiring indicate a loose, over tightened or corroded connection with increased resistance and faulty fuses indicate its saturated capacity, which thus become warm (FLIR, 2011b). If the faulty electrical equipments are left unchecked, heat can rise to the point where connections start to melt resulting in sparks to start a fire (FLIR, 2011a & 2011b).

The radiated heat from an electrical device can be measured on the infrared spectral band of the electromagnetic spectrum using thermal imaging (FLIR, 2011b, Haidar, Asiegbu, Hawari, & Ibrahim, 2012). If the difference in temperature between similar components under similar loads exceeds 15 °C (~25 °F), it indicates requirement of immediate repairs (FLIR, 2011b). Thus, any of the electrical problems can be avoided with the use of a thermal imaging camera, helping to detect anomalies that would normally be invisible to the naked eye and to solve problems before production goes down or a fire occurs (FLIR, 2011b).

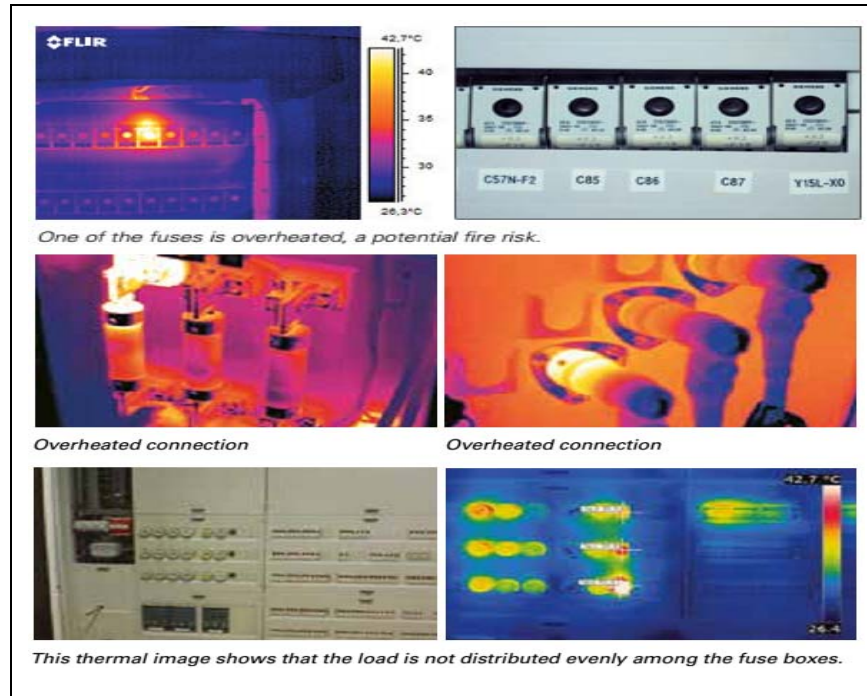


Figure 3: Use of thermal image in detecting faulty electrical instruments (Source: FLIR, 2011a & 2011b)

Mechanical systems heat up if there is a misalignment at some point in the system, or when mechanical components become worn and less efficient. Again, increased surface temperatures can be the result of internal faults. Excessive heat can also be generated by friction in faulty bearings due to wear, misalignment or inadequate lubrication. When these overheated machines come to contact with electrical equipments or any combustible or flammable materials, this results in fire to ignite. Thermal images help to inspect overheated mechanical installations in the factories. Interpretation of results should be based on comparison between components operating in similar conditions under similar loads (Source: FLIR, 2011b).

## 2 METHODOLOGY OF THE STUDY

The research has been conducted with the following methodology:

### 2.1 STUDY DESIGN

In Old Dhaka fire incidents are very common, but for lack of knowledge about the reasons behind such frequent fire incidents proper initiatives for the fire prevention cannot be taken for the area. Thereby, objective of the study was defined to find out the causes of fire incidents in Old Dhaka. Then methodology of the study was defined based on literature review.

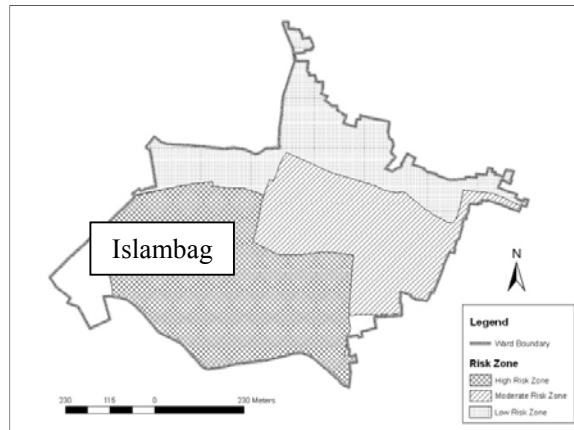


Figure 4: Fire risk zone in Ward 65

### 2.2 STUDY AREA SELECTION

The Islambag area of Ward No. 65 of Old Dhaka is selected as the study area. The total area of Ward No. 65 is 118.1668 acres (0.478 Square Kilometer). Ward No. 65 is divided into three risk zones including high risk zone, moderate risk zone and low risk zone according to their land use from expert opinion (Figure 4). High risk zone is 52.84 acres (44.72%) where dominant land use are plastic processing industries; moderate risk zone is 30.89 acres (26.14%) where dominant land use are processing factory and different warehouse (plastic warehouse, cattle food storage etc), and low risk zone is 27.95 acres (23.65%) where dominant land use are residential use with commercial facilities (retail shop, office, bank and storage) (calculated from GIS). Islambag area lies in the high risk area as the livelihoods of the inhabitants of this area are primarily based on plastic processing industries.

### 2.3 PREPARATION OF QUESTIONNAIRE

For achieving the objectives, depending on the literature review a questionnaire for the study has been designed which has been modified on the basis of findings from pilot survey.

### 2.4 FINDING OUT REASONS BEHIND FIRE HAZARD

The reasons behind fire hazard in the study area was assessed by identification and observation of the sources of fire hazard, i.e. ignition sources, sources of ignition, fuel and oxygen, assessment of structural condition, and identification and observation of availability of safety measures. Considering these factors, the methodology for fire hazard assessment was developed, which involves both questionnaire survey and visual assessment.

### 3. REASONS OF FIRE HAZARD IN THE STUDY AREA

Fire hazards are mainly initiated in the factories or small scale industrial buildings in the study area. In this study, 20 number of buildings have been surveyed which are mainly factories or small scale industrial buildings. In the following section of the report, detailed findings from the survey have been described.

#### 3.1 GENERAL CONDITION OF THE BUILDINGS

Number of storey of the surveyed buildings ranged from one to seven. Table 1 shows the frequency of buildings surveyed with respect to occupancy and number of storey.

Table 1: Frequency of the building surveyed with respect to building occupancy and number of floors

No. of floors Building occupancy	No. of floors			Total
	1 Floor	2 Floors	Greater than 2 floors	
Welding Shop	1	0	0	1
Plastic Factory	7	0	0	7
Plastic Storage	1	0	0	1
Machine Shop	1	0	0	1
Welding shop and plastic storage	0	1	0	1
Welding shop and residential use	0	1	1	2
Machine shop and residential use	0	0	2	2
Plastic storage and residential use	0	0	1	1
Plastic factory and residential	0	0	1	1
Plastic shoe factory	1	0	0	1
Machine shop and plastic storage	0	1	0	1
Plastic shoe factory and residential	0	0	1	1
Total	11	3	6	20

### 3.2 IGNITION SOURCES OR SOURCES OF HEAT

Figure 5 shows ignition sources of fire in the surveyed buildings with respect to number of buildings containing the source. The main ignition sources in the surveyed buildings are the unsafe electrical conditions. In the study area, the overhead electric supply pole and wires are arranged in much disorganized way, which may cause rapid spread of fire in the area. Almost all the surveyed buildings pose similar electrical unsafe conditions which include: improper wiring system, defective switches and outlets, defective fuses, cable conduit on wall not clipped properly and low quality electrical equipments, among which use of low quality equipments, defective wiring system, and defective cutouts and fuses are most common (Figure 5).

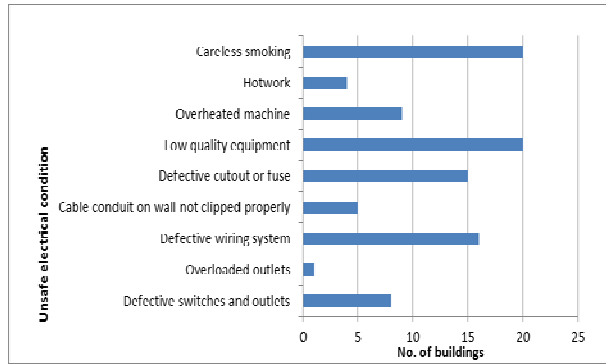


Figure 5: Fire ignition sources in the study area

Among the surveyed buildings, plastic factories and machine shops contain machines and equipments. Most of the machines are not lubricated properly causing overheating. Thus, nine buildings among twenty have the problem of overheated machine (Figure 5). Moreover, for lack of proper maintenance, the machines and equipments used in the factories have a layer of oil cover which accelerates the possibility of ignition of fire. In these factories, the electric equipments and machines are observed in close proximity, which increases the risk of fire hazard.

In the welding shops, the operations involve hot works which produce open flame. In all the surveyed buildings, careless smoking is very common according to the workers. Other significant ignition source that was observed in one of the plastic storage is the use of candle light at the time of load shedding. Close proximity of the stored plastic materials and candle light may also cause a fire to initiate. One of these factors may contribute to ignition of fire in the buildings and the study area.

### 3.3 SOURCES OF FUEL

Figure 6 shows sources of fuel of fire in the surveyed buildings with respect to number of buildings containing the source. Most common combustible materials used, produced and preserved in the surveyed buildings are plastic products and materials soaked in oil (Figure 6). Again close proximity of ignition sources and fuel sources increase the risk of fire hazard in the area.

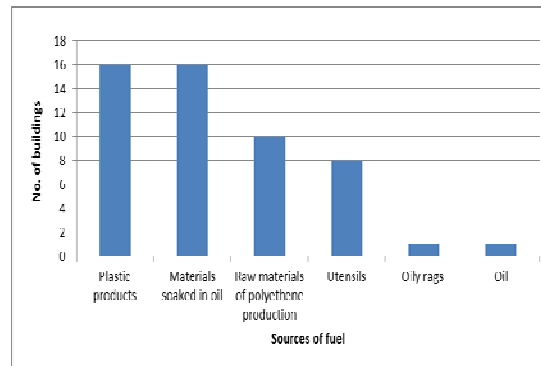


Figure 6: Sources of fuel of fire in the study area

### 3.4 SOURCES OF OXYGEN

For assessment of sources of oxygen in the study area, the air circulation systems in the buildings were assessed. In plastic factories and storages, smoke and heat vents are installed, whereas in machine shop and welding shops there are no sufficient ventilation systems. Thus among twenty surveyed buildings thirteen buildings have smoke and heat vents, among which seven have sufficient ventilation. In storages of plastic materials, heat vents are mainly located in the walls which are mostly small in size, very few in numbers and are placed in distant locations. In plastic factories, heat vents are mainly located in the ceilings which are mostly large in size as the plastic production activity creates greater heat and smoke. In all the cases, smoke and heat vents are kept open. Thus among thirteen buildings, Thus, most of the buildings lack proper air circulation system, which may result in rapid spread of fire in the area.

### 3.5 STRUCTURAL CONDITION

Spreading of fire and success of fire rescue and firefighting operation largely depend on structural condition. The structural conditions includes, i.e. building material, condition of wall and roof, condition of exit door, condition of stair, etc. Figure 7 shows components of building structures in the surveyed buildings according to building material with respect to number of buildings. The structures made of brick have heat resistance time of three hours and concrete have heat resistance time of three hours (Brick Industry Association, 2008 and Beall, 1994). Thus the buildings with components made of brick are safe for fire hazard. The buildings of single storey are constructed

with tin roof which are highly vulnerable to fire. The buildings with two storeys are constructed with wooden roof and the second floors are constructed of tin and wood, which are also highly vulnerable to fire hazard.

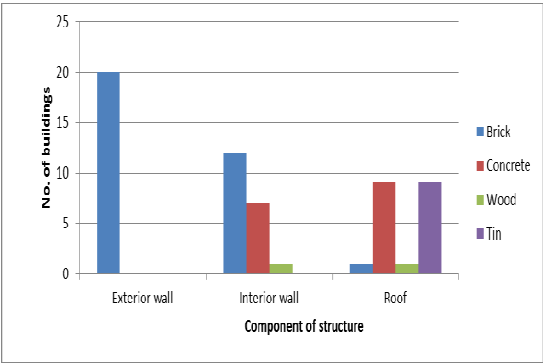


Figure 7: Component of structure with respect to material in the surveyed buildings

The minimum safe dimension of exit doors is minimum two feet width and minimum seven feet height, which is required for safe evacuation. In all of the factories, the exit doors are steel shutter, which are wide enough. Thus, sixteen out of twenty buildings have safe exits which are suitable for evacuation. Figure 8 shows condition of stairs in the surveyed buildings with respect to number of buildings.

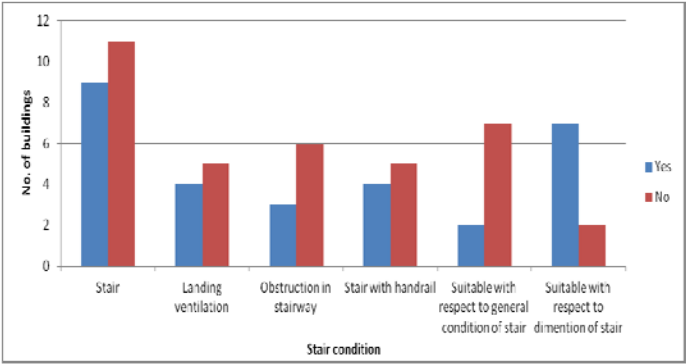


Figure 8: Condition of stair in the surveyed buildings

Among twenty surveyed buildings nine have stairs, among which seven buildings have concrete stair and two have steel stairs. Steel stairs are highly vulnerable to fire hazard due to its heat capacity. Stairs are the weakest part of a construction, whereas in the surveyed buildings the stairs are in deteriorated condition. Among nine buildings with stair, four do not have landing ventilation, three have obstruction in stairway and four have handrails. Thus, only two are suitable with respect to general condition of stair and seven are suitable with respect to dimension. So, conditions of the stairs are required to be improved. Thus, structurally the surveyed buildings are highly risky to fire hazard.

### **3.6 AVAILABILITY OF SAFETY MEASURES**

In most of the cases, width of access roads is on an average 15 ft. Thus, in case of any fire incident, fire vehicles will be able to enter the area through the adjacent roads, though they will have to continue the firefighting operation on feet within the narrow access roads. Among twenty surveyed buildings, only two have firefighting operation system. Again only six buildings among twenty have water source through underground and overhead tank due to their mixed use with residential use. Moreover, capacities of these water sources are not sufficient. According to Bangladesh National Building Code, buildings should have underground reservoir of 50000 liters and overhead reservoir of 25000 liters (BNBC, 2006). Thus, safety measures are not sufficient in the buildings.

### **4. PREVENTION STRATEGY**

Based on the findings of the study, fire prevention plan can be developed for the small scale industrial buildings of Old Dhaka to avoid any fire or explosion risks by eliminating either the potential ignition sources or potential fuel sources, or both (HSE, 2012). However, it is not possible to eliminate all the sources, so strategies can be developed to reduce fuel loads, eliminate ignition sources or prevent the fuel/ignition interaction by keeping potential ignition sources apart from potential fuel, then fire loss and human death and injury can be reduced (HSE, 2012). Particular strategies to prevent fire hazard in Old Dhaka are described below:

- Faulty electrical issues should be taken care of. The relevant strategies should include: correction and improvement of wiring system, replacement of damaged wiring, fuses, switches and plugs, avoid use of extension cords and ensure proper covering of all outlets, junction boxes and electrical panels.
- Machines and equipments should not be used by overloading their capacities to prevent overheating. Other measures should include: cleaning of all work areas of oil to prevent buildup and all power equipments should be turned off or unplugged after use.
- Hot works, i.e. welding or working with an open flame or other ignition sources, should be done in controlled and well-ventilated areas.
- Smoking should be strongly prohibited in the work place.
- Combustible or flammable materials should be kept in safe distance from the potential ignition sources and should be stored in safer places.
- Well ventilation in workplace should be ensured.
- Regular inspection in the factories should be ensured to keep the work place free of dust. The equipments should be kept in good working order. Electrical equipments should be turned off when not in use.

- Minimum fire protection instruments should be stored in the factories. Based on the type of source of a fire hazard, different fire protection instruments should be used, as some fire may be sensitive to certain types of fire extinguishers. Based on source of fire, fire incidents may be classified into five classes, for which certain extinguishing media may be required, which is shown in table 2.

Table 2: Classification of fire with respect to source and required extinguishing media

<b>Class of fire</b>	<b>Materials causing the fire</b>	<b>Extinguishing media required and their characteristics</b>	<b>Extinguisher that should not be used</b>
A	Ordinary combustible material: wood, paper, rags, rubbish, rubber and plastic.	Water and dry chemicals: Douse flames quickly and prevent spreading of fire.	
B	Flammable or combustible gases and liquids: gasoline, kerosene, thinners, paints, grease and similar materials.	Carbon dioxide, dry chemicals, foam and halogenated hydrocarbons: Limit supply of air. Water spray: to cool the containers which are likely to catch fire.	Water: Use of water may spread the fire.
C	Electric equipments	Carbon dioxide or dry powders: Non-conducting materials.	Water and foam: They may cause short circuiting, electric shock and damage to the equipment.
D	Metals: Magnesium sodium, titanium, potassium, zirconium.	Special extinguishing agents.	Normal extinguishing agents: Increase intensity of fire.

Source: Adopted from AmeriCares, n.d.

## 5. CONCLUSION

After an in depth assessment of the buildings with commercial and industrial use in Old Dhaka, it can be said that the buildings are vulnerable to fire hazard and the overall condition of buildings are not suitable for firefighting. Although this study was not conducted on a large number of building samples, it represents the miserable condition of the buildings in Old Dhaka increasing the risk of fire hazards in the area. It is not possible to eliminate all the sources of fire hazard in the area, but at least some initiatives can be taken to minimize the loss. Thus, for improving the condition some fire prevention strategies have been suggested in this study. For further development in the area, all

buildings should follow the provision provided by Bangladesh National Building Code and Bangladesh Fire Service and Civil Defense during construction. To prevent violation of regulation strict inspection and actions are required from corresponding authority. The good practices of fire hazard prevention in the building codes of other countries need to be studied and adopted according to Bangladesh's context. In addition, to create public awareness, workshops and seminars may be arranged. Electronic and printing media can play an important role for increasing awareness. A pragmatic fire safety plan may be developed for all the buildings with the help of Bangladesh Fire Service department.

## REFERENCES

- Bangladesh Fire Service and Civil Defense (BFSCD). (2003). *Fire Fighting & Extinguishing Law*.  
*Bangladesh National Building Code (BNBC)*. (2006). Published by HBRI-BIDS.
- AmeriCares. (n.d.). *Fire Prevention and Fire Safety: Health Worker Safety Training Module 5*. Retrieved October 11, 2014, from:  
<http://www.americares.org/assets/downloads/pdf/modules/hws/HWS-5-fire-safety.pdf>
- OSHCN. (2006). *Sample Written Program for Fire Prevention Plan*. Occupational Safety and Health Consultation Program (OSHCN), Texas Department of Insurance, Division of Workers' Compensation, Publication No. HS03-013A (1-06). Retrieved October 11, 2014, from:  
<http://www.tdi.texas.gov/pubs/videoresource/ofirepreventio.doc>
- EHSS. (2011). *Fire Prevention Planning*. Environmental, Health and Safety Services (EHSS), Virginia Polytechnic Institute and State University. Retrieved October 11, 2014, from:  
[http://www.ehss.vt.edu/uploaded\\_docs/200802261709470.Fire%20Prevention%20Planning.ppt](http://www.ehss.vt.edu/uploaded_docs/200802261709470.Fire%20Prevention%20Planning.ppt)
- UoC. (2005). *Basic Fire Prevention Measures*. Environmental Health and Safety, Division of Agriculture and Natural Resources, University of California, Safety Note #72. Retrieved October 11, 2014, from:  
<http://safety.ucanr.org/files/1468.pdf>
- Margentino, M. R., & Malinowski, K. (1992). *Fire prevention and safety measures around the Farm*. Rutgers Cooperative Extension, University of New Jersey: document FS608. Retrieved October 11, 2014, from:  
[http://nasdonline.org/static\\_content/documents/1048/d000843.pdf](http://nasdonline.org/static_content/documents/1048/d000843.pdf)

- HSE. (2012). *Guidance on the prevention and control of fire and explosion at mines used for storage and other purposes*. Great Britain: Health and Safety Executive (HSE). Retrieved October 11, 2014, from: <http://www.hse.gov.uk/mining/festorage.pdf>
- Beall, C. (1994). Calculating Masonry's Fire Resistance. *Mag. Masonry Constr.*, 7(8), 372-391. Retrieved 24 November, 2014 from:  
[http://www.masonryconstruction.com/Images/Calculating%20Masonry%27s%20Fire%20Resistance\\_tcm68-1375295.pdf](http://www.masonryconstruction.com/Images/Calculating%20Masonry%27s%20Fire%20Resistance_tcm68-1375295.pdf)
- Brick Industry Association. (2008). Technical Note 16: Fire Resistance of Brick Masonry. Brick Industry Association, Reston, Virginia. Retrieved 24 November, 2014 from:  
<http://www.gobrick.com/portals/25/docs/technical%20notes/tn16.pdf>
- FLIR. (2011a). Thermal Imaging Guidebook for Building and Renewable Energy Applications. FLIR Systems AB.
- FLIR. (2011b). Thermal Imaging Guidebook for Industrial Applications. FLIR Systems AB.
- Haidar, A., Asiegbu, G. O., Hawari, K., & Ibrahim, F. A. (2012). Electrical defect detection in thermal image. *Advanced Materials Research*, 433, 3366-3370. Retrieved 24 November, 2014 from:  
<http://ro.uow.edu.au/infopapers/2315/>
- Taib, S., Jadin, M., S., & Kabir, S. (2012). Thermal Imaging for Enhancing Inspection Reliability: Detection and Characterization. In Prakash R., V. (Ed.). *Infrared Thermography*. InTech, ISBN: 978-953-51-0242-7. Retrieved 24 November, 2014 from:  
<http://www.intechopen.com/books/infrared-thermography/thermal-imaging-forenhancing-inspection-reliability-detection-and-characterization>



**BANGLADESH NETWORK  
OFFICE FOR URBAN SAFETY**



## **PART-VI**

# **SEISMIC MICROZONATION OF COX'S BAZAR MUNICIPAL AREA BANGLADESH**

**BANGLADESH NETWORK OFFICE FOR URBAN  
SAFETY (BNUS), BUET, DHAKA**

**Prepared By: Afifa Imtiaz**

**Mehedi Ahmed Ansary**

## 1. INTRODUCTION

Cox's Bazar Municipal is located in the Southeastern part of Bangladesh, beside the Bay of Bengal under the district Cox's Bazar. The area is famous for her outstanding natural beauty. The district has an area of 2491.9 sq km with a population of 1.8 Million (BBS, 2001). Cox's Bazar municipality covering an area of 6.85 sq. km is located at 21.58°N, 92.02°E. Cox's Bazar falls in zone 2 with a seismic coefficient of 0.15g. Recent earthquakes in adjoining areas of Cox's Bazar indicate a warning that the people of that area should take adequate measures against earthquakes.

Anbazhagan and Sitharam (2010) presented seismic site classification using boreholes and shear wave velocity and assessed the suitable method for shallow engineering rock region. Islam and Hossain (2010) estimated liquefaction potential of selected reclaimed areas of Dhaka city based on standard penetration test and shear wave velocity. Motazedian et al. (2011) applied four different seismic methods which were down hole interval vs. measurements at 15 borehole sites, seismic refraction–reflection profile measurements for 686 sites, high-resolution shear wave reflection “landstreamer” profiling for 25 km in total, and horizontal-to-vertical spectral ratio (HVSr) of ambient seismic noise to evaluate the fundamental frequency for ~400 sites for development of a Vs30 (NEHRP) map for the city of Ottawa, Ontario, Canada. Louie et al. (2011) made earthquake hazard class mapping by Parcel in Las Vegas Valley which included more than 10,000 measurements that classify individual parcels on the NEHRP hazard scale. Another earthquake hazard class mapping by Parcel was made by Louie et al. (2012) which included 10,721 surface-wave array measurements that classify individual parcels on the NEHRP hazard scale. Cox et al. (2012) worked on frozen and unfrozen shear wave velocity seismic site classification of Fairbanks, Alaska which was based on 59 shear wave velocity (Vs) profiles collected using the spectral analysis of surface waves (SASW) method. Mohanty and Patra (2012) assessed liquefaction potential of pond ash at Panipat in India using SHAKE2000 where the liquefaction analysis of pond ash was carried out by using Seed and Idriss method and 1-D ground response analysis. Irfan et al. (2012) worked on local site effects on seismic ground response of Dubai-Sharjah metropolitan area where dynamic properties of selected soil profiles were evaluated using empirical relations between Standard Penetration Test (SPT) N-values and shear wave velocity (Vs). Manne and Satyam (2013) estimated the local site effects using microtremor testing in Vijayawada city, India where microtremor surveys were carried out at 75 different locations in the Vijayawada urban area and analysis was carried out using the Nakamura technique. Natural Resources Canada (NRCan) (2013) adapted Hazus for seismic risk assessment in Canada which was a standardized best-practice methodology developed by the US Federal Emergency Management Agency (FEMA) for estimating potential losses from common natural hazards, such as earthquakes, floods, and hurricanes. Thaker and Rao (2014) worked on seismic hazard analysis for urban territories at Ahmedabad region in the state of Gujarat, India where earthquake data has been analyzed statically and the seismicity of the region is evaluated by defining 'a' and 'b' parameters of the Gutenberg-Richter relationship. Desai and Choudhury (2014) worked on deterministic seismic hazard analysis for Greater Mumbai, India where the seismic sources were identified from the seismotectonic atlas of India within the control region of 300 km radius around Mumbai City and the epistemic uncertainty involved in estimation of different input parameters was accounted within a logic tree framework. Sil and Sitharam (2016) researched on detection of local site conditions in Tripura and Mizoram using the topographic gradient extracted from remote sensing data and GIS techniques where Peak Ground Acceleration (PGA) at the bedrock for the states of Tripura and Mizoram in NE India was estimated using Probabilistic Seismic Hazard Analysis (PSHA), which considered linear sources and events (from 1731 to 2010) with appropriate ground motion prediction equations applicable for NE India.

In this study, for microzonation purposes, bore holes with SPT data and historical large earthquakes were used as scenario events. From attenuation laws, Peak Ground Acceleration (PGA) in the bedrock level was estimated and used to develop a regional combined seismic hazard map based on site liquefaction, amplification and slope stability.

## 2. GEOLOGY OF THE AREA

Cox's Bazar town is located at the Middle-West part of the district bounded by the Bakkhali River on the North and North-East. The area lies within the Eastern flank of Inani Anticline, trending towards NNW-SSW, whose Western Flank is eroded. The existing Eastern Flank of the anticline is also in the process of continuous erosion. Figure 1 shows the Surface Geology of Cox's Bazar Municipal area according to the Geological Map of Bangladesh (Alam et al., 1990). The Western Figure reveals that the area around the city of Cox's Bazar predominantly composed of Valley Alluvium and Colluvium and Dihing Formation of Pliocene-Pleistocene age. Rocks of the Pliocene, Pliocene and Neogene ages are also exposed in the area. The exposed rock units are mostly

have been observed from the Geological Map of Bangladesh. To the west of the Municipal Boundary, the strand of coastal Deposit, Beach and Dune Sand, lies extending towards south. To the East of Beach and Sandstone, there lies another narrow zone of Boka Bil Formation of Neogene age. A slight narrow zone Tipam Sandstone of Neogene age forms the Eastern side of BokaBil zone. Along the East of Tipam Sandstone zone, another formation of Bedrock from Tipam Group that is Girujan Clay of Pleistocene and Neogene age lines. The North Eastern boundary of the town consists of Alluvial Deposits of Valley Alluvium and Colluvium. The south eastern part of the town has basically Dihing Formation Bedrock which is characterized as yellow to yellowish-grey, massive, fine to medium grained poorly consolidated sandstone and clayey sandstone. Dupi Tila Formation of Pleistocene and Pliocene age lies to the south of Dihing Formation which might have a slight influence in the surface geology of the city. Dupi Tila is characterized as yellow to ochre, pink, light-brown, light-grey to grayish-white or bluish-grey sandstone, siltstone and conglomerate.

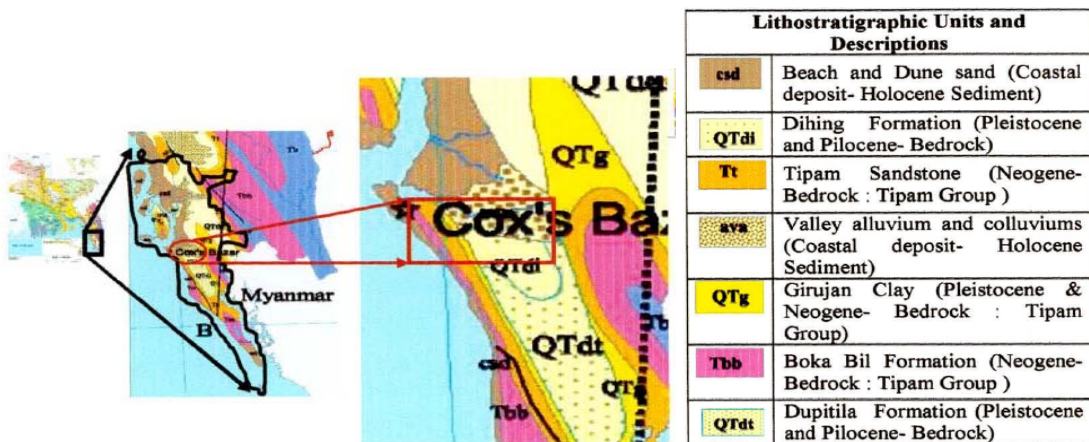


Figure 1: Geology of Cox's Bazar Municipal (after Alam et al, 1990)

### 3. SEISMOTECTONIC SETUP

The generalized tectonic map of Bangladesh and adjoining areas is given in Figure 2. The junction between the platform and the fore deep running southeast from Mymensingh to Calcutta (the Hinge line) is considered to be a zone of weakness. Some major earthquakes can be related to the Dauki fault which terminates the fore deep in the Northeast. Most recorded earthquakes had epicenter further East in Burma. The Himalayan arc can be regarded as one of the most intensely active seismic regions in this area. In Northeast India, the Shillong plateau and adjacent syntax is between the two accurate structures are one of the most unstable regions in the Alpine-Himalayan belt. Earthquake data suggest that the basement of the Indian plate below the Indo-Burma ranges is moving north. Thus the shortening in the overlying rocks is partly decoupled from the basement. The Main Boundary Thrust (MBT) fault initiated in late Miocene or Pliocene time is regarded as the present thrust front of the Himalayas and forms the northern margin of the Himalayan foredeep. Bengal Basin is bounded on the East by the western fold belt of the Indo-Burma ranges. The northern and the Central portion of this fold belt are seismically active. Tripura fault zone is characterized by the high concentration of earthquake events. A number of

morphotectonic lineaments have been identified. Among these the Kopili lineament trending NW-SE is remarkable. At the north of this zone Halflong-Dissang thrust is present. Morphotectonic lineaments around the Halflong-Dissang thrust zone trend NE-SW, E-W and NW-SE. Mikir hill is present to the northeast corner of the Halflong-Dissang thrust, which separates the Shillong plateau by Kopili fault.

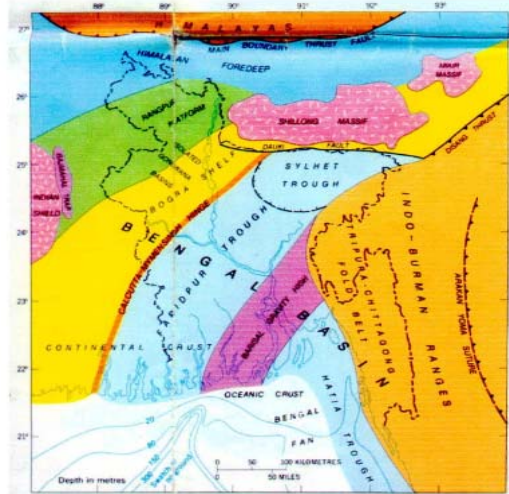


Figure 2: Generalized tectonic map of Bangladesh and adjoining areas (after GSB, 1991)

#### 4. REGIONAL TECTONICS

According to Molnar and Tapponier (1975), for the past 40 million years the Indian subcontinent has been pushing northward against the Eurasian plate at a rate of 5 cm/year, giving rise to the severest earthquakes and most diverse land forms known. Figure 3 shows continued drift of the Indian plate towards the Eurasian plate. Recently, Bilham et al. (2001) pointed out that there is high possibility that a large earthquake may occur around the Himalayan region based on the difference between energy accumulations in this region. There is a seismic gap that is accumulating stress, and a large earthquake may occur some day when the stress is relieved. Figure 3 shows the estimated slip potential along the Himalaya. The major earthquakes that have affected Cox’s Bazar area are presented in Table 1.

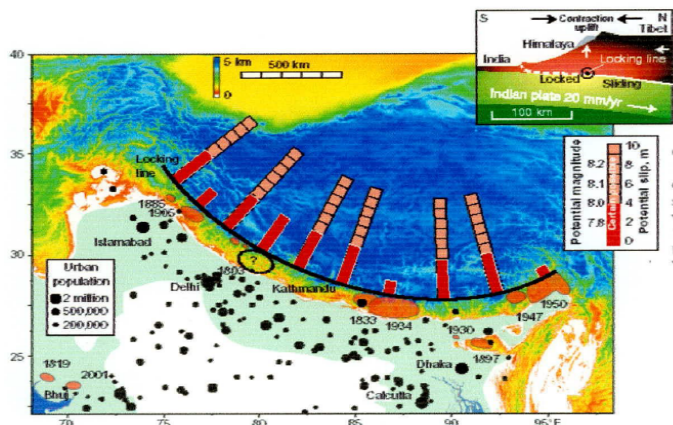


Figure 3: Estimated slip potential along the Himalaya (after Bilham et al., 2001)

## 5. DATA COLLECTION

A total of 26 borelogs were used in this study. SPT were carried out in each boring at nominal 1.5 m intervals to study site amplification as well as soil liquefaction potential characteristics of municipality area. Among them, twelve subsoil investigations were carried out by the first author (Imtiaz, 2009). The other fourteen borelogs up to a depth of 30 meters were collected from a research project on Cox's Bazar District (Dhar et. al. 2008). Figure 4 shows 26 borehole locations.

Table 1: Large earthquakes in and around Cox's Bazar

Year	Name	Epicentre	Magnitude (M)
1762	Arakan Earthquake	50 km northwest of Cox's Bazar	8.5
1858	Prome Earthquake	Sandaway, Myanmar	7.0
1912	Mandalay Earthquake	Sagaing, Myanmar	7.7
1956	Sagaing Earthquake	Sagaing, Myanmar	7.1
1997	Bandarban Earthquake	Ruma, Bandarban	6.0
1999	Moheskhal Earthquake	Moheskhal Island	5.1

At entire area under Cox's Bazar Municipality necessary data such as subsoil reports and geology, topography etc was collected from different relevant sources. The GPS locations of all the borehole investigation points and hill soil samples have been presented on the digitized municipality map and were saved in MS Excel. For assessment of landslide potential Geological Map and Aerial Photograph were not available in the concerned authorities' office considering this limitation this study was carried out.

For slope stability analysis, hilly regions of this area have been surveyed and data of location, height, and slope have been collected (see Figure 5). Where eleven disturbed samples from different locations of the municipal area were collected for laboratory investigations including specific gravity test, grain size analysis, Atterberg limits, Standard compaction test and direct shear test.

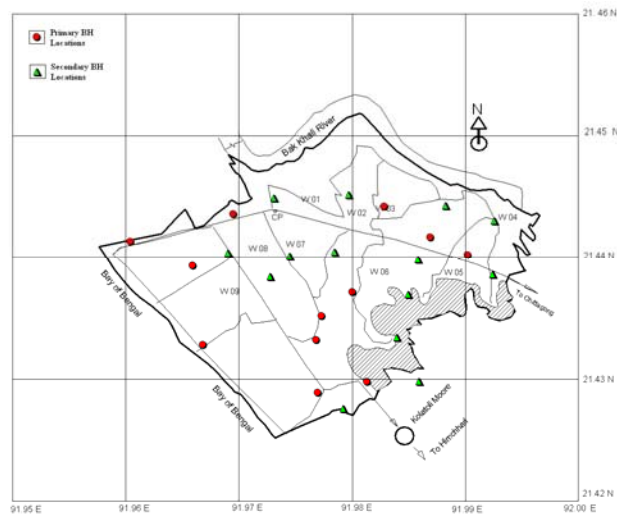


Figure 4: Cox's Bazar municipal area map showing soil borehole locations

## 6. ASSESSMENT OF SEISMIC HAZARD

The first step in reducing the risk of the society from earthquake hazard is the assessment of the hazard itself. Seismic microzonation map for strong-ground shaking, liquefaction, and landslide can play a significant role in mitigating the effects of earthquake in urbanized regions. The seismic hazard evaluation at a specified site depends upon the definition of the following four models:

**Earthquake source model:** It is based on geological evidence, Seismic sources are identified and modelled as a point, line, area or dipping plane. In this study, a point source model is used.

**Seismicity model:** The seismicity of each of the modeled sources is first determined from past data available. The recurrence relationship relating the size of the past events in terms of Magnitude (M) and Peak Ground Acceleration (PGA) is derived, the seismicity model used in Molas and Yamazaki (1994) is usually taken as

$$\log(v) = a + b * M \quad (1)$$

$$\log(v) = a + b * \log(y) \quad (2)$$

Where M is the earthquake magnitude and y is the peak ground acceleration. v is occurrence rate per year and a and b are regression constants. These relations can be written as

$$M = (-\log(T) - a) / b \quad (3)$$

$$\log(y) = (-\log(T) - a) / b \quad (4)$$

where  $T (=1/v)$  is the return period in years. Thus, the above equations represent magnitude and the peak ground acceleration for a return period of  $T$  years.

**Attenuation model of ground motion:** This describes the transfer of ground motions from the source to a particular site as a function of magnitude, distance and soil conditions. Here, the peak ground acceleration is used to characterize the ground motion; the attenuation law is in the form

$$\log(y) = b_1 + b_2 (Ms) - b_3 \log(r) - b_4(r) \quad (5)$$

where,

$$r^2 = d^2 + h^2,$$

$r$  = the hypo central distance (km),

$d$  = the epicentral distance (km),

$h$  = the focal depth and  $Ms$  is the surface-wave magnitude.

The attenuation law is required to determine the peak ground acceleration at the site for different events and then to determine the regression constants  $a$  and  $b$ .



## 6.1 Selection of Attenuation Law for Peak Ground Acceleration

To select the most suitable attenuation law for predicting rock motions, the formula adopted in the previous studies were followed (Sabri 2001, Sharfuddin 2001). From these studies, it was found that McGuire (1978) as well as Joyner and Boore (1981) equations follow the PGA trend of most large earthquakes in and around Bangladesh. Since, McGuire equation was already used for Bangladesh for seismic hazard analysis (Sharfuddin, 2001) and due to its simple form, it was selected for further use. The attenuation laws for rock used in this study, are presented below:

$$\text{PGA (from McGuire)} = 0.0306e^{0.89M}r^{-1.17} \quad (7)$$

$$\text{PGA (from Joyner \& Boore)} = 0.0955e^{(5.73M)}d^{-1}e^{(0.0058)h} \quad (8)$$

Where,

M = Earthquake Magnitude,

d = Epicentral Distance,

r = Hypocentral Distance and

h = Depth

## 6.2 Regression Analysis

Seismic parameter b was evaluated from G-R relationship (Gutenberg and Richter, 1944), a method utilizing extreme, instrumented and complete catalogs. Linear regression was applied to each site which is taken as the centre of an area of 250 km radius where past earthquakes are likely to occur again. The hazard curves of Mean Annual Rate of Exceedance ( $\nu$ ) versus Peak Ground Acceleration (PGA) and Mean Annual Rate of Exceedance ( $\nu$ ) versus Earthquake Magnitude (M) were generated at the rock levels. The hazard in terms of the rock level PGA values and probable earthquake magnitude corresponding to return periods of 200 years are quantified from equation 3 and 4 as, 0.18g and 8.3 consecutively. Since the largest Magnitude earthquake around the 350-450 km radius of the study area exceeds 7.9 and around 250 km radius is 6.5, a cut-off Magnitude of 7.5 earthquake was considered as the expected one in 200 years return period and thus used for further analyses.

## 7. SITE AMPLIFICATION ANALYSIS

For site amplification, in this study, the engineering bedrock was assumed to be the layer at which the shear wave velocity ( $V_s$ ) exceeds 400 m/s, which exist almost 30 m deep from the surface of the study area. The calculations show that the shear wave velocities at bedrock level vary from 400 m/s to 500 m/s. Vibration characteristics plotted as transfer functions at different points of the study area were estimated by employing one dimensional wave propagation program SHAKE. The computations were made in the frequency range 0 to 20 Hz at frequencies every 0.05 Hz interval. The loss of energy of seismic waves in the soil layers was also considered. The computed results from the site amplification potential analysis were exported to a GIS environment for further processing and visualization. They were classified into different classes according to the extent of amplification factors and plotted on the Cox's Bazar municipal map (see Figure 7).

From the site amplification study, the average amplification factor was found to be 2.3 and 1.7 respectively for extreme and average conditions. The rock level PGA for return period of 200 years was estimated as 0.18g. Thus the surface level PGAs calculated by multiplying the rock level PGA with amplification factor were 0.4g at extreme condition and 0.31 g considering AHSA.

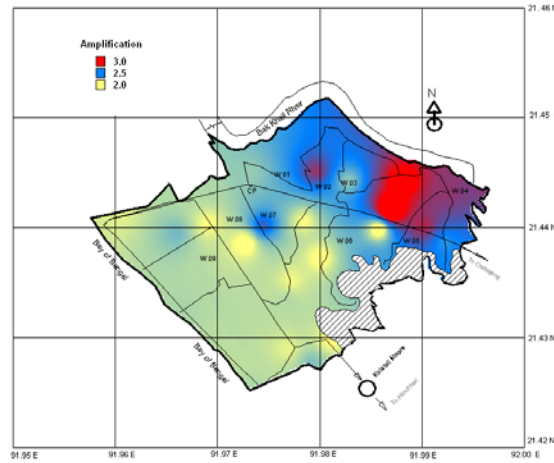


Figure 7: Microzonation map based on amplification at fundamental frequencies

## 8. LIQUEFACTION ANALYSIS

The first step in calculation of liquefaction potential is to determine whether the soil has the potential to liquefy during the earthquake. This analysis is usually carried out by using simplified empirical procedure, originally developed by Seed and Idriss (1971). Since the largest earthquake magnitude has been considered as 7.5, the relevant Magnitude Scaling Factor (MSF) was selected as 1.0. The Factor of Safety against Liquefaction for earthquakes other than that of magnitude 7.5 and calculated as

$$FS = FL \frac{CRR_{7.5}}{CSR} MSF \quad (9)$$

Where,

CRR<sub>7.5</sub>= Cyclic Resistance Ratio for the earthquake of magnitude 7.5

CSR= Cyclic Stress Ratio

The severity of foundation damage caused by soil liquefaction depends to a great extent on the severity of liquefaction, which cannot be evaluated solely by the FL. Liquefaction under the following condition tends to be severe:

1. The liquefied layer is thick
2. The liquefied layer is shallow
3. The FL of the liquefied layer is far less than 1.00

In this method, the factor of safety values, FL (Seed and Idriss, 1971) against resistance to liquefaction have been computed up to top 20 meters depth for all the boreholes and these values have been subsequently converted into liquefaction potential index (IL) given by the following equation (Iwasaki et al., 1982):

$$IL = \int_0^{20} F(z)w(z)dz \quad (10)$$

Where,

$$F(z) = (1 - FL); \quad \text{for } FL \leq 1.0$$

$$F(z) = 0; \quad \text{for } FL > 1.0$$

$$W(z) = (10 - 0.5z); \quad \text{for } z \leq 20 \text{ m}$$

$$W(z) = 0; \quad \text{for } z > 20 \text{ m}$$

The value of liquefaction potential, IL indicates that a soil mass is susceptible to liquefaction if  $IL > 0$ . If the value of IL is large, the soil is very susceptible for liquefaction. Severity of liquefaction is then expressed as shown below:

- IL = 0; No liquefaction
- = 0-5; Low liquefaction
- = 5-15; Moderate liquefaction
- = >15; High liquefaction

IL has been used to express the measure of liquefaction potential for a particular location and for further zonation of the area based on a particular range of this index. Table 2 shows the interpretation of liquefaction potential in terms of intensity and ground susceptibility.

Table 2: Summary of the liquefaction potential index (after Iwasaki et al., 1986)

Liquefaction Potential	Criteria	Explanation
High	$15 < IL$	Ground Improvement is indispensable
Moderate	$5 < IL \leq 15$	Ground Improvement is required. Investigation of important structure is indispensable
Low	$0 < IL \leq 5$	Investigation of Important structure is required.
Very low	$IL = 0$	No measure is required.

Liquefaction resistance factor, FL, for the top 20 m of soil, and the resulting liquefaction potential IL for the 26 sites was calculated. The flow chart of liquefaction analysis used in this study and the result of Liquefaction potential was provided in tabulated form. The computed results from the liquefaction potential analysis were exported to a GIS environment and plotted on the Cox's Bazar district map dividing the study area into different zones according to the ranges of liquefaction potential index values (Table 2). Thus microzonation maps were developed for liquefaction potential as shown in Figure 8.

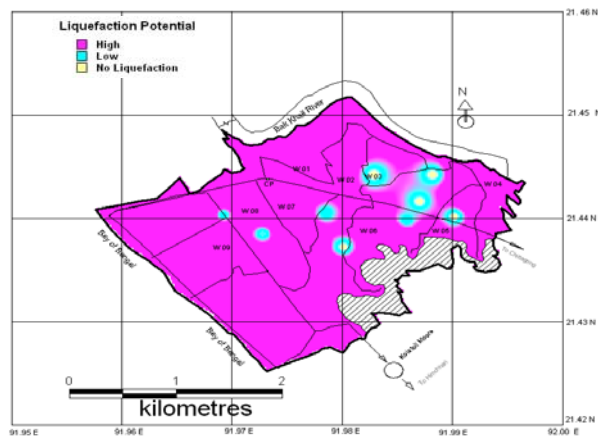


Figure 8: Microzonation map based on regional distribution of liquefied areas

## 9. LANDSLIDE POTENTIAL ANALYSIS

The overall stability failure mechanism is development of slip circles resulting in deep sliding surface which is a conventional soil mechanics stability problem. Preexisting slip planes within the soil, cracker material can have a significant effect on slope stability. Stability analysis is carried out to evaluate the factor of safety against bearing capacity failure. The program used for stability analysis is XSTABL which is a fully integrated slope stability analysis program. The landslide potential was categorized as 'high' and 'low' for Factor of Safety being greater than or equal to 1.2 and less than 1.2 consecutively. The corresponding Factor of Safety values have been exported to GIS and plotted on the Cox's Bazar municipality range. Thus the microzonation map based on landslide potential was developed as shown in Figure 9.

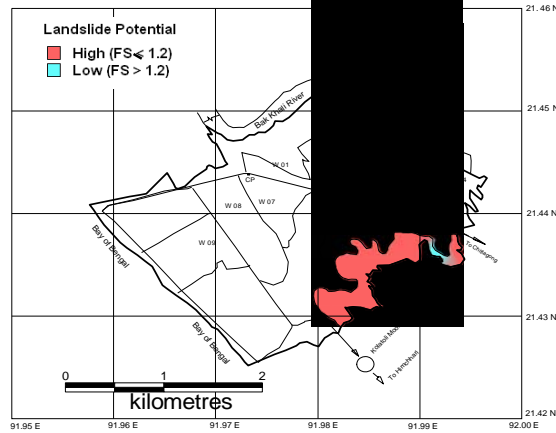


Figure 9: Microzonation map based on landslide potential in Cox's Bazar Municipality area

## 10. SEISMIC HAZARD INTEGRATION

The most important endeavor of this study was the estimation of seismic hazards linked with the local site attributes of soil amplification, liquefaction, and landslide and then integrating them in such a manner so that a reflection of probable actual disaster consequences can be represented. It is not feasible to resolve how much of the potential hazard is discretely attributed by each local site effect; consequently the ultimate regional seismic hazard distribution is established on a weighted average combination of the hazards related with each effect.

The rules for combining the various hazards were based on expert opinion (Stephanie and Kiremidjian, 1994) about the relative accuracy of the hazard information and the behavior of the local geology. It was assumed that the final combined seismic hazard would be quantified in terms of Modified Mercalli Intensity (MMI). At the end, different possible hazards were integrated to investigate the combined effects of more than one hazard. The results of the combined hazard analysis were summarized in Table 3.

Table 3: Final Combined Intensity and affected areas for different hazard combinations

Combined Intensity (MMIF)	Combination of Possible Hazards	Area (%)
X	2.0 times Amplification + High Liquefaction	43.12
	2.5 times Amplification + High Liquefaction	35.40
	3.0times Amplification + High Liquefaction	7.72
	2.0 times Amplification + High Landslide	1.65
		6.25

2.5 times Amplification + High Landslide		
IX	2.5 times Amplification + Low Liquefaction	0.93
	3.0 times Amplification + Low Liquefaction	2.75
	2.5 times Amplification + Low landslide	0.23
VIII	2.0 times Amplification + Low Liquefaction	1.95

## 11. CONCLUSION

This study proposed a methodology for seismic hazard assessment for Cox's Bazar, Bangladesh. In this study, seismic microzonation maps were developed on the basis of potential of earthquake occurrences and ground susceptibility to earthquake. SPT data from 26 boreholes were used to study site amplification as well as soil liquefaction potential characteristics. Using historical seismicity records and attenuation laws of Peak Ground Acceleration (PGA), the bedrock PGA was estimated as 0.18g for magnitude 7.5 earthquake with 200 years return period. The surface PGA was calculated as 0.41g and 0.31g adopting on First Peak Amplification and Average Horizontal Spectral Amplification, respectively. The liquefaction potential of the boreholes points were assessed by including these PGAs. Landslide potential was assessed using a slope stability program. The results obtained from these three analyses, were developed in GIS environment and were presented in the form of microzonation maps. The final combined hazard ( $MMI_F$ ) is computed as a weighted sum of those three hazards.

## 12. REFERENCES

- Alam M.K., Hasan A.K.M. and Khan M.R. (1990) Geological Map of Bangladesh, Geological Survey of Bangladesh, Govt. of the People's Republic of Bangladesh.
- Anbazhagan, P. and Sitharam, T. (2010) "Seismic Site Classification Using Boreholes and Shear Wave Velocity: Assessing the Suitable Method for Shallow Engineering Rock Region". *GeoFlorida 2010*, pp. 1059-1068.
- Ansary, M.A., Hussaini, T.M.AI, Sharfuddin, M. and Choudhury, J.R. (1999) "Report on Moheshkhalī earthquake of July 22, 1999", Earthquake Engineering Series, Research report No. BUET/CE/EQE-99-01, Department of Civil Engineering, BUET, Dhaka, August, 1999.
- Ansary, M.A. (2009) Earthquake Database of Bangladesh. Unpublished Report. Department of Civil Engineering, BUET, Dhaka, Bangladesh.
- BBS (2001) Population Census 2001: Preliminary report, August, 2001. Statistics Division, Ministry of Planning, GOB.
- Bilham, R., V.K. Gaur and P. Molnar (2001) "Himalayan Seismic Hazard". *SCIENCE*. Volume 293.
- Cox, B., Wood, C., and Hazirbaba, K. (2012) "Frozen and Unfrozen Shear Wave Velocity Seismic Site Classification of Fairbanks, Alaska." *J. Cold Reg. Eng.*, 10.1061/(ASCE)CR.1943-5495.0000041, 118-145.
- Desai, S. and Choudhury, D. (2014) "Deterministic Seismic Hazard Analysis for Greater Mumbai, India". *Geo-Congress 2014 Technical Papers*: pp. 389-398. doi: 10.1061/9780784413272.038.
- Manne, A. and N. D. Satyam (2013) "Estimation of local site effects using microtremor testing in Vijayawada city, India". doi: <http://dx.doi.org/10.1680/geolett.13.00033>.
- Motazedian, J. A. Hunter, A. Pugin, H. Crow (2011) "Development of a Vs30 (NEHRP) map for the city of Ottawa, Ontario, Canada". *Canadian Geotechnical Journal*, 48(3): 458-472, 10.1139/T10-081.

- Dhar, A.S., Ansary, M.A., Imtiaz, A.B.A., and Saha, R., (2008) Earthquake Vulnerability Assessment of Cox's Bazar District, prepared for United Nations Office for Project Services (UNOPS).
- Gutenberg, B., Richter, C. F. (1954) "Seismicity of the earth and associated phenomena", 2nd Edition, Princeton, Princeton University press.
- Imtiaz, A. (2009) Seismic Microzonation Of Cox's Bazar Municipal Area', MSc. Engg. Thesis, Department of Civil Engineering. Bangladesh University of Engineering and Technology. Dhaka, Bangladesh.
- Irfan, M., El-Emam, M., Khan, Z., and Abdalla, J. (2012) "Local Site Effects on Seismic Ground Response of Dubai-Sharjah Metropolitan Area". GeoCongress 2012: pp. 1869-1878. doi:10.1061/9780784412121.192.
- Islam, M. and Hossain, M. (2010) "Earthquake Induced Liquefaction Potential of Reclaimed Areas of Dhaka City". Soil Dynamics and Earthquake Engineering: pp. 326-332. doi: 10.1061/41102(375)40.
- Iwasaki, T., Tokida, K., Tatsuoka, F. Watanabe, S., Yasuda, S. and Sato K, (1982) "Microzonation for soil liquefaction Potential using Simplified Methods". 3<sup>rd</sup> International Microzonation Conference, Proceedings, 1319-1329.
- Iwasaki, T. (1986) "Soil liquefaction Studies in Japan: State of the Art". Soil Dynamics and Earthquake Engineering, 5(1), 2-68
- Joyner, W.B., and D. W. Boore (1981) "Peak horizontal acceleration and velocity from strong motion recorded including records from the 1979, Imperial Valley, California, earthquake". Bull. Seism. Soc. Am., 71, 2011-2038.
- Stephanie, A. King, and Anne S. Kiremidjian, (1994) Regional Seismic Hazard and Risk Analysis through Geographic Information System, PhD Thesis, Stanford University, USA.
- Louie, J., Pullammanappallil, S., Pancha, A., and Hellmer, W. (2012) "Earthquake Hazard Class Mapping by Parcel in Las Vegas Valley". GeoCongress 2012: pp. 2746-2755. doi: 10.1061/9780784412121.281.
- Louie, J., Pullammanappallil, S., Pancha, A., West, T., and Hellmer, W. (2011) "Earthquake Hazard Class Mapping by Parcel in Las Vegas Valley". Structures Congress 2011: pp. 1794-1805. doi: 10.1061/41171(401)156.
- McGuire, R. (1978) "Seismic ground motion parameters relations". Journal of Geotechnical Division, ASCE, Volume 104, pp. 461 - 490.
- Mohanty, S. and Patra, N. (2012) "Assessment of Liquefaction Potential of Pond Ash at Panipat in India Using SHAKE2000". GeoCongress 2012: pp. 1829-1838. doi: 10.1061/9780784412121.188.
- Molas, G. I. and F. Yamazaki (1994) "Seismic macrozonation of the Philippines based on seismic hazard analysis". Journal of Structural Mechanics and Earthquake Engineering, JSCE, 489 (1-27), 59-69.
- Molnar, P. and P. Tapponier. (1975) "Cenozoic tectonics of Asia, effects of a continental collision". Science, Volume 189(8), pp. 419-426.
- Sabri, S. A., (2001) Earthquake intensity-attenuation relationship for Bangladesh and its surrounding region. M.Engg. Thesis, BUET, Dhaka, Bangladesh
- Seed, H.b. and Idriss, I.M. (1971) "Simplified Procedure for Evaluating Soil Liquefaction Potential". Journal of the Soil Mechanics and foundations Division, ASCE, 97(SM9), 1249-1273.
- Seed, H. B., and Idriss, L M., (1982) "Ground Motions And Soil Liquefaction During Earthquakes". Earthquake Engineering Research Institute. Oakland, California, Monograph Series, p. 13.

- Seed, H. B., I. M. Idriss and L Arango (1983) "Evaluation of liquefaction potential using field performance data". Journal of Geotechnical Engineering. Volume 109, No. 3, pp. 458-482.
- Sharfuddin, M. (2001) Earthquake Hazard Analysis for Bangladesh. M.Sc. Engg. Thesis, Bangladesh University of Engineering and Technology (BUET). Dhaka.
- Sil, A. and Sitharam, T. (2016) "Detection of Local Site Conditions in Tripura and Mizoram Using the Topographic Gradient Extracted from Remote Sensing Data and GIS Techniques." Nat. Hazards Rev.10.1061/(ASCE)NH.1527-6996.0000228, 04016009.
- Thaker, T. and Rao, K. (2014) "Seismic Hazard Analysis for Urban Territories: A Case Study of Ahmedabad Region in the State of Gujarat, India". Advances in Soil Dynamics and Foundation Engineering: pp. 219-228. doi: 10.1061/9780784413425.023.



## **PART-VII**

# **EARTHQUAKE RELATED RESEARCH AND ACTIVITIES IN BANGLADESH DURING THE LAST SIX YEARS (2010-2016)**

**BANGLADESH NETWORK OFFICE FOR  
URBAN SAFETY (BNUS), BUET, DHAKA**

**Prepared By: Mehedi Ahmed Ansary**

## 1. INTRODUCTION

In the recent past, Bangladesh has not suffered any damaging large earthquakes, but in the past few hundred years, several large catastrophic earthquakes struck this area. So far, all the major recent earthquakes have occurred away from major cities, and have affected relatively sparsely populated areas. This has limited the human casualty and the economic losses. However, the 1993 Killari and 2001 Gujarat earthquakes in India has amply demonstrated that inappropriate construction technology may lead to high casualty levels even for moderate earthquakes (Sinha and Goyal, 1994).

In 1897, an earthquake of magnitude 8.7 caused serious damages to buildings in the northeastern part of India (including Bangladesh) and 1542 people were killed. Recently, Berryman et al. (2014) pointed out that there is high possibility that a huge earthquake will occur around the Himalayan region based on the difference between energy accumulation in this region and historical earthquake occurrence (see Figure 1). More recently, Steckler et al. (2016) suggested that the presence of a locked mega thrust plate boundary under the Indo-Burman ranges represents an underappreciated hazard in one of the most densely populated regions of the world (see Figure 2). The population increase around this region is at least 50 times than the population of 1897 and cities like Dhaka, Kathmandu, Guwahati have population exceeding several millions. It is a cause for great concern that the next great earthquake may occur in this region at any time.

A strong earthquake affecting major urban centres like Dhaka, Chittagong, Sylhet may result in damage and destruction of massive proportions and may have very severe long-term consequences for the entire country. After the 1971 independence, most major urban centres of Bangladesh have grown tremendously due to unabated migration from the smaller towns and rural areas. As a result, the cities have developed in haphazard fashion with little consideration for proper town-planning norms. There is, consequently, a need to be prepared against all possible natural and man-made disasters that are likely to occur in Bangladesh. For this purpose, it is essential to have realistic understanding of the consequences of likely damage in major cities due to different disasters. This will permit rational planning of mitigation efforts in order to minimise effects of these disasters.

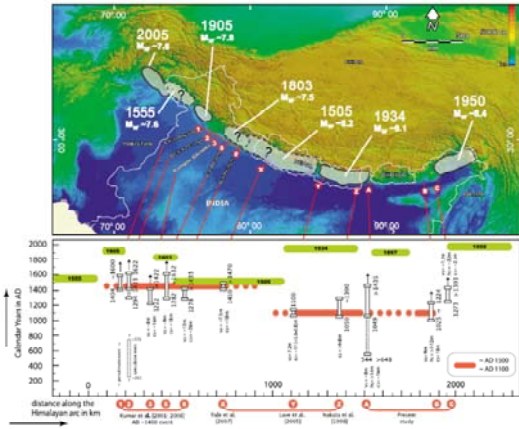


Figure 1: Synopsis of historical and paleoseismic history along the Himalayan Frontal Thrust (HFT) [after Berryman et al., 2014]

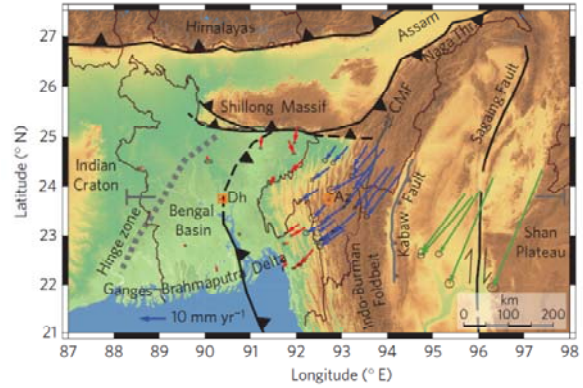


Figure 2: Topographic map of the Ganges–Brahmaputra Delta and Indo-Burman Fold belt showing GPS velocities (after Steckler et al., 2016)

The extent of damage to structures and casualty level due to an earthquake in the future can be reduced by the introduction of suitable mitigation measures. These mitigation measures can be categorized as structural and/or non-structural. The structural measures are those that directly influence the performance of building stock through strengthening of code provisions and the prevalent construction practice. Incorporating the appropriate structural mitigation measures can reduce the vulnerability of any building type. The non-structural mitigation measures include improvement in the state of awareness and preparedness before a disaster, land-use control and other government policies, and the infrastructure related to response following a disaster. The non-structural measures help to reduce the severity of casualty levels following an earthquake. In order to reduce the consequences of a major earthquake in the cities of Bangladesh, it is necessary that appropriate structural as well as non-structural measures be undertaken.

In this paper a brief summary of the activities and researches undertaken in the field of earthquake engineering in Bangladesh for the last six years have been presented. In an earlier publication, similar activities for two decades (1993-2013) have been published (Ansary, 2014).

## 2. BANGLADESH UNIVERSITY OF ENGINEERING & TECHNOLOGY (BUET)

Department of Civil Engineering, BUET offers postgraduate courses on Earthquake Engineering, Soil Dynamics, Structural Dynamics and Vibration Analysis. Until 1996, their

existed only two postgraduate theses linked with Earthquake Engineering. But after 1996, at least thirty more postgraduate theses related to this field were completed. Currently five students are pursuing their PhD and several more students are pursuing for their Master's thesis in the Department in Earthquake Engineering field. BUET has also undertaken research jointly with different local industry in the field of Geotechnical-Earthquake and Structural-Earthquake engineering fields (see Figures 3 and 4).

Recently, BUET with the help of Japanese government also established a new institute on Disaster Prevention and Urban Safety, named BUET-JIDPUS (see Figure 5).

### 3. GOVERNMENT AGENCIES

Disaster Management Bureau (DMB) was established with the help of UNDP and UNICEF in 1993. Although initially it was established to manage flood and cyclone, after the 1997 earthquakes in Chittagong and Sylhet region, Bureau started to train different government officials and volunteers about pre and post-earthquake preparedness and management techniques. For the last couple of years, Bureau conducted fifty or more earthquake training workshops in different regions of Bangladesh. In 2002, it also published a Disaster Management Training Manual. The second part of the manual has a complete chapter on Earthquake Training Module and Public Awareness Guidelines. Recently, under the Disaster Management Act 2012, DMB and DRR were merged to form a new Directorate called Department of Disaster Management (DDM).

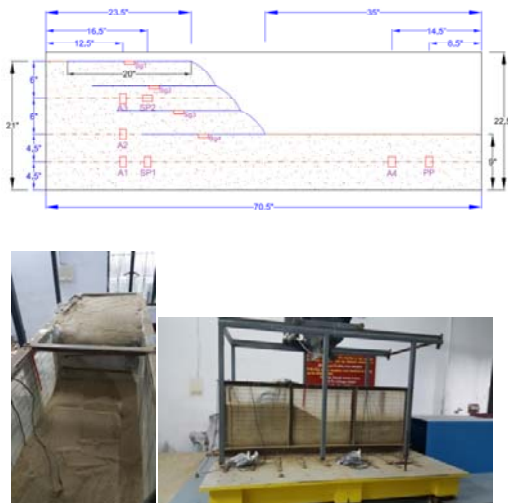


Figure 3: Shaketable test on sloped geotextile using Sylhet sand



Figure 4: Prototype models of Bangladeshi RCC structures to be tested on shaketable

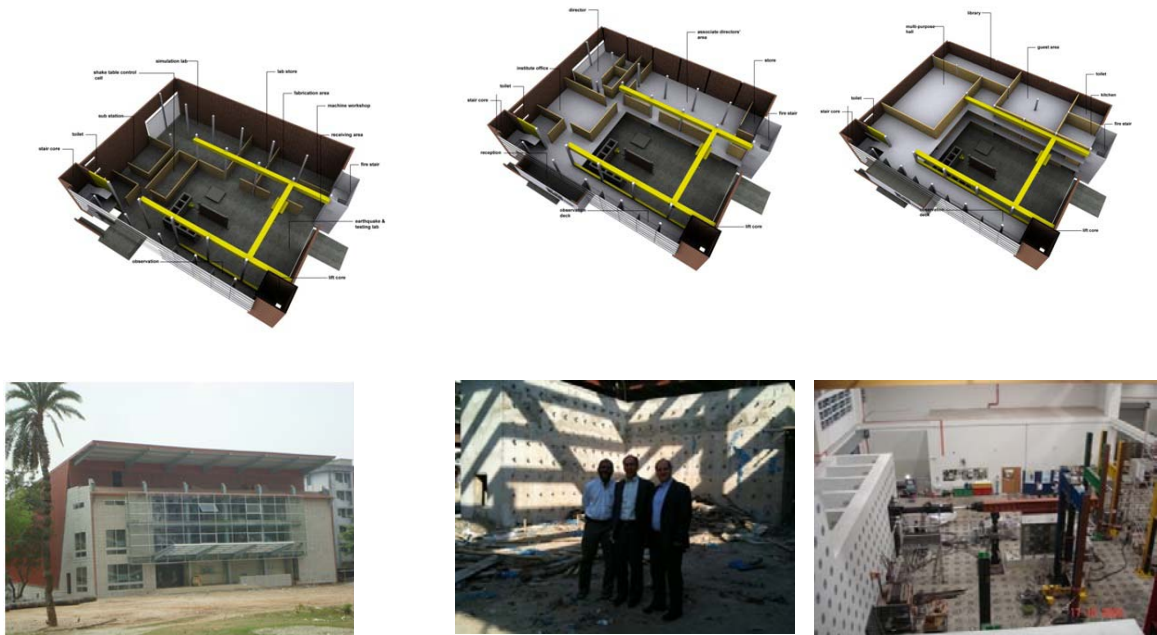


Figure 5: Floor plans and outside view of BUET-JIDPUS

The Ministry of Disaster Management & Relief (MoDMR) is currently working as the government coordinator for all activities regarding earthquake. Recently, they asked all the concerned ministries, departments and armed forces division to submit Contingency Plan regarding earthquake. The Ministry also compiled a list of available rescue and recovery equipment available in the country. Some recent publications, activities of the MoDMR and other government agencies are shown in Figures 6 to 12.

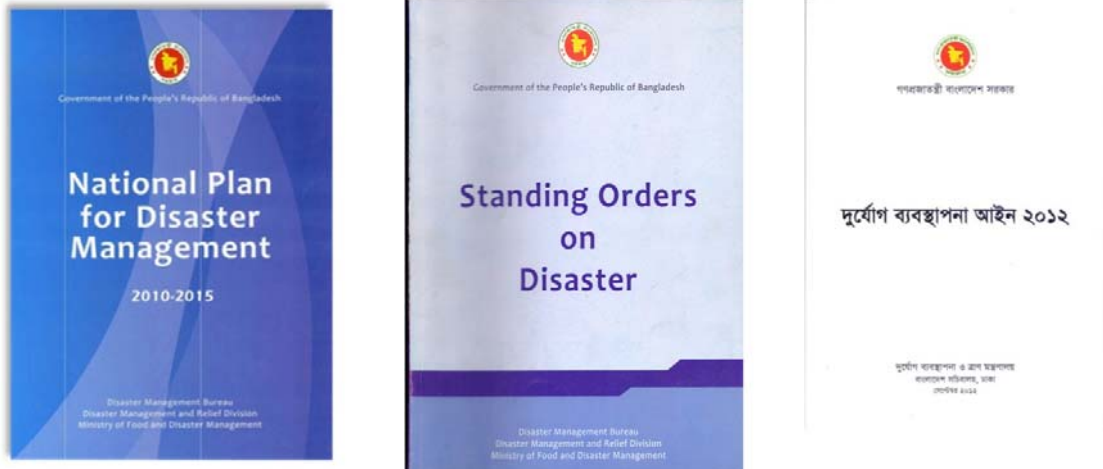


Figure 6: NPDM, Revised SoD and DM Act published by MoDMR

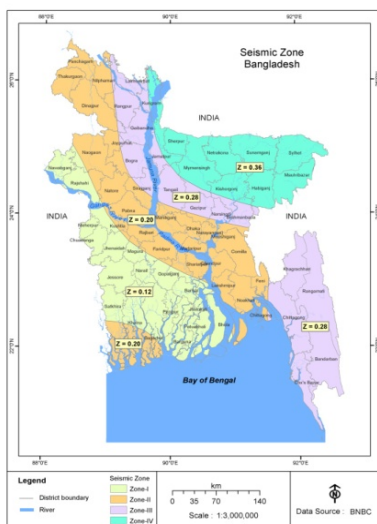
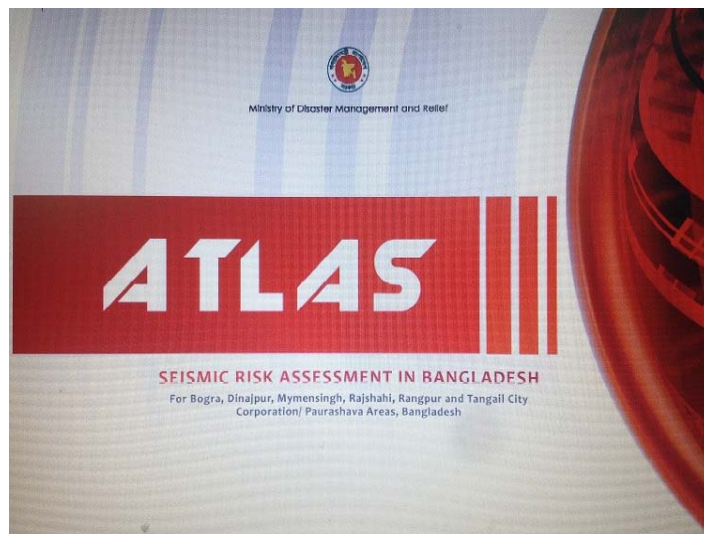


Figure 7: Proposed seismic zoning map of Bangladesh



2015

Figure 8: Vulnerability atlas for six cities of Bangladesh



Figure 9: Awareness raising rally and posters

CDMP Phase II (2010–14) builds upon and expands Phase I achievements by ensuring that the institutionalization of risk reduction and climate change adaptation occurs across all levels of government. The main tasks are:

Task-I : Seismic risk and damage assessments and subsequent development of scenario-based contingency planning for Rangpur, Dinajpur, Mymensingh, Tangail, Bogra, and Rajshahi municipalities/city corporations of Bangladesh

TaskII: Development of detailed building and infrastructures database of Dhaka and Chittagong City corporation areas



Figure 10: Training of urban volunteers



Figure 11: Training of masons and bar binders



Figure 12: Youth Campaign for earthquake preparedness

Task-III: Development of Ward level Spatial Contingency Plans for Dhaka, Chittagong and Sylhet City Corporation Areas in Bangladesh. The purpose of the plan is

- To support with immediate local response initiatives to save maximum number of lives in case of an earthquake emergency in the particular ward, with a goal of stabilizing the event within the first 72 hours.

Recently PWD completed a project funded by JICA. The overall goals are:

1. Retrofitting of public buildings including government building, hospital, fire station, school, shelter, etc. has been implemented. A retrofitted Fire Station at Tejgaon is shown in Figure 13.
2. Ministry of Housing and Public Works issues official license to the engineers upon completion of the training program introduced by the Project.
3. Manuals and the concepts prepared through the Project are incorporated in future edition of Bangladesh National Building Code (see Figure 14).

The “Urban Building Safety Project” is a US\$ 116 million investment, US\$ 100 million financed by JICA and US\$ 16 million by the Government of Bangladesh. The project aims to strengthen the building safety in Urban Cities by financing loans for building safety for private buildings through Participating Financial Institutions (PFI), and by improving the building safety for public buildings, thereby contributing to improvement of the social vulnerability of urban cities. Under this project, one new fire service headquarter building (see Figure 15) will be constructed, ten FSCD stations will be retrofitted and several RMG factories will get fund for retrofitting purposes.

The “Urban Resilience Project” is a US\$ 179.5 million investment, US\$ 173 million financed by the World Bank and US\$ 6.5 million by the Government of Bangladesh. The project aims to strengthen the capacity of Government of Bangladesh agencies to respond to emergency events and to strengthen systems to reduce the vulnerability of future building construction to disasters in Dhaka and Sylhet. The above two projects have been jointly launched by the Government of Bangladesh, JICA and WB on December 19, 2015.

Under the WB project, GEODASH (supported by Geonode) has been developed which is a Platform for Sharing of Earthquake Hazard and Vulnerability Data (see Figure 16).



Figure 13: Tejgaon fire station before and after retrofitting

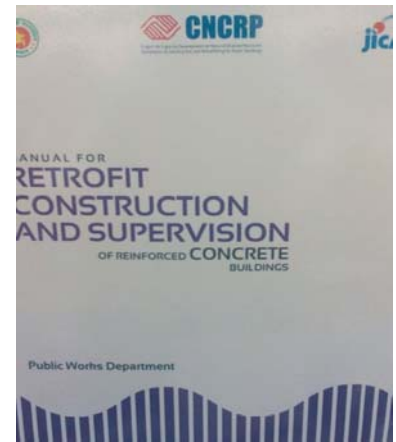


Figure 14: PWD published manuals



Figure 15: Proposed new FSCD Headquarter with base isolation technology funded by JICA

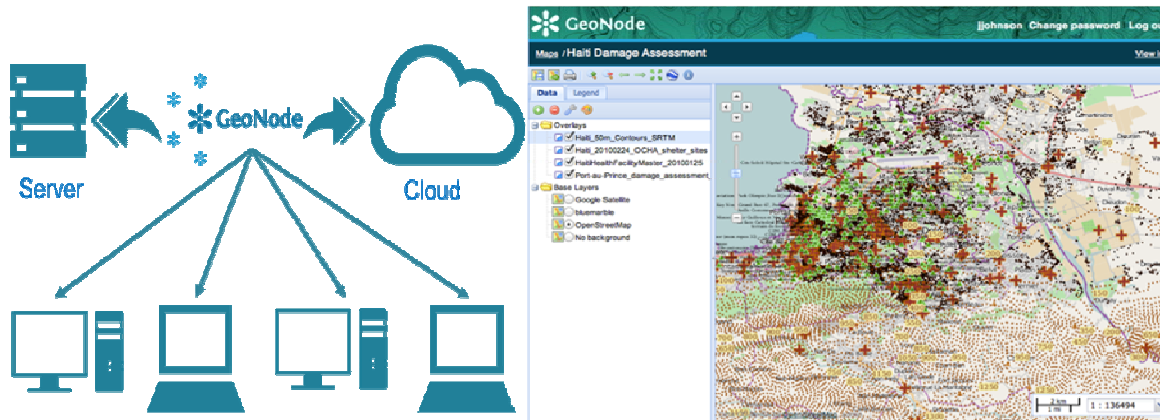


Figure 16: Geonode, a WB supported data sharing platform also used in Haiti damage assessment

Proposed Bangladesh Urban Resilience Project of WB: City-level actors are critical to the effort to develop resilient and livable cities in Bangladesh. This project seeks to create an enabling environment for coordinated, locally managed DRM. There are three core pillars of disaster resilience in urban settings, including: i) effective emergency management; ii) improving structural resilience through reduction of existing physical vulnerability; and risk sensitive land use planning and safe construction standards and practices to ensure sustainable growth.

A comprehensive approach to increasing urban resilience requires coordinated long-term investment across the three pillars. The Bangladesh Urban Resilience Project (BURP) would serve as the first in a series of interventions, which will initially focus on Pillar 1, to improve the critical capacity and infrastructure for emergency planning and response. The proposed project will also lay the foundations for subsequent investments in Pillars 2 and 3 by identifying key risks in the built environment and developing the practice of risk sensitive urban development.

With the key elements of effective urban response in place, future attention could then shift to reversing the trend of risk accumulation, and to increasing physical resilience through broader investments in priority sectors. Under this strategy, a second project would seek to further improve construction standards for future developments and reduce the existing physical vulnerabilities in Dhaka and major cities across Bangladesh. A third project could consider broader investment in priority sectors, for example critical facilities, water system, power system, transport, and construction of protective infrastructure.

The BURP consists of four main components that focus on emergency response and preparedness, establish an understanding of risk for critical facilities and essential facilities, support improvements in urban development and construction, and provide the institutional arrangements for implementation, monitoring and evaluation to ensure efficiency, transparency, and accountability in the implementation of project activities.

Component A: Reinforcing the Country's Emergency Management Response Capacity. There are several elements under Component A as follows:

- Creation of National Coordination Center and National Disaster Management Research and Training Center that will operationalize and sustain a program for well-coordinated emergency planning and response operations, and undertaken training, educational and awareness activities.
- Enhancement of the emergency management planning and response capability of the Fire Services and Civil Defense
- Building the emergency management capability along with establishing EoCs of the Dhaka City Corporations and Sylhet City Corporation (see Figure 17)



Figure 17: Examples of EoCs

Component B: Program on Assessment of Vulnerability of Critical and Essential Facilities. There are several elements under Component B as follows:

- Assessment of Vulnerability of Critical and Essential Facilities and Lifelines
- Data Sharing Platform to Support Risk-Sensitive Development

Component C: Improved construction, urban planning, and development. There are several elements under Component C as follows:

- Creation and Strengthening of URU

- Electronic Construction Permitting
- Professional Accreditation Program
- Building Code Enforcement

Component D: Project Implementation, Monitoring, and Evaluation.

In view of the recent earthquake trend in Southeast Asia, Directorate General of Health Services (DGHS), Government of the People’s Republic of Bangladesh, has undertaken an assessment to gain better understanding of the existing non-structural vulnerability of hospitals at upazila and district level in order for making the hospitals seismic resilient. Findings and recommendations from the assessment are believed to support DGHS to plan and stimulate efforts to reducing non-structural vulnerability to earthquake so that the hospitals continue to function and contribute to response and recovery process after an event of earthquake.

The assessment involved physical inspection of non-structural components of hospitals. The work is done on 15 hospitals (5 district hospitals and 10 upazila health complex) in the northern part of Bangladesh spread over active seismic Zone-One. Much importance provided in the selection of district and upazila hospitals to maximize representation of active seismic zone-one. The hospitals are located in Moulvibazar, Sunamganj, Lalmonirhat, Kurigram and Sherpur district. Depending upon the capacity, there are four types of hospital: 31 bed, 50 bed, 100 bed and 250 bed. The buildings of the hospitals are mostly RCC. A team comprised of six well trained data collectors dividing into three groups carried out the inspection of non-structural elements during 24 April – 15 May 2016.

#### **4. NON-GOVERNMENT AGENCIES**

In 2011-2012 fiscal years, six International NGOs (Action Aid, Concern Universal, Concern Worldwide, Islamic Relief Worldwide, Oxfam GB and Plan Bangladesh) represents consortium on disaster management called National Alliance for Risk Reduction and Response Initiatives (NARRI), Bangladesh and BNUS agreed to work on the following issues:

- Training module and resource material on Earthquake resistant construction developed for the training of
  - Civil engineers
  - Architect

- Masons and bar binders
- 30 number of civil engineers, 20 numbers of architects, 75 numbers of masons / bar binders are trained on earthquake resistant construction
- 01 number of shake table demonstration on February, 2012 at Dhaka followed by open discussion facilitated by relevant prominent experts in pre-identified schools, markets, high rise building etc.
- Structural safety (in view of Earthquake) assessment of 20 number of selected buildings are carried out with a concise report highlighting recommendations
- Review of existing Bangladesh National Building Code in view of Earthquake safety is conducted along with recommendations and documented Advocacy material and IEC on building codes are developed targeting general community residing in urban settings, Engineers / Architect, builders and policy makers
- 02 number of advocacy workshops / seminars are organised to advocate and promote at both Dhaka and Sylhet level
  - Enforcement of improved building codes / bylaws in view of Earthquake safety
  - Required changes in existing syllabus of undergraduate courses in civil engineering and architecture in view of seismic safe construction
  - Certification of engineers / architect and masons / bar binders trained on seismic safe construction \
  - Establishment of appropriate institutional arrangement to monitor implementation of building codes.

Under this project, A Manual for Architects, A Manual for Engineers, A Manual for Masons was developed. Also structural assessment of some selected schools of Sylhet city was carried out.

## **5. DISASTER MITIGATION IN BANGLADESH**

Bangladesh achieved remarkable success in managing frequently occurring hazards such as cyclones and floods. The country has a well-organized Cyclone Preparedness Plan (CPP), which boasts a volunteer list of around 44000. Even country like India and Sri-Lanka try to emulate CPP. To cope with the earthquake disaster a similar Earthquake Preparedness Plan (EPP) need to be implemented. Currently FSCD started training 62000 urban volunteers to enrich EPP.

For earthquake disaster mitigation professional as well as government solution is required. Architects, engineers, geologists, planners etc. will provide technical aspects and NGOs, mass media and social scientists will provide social aspects of professional solution. Builders, financial institutions, land developer would be required to support professional solution. Government agencies can help to implement professional solution through policymaking and policy enforcement. Government solution should clearly point out regulatory jurisdiction of each organization. For earthquake disaster mitigation following pre and post measures should be undertaken on an urgent basis.

#### **Awareness and capacity building**

- Increase public awareness through education (school children), earthquake drills, interactive website, mass-media, publication, training etc.
- Training of building inspectors, community leaders, construction workers and masons.
- Updating earthquake engineering course curriculum.

#### **Earthquake engineering research**

- Installation of free field accelerographs and seismographs for engineering and seismology studies.
- Seismic hazard assessment based on free field data and source models.
- Vulnerability assessments of structures using structural analysis and nondestructive testing.
- Develop laboratory and testing facilities.
- Development of indigenous and cheap retrofitting measures. Microzonation of urban areas based on different soil effects.
- Updating building code.

#### **Earthquake resistant construction**

- Legal enforcement of building code.
- Proper use of ductile steel and lateral force resisting systems.
- Building insurance to promote earthquake resistant construction.

- Retrofitting critical structures such as schools, hospitals and fire offices.
- Urban and regional planning to mitigate earthquake effects.

### **Post-earthquake response**

- Develop automatic safety shutdown system for electricity, gas, telephone and water supply system whenever the ground shaking exceeds a certain limit.
- Develop facilities for post earthquake search and rescue operation.
- Local people and organizations most effectively do rescue of victims because they are able to carry this out more quickly than outside agencies. Community based voluntary group should be trained who can actively participate in rescue operation just after an earthquake disaster.
- Prepare contingency plans.
- Coordination among different interest groups those will be involved in the post earthquake rescue effort.
- Arrangement of emergency medical treatment facilities for injured people.

### **REFERENCES**

- Ansary, M.A., 2014. Earthquake Related Research and Activities in Bangladesh during the last two decades, published by BSRM in June, 2014.
- Berryman, K., W. Ries, N. Litchfield, 2014. The Himalayan Frontal Thrust: Attributes for seismic hazard, Report produced in the context of the GEM Faulted Earth Project.
- Sinha, R. and Goyal, A., 1994. Damage to buildings in Latur earthquake, *Current Science* 67, 380-385.
- Steckler, M., Dhiman Ranjan Mondal, Syed Humayun Akhter, Leonardo Seeber, Lujia Feng, Jonathan Gale, Emma M. Hill and Michael Howe 2016. Locked and loading mega thrust linked to active subduction beneath the Indo-Burman Ranges, *Nature Geoscience* · July 2016.



## **PART-VIII**

# **USE OF JET GROUTING IN RETROFITTING OF A RMG FACTORY BUILDING IN CHITTAGONG, BANGLADESH**

**BANGLADESH NETWORK OFFICE FOR  
URBAN SAFETY (BNUS), BUET, DHAKA**

**Prepared By: Mehedi Ahmed Ansary**

## INTRODUCTION

The retrofit process is a general term that consists of a variety of treatments, including: preservation, rehabilitation, restoration and reconstruction (Kelley, 1996). When an existing building found potential for severe damage due to lack of capacity against various possible loading, is considered for retrofitting. Most of the structures built prior to 2000s in Bangladesh were typically not designed with proper details to perform adequately during earthquakes. While Details Engineering Assessment (DEA) conducted in several buildings, most of them have been found vulnerable against seismic load. Recent events like collapse of Rana Plaza in Bangladesh have increased the awareness among building owners as well as building users for various purposes. The seismic retrofitting design and construction have recently been initiated in Bangladesh for vulnerable buildings. In retrofitting, strengthening of all structural elements has been considered as per requirements and relevant deficiencies.

Jet grouting columns are frequently adopted in foundation engineering as an alternative to piles with the aim of strengthening weak subsoil and transferring loads to deeper and more competent strata (Modoni et al, 2010). Jet grouting, among all kind of soil improvement, has certainly acquired a special place due to its widespread use in all kind of soil and capability of giving convenient solutions to most geotechnical problems. Jet grouting technology can give practical and cost-effective solutions to a number of difficult situations, such as for excavation support, ground-water barrier, bottom sealing to prevent pollutants from entering excavations, protection of bridges against scour, stabilization of slopes and underpinning of existing foundations in commercial and industrial settings (Croce et al., 2014). It is commonly recognized that jet grout was first applied to soils by the Japanese in 1960's (Nakanishi 1974). The experience on the use of high-speed jets in late 1960s for cutting rock and rock-like materials (Farmer and Attewell, 1965) inspired a group of Japanese specialists to investigate their use as a ground improvement tool. They developed an idea of injecting fluid binders within previously drilled boreholes to erode and mix in place the soil. Chemical binders were used in the first patented version, known as the Chemical Churning Pile (CCP) (Miki 1973; Nakanishi 1974), but these products were soon replaced by water-cement grouts. In the subsequent decades, the technique has developed significantly and is now being widely used around the world. The CCP and Jet Grout methods came to the attention of European companies in general and Italian companies in particular on the occasion of the international competition on the methods for the stabilization of the Pisa Tower in the early 1970s (Croce et al., 2014). Currently, jet grouting is used all over the world (Ryjeski et al. 2009).

This paper presents the first ever use of Jet Grout in Bangladesh for retrofitting of an existing foundation of a four storied RMG building, situated in Chittagong Export Processing Zone, Bangladesh. Figure 1 shows the building before and after retrofitting. The building is a RC beam-column structural frame system and the structural configuration is regular in pattern. This building has been constructed in 2001. A DEA has recently been carried out by EIMS to ensure the serviceability of the building. After completion of the DEA, the building has been found structurally inadequate due to highly stressed conditions of several columns and existing mat foundation considering existing gravity and lateral loads as per Bangladesh National Building Code (HBRI, 1993). The report suggested preparing retrofitting design and construction of the building to sustain lateral load as per BNBC. When it comes to retrofitting design, preparing a constructible design is the main challenge for structural engineers due to its existing condition. Considering all difficulties of construction, column jacketing and concrete shear wall scheme have been proposed to give the super structure an overall stability against all kind of possible loading. To overcome the foundation inadequacy deep beams have been inserted in two opposite side of the mat resting on Jet Grout Columns (JGC). While constructing the JGCs, there are several obstacles due to existing condition. The sizes of the JGCs have been adjusted as per field condition. Full control of jet grouting application has been maintained by monitoring all jet grouting phases carefully. The diameter of the pile has been checked by digging up to a depth of several feet for most cases. The core sample has been collected from grout piles and compressive strength has been evaluated. Subsoil investigation and Static Pile load test have also been carried out.

In this paper methodology of retrofitting design for both super and sub-structure is discussed along with the changes that have been made due to field condition. Construction process, impediments and relevant changes are also included. In addition, type of treatment, application procedure and operational parameters for jet grouting are discussed.



**Figure 1: Building (a) before and (b) after retrofitting**

### **BUILDING INFORMATION AND DEFICIENCIES**

The evaluated building is a four-storied concrete moment resisting frame. The structural configuration of this building is regular in pattern. All of the interior columns are circular having 650mm in diameter and all edge and corner columns are square in shape having 500mm x 500mm in size. Typical floor beams are 250mmx700mm in size along both principle directions of the building. Crushed stone chips have been used as coarse aggregate for concrete and steel deformed bars have used as reinforcement. The ground floor height is 5.55m and other typical floor height is 3.6m. The existing floor system is a two way edge beam supported floor having 160 mm thickness. The plan dimension of the building is 21.4mx21.4m. The existing foundation is mat foundation having a thickness of 500mm. The ground floor is a structural floor with proper reinforcement and thickness is 200mm. The evaluated concrete strength as per ACI 562 (2013) is 18.4MPa and the yield strength of deformed bar is 420MPa. The main use of the building is to supply electricity to others buildings. There are several high voltage generators and other machineries related to electrical connections and supply in the ground floor. The other floors are used for office purposes and the top floor for garments product.

Based on DEA, several structural deficiencies have been identified. Most of the columns are inadequate in capacity due to earthquake forces. The reinforcements of mat foundation along both principle directions is inadequate for bending moments due to upward soil pressure caused by the action of gravity loads. The underneath soil of the existing mat foundation is found to be compacted. The estimated settlement is acceptable.

## **SEISMIC RETROFITTING DESIGN AND CONSTRUCTION**

Since the structural elements are mainly inadequate due to lateral forces and the access for strengthening the interior columns are not possible due to existing condition, additional concrete shear walls are attached to the exterior columns at front and rear sides of the building. From numerical analysis, it has been observed that shear wall increased overall lateral stiffness of the building, also the inter-storey drift of the first floor remains within tolerable limit. Along with shear wall, two columns are also strengthened as per conventional column jacketing procedure using high strength concrete. Concrete shear wall required deep foundation to resist the uplift force action due to lateral forces. For this purpose cast-in-situ piles in addition have been considered below the foundation of the shear walls.

Inadequacy of the foundation occurs due to upward soil pressure that reacts against the vertical loading of the building. To rectify this inadequacy reinforcement of top layer need to be increased in both principle directions. This is practically impossible due to the setup of electric generator at the ground floor and presence of active electric lines under the ground floor slab. The designer has proposed to let the mat distribute its load in such a way that it will reduce soil pressure on it. Mat connecting deep beams (thicker than the normal beam) have been proposed along the front and rear sides of the building. These two deep beams have been connected with the mat. The mat behaves like a two way edge supported slab and the moment due to upward pressure of underneath soil will be transferred by the deep beams. The compacted soil is not fully capable to support the beams. Therefore continuous cement grout columns (JGC) are considered. These JGCs will be able to reduce the deflection of deep beams. Figure 2 shows the location of JGCs.

The retrofitting construction has been completed within three months. Within this time period, forty six Jet Grout columns (JGC), sixteen bored piles, two 21m long mat connecting deep beams, eight pile caps, six mat beams, two column jacketing and eight shear walls have been constructed. Figure 3 shows construction of different new building elements for retrofitting purposes.



proposed treatment zone at which high velocity injection of fluids (often sheathed in air) are initiated as the monitor is slowly rotated and lifted. The jet erode and flush out a portion of the in situ soil and mix the remaining soil with cement grout to form a mass of stabilized soil, referred to as jet grouted soil (Sweeney et al., 2001). Currently, there are three major forms of jet grouting which involve the injection of a single fluid, two fluid or three fluids (Kauschinger and Welsh, 1989). Double fluid system has been used in the present case.

### **1. Selection of Jet Grout for this Project**

The major concern of the project is laying the deep beam in a base with sufficient bearing capacity or transfers the load to other load bearing elastic foundation. The soil needs to be treated to increase its bearing capacity having settlement within tolerable limit. Otherwise install a deep foundation under the beam. The deep beams to be constructed are adjacent to the building and the working space is congested. In this working space, installation of a deep foundation is almost impossible. Due to this reason, improving the soil improvement through JGC is the only viable solution. JGC is the most viable solution due to its capability to create large columns of cemented material by drilling small holes into the ground, with limited disturbance of the surrounding subsoil. Moreover jet grouting is an erosion-based process, and subsequently can be effective across the widest soil spectrum (Burke and Sehn, 2003). With a number of jet grouted column in a row will provide a level platform which will prevent any detrimental settlement. For the above reasons jet grout columns have been selected for this project.

### **2. Design Methodology**

In designing jet grout, the first thing is to decide how much of soil need to be improved to attain the desirable soil properties. Based on that designer decides the volume of jet grout to be done and the arrangement of jet grout columns as per volume requirement. Design process, strictly related to the quantification of the technological effects: the choice of the jet grouting procedure, the quantification of treatment parameters, the prediction of the dimensions and the mechanical properties of the jet grouted piles and the analyses of possible undesired collateral effects on the surrounding constructions and on the environment. In this project, the main purpose of jet grout column is to transfer loads to deeper and more competent subsoil strata, bypassing weaker or more deformable soils. Also to prevent any detrimental settlement to provide the deep beam an elastic base foundation. The design of jet

grout column is done as per subsoil condition as shown in Figure 4. The soil report shows that the soil is mainly silty fine sand up to a depth of 24.4m except from 7.62m to 10.67m, the soil is soft clayey silt. The capacity (tip resistance and skin friction) of a single JGC has been estimated based on the available data which is obtained from the subsoil investigation report.

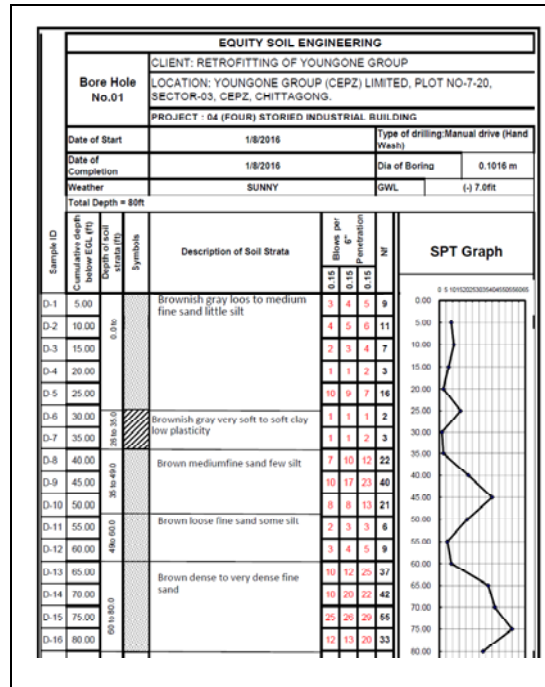


Figure 4: Subsoil report at the project site

As per site condition, three different diameter of grout columns have been selected, they are 800mm, 600mm and 500mm. Due to lack of access in some locations, higher diameter columns have been used as the spacing is higher. Also when the spacing is less, the smaller diameter has been used. The length of the designed column is 18.3m. For this project site, the estimated column capacity for 600mm diameter is 300kN, for 500mm diameter the estimated column capacity is 235 kN and for 800mm diameter the estimated column capacity is 500 kN. This has later been verified by static pile load test (ASTM 1143, 1994) for the for 600mm diameter column. Jet grout strength is primarily determined by the soil type; however the amount of cement used per unit volume and the water-cement ratio also has an effect. In design, the compressive/bearing strength of the soil is assumed to be 3000kN/m<sup>2</sup>, which is also verified by collecting cores from the JGCs constructed at the site. The grout mix is composed of water and cement dosed according to weight ratios (W/C), usually ranging

between 0.6 and 1.3. Selection of these parameters is very important for achieving design strength. In this project, the selected the water and cement is 1:1.

### **3. Construction Methodology**

Jet grout columns are installed by initially drilling a small hole, typically 100 mm in diameter to the required depth. In the double fluid system, the grout is encased within a shroud of compressed air. The air acts as a buffer between the groundwater and the grout, greatly increasing the cutting efficiency. It also creates turbulence in the waste spoil, improving the efficiency of its removal. In this method a special coaxial drill string and jet monitor has been used. The cutting jets are located above the grout supply, which allows a nearly complete replacement of the soil with grout as the monitor is withdrawn. The double fluid jet grouting system used for this project is shown in Figure 5. Double fluid jet grouting is typically constructed from the bottom upwards. Column size is dependent on parameters such as rotation rate, lift rate, injection pressure and grout flow rate. Selection and control of these parameters are the main task in construction stage to attain desirable results for the structure.

### **4. Application procedure**

In construction of the project, all necessary machinery for jet grouting needs to be placed in a convenient way to facilitate the work condition. For jet grouting pump machine a temporary work station has been selected. The air compressor as shown in Figure 5 (c) has been placed near the work station. Near this place the mixing plant for grout has also been set. The drilling rig has been positioned on top of two pipes so that the machine can easily be moved to its desired point. In this project, jet grouting pile installation process has been executed with the help of four operators. A supervisor has also been involved to take care of the grout mixing. After finishing one jet grout column, the machine has been shifted to the alternative point of jet grout column, skipping the adjacent pile. This way time is given to newly installed pile to be cured, at the same time maintaining the time schedule.

### **5. Type of Treatment**

The soil beneath the deep beam needs to be treated. The deep beam is about 600mm in width and length of around 21m. The soil beneath the beam needs to be improved for an area of 21m long strip with a width of 600mm. In that case, a series of jet grouted pile needs to be installed in a single row along the strip having a diameter of around 600mm as shown in Figure 2. As per design, to transfer the imposed load to a hard stratum, JGCs has been formed

up to a depth of 18.3m. It has been observed that during actual construction some of the JGCs can't be placed according to the design as shown in Figure 2 due to existing pipes and other installations. For this reasons, the diameter of some of the JGCs have been increased or decreased as per requirement so that the overall objective of grouting may be fulfilled (as discussed in design methodology).

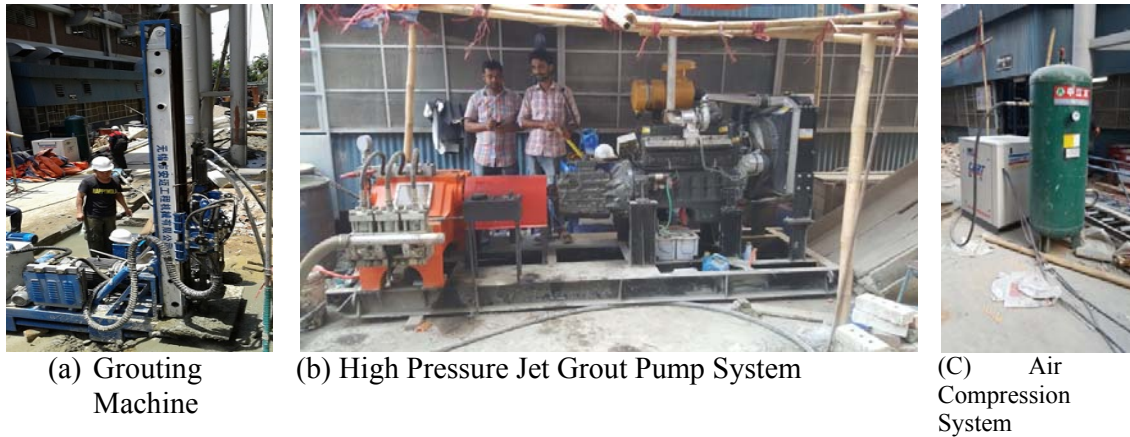


**Figure 5: Jet Grout Column Construction on site**

## 6. Operational parameter

In JGC construction, the operational parameters are injection pressure, number and diameter of nozzles, rotation and lifting speed of the rods and flow rates. These parameters have been set according to appropriate calculation and as a result of required diameter according to the design. Following factors may affect the selection of operational parameter: subsoil condition, desire pile diameter, desire jet grouted soil bearing capacity, applied jet grouting technique. For this project, operational parameter has been determined by a field trial. The operational parameters used in this project are presented in Table 1.

**Table 1: Operational Parameters of JGC construction at the project**

Operational Parameter	Unit	Value for different diameter, D of Jet Grout Column		
		D=800mm	D= 600mm	D= 500mm
Injection Pressure	MPa	20~35	20~35	20~35
Number of Nozzles	No	2	2	2
Diameter of Nozzles	Mm	1.8	1.8	1.8
Rotational Speed	Rpm	20	20	20
Lifting Speed	cm/min	15	20	25
Flow rate	Liters/min	5.25	2.65	1.81

## 7. Performance

As the project is the first project for the designer and the contractor, the result of their assumption need to be verified by field trials. The first thing is to check the diameter of the grout piles. The diameter is physically checked by excavating the JGC heads. It has been found that the diameters are okay as per design requirements. Figure 7 shows one of the excavated areas to find out grout pile diameter and the process of core collection. The compressive strength has been ascertained for eight collected core samples. Table 2 shows the core test results.

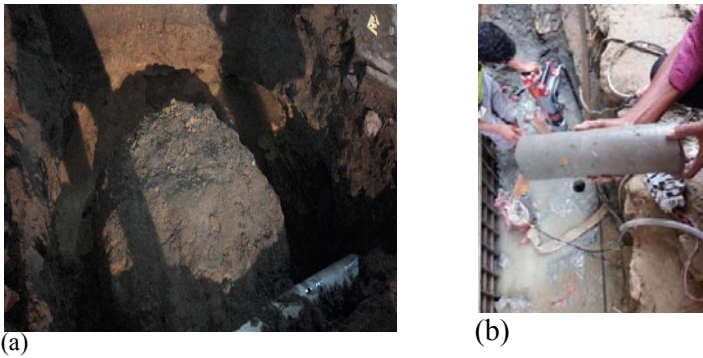


**Figure 6: Exposed (a) JGC and (b) Sample Core Collection**

The average compressive strength of all the cores is 2700 kN/m<sup>2</sup>, slightly lower than the design value of 3000 kN/m<sup>2</sup>. Static pile load test on a test JGC of diameter 600mm has also been carried out as per ASTM 1143 (1994) up to failure of the pile. The pile load test setup is shown in Figure 7.

**Table 2: Crushing Strength of Jet Grout Core**

Sl No	Grout Pile Diameter	Crushing Strength (MPa)
1	800mm	3.6
2	800mm	1.4
3	600mm	2.6
4	600mm	2.6
5	500mm	3.1
6	500mm	2.7



**Figure 7: (a) Static Loading System on top of a JGC and (b) Hydraulic Jack and dial gage setup**

The load versus settlement curve for the tested JGC is shown in Figure 8. The ultimate capacity of the tested JGC is approximately 1000 kN. For a factor safety of 2, the allowable capacity is 500kN which satisfies the designed value of 300 kN for 600mm diameter column.

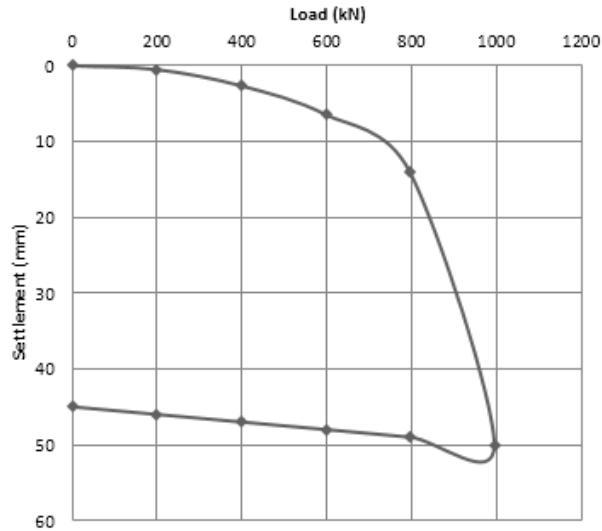


**Figure 8: Load versus settlement curve**

## CONCLUSIONS

Foundation bearing improvement of a four-storied RMG factory in Chittagong is one of the first applications of Jet Grout Column in Bangladesh. As a result of this soil improvement, the predicted settlement under the existing raft will be low as well as the raft will be able to carry additional loads coming from the new shear walls inserted on the superstructure. The high speed of jet grouting application allowed the other construction phases take place immediately such as lean concrete works, drainage, deep beams, new shear walls etc. The appropriate selection of the operational parameters resulted in a successful treatment that has been proved by technical methods such as trial excavations, core sampling and static pile load tests.

## REFERENCES

- ACI (American Concrete Institute) Committee 562. (2013) *Code Requirements for Evaluation, Repair, and Rehabilitation of Concrete Buildings (ACI 562-13) and Commentary*, ISBN: 9780870318085
- ASTM (American Society for Testing Material) Designation D 1143//D 1143M – 07 (1994). “Standard Test Method for Piles under Static Axial Compressive Load”.

- Burke, G.K. and Sehn, A.L. (2003). “The influence of ground improvement on geotechnical design”. *ASCE/PENNDOT 20<sup>th</sup> Central PA Geotechnical Conference*, October 29-31, 2003.
- Croce, P., Flora, A., Modoni, G., (2014). “Jet Grouting Technology, Design and Control” CRC Press, ISBN 9780415526401 - CAT# Y136059
- Farmer, W. and Attewell, P. B. (1965). “Rock penetration by high-velocity jet”. *International Journal of Rock Mechanics and Mining Sciences 2*: pp. 135–153.
- HBRI-BSTI (1993). Bangladesh National Building Code.
- Kauschinger, J. L. and Welsh, J. P. (1989). “Jet Grouting for Urban Construction,” *Proc., Geotechnical Lecture Series, Boston Society of Civil Engineering: Design, Construction, and Performance of Earth Support Systems*, MIT, Cambridge, MA.
- Kelley, S. J.(1996). “Standards for preservation and rehabilitation”, *West Conshohocken, PA, ASTM*, 1996.
- Modoni G., Bzówka J., and Pieczyrak, J. (2010). “Experimental investigations and numerical modelling on the axial loading of jet grouting columns” *Architecture Civil Engineering Environment Journal (ACEE)*, Silesian University of Technology, ISSN 1899-0142 (code E201327)
- Nakanishi, W. (1974). “Method for Forming an Underground Wall Comprising a Plurality of Columns in the Earth and Soil Formation”, *U.S. Patent 3,800,544*: 8 p.
- Ryjevski, M., Shramko, K., and Baghirova, E. (2009). “Jet grouting application forDubai Metro Construction”, *Proceedings of the World Tunnel Congress*, Budapest, Hungary, May 23-28, 2009.
- Sweeney, B.P., Wheeler, J.R., and Henry, L.B. (2001). “Design and Construction of a Jet-Grouted Excavation Support Wall in an Urban Environment.” *Foundation and ground Improvement*, Proceeding of the conference, American Society of Civil Engineers.



## **PART-IX**

# **AMBIENT VIBRATION ANALYSIS OF HERITAGE UNREINFORCED MASONRY BUILDINGS IN BANGLADESH**

**BANGLADESH NETWORK OFFICE FOR  
URBAN SAFETY (BNUS), BUET, DHAKA**

**Prepared By: B.S.P. Biswas**

**Mehedi Ahmed Ansary**

## 1. Introduction

Bangladesh is located in a seismically moderately region in Global Seismic Map prepared by Global Seismic Hazard Assessment Program (GSHAP, 1992). Although no major earthquakes occur in this country in the last few decades. During the past few earthquakes and also in the time of recent earthquakes, the masonry structure of Bangladesh shows poor structural behavior. Ancient masonry structures are particularly less vulnerable to dynamic actions, especially seismic actions.

Unreinforced masonry was a very common practice and used technology. Those heritage unreinforced masonry structures have been named according to their extent of Bengali civilization, cultures and religions. Few of those are- Pala Buddhist architecture, Islamic and Mughul architecture, Terracotta temple architecture, Common Bungalow style architecture, Indo-Saracenic revival architecture etc.. Later on the British colonial age predominantly represent the buildings of the Indo-European style developed, which is mainly a mixture of Indian European and Central Asian components. The more prominent works amongst them are Ahsan Manzil in Dhaka and Tajhat Palace in Rangpur City. All of them are mostly masonry, sometimes in combination with stones and other local materials <sup>[1]</sup>.

The remains of the ancient archaeological sites bear ample testimony to the fact that the art of building was practiced in Bengal from early period of her history. A satisfactory reconstruction of the history of architecture in ancient Bengal has been found from the evidence of the disappeared materials. The structures were rudimentary wattle and daub construction with beaten earth flooring. The early period of the history has witnessed the spouting of a number of urban centers at sites like Mahasthan at Bogra City in Bangladesh and in west Bengal at Bangarh at Dinajpur City, Chandraketurgh at 24 Paraganas district, Mangalkot at Burdwan district, Pokharana and Dihar. Traces of mud ramparts, noticed at several of these sites suggested that an early Bengal City often contained an acropolis.

In addition mud, bamboo and timber and occasionally burnt bricks were used for building houses. Terracotta drainpipes and ring wells were also found. But later after, during the succeeding periods, represented by sites like Banarh and Mahasthan, the houses became more and more complex, with a simultaneous increase in the use of burnt bricks <sup>[2]</sup>.

Mosque architecture (1205-1765) was introduced by the Muslims to ritual needs of their religion, Islam after the establishment of Muslim rule in Bengal. For this consequence numerous mosque were built during the five and a half centuries of the Muslim period before the British colonial period. Most the building were constructed with burnt bricks and stones. Bricks an easily manufactured material from the abundantly available clay of the delta, has been the traditional building material of Bengal from the ancient times, as seen in the ruined but monumental Mainamati and Paharpur, monasteries in Bangladesh.

Although rooted in the 15<sup>th</sup> century architectural traditions of Bengal, their stark, unadorned exteriors, circular engaged corner towers and massive appearance shows the considerable influence from Tughluq architecture of Delhi. The most important of this approach is the Shatgumbad Mosque in Bagerhat district of Bangladesh. The mosque has eleven bays and seven aisles, with the largest bay in the center. This central bay is divided into seven independent, rectangular bays that are covered by the chau-chalas; this being the earliest use of the form in Bengal. The interiors of the miniature chau-chalas have thin, raised bands of brick that imitate the rafters and purlins of bamboo hut frames. There are seven entrances each on the north and south sides. It seems that the stone pillar once had brick casings, because there are traces of brickwork around some of their bases.

The Chhota Sona Mosque in Gaur dated by inscription to the reign of sultan Alauddin Husain shah (1494-1519), and was built by a high official in the royal court. This rectangular mosque is completely faced with stone in the exterior, while inside there is stone up to the springing of arches. Pillars, pilasters and the platform in the northwest corner are of stone. There is abundant stone carving in low relief in the exterior and ornamental niches within rectangular panels, rosette and pot motifs that are used repeatedly.

The Chatmohar mosque in Pabna district dated 989 AH (1581-82) and the Kherua mosque in Sherpur district dated 989 AH (1582). These mosques used the single aisle, three bayed plan which was to become the paln par excellence for Mughal mosques in Bengal from the 17<sup>th</sup> century onwards. In elevation the octagonal corner towers, the curved cornices. Low drum less domes, brick surface and pointed arches link them to the Sultanate style.

A refined Mughal provincial style was developed in the capital city Dhaka in the 17<sup>th</sup> century. The Lalbagh Fort Mosque in Dhaka dated 1059 AH (1649) and 1194 AH (1780) conforms to the typical Mughal mosque plan which was mostly masonry <sup>[3]</sup>. Kantanagar Temple, commonly known as the Kantajiu Temple is a late-medieval Hindu temple in Dinajpur district of Bangladesh. The Kantajew Temple is one of the most magnificent religious edifices belonging to the 18<sup>th</sup> century. The temple was built by Maharaja Pran Nath, its construction started on 1704 CE and ended in the region of his son Raja Ramnath on 1722 CE. It boasted one of the greatest example on terracotta architecture in Bangladesh and once had nine spires, but all were destroyed during the great Indian Earthquake that took place on 1897 <sup>[4]</sup>.

One of the most vulnerable forms of construction to damage in construction is unreinforced masonry. The 1989 Newcastle, Australia, earthquake was a recent event that demonstrated this vulnerability. The majority of damage in Newcastle was to older load bearing masonry construction or nonstructural masonry. Also a large number of small and large masonry performed well during the earthquake <sup>[5]</sup>.

Historical structures have been built without accounting for the seismic actions and are vulnerable even to moderate events but, due to their historical importance and to the daily presence of tourists,

their seismic rehabilitation is quite delicate, aiming at the protection of both human life and cultural heritage. Seismic preservation should be based on a good knowledge of the dynamic characteristics of the structure and a suitable choice of the intervention, if necessary. The first step is very important in order to assess, also by means of a suitable numerical model, the possible dynamic behavior of the structure during strong events. But it is not easy for several reasons: the structural size of the various elements (walls, floors, etc.) cannot be evaluated with the needed accuracy; the material characteristics, such as the tension-strain relationship, the strength, etc., are not known; structure and materials often exhibit inelastic behavior; horizontal structures are not effective in joining the vertical ones; the depth of the foundations is often variable as well as their geometry and material properties, including the soil characteristics; buildings are often connected to other constructions, so that their behavior is very complicated. For such kind of structures the experimental analysis is often the only way to improve our understanding about their dynamic behavior [6, 7, 8, 9 & 10].

## **2. Methodology**

### **2.1 Study Design**

Masonry is the building of structures from individual units laid in and bound together by mortar; the term masonry can also refer to the units themselves. The common materials of masonry construction are brick, building stone such as marble, granite, travertine, and limestone, cast stone, concrete block, glass block, and cob. Masonry is generally a highly durable form of construction. However, the materials used, the quality of the mortar and workmanship, and the pattern in which the units are assembled can significantly affect the durability of the overall masonry construction.

This research was initiated to collect preliminary information for heritage unreinforced masonry buildings in the Dhaka City. The purpose of conducting ambient vibration testing in general is to obtain the dynamic characteristics of a structure, its natural frequencies, corresponding mode shapes and damping estimates. The structure is assumed to be excited by wind, traffic and human activity. The measurements, typically accelerations, are taken for a long duration to ensure that all the modes of interest are sufficiently excited. Microtremor measurements were carried out to characterize the site dynamics. Five sensors were used for the measurement. The buildings are typically two storied with some part three storied. Three sensors were placed at different three stories on the line of stiffness of every floor. Other two sensors were placed on the ground to record the soil dynamics.

The present state of knowledge concerning shear strength and shear load-displacement behavior of masonry is far less advanced than that concerning masonry behavior in compression, even though shear failure is an important, often governing mode of failure in many masonry buildings<sup>[14]</sup>. This lack of understanding is reflected by the low values of shear resistance allowed by present U.S. building codes (ASCE 31 02). Information on the post-peak behavior and on the deformations

associated with pre-peak and post-peak responses are also lacking. Only recently, the terms softening and dilatancy were introduced in the research community [15]. Knowledge of such behavior is essential if adequate analytical models are to be developed to describe the in-plane behavior of masonry walls. Most of the research conducted to date regarding the masonry shear behavior has been limited to determining the peak shear stress and affecting parameters.

Lime mortar was used as the bonding material in all the three study buildings. It was required to check the shear stress of the bonding mortar of masonry. Direct shear test has been carried out to find the best result for mortar strength at one building (Old academic Building of BUET) as identical as all the three buildings are similar in bonding material. This paper describes the buildings tested, the tests and results, and the methodologies and equipment used.

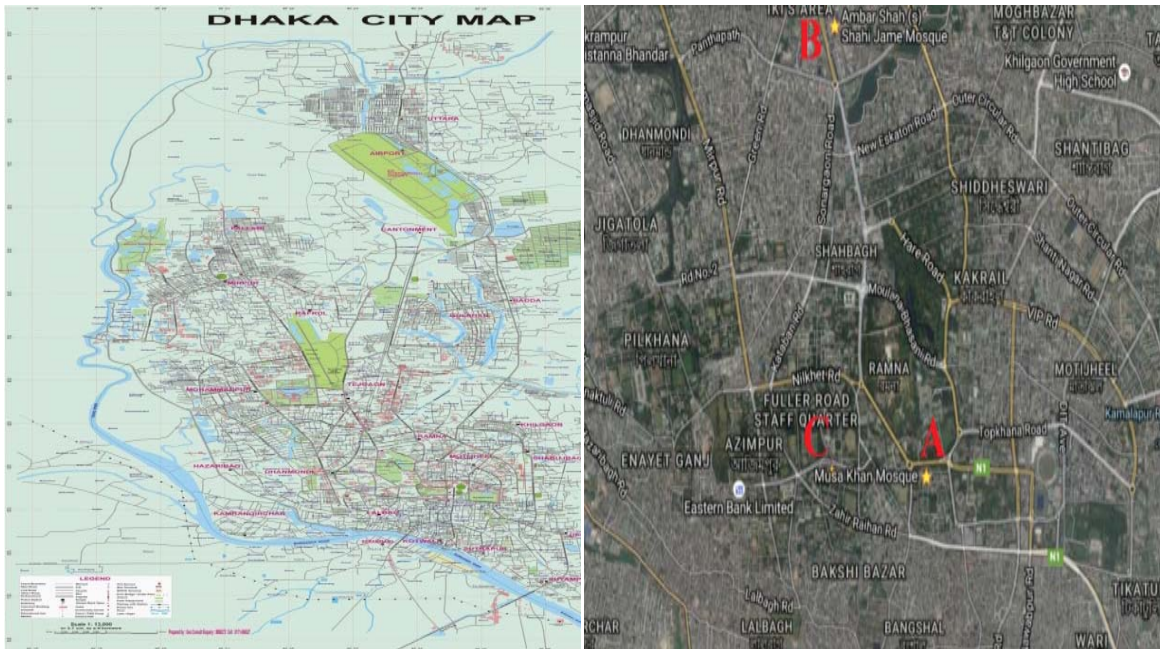


Figure 1A: Dhaka City Map (source: Dhaka Map of RAJUK website)

Figure 1B: Location of Study Area (source: Google map)

## 2.2 Study Area Selection

The tests were performed on and around three buildings of Dhaka City. Figure 1A shows the map of Dhaka City and figure 1B shows the locations of the three buildings tested in the Dhaka City. The buildings were the Curzon Hall Musa Khan Mosque Building, shown as Point A, the Aambour Shah

Shahi Mosque, shown as Point B, and the Old Academic Building of Bangladesh University of Engineering and Technology (BUET), shown as Point C. The points were taken for the microtremor measurements. The three buildings feature similar structural systems, with unreinforced masonry load bearing walls at the sides of the buildings with a mix combination of wood and I-Joist steel diaphragm floors connecting them.

## 2.3 Description of Buildings

### 2.3.1 Musa Khan Mosque at Curzon Hall

This mosque is located at Curzon hall in Dhaka University at latitude  $23^{\circ}43'38.5''N$  and longitude  $90^{\circ}24'06.9''E$ . The Musa khan mosque (Figure 2) belongs to oblong shaped plan measuring 15.17 m by 7.54 m externally with a 1.52 m thick surrounding brick wall. The prayer hall is entered from the eastern side by three archways and the other two side walls have one pointed-arch openings each. To articulate the main mihrab niche from outside, the kibla wall is projected in the centre towards the west. The whole length of the rectangular hall is divided into three unequal bays by means of two 1.06 m wide arches springing from the east and west walls. The side bays are rectangular in shape and smaller in width, but the central one is bigger and square. With the help of brick pendentives the square central bay is transformed into an octagonal area. By introducing a series of sequences the octagonal area is transformed into a circular supporting area, upon which the dome supports. The two smaller rectangular side bays are converted into square supporting areas for the dome by using two half domed vault springing from the eastern and western walls. Plan and front elevation of the mosque are shown in Figure 3 and Figure 4 respectively.

### 2.3.2 Aambour Shah Shahi Mosque at Karwanbazar

One of the most well preserved mosque complex of Dhaka city belonging to the 17th century is the Aambour Shah Shahi Mosque (Figure 5). It is located at Karwan bazaar in Dhaka City at latitude  $23^{\circ}45'11.6''\text{N}$  and longitude  $90^{\circ}23'35.0''\text{E}$ . The mosque proper has the usual oblong shaped plan measuring 13.41m by 7.30m externally with a 1.2m thick along east-west direction and 1.6m thick along north-south direction brick wall. The prayer hall is entered from the eastern side by three archways and the other two side walls have also one arch opening each. Corresponding to the three frontal openings, the kibla wall is niched with three mihrabs. The rectangular shaped prayer room is divided into three square bays by two wide transverse corbelled cusped arches supported by twin brick pilasters embedded in the east and west walls. With the help of half domed squinch at each corner, each square area is transformed into a circular supporting area, upon which the dome supports. All the three domes, with a very low shouldered dome on a cylindrical drum, are crowned with lotus and kalasa finial. The central one is slightly higher than the flanking ones. Plan and front elevation of the mosque are shown in Figure 6 and Figure 7 respectively.

### 2.3.3 Old Academic Building (OAB) of BUET

The Old Academic Building of Bangladesh University of Engineering and Technology (BUET) at latitude  $23^{\circ}43'39.0''\text{N}$  and longitude  $90^{\circ}23'34.2''\text{E}$  was built on the early 1900's (Figure 8). Some parts of the building is two stories and some parts is three storied. The OAB building has a mixed used of office cum academic. The OAB's proper has plan measuring 70.5m by 48m externally with a 1.1m thick brick wall every direction. It is Unreinforced Masonry Bearing Walls with Stiff Diaphragms (Building Type 15 according to ASCE/SEI 31-03) <sup>[13]</sup>. First floor (2<sup>nd</sup> story) is slab supported on masonry wall, Ground floor (1<sup>st</sup> story) is slab on grade. It is mainly unreinforced burnt clay brick masonry with lime mortar. Plan of the OAB is shown in Figure 9.



Figure 2: Musa Khan Mosque

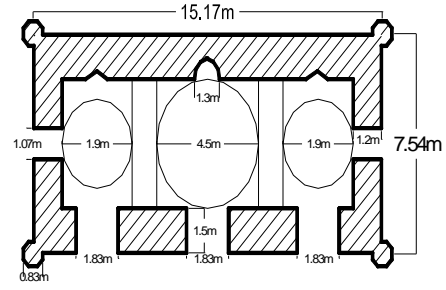


Figure 3: Plan of Musa Khan Mosque

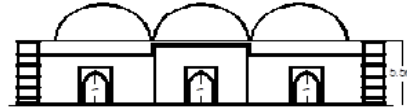


Figure 4: Front Elevation of Musa Khan Mosque



Figure 5: Aambour Shah Shahi Mosque

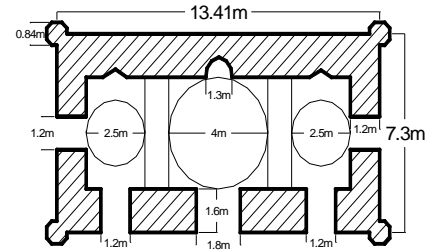


Figure 6: Plan of Aambour Shah Shahi Mosque

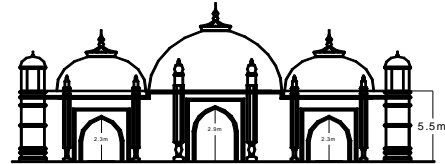


Figure 7: Front Elevation of Aambour Shah Shahi Mosque



Figure 8: Old Academic Building of BUET



Figure 9: Plan of Old Academic Building

## 2.4 Data Collection Using Microtremor

The purpose of conducting Microtremor measurements is to obtain an estimation of site response for a particular location. Three approaches are commonly used to analyze microtremor data; power spectral densities obtained directly from the Fourier amplitudes, spectral ratios relative to a reference site, and Nakamura's technique <sup>[12]</sup>, which is defined as the spectral ratio of horizontal components to vertical components recorded at the same site (H/V ratio). It is common to perform tests over a period of time to observe the stability of the measured site response, in order to provide a reliable prediction of the period of potential earthquake motion at that site.

Nakamura's technique describes the microtremors as Rayleigh waves propagating in a single layer over a half-space, and assumes that the microtremor motion is due to local sources such as traffic and human and construction activity nearby. It further assumes that the vertical component of ground motion is not amplified by the soil layer. Hence, the spectral ratio of the horizontal to the vertical components at the surface (H/V ratio) gives an estimate of the period at which it peaks, corresponding to the site period.

The equipment used for the microtremor testing system consists of five velocity transducers; two horizontal and one vertical, an amplifier and a laptop computer used for data acquisition. For the selection of the test location, care is taken to avoid heavy traffic, manholes, foundation sand other underground structures. The sensors are placed so that the two horizontal sensors are orthogonal, preferably facing North and East. The analysis is carried out using Nakamura's method, plotting the H/V spectral ratios that are the result of taking the RMS of the east and North spectral ratios. The most significant peak of the H/V spectral ratio is taken to be the dominant frequency of the site.

Methods to get geophysical information from the microtremor measurement were 1) obtaining the phase velocity by array observation of microtremor and 2) obtaining H/V spectrum by using 3 component sensors. After obtaining the phase velocity or H/V spectrum, S-wave velocity profiles should be interpreted by applying an inverse analysis. All 5 sensors were placed in a single row with the distance of 15m and 30 min data was taken.

Soil characteristics can be assessed by Microtremor measurement. Hard soil gives high frequency and soft soil gives low frequency. A structure may experience a vibration period at which it oscillates in the earthquake vibration motion and will tend to respond that. Natural frequency is obtained based on the spectral ratio of horizontal component of the structure to that of ground. Wave propagation mechanism of Microtremor and its relation with ground vibration characteristics were studied from the beginning of Microtremor studies <sup>[11]</sup>. Figure 10 shows the microtremor testing equipment.



Equipment arrangement



Microtremor Sensor

Figure 10: Microtremor Equipment

### 2.5 Data Collection Using Direct Shear Test

The direct shear test to measure the shear stress due of mortar bond of Old Academic Building of BUET has been performed by using Hi-Force Hydraulic Jack. Figure 11 shows the testing activity of direct shear test.



Figure 11: Direct Shear Test

## 3. Data Processing and Analysis

The analysis has performed using the GeoSiG software and D-Plot software. For microtremor observation at the selected buildings, initially the sensors were deployed. Three sensors were fixed on the different stories of the building and another one on the free field near the surface. After taking the observation with the help of microtremor, the time domain velocity data was converted into to frequency domain data and natural frequency if the structures are determined.

### 3.1 Curzon Hall Musa Khan Mosque

The intention of the tests described in this research was to provide some preliminary information about the dynamic behavior. The Microtremor analysis of Curzon Hall Musa Khan Mosque has been illustrated as below in figure 12 and figure 13.

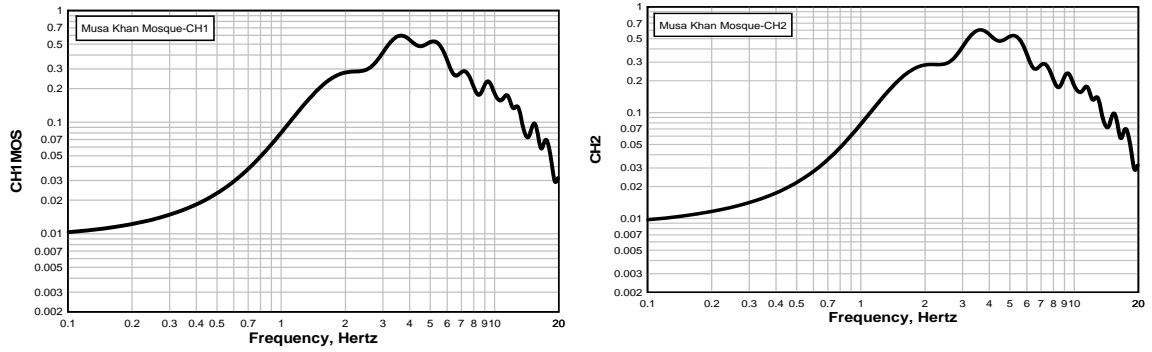


Figure 12: The corresponding FFT of recorded time series of the Curzon Hall Musa Khan Mosque

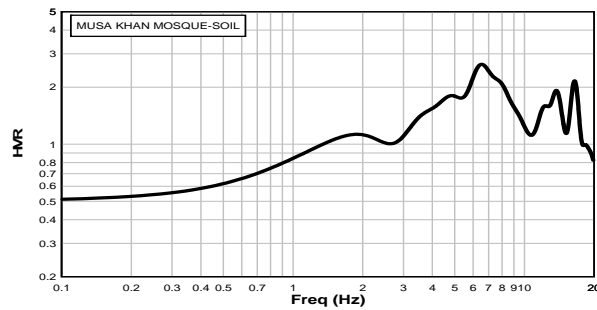


Figure 13: The corresponding H/V ratio of the Curzon Hall Musa Khan Mosque

### 3.2 Aambour Shah Shahi Mosque

Observation of microtremors can give useful information on dynamic properties of the site such as predominant period and amplitude. Microtremor observations are easy to perform, inexpensive and can be applied to places with low seismicity as well. The Microtremor analysis of Aambour Shah Shahi Mosque has been depicted as below in Figure 14 and Figure 15.

### 3.3 Old Academic Building (OAB) of BUET

Seismic noise is relevant to any discipline that depends on seismology, such as geology, earthquake engineering and structural engineering. It is often called ambient wave field or ambient vibrations.

The Microtremor analysis of Old Academic Building of BUET has been shown as below in figure 16 and Figure 17.

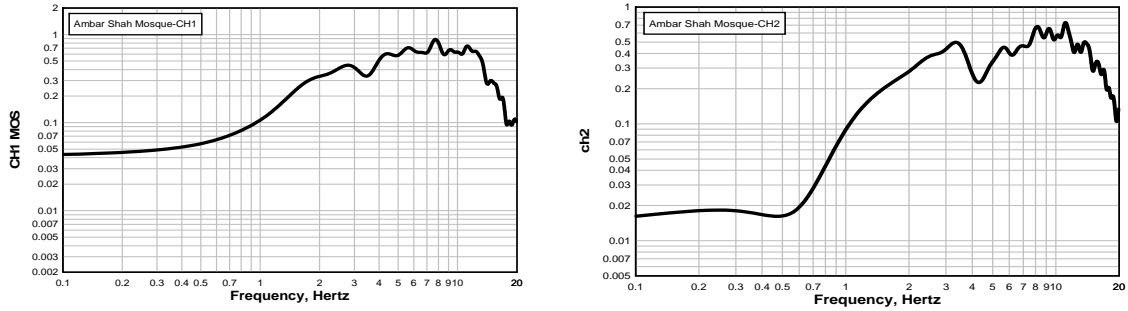


Figure 14: The corresponding FFT of recorded time series of the Aambour Shah Shahi Mosque

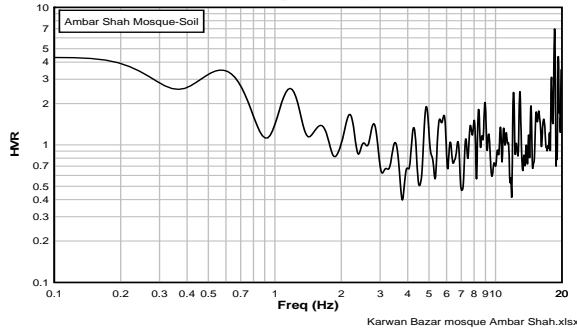


Figure 15: The corresponding H/V ratio of the Aambour Shah Shahi Mosque

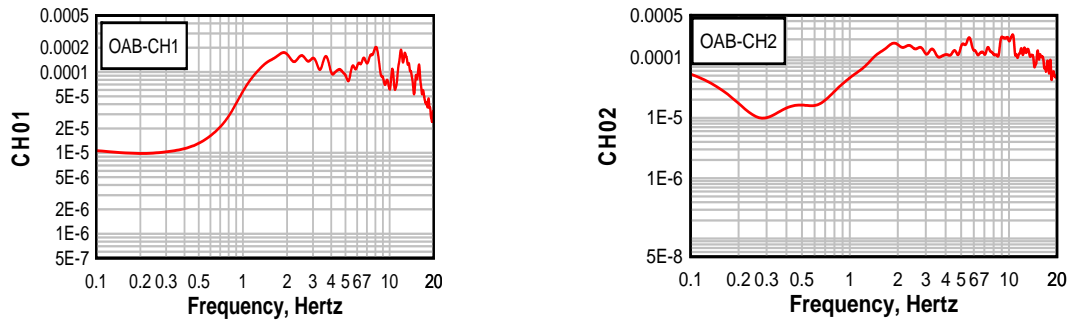


Figure 16: The corresponding FFT of recorded time series of the OAB

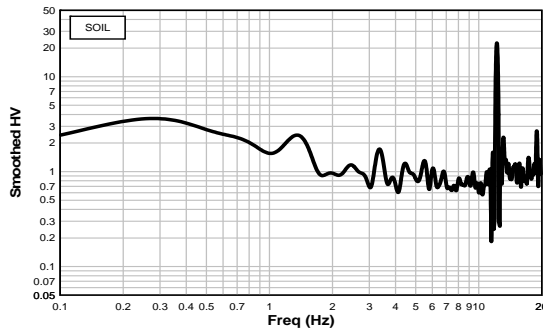


Figure 17: H/V ratio of recorded time series of the OAB

### 3.4 Direct Shear Test of Old Academic Building (OAB) of BUET

Shear failure is the dominant mode of failure observed in many masonry buildings subjected to lateral loading due to earthquakes, wind (in tall and slender structures), support settlements, or unsymmetrical vertical loading. Lateral loading can produce both diagonal cracking failures and shear failures of the horizontal joints. Joint resistance is of particular concern in the analysis of the load-bearing unreinforced masonry structures that are rather common among older buildings in many countries in the world. The shear generally acts in combination with compression caused by the self-weight and floor loads. Confinement by, for instance, structural frames to in-fill walls may also lead to shear compression.

The in-place shear test, also known as the push test, provides a direct measurement of the shear resistance of mortar joints in masonry. The test is suitable for masonry that has relatively strong units and weak mortar so that shear cracks form in the typical stair step pattern along mortar joints and the units remain uncracked. In this type of construction, the shear strength of the mortar joints limits the shear strength of the masonry wall <sup>[16]</sup>.

The Uniform Code for Building Conservation (UCBC) provides an empirical relationship that relates the mortar joint shear strength to the masonry wall shear strength, assuming that wall shear strength is limited by the shear of the mortar joints rather than shear through the units. The method is not applicable for determining shear strength of modern masonry with high strength mortars <sup>[17]</sup>.

A calculation on direct shear test of lime mortar as bonding material of Old Academic building has been made. The calculation is given below-

Direct Shear Test of Old Academic Building of BUET	
Jack diameter	35 mm
Area	962.12 mm <sup>2</sup>
Brick Size	254 mm (Length); 114.3 mm (Width)
Contact Area	77419.2 mm <sup>2</sup>
Dial Gauge Reading	650(Kg/cm <sup>2</sup> ); 89846.22 (N)
Shear Strength of the Sample, $\tau$	1.161 N/mm <sup>2</sup>
Nos. of bricks above testing brick	100 Nos.
Height of wall above testing brick	9.15 m
Unit weight of wall	19 KN/m <sup>3</sup>
Vertical Pre-stress on testing brick, $\sigma$	173.85 KN/mm <sup>2</sup>
$\sigma * \mu$	0.174 N/mm <sup>2</sup>
Shear Stress due to mortar bond only	$\tau - \sigma * \mu = 0.987$ N/mm <sup>2</sup>

Reliable information on shear resistance is needed when performing retrofits and seismic upgrades of masonry buildings. While shear strength of a masonry wall is difficult to measure without resorting to large-scale testing, less destructive in-place tests of single masonry units provide a comparative figure

that can be correlated to full-scale wall behavior. This less destructive alternative is more economical than large-scale testing and is desirable when a building's historic integrity must be maintained.

#### 4. Results and Discussions

For the three buildings described earlier in this paper, both vertical and horizontal measurements were recorded, with a sampling rate of 200Hz and duration of 30 minutes for each. From the analysis of the normalized H/V ratio plots and FFT of the three buildings, the pertinent information obtained is presented in Table 1.

Table 1: Comparison of Microtremor Result of Soil (H/V ratio) and Building (FFT)

Test points	Predominant Frequency of Soil (HVR)	Structural Predominant Frequency	Remarks
Curzon Hall Musa Khan Mosque	1.8 Hz	3.6 Hz	Possibility of no seismic resonance
Aambour Shah Shahi Mosque	1.2 Hz	2.6 Hz	Possibility of no seismic resonance
Old Academic Building of BUET	1.6 Hz	1.9 Hz	Possibility of seismic resonance

The predominant frequency of the building of the Curzon Hall Musa Khan Mosque has found 3.6 Hz which is different from the predominant frequency of the site soil (1.8 Hz). So there's no possibility of soil structure interaction during any severe earthquake. It is also similar in case of the Aambour Shah Shahi Mosque. But the predominant frequency of building of the Old Academic Building of BUET is in the range of the peak frequency of the soil. This value is close to the range of the higher modes of vibration for the buildings measured as shown in the figure 16 and figure 17. This raises the possibility of soil-structure interaction.

The direct shear test was done to find the mortar strength. From the analysis the shear stress due to mortar bond only was found about 0.987 N/mm<sup>2</sup> which is below the standard value. The direct shear test result suggested that as the mortar bond was not strong enough, the OAB building will be unable to resist lateral forces due to an strong earthquake. A detailed assessment has been done by following the guidelines of Arya (1986)<sup>[18]</sup>. Retrofitting of the masonry wall is mandatory. Currently, the OAB is being retrofitted.

## 5. Conclusions

The intention of the tests described in this paper was to provide some preliminary information about the dynamic behavior and the dynamic site conditions for three masonry buildings in Dhaka City. The Curzon Hall Musa Khan Mosque, Aambour Shah Shahi Mosque and the Old Academic Building (OAB) of BUET were each tested by researchers of BUET. Among the three historical buildings, from the dynamic analysis it has found that two buildings (Curzon Hall Musa Khan Mosque, Aambour Shah Shahi Mosque) are safe from seismic resonance whereas the Old Academic Building of BUET has the strong probability of severe seismic resonance. Also the direct shear test result on brick mortar of OAB shows that the mortar strength is below the standard value which indicates that the load bearing masonry wall is unable to withstand the lateral seismic force. This means the OAB needs to be retrofitted. In this case, the earthquake resistant guidelines for non-engineered construction of Arya (1986) have been followed to retrofit the OAB.

## References

- [1] [https://en.wikipedia.org/wiki/Architecture\\_of\\_Bangladesh](https://en.wikipedia.org/wiki/Architecture_of_Bangladesh)
- [2] <http://en.banglapedia.org/index.php?title=Architecture>
- [3] [http://en.banglapedia.org/index.php?title=Mosque\\_Architecture](http://en.banglapedia.org/index.php?title=Mosque_Architecture)
- [4] [https://en.wikipedia.org/wiki/Kantajew\\_Temple](https://en.wikipedia.org/wiki/Kantajew_Temple)
- [5] PAGE, A.W., KLEEMAN, P.W., STEWART, M.G., and MELCHERS, R.E., “Structural aspects of the Newcastle Earthquake” Proceedings of the Institute of Engineering, Australia Structural engineering Conference, Adelaide, South Australia; 3-5 October, 1990.
- [6] De Stefano A., Clemente P. (2009). “Structural health monitoring of historic buildings”, In Karbhari V.M. and Ansari F. (Eds), Structural Health Monitoring of Civil Infrastructure Systems, Woodhead Publishing Ltd
- [7] Clemente P., Rinaldis D. (2005). “Design of temporary and permanent arrays to assess dynamic parameters in historical and monumental buildings”. In Ansari F. (ed), Sensing Issues in Civil Structural Health Monitoring (Proc., North American Euro-Pacific Workshop, CSHM, Honolulu, 10-13 November 2004, invited paper), Springer, 107-116.
- [8] Rinaldis D., De Stefano A., Clemente P. (2005). “Design of seismic arrays for structural systems”. In Ou J.P., Li H. & Duan Z.D. (eds), Structural Health Monitoring of Intelligent Infrastructure (Proc., 2nd International Conference SHMII-2, Shenzhen, Nov.16-18, 2005), Vol. 2, 1447-1453, Taylor & Francis/Balkema, Leiden, The Netherlands.
- [9] De Stefano A., Clemente P. (2005). “S.H.M. on historical heritage. Robust methods to face large uncertainties”. Proc., 1st International Conference on Structural Condition Assessment, Monitoring

and Improvement, (12-14 Dec. 2005, Perth, W. Australia), 09-22, CI-Premier Conference Organisation, Singapore.

[10] Clemente P., Buffarini G. (2009). “Dynamic Response of Buildings of the Cultural Heritage”, In Boller C., Chang F.K., Fujino Y. (eds), Enciclopedia of Structural Health Monitoring, John Wiley & Sons Ltd, Chichester, UK, 2243-2252.

[11] Aki, K. (1957). Space and time spectra of stationary stochastic waves, with special reference to microtremor. Bull. of earthquake research Institute , 415-456.

[12] Nakamura, Y. (1989) “A method for Dynamic Characteristics Estimation of Subsurface using Microtremor on the Ground Surface”, QR of RTRI, Vol. 30, No. 1, pp. 25-31

[13] Seismic Evaluation of Existing Buildings, ASCE/SEI 31-03.

[14] Van Zijl, G. P. A. G. (2004). “Modeling masonry shear-compression: Role of dilatancy highlighted.” J. Eng. Mech., 10.1061/ (ASCE) 0733-9399 (2004)130:11(1289), 1289–1296.

[15] Lourenço, P. B., Rots, J. G., and Blaauwendraad, J. (1998). “Continuum model for masonry: Parameter estimation and validation.”J. Eng. Mech., 10.1061/ (ASCE) 0733-9445(1998)124:6(642), 642–652.

[16] ASTM C 1531-02, Standard Test Methods for In Situ Measurement of Masonry Mortar Joint Shear Strength Index.

[17] Uniform Building Code (UBC) Standard 21-6, In Place Masonry Shear Tests.

[18] A. S. Arya (1986). Guidelines for Earthquake Resistant Non-engineered Construction. International Association for Earthquake Engineering. p. 158



## **PART-X**

# **EFFECTS OF RELATIVE DENSITY AND EFFECTIVE CONFINING PRESSURE ON LIQUEFACTION RESISTANCE OF SANDS**

**BANGLADESH NETWORK OFFICE FOR  
URBAN SAFETY (BNUS), BUET, DHAKA**

**Prepared By: Mohammad Mominul Hoque  
Mehedi Ahmed Ansary**

## 1 INTRODUCTION

The first widespread observations of damage attributed to soil liquefaction were made in the 1964 Niigata and Alaska earthquakes. Spectacular examples of liquefaction induced failure have also been widely observed during most moderate to large size earthquakes around the world. Since 1964 Alaska and Niigata earthquakes, liquefaction has been studied extensively by many investigators and substantial advances have been made in both understanding and practice with regard to assessment and mitigation of liquefaction induced hazards. However, major advances have occurred in the field of seismically induced soil liquefaction, catastrophic failures in recent earthquakes have provided a sobering reminder that liquefaction of soils as a result of earthquake poses a major threat to the safety of infrastructures. There is no reported case history of seismically induced soil liquefaction in Bangladesh, but location of this country in world seismic map, geologic formation and frequent earthquakes in and around the country remind the great danger of seismically induces soil liquefaction. This research aimed to examine the effects of relative density and initial effective confining pressure on liquefaction resistance of saturated sands using laboratory cyclic triaxial test.

## 2 LITERATURE REVIEW

The effects of relative density and initial effective confining pressure on liquefaction resistance of saturated sands under cyclic loading condition have been extensively investigated by many researchers in the laboratory cyclic triaxial tests. The outcome of these studies generally agreed that, the resistance to liquefaction of sands tends to increase with an increase in relative density and decrease with increase in effective confining pressure. Extensive laboratory investigations on Toyoura sand revealed that, up to a relative density of 70%, liquefaction resistance tends to increase linearly with the relative density, but for the density in excess of 70%, the cyclic strength goes up sharply (Tatsuoka et al. 1986). Undrained cyclic triaxial tests results on clean Ottawa sand (Carraro et al. 2003) and white natural quartz sand (Stamatopoulos 2010) have also illustrated that, the resistance to liquefaction increases as the relative density increases. Other laboratory studies (Liu and Xu 2013, Belkhatir et al. 2010, Vaid and Sivathayalan 2000) have equally provided strong evidence that the liquefaction resistance of sand increases with increase in relative density.

Laboratory research on rounded Ottawa sand and angular tailing sand illustrated that, substantial decrease in resistance to liquefaction occurred for both sands with increase in

effective confining pressure in the range of 200 kPa to 2500 kPa (Vaid et al. 1985). It was apparent that, the resistance to liquefaction for both sands at all level of confining pressure tends to converge around a relative density of 50-55%. This implies that, the influence of confining pressure on reduction of resistance against liquefaction may be significant only for densities larger than a certain minimum. In addition, laboratory test results confirmed that, initial effective confining stress does not have any influence on the resistance to liquefaction at loose density ( $D_r = 19\%$ ) state (Thomas 1992). But at high relative densities of 40% and 59%, resistance to liquefaction decrease with increase in initial effective confining stress, height decrease being associated with the densest state. So, it is obvious that resistance to liquefaction of sand decrease with increase in initial effective confining pressure and this effect is more pronounced as the sand specimens become denser.

A significant amount of research has been conducted in the field of soil liquefaction around the world, but there are very limited numbers of laboratory research (Hoque et al. 2013, Karim and Alam, 2014) have been undertaken to evaluate liquefaction resistance of local soils. A study was therefore carried out to examine the liquefaction resistance of locally available soils.

### 3 EXPERIMENTAL INVESTIGATIONS

#### 3.1 Test Materials

For this research, two different types of poorly graded sands were collected; one from subsurface at Rooppur, Pabna and another from the bed of Piyain river at Jaflong, Sylhet. Index properties of the tested sands are given in Table 1. Both sands are grey in color and composed of subrounded particles in shape. According to Unified Soil Classification System these sands are classified as poorly graded sands with silt (SP-SM).

Table 1. Index properties of the sands

Index Properties	Rooppur sand	Piyain river sand
Specific gravity	2.66	2.65
Fineness Modulus	0.5	1
Mean grain size, $D_{50}$ (mm)	0.15	0.21
Fines (%)	13	11.7
Minimum density ( $\text{kN/m}^3$ )	13.15	12.15
Maximum density ( $\text{kN/m}^3$ )	17.95	16.7

Particle size distribution curves for Rooppur sand and Piyain river sand are presented in Figure 1. From these curves it can be observed that, both sand samples contain appreciable amount of fine particles.

### 3.2 Specimen Preparation

Soil specimens of size 142 mm in height and 71 mm in diameter were prepared using wet tamping technique. After taking required amount of dry sand in a container, a measured amount of de-aired water was added to the sand to bring the moisture content approximately to 10 percent by weight of dry sand. The sand and water was then mixed thoroughly and the container was sealed and kept for half an hour to insure uniform water content distribution throughout the sand. The moist sand was then placed into the mold in six separate layers of equal mass and thickness. The layer mass was determined from the target relative density of the specimen. Each layer was compacted using a manually operated aluminum hammer of diameter 35.5 mm, weight of 1000 gm and equipped to provide a free fall height of 152.4 mm. The numbers of blows required on each layer to achieve target relative density was determined by several trials.

A total of 26 soil specimens were prepared using Rooppur sand at three different relative densities of 30%, 50% and 70% and tested at a constant initial effective stress of 100 kPa. Using Piyain river sand, a total of 11 specimens were prepared at a constant relative density of 55% and tested at two different effective confining pressures of 50 kPa and 100 kPa. In both test series, cyclic stress ratio was kept in the range of 0.10 to 0.40.

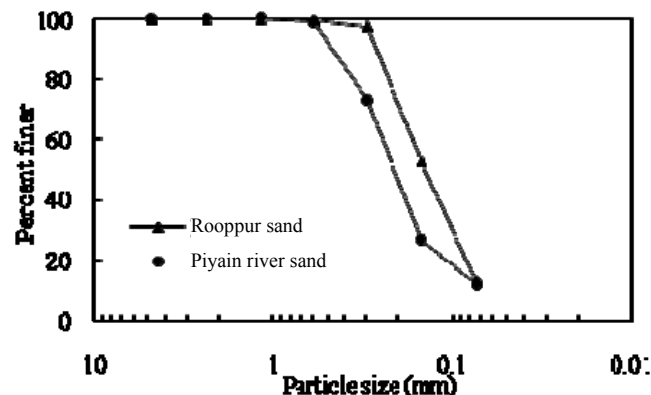


Figure 1. Particle size distribution curves

### 3.3 Cyclic Triaxial Test

The prepared specimen was sealed in a water tight rubber membrane with O-ring and confined in a triaxial chamber where it was subjected to a confining pressure of 20 kPa. In

order to improve initial saturation of the specimen, carbon dioxide (CO<sub>2</sub>) was allowed to flow through the specimen at a low pressure (less than 20 kPa) in order to replace the air in the specimen pores. This was done because CO<sub>2</sub> has a much higher solubility in water than air, allowing a higher degree of saturation to be reached at lower backpressure. After 30 minutes, the flow of CO<sub>2</sub> was stopped and a tank of de-aired water was attached to the drainage line on the bottom platen. The de-aired water was then percolated from the bottom trough the top of the specimen by gravitational force in order to increase the degree of saturation and percolation was continued until all CO<sub>2</sub> from specimen's pores has been replaced. Once the desired volume of de-aired water had flowed through the specimen, the drainage valves on the cell were closed and the de-aired water line removed. The drainage line is then connected to the pore pressure line. The specimen was then saturated with de-aired water using backpressure saturation. The backpressure was increased gradually while maintaining the effective confining pressure at 10 kPa. This process was continued until the Pore Pressure Parameter B value exceeded 0.95. Following saturation, the sand specimen was isotropically consolidated to desired effective stress. At the end of the consolidation it was ensured that the pore pressure parameter B remains unchanged.

Undrained cyclic loading was then applied on the specimen using stress controlled method. The magnitude of cyclic load to be applied on the soil specimens for the desired cyclic stress ratio was automatically calculated by operating software based on the initial input parameters. In the entire test program, a harmonic cyclic load was applied using sine wave with a frequency of 1 Hz. The maximum peak to peak axial strain of 10% was recorded. The numbers of loading cycles was limited to 200 cycles with a specified data recording speed of 100 data points per cycle to give the adequate resolution to measure sample response in terms of load, deformation and pore water pressure. During the whole test procedure enormous amount of data were recorded such as axial deformation, cell pressure, cyclic load, and sample pore water pressure, normal stress, and shear stress using the cyclic triaxial software.

### 3.4 Data calculation

As the deviator stress cycles between compression and extension, pore water pressures in the specimen builds up steadily, effective stress decreases, and the specimen undergoes axial deformation. Excess pore water pressure builds up steadily with the applied loading cycles, and eventually approaches a value equal to the initially applied confining pressure, thereby producing an axial deformation of about 5% in double amplitude. Such a state has been referred to as initial liquefaction or simply liquefaction. Typical undrained response of a

specimen in the form of deviator stress, axial deformation and induced excess pore water pressure with number of loading cycles obtained at cyclic stress ratio of 0.22 and initial effective confining stress of 100 kPa at relative density of 50% are given in Figure 2.

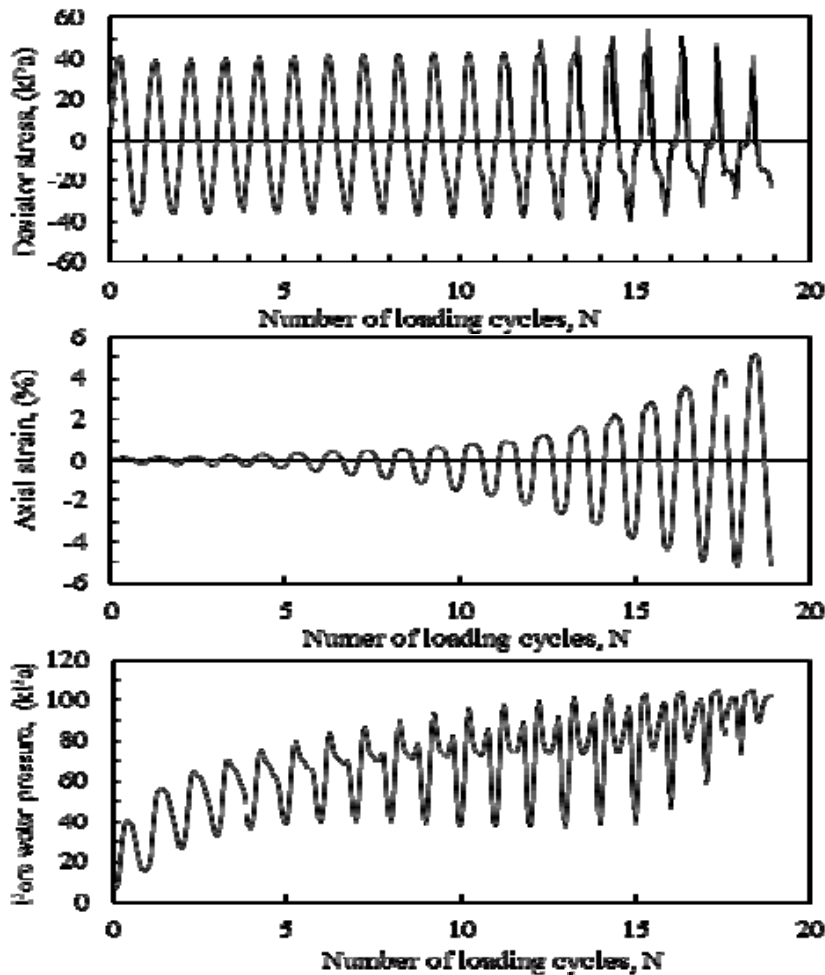


Figure 2. Typical undrained response of a specimen (a) deviator stress, (b) axial strain, and (c) induced excess pore water pressure with number of loading cycles

It can be seen from Figure 2 that, under constant amplitude of cyclic deviator stress applications the excess pore water pressure increases gradually and reached the value just equal to the initial applied effective confining pressure. At the beginning of the test development excess pore water pressure in the specimen is relatively slow and the axial deformation in the specimens is small. As the pore water pressure start to increase rapidly, axial deformation also speeds up. When excess water pressure reached just equal to initial effective confining pressure, it take only few cycles to reach 5% double amplitude axial strain, which is defined as initial liquefaction.

For each cyclic stress ratio, number of cycles required to reach 5% double amplitude axial strain are recorded. Such data from several tests are then combined and plotted as cyclic stress ratio versus number of cycles required to reach initial liquefaction, which is commonly known as liquefaction resistance or cyclic triaxial test strength curve. From cyclic strength curve, the liquefaction resistance of the specimen is specified in terms of magnitude of cyclic stress ratio (CSR) required to reach 5% double amplitude axial strain in 20 cycles of uniform load application.

## 4 RESULTS AND DISCUSSION

### 4.1 Effects of relative density

Cyclic shear strength curves constructed based on 26 undrained cyclic triaxial tests on Rooppur sand at three different relative densities are shown in Figure 3 and the assessed liquefaction resistance corresponding to relative densities of 30%, 50% and 70% are 0.15, 0.21 and 0.24 respectively. It can clearly be seen from Figure 3 that, the increase in relative density results in increase in liquefaction resistance. Controlling initial test conditions and test procedures identical it was noticed that, the change in relative density from 30% to 50% results in 40% increase in liquefaction resistance, while change in relative density from 30% to 70% results in 60 % increase in liquefaction resistance. It is also apparent that the cyclic strength curve corresponding to each relative density shifts consistently to the right along x-axis as the relative density becomes higher. Which implies that, the number of cycles required to occur initial liquefaction increase with increase in relative density. So, an increase in relative density causes significant increase in resistance against liquefaction, thereby making soils less susceptible to liquefaction.

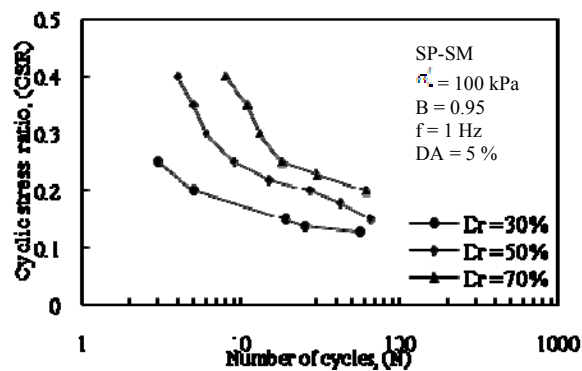


Figure 3. Cyclic shear strength curves for relative density of 30%, 50% and 70% at initial effective confining pressure of 100 kPa

#### 4.2 Effect of Confining Pressure

Liquefaction resistance curves generated based on a total of 11 undrained cyclic triaxial tests on Piyain river sand at two different initial effective confining pressure of 50 kPa and 100 kPa at a constant relative density of 55% are depict in Figure 4. It can be clearly seen from Figure 4 that, increase in initial effective confining pressure results dramatic reduction of resistance against liquefaction. Remaining initial test conditions and test procedures identical it was observed that, an increase in initial effective confining pressure from 50 kPa to 100 kPa caused liquefaction resistance to decrease from 0.30 to 0.12. Hence, soils at high effective confining stress are more susceptible to liquefaction than those at low effective confining pressure.

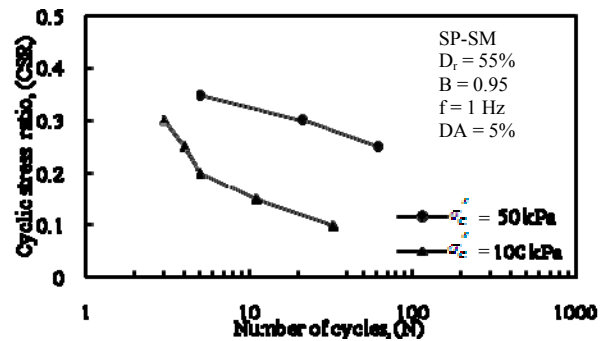


Figure 4. Cyclic shear strength curves for initial effective confining pressure of 50 kPa and 100 kPa at relative density of 55%

#### 5 CONCLUSIONS

Series of laboratory undrained cyclic triaxial tests were carried out on two different sands at different relative densities and effective confining pressures in order to examine the effects of relative density and initial effective confining pressure on liquefaction resistance of saturated sands. Two local sands were used in this investigation. Laboratory tests results illustrated that, relative density and initial effective confining pressure has great influence on liquefaction resistance. Increase in relative density results significant increase in resistance against liquefaction. The rate of increase is almost linear with relative density. On the other hand, resistance against liquefaction decreased dramatically as the initial effective confining pressure increased. As the initial effective confining pressure was doubled from 50 kPa to 100 kPa, the value of CSR decreased to about one-third from the value at initial confining pressure of 50 kPa. The results obtained in this research are reasonably in agreement with the results reported in literature considering initial test conditions and test procedures.

#### 4 REFERENCES

- Tatsuoka F., OchiK.,Fujii S. and Okamoto M. 1986b. Cyclic undrained triaxial and torsional shear strength of sands for different sample preparation methods. *Soils and Foundations*26(3), 23- 41.
- Carraro J.A.H., Bandini P. and Salgado R. 2003. Liquefaction resistance of clean and nonplastic silty sands based on cone penetration resistance. *Journal of geotechnical and geoenvironmental engineering* 129 (11), 965-976.
- Stamatopoulos C.A. 2010. An experimental study of the liquefaction strength of silty sands in terms of the state parameter. *Soil Dynamics and Earthquake Engineering*30 (8), 662-678.
- Liu C. and Xu J. 2013. Experimental study on the effects of initial conditions on liquefaction of saturated and unsaturated sand. *International Journal of Geomechanics* 15 (6), 04014100.
- Belkhatir M., Arab A., Della N., Missoum H., and Schanz T. 2010. Liquefaction resistance of chlef river silty sand: effect of low plastic fines and other parameters. *Acta Polytechnica Hungarica* 7 (2), 119-137.
- Vaid Y.P. and Sivathayalan S. 2000. Fundamental factors affecting liquefaction susceptibility of sands. *Canadian Geotechnical Journal* 37 (3), 592-606.
- Vaid Y., Chern J. and Tumi H. 1985. Confining pressure, grain angularity and liquefaction. *Journal of geotechnical and geoenvironmental engineering* 111 (10), 1229–1235.



## **PART-XI**

# **EVALUATION OF LIQUEFACTION POTENTIAL FROM SPT AND CPT: A COMPARATIVE ANALYSIS**

**BANGLADESH NETWORK OFFICE FOR  
URBAN SAFETY (BNUS), BUET, DHAKA**

**Prepared By: Mohammad Mominul Hoque  
Mehedi Ahmed Ansary**

## 1 INTRODUCTION

The Standard Penetration Test (SPT) and Cone Penetration Test (CPT) are the two most widely used in-situ tests for evaluating the liquefaction characteristics of soils. The basic framework for liquefaction evaluation methods (Seed and Idriss, 1971) based on SPT first began to evolve after the wake of a pair of devastating earthquakes that occurred in Alaska and Niigata in 1964. Countless effort of numerous researchers (Seed et al. 1985, 2003, Youd et al. 2001, Boulanger and Idriss, 2014) have made subsequent progresses of liquefaction evaluating methods and continue to evolve today. The SPT based deterministic relationship (Seed et al. 1985) is one of the most widely accepted correlation for evaluation of seismically induced soil liquefaction and which has set standard for practicing engineers. On the other hand, CPT based correlations is increasingly used for liquefaction studies because of its consistency and efficiency, and is now represent nearly co-equal status with regard to accuracy and reliability relative to SPT based correlations. The fundamental of both methods, as adopted by numerous researchers, compares the earthquake induced cyclic stress ratios (CSR) with the cyclic resistance ratios (CRR) of the soil, usually determined from in-situ parameter such as SPT N-value or CPT cone tip resistance. Both SPT and CPT methods have significant relative advantages, and both tests are far better when used in combinations. This research intended to evaluate and compare liquefaction potential using both SPT and CPT based deterministic correlations.

## 2 FIELD INVESTIGATIONS

In this research, field investigations were carried out along the riverbank of the Jamuna River, Bangladesh. The geologic formations of the research site are mainly consisting of alluvial sand and silt deposits of Holocene age. The alluvial sands are light to brown-grey coloured, coarse to fine silty sand of subrounded in shape. The sand contains mostly quartz, feldspar, mica and significant amount of heavy minerals. The alluvial silts have the same color as the sands, but are fine sandy to clayey silt and are poorly stratified (Alam et al. 1990).

A total of four pairs of SPT and CPT tests were performed in different locations within the study area and each pair was carried out as close as possible, maximum horizontal distance not greater than 10m. Boreholes for the SPT were advanced by percussion method with bentonite slurry and an automatic type SPT hammer-release was used for the measurement of N-values from SPT. Potential source of uncertainty that may affect N-values have been carefully taken into account. The split spoon sampling method was used to obtain

representative disturbed soil samples from boreholes and used for laboratory investigations. The SPT N-value and samples were collected every 1.52 m intervals.

CPT soundings were advanced using a Hogentoglar type piezocone penetrometer with a cross sectional area of  $10 \text{ cm}^2$  and which can measure the pore water pressure ( $u_2$ ), as well as the cone tip resistance ( $q_c$ ) and sleeve friction ( $f_s$ ). To perform CPT sounding, the cone was pushed vertically into the ground at a constant rate of approximately 20 mm/sec. During the advancement, measurements of dynamic pore water pressure, cone tip resistance and sleeve friction were recorded continuously at increments of 10 mm. The modified cone tip resistance ( $q_{c,1,mod}$ ) in MPa (top scale) and normalized SPT  $N_{1,60}$  values (bottom scale) are presented in Figure 1.

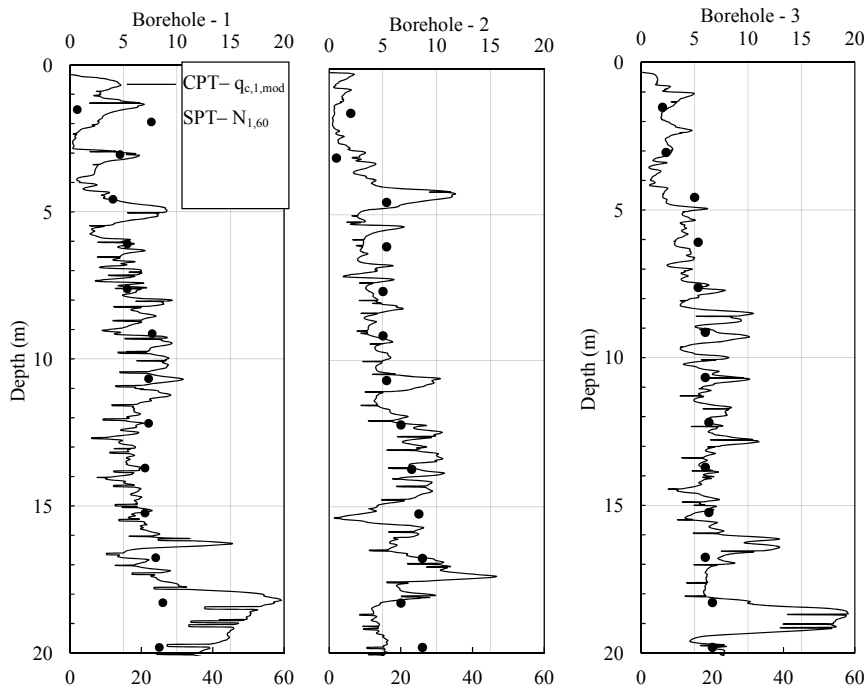


Figure 1. Penetration depth vs. modified cone tip resistance  $q_{c,1,mod}$  and normalized  $N_{1,60}$  values for all boreholes.

It has been found that, the soils within the test area primarily comprised of silt, fine and medium sands, and clay. As such, the combination of silt and sand are generally non-plastic and the combination of silt, clay and sand are low-plastic. Soils are moist from ground surface and ground water table is located approximately at 3 m below from ground surface. Density state of soil at different depths varies from loose to medium dense.

### 3 LABORATORY INVESTIGATIONS

Laboratory investigations included mainly visual observations and mechanical sieve analysis. Soil samples recovered from various depths were individually assessed and classified based on sieve analysis. Samples are light brown to grey in colour and grains are mostly subrounded in shape. Out of 52 recovered samples, 44 samples were used for sieve analysis. Soil samples obtained from 1.52 m and those contained considerable amount clay were excluded from sieve analysis. From sieve analysis it was observed that soils are containing appreciable amount of fines (material finer than 0.075 mm) ranging from 3.5 to 39.2 percent, fineness modulus (F.M.) varied from 0.18 to 1.11 and mean grain size ( $D_{50}$ ) in the range of 0.09 to 0.23 mm. Based on the sieve analysis results, the soils were generally classified into two groups; either well graded sands with little silt or poorly graded sands with silt. According to unified soil classification system, the soils can be symbolized as SW and SP-SM respectively. As fines content is one of the important parameter in liquefaction analysis from deterministic relationships, only fines content for each borehole are presented in Table 1.

Table 1. Fines content of sand at different boreholes.

Depth (m)	<i>BH-1</i>	<i>BH-2</i>	<i>BH-3</i>	<i>BH-4</i>
3.05	26.8	ND*	17.96	ND*
4.57	32.5	32.44	16.89	ND*
6.10	32.5	26.39	19.8	ND*
7.62	38.4	36.35	20.7	5.85
9.14	11.3	39.2	16.95	6.25
10.67	12.4	38.1	17.8	5.5
12.19	8	38	7.44	5.5
13.72	17.3	22	5.5	5.39
15.24	12.5	24.4	4.15	5.4
16.76	7.68	5.85	5.05	5.15
18.29	32.03	7.5	4.95	6.75
19.81	22.7	6.85	3.5	6

BH = Borehole and ND\* = not determined

### 4 DATA ANALYSIS

The SPT and CPT based deterministic relationships compares the earthquake-induced cyclic stress ratios ( $CSR_{eq}$ ) with the in-situ equivalent uniform cyclic stress ratios ( $CSR_{eq,M=7.5,1atm}$ ) of the soil. The soil's  $CSR_{eq,M=7.5,1atm}$  is correlated to in-situ parameters obtained from SPT blow count (N-values) and CPT penetration resistance (cone tip resistance,  $q_c$ ). The measured

SPT N-values, normalized for both effective overburden stress and energy, equipment and procedural factors affecting SPT testing to  $N_{1,60}$  values and CPT cone tip resistance,  $q_c$  is normalized and modified to  $q_{c,1,mod}$  for effective overburden stress and the frictional effects of apparent fines content and character. Normalized  $N_{1,60}$  and modified  $q_{c,1,mod}$  is then used to calculate  $CSR_{eq,M=7.5,1atm}$  from deterministic relationships. In the deterministic correlations both  $N_{1,60}$  and  $q_{c,1,mod}$  represented as a function of fines content. It should be noted that,  $CSR_{eq,M=7.5,1atm}$  is obtained after adjusting both for magnitude-correlated duration weighting factor and effective initial overburden stress (expressed through a  $K_\sigma$  factor). Factor of safety (often known as liquefaction potential or liquefaction resistance) against liquefaction can now be obtained from the ratio of  $CSR_{eq,M=7.5,1atm}$  to  $CSR_{eq}$ . In general, it is assumed that, if the value of safety factor greater than unity, the deposit is safe against liquefaction for a given earthquake.

#### 4.1 Earthquake-induced Cyclic Stress Ratio

The earthquake-induced cyclic stress ratio, at a given depth, within the critical soil stratum, is usually expressed as a representative value (or equivalent uniform value) equal to 65% of the maximum cyclic shear stress ratio as –

$$CSR_{eq} = 0.65 \times (a_{max}/g) \times (\sigma_v/\sigma'_v) \times (r_d) \quad (1)$$

Where,  $\sigma_v$  and  $\sigma'_v$  are the vertical total stress and effective stress at a given depth,  $a_{max}/g$  is the maximum horizontal acceleration (as a function of gravity) at the ground surface, and  $r_d$  is the shear stress reduction factor that accounts for the dynamic response of the soil profile. In this research maximum horizontal acceleration at the ground surface was taken 0.25g and values of  $r_d$  were estimated from the depth vs.  $r_d$  correlation (after Cetin and Seed, 2000).

#### 4.2 In-situ Uniform Cyclic Stress Ratio

The measured SPT N-values were first corrected for effective overburden stress, energy, equipment, and procedural effect to obtained fully standardized  $N_{1,60}$  values as –

$$N_{1,60} = (1/\sigma'_v)^{0.5} \times C_R \times C_s \times C_B \times C_E \quad (2)$$

Where,  $C_R$  is the correction for rod length,  $C_s$  is the correction for non-standardized sampler configuration,  $C_B$  is the correction for borehole diameter, and  $C_E$  is the correction for hammer energy efficiency.

Similarly, measured cone tip resistances,  $q_c$  were normalized and modified for effective overburden stress and the frictional effects of apparent fines content and character to obtained to  $q_{c,1,mod}$  values as

$$q_{c,1,mod} = (q_c \times (P_a/\sigma'_v)^c) + (\ddot{A}q_c) \quad (3)$$

Where,  $P_a$  is the atmospheric pressure, normalization exponent ( $c$ ) is a function of both normalized tip resistance ( $q_{c,1}$ ) and friction ratio ( $R_f$ ),  $\ddot{A}q_c$  is the function of  $q_{c,1}$ ,  $R_f$  and  $c$ .

Then, normalized  $N_{1,60}$  and modified  $q_{c,1,mod}$  were used to calculate  $CSR_{eq,M=7.5,1atm}$  from deterministic relationships (Seed et al, 2003). An earthquake magnitude of  $M_w = 7.5$  was assumed for the adjustment of magnitude-correlated duration weighting factor. Soil's unit weights were back calculated from SPT N-value vs. unit weight correlation (Bowles, 1982) to estimate total and effective overburden stresses.

## 5 RESULTS AND DISCUSSIONS

Factor of safety obtained from SPT and CPT based deterministic relationships are presented in Figure 2 for different boreholes. As SPT N-values were recorded every 1.52 m intervals, factor of safety for both SPT and CPT were also evaluated at same depth intervals. In case of CPT, an average value of cone tip resistances over 0.30 m were taken as penetration resistance, at same depths where SPT blows were counted. For all boreholes it can be observed from Figure 2 that, majority of the cases safety factors obtained from CPT based relationship gives lower values as compared to SPT based relationship. Although safety factors obtained both SPT and CPT are found to be mostly identical throughout the boreholes depth, for some depths, factor of safety obtained from CPT are higher than that from SPT. Safety factors obtained from CPT analysis indicate that, liquefaction can occur throughout the entire depth of 20m in all the boreholes, except some thin layers in borehole-2 and borehole-3. On the other hand, safety factors obtained from SPT analysis indicate that liquefaction can be expected in all borehole locations at depths less than 10 m and 12.5 m in borehole-1 and borehole-2 respectively.

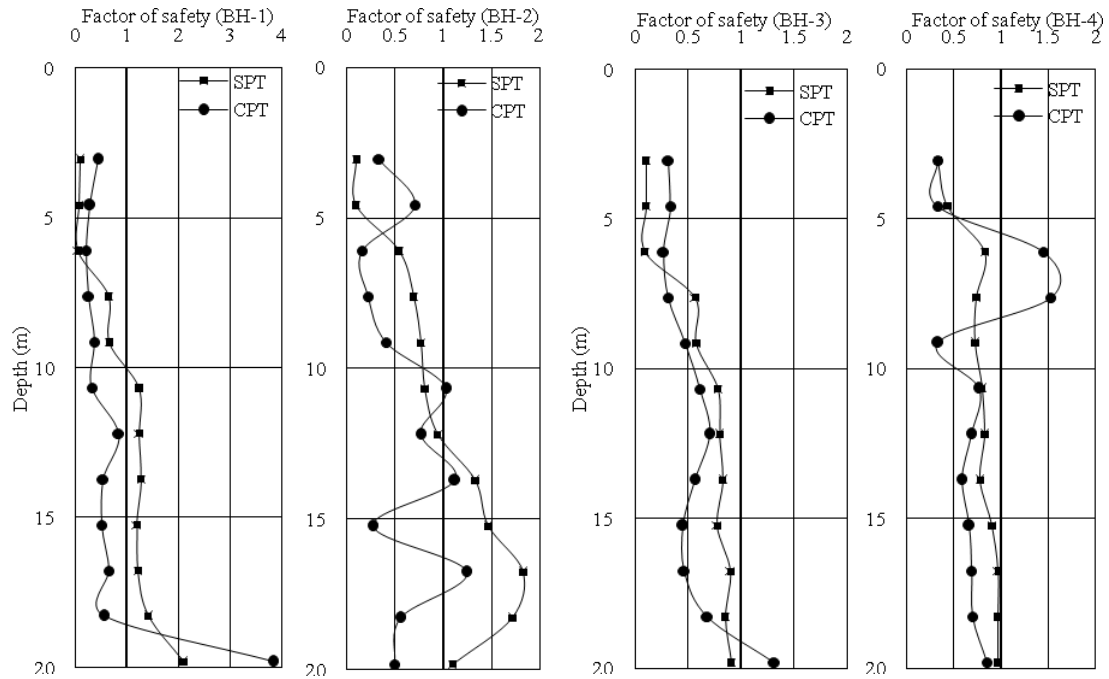


Figure 2. Factor of safety against liquefaction from SPT and CPT.

Inconsistency in safety factors evaluated from SPT and CPT may be resulted due to the variations in recorded SPT N-values and CPT cone tip resistances at same depth. Probably these variations were due to boreholes distance between each pair of SPT and CPT. In addition to that, energy efficiency of SPT hammer was not directly estimated in the field and efficiency ratio was assumed as 60% of the applied energy. Due to this reason, factor of safety against liquefaction from SPT may have resulted in over estimation compared to CPT.

## 6 CONCLUSION

Four pairs of SPT and CPT tests were carried out to evaluate and compare liquefaction potential from SPT and CPT based deterministic relationships. It was observed that, the recorded SPT N-value and CPT resistance considerably vary at same depth. Due to this inconsistency, safety factors against liquefaction results an over and/or under estimation compare to each other. So, it is highly recommended to ensure high quality tests data to confirm accurate and reliable results when both methods are used in combinations.

## 7 REFERENCES

- Alam M.K., Hasan S.A.K.M., Khan M.R. and Whitney J.W. 1990. Geological Map of Bangladesh. Geological Survey of Bangladesh, Dhaka.
- Bolton Seed H., Tokimatsu K., Harder L.F. and Chung R.M. 1985. Influence of SPT procedures in soil liquefaction resistance evaluations. *Journal of Geotechnical Engineering* 111(12), 1425-1445.
- Boulanger R.W. and Idriss I.M. 2014. CPT and SPT based liquefaction triggering procedures. Rep. No. UCD/CGM-14, 1.
- Bowles, J.E. 1982. *Foundation Analysis and Design*. McGraw-Hill, New York.
- Cetin K.O. and Seed, R.B. 2000. Earthquake-Induced Nonlinear Shear Mass Participation Factor ( $r_d$ ). Geotechnical Engineering Research Report No. UCB/GT2000/08. University of California, Berkeley.
- Seed H.B. and Idriss I.M. 1971. Simplified Procedure for Evaluating Soil Liquefaction Potential. *Journal of the Soil Mechanics and Foundations Division* 97 (9), 1249-1273.
- Seed, H. B., Tokimatsu, K., Harder, L. F., Chung, R. M. 1985. Influence of SPT procedures in soil liquefaction resistance evaluations. *Journal of Geotechnical Engineering*, 111(12), 1425-1445.
- Seed R.B., Cetin K.O., Moss R.E. Kammerer A.M., Wu J., Pestana J.M., Riemer M.F., Sancio R.B., Bray J.D., Kayen R.E. and Faris A. 2003. Recent advances in soil liquefaction engineering: a unified and consistent framework. In *Proceedings of the 26<sup>th</sup> Annual ASCE Los Angeles Geotechnical Spring Seminar*. Long Beach, California.
- Youd T.L., Idriss I.M., Andrus R.D., Arango I., Castro G., Christian J.T., Dobr, R., Finn W.L., Harder Jr L.F., Hynes M.E. and Ishihara K. 2001. Liquefaction resistance of soils: summary report from the 1996 NCEER and 1998 NCEER/NSF workshops on evaluation of liquefaction resistance of soils. *Journal of geotechnical and geoenvironmental engineering* 127(10), 817-833.



## **PART-XII**

# **CPT-SPT BASED CORRELATIONS FOR COHESIONLESS SOIL FOR UTTARA 3<sup>RD</sup> PHASE, DHAKA**

**BANGLADESH NETWORK OFFICE FOR  
URBAN SAFETY (BNUS), BUET, DHAKA**

**Prepared By: Zinan A. Urmi**

**Mehedi Ahmed Ansary**

## 1 INTRODUCTION

Standard Penetration Test (SPT) and Cone penetration Test (CPT) are the most commonly used in situ tests to demarcate soil stratigraphy. It is also important for determining the geotechnical engineering properties of surface/ subsurface soils. Several geotechnical design parameters of the soil are associated with the SPT. On the contrary CPT is becoming progressively more popular for site investigation and geotechnical design, based on the soil type and testing method. For many construction projects, SPT for the preliminary soil investigation is generally used, while CPT is used for detailed soil investigation and construction quality control. For this reason, it is very imperative to correlate the SPT N-value to CPT data so that the available data could be effectively utilized.

## 2 BACKGROUND

Since last few decades, much research has taken place to properly utilize abundant experiences and available database on SPT to more reliable CPT. As a result, a considerable number of correlations have been proposed by several researchers between CPT cone tip resistance ( $q_c$ ), SPT N-values and other engineering soil properties. These correlations can be considered in three major groups. Most of the primary correlations considered  $q_c/N_{60}$  as a function of grain characteristics, such as mean grain size ( $D_{50}$ ) and/or fines content ( $f_c$ ). Some other researchers proposed a constant value of  $q_c/N_{60}$  for different soil types in a chart of corrected cone tip resistance ( $q_t$ ) versus friction ratio ( $R_f$ ).

Many researchers have pointed out the importance of CPT -SPT correlations, it shows that there is a need for reliable CPT-SPT correlations so that CPT data can be used in existing SPT-based design approaches.

Kulhawy and Mayne emphasize on the advantages of having a procedure to interrelate  $N_{60}$  and  $q_c$ . These tests represent the most common in situ soil testing used worldwide and both of them representing soil resistance to penetration (although the SPT is dynamic and the CPT is quasi-static).

Back in the late 1950s and early 1960s, several researchers suggested constant values of  $q_c/N_{60}$  for different soil types. A number of researchers proposed that the  $q_c/N_{60}$  ratio is a function of the mean grain size ( $D_{50}$ ) of the soil. They concluded that the smaller the  $q_c/N_{60}$  ratio, the finer grained the soil. The proposed classification chart was recommended to

estimate the mean particle size. Clearly, the  $q_c/N_{60}$  ratio increases with increasing grain size ( $D_{50}$ ); conversely, the ratio decreases with increasing fine material. Scatter in data tends to increase with the increase in sand grains size ( $D_{50} > 1.0$  mm). This may have related to the significant effect of large particles on the penetration.

Other investigators reported that the correlation could be more relevant by relating the fine contents ( $F_c$ ) to the  $q_c/N_{60}$  ratio. Similarly, their study results indicate that the  $q_c/N_{60}$  ratio is smaller with sands of high fines content than for clean sands. Kulhawy and Mayne have compiled a number of studies in one graph to verify a general trend between the  $q_c/N_{60}$  ratio and the fines content. The  $N_{60}$ -values used in that research were the uncorrected due to some limitation of the data.

Robertson et al. (1983) presented the  $q_c/N_{60}$  ratio as a function of mean grain size, ' $D_{50}$ '. They proposed a soil behavior-type classification, giving  $q_c/N_{60}$  ratio for each soil classification zone based on cone penetration test with pore pressure measurement tests (CPTU, piezocone).

Ismael and Jeragh (1986) correlated CPT  $q_c$  values with SPT N-values for calcareous desert sands in Kuwait and compared their results with the values presented by Schmertmann (1970) for clean, fine to medium sands and slightly silty sands. Their proposed n- values were higher than those proposed by Schmertmann for clean, fine to medium sands and slightly silty sands. A close agreement of their test results in the form of  $q_c/N_{60}$  versus mean grain size ' $D_{50}$ ' were found when compared with the historical data of Robertson et al. (1983).

Danziger and de Velloso (1995) proposed a correlation between CPT and SPT for some Brazilian soils. Values found were in the same range obtained by Schmertmann (1970). Different types of correlation were tested, and a linear correlation was found better suited for practical applications. A general trend was obtained in a similar pattern of Robertson's curve (increasing n-values with increasing grain size).

Lunne et al. (1997) cited Jefferies and Davies (1993) who presented a soil classification chart estimating N-values. This new development considers  $q_c$  by taking into account pore water pressure ( $u$ ) and overburden stress, using piezocone.

Akca (2003) proposed SPT-CPT correlation for United Arab Emirates Soils. Results of his study showed higher values of  $n = q_c/N_{60}$  when compared to values found in the literature.

He explained that higher values are due to cementation, densification and Shelly structure or gravel layers in the United Arab Emirates soils.

McNulty & Harney (2010) have compared effective angle of internal friction estimated from the CPT with those determined from SPT N-values and laboratory triaxial tests. Their study revealed that effective angle of internal friction obtained from triaxial tests correlated well with those obtained from the CPT and SPT below the water table, but above the ground water obtained values from CPT and SPT were significantly high compared to laboratory measurement.

Research by Elbanna et al. (2011) suggested that, in the absence of site specific CPT-SPT correlations, it is suitable to use the general correlation proposed by Robertson, et al (1983). In the absence of grain size data, they have also proposed a new correlation using the  $q_t/(N)_{60}$  ratio of 0.45. However, some of the existing correlations provide best estimated relationship between  $q_c$  and N-value, but region specific study result presented by Elkateb and Ali (2010) represents quite inapplicability of existing correlations. Therefore, direct application of the average relationship presented in several correlations may lead to significant deviation from exact result.

Shahri et al. (2014) proposed a correlation between  $q_c$  and N-value for various soil layers, particularly in clayey soils with significant clay content in an area in southwest Sweden. They proposed linear and power relationships to predict  $q_c$  using N-value. The results of their study showed a good agreement with previous work by other researchers.

Tarawneh (2014) developed a multiple linear regression (MLR) and a symbolic regression (SR) models to predict N-value using CPT data for sand, sandy silt, and silty sand soils.

Asci et al. (2015) proposed exponential models to predict CPT  $q_c$  value from SPT N-values for silty clay, clayey silt, clay, and sandy silt.

#### **4 OBJECTIVE OF THE RESEARCH**

The primary objective of this research is

1. To examine the applicability of various existing CPT-SPT correlations for Uttara 3rd phase soils
2. To propose possible new correlations
3. To provide useful contribution for further improvement of region specific CPT-SPT correlations.

## 6 FIELD INVESTIGATION

By the appliance of cone penetration testing (CPT) and standard penetration testing (SPT) field investigations were carried out mostly. Six pairs of CPT and SPT were performed in different locations within the study area. In this research, field investigations were carried out in Uttara Residential Model Town (3<sup>rd</sup> Phase), Dhaka , Bangladesh in which each pair of CPT and SPT was carried out as close as possible and the horizontal distance was not greater than 1m. A map of Uttara Residential Model Town (3<sup>rd</sup> phase) is shown in Figure 6.1.

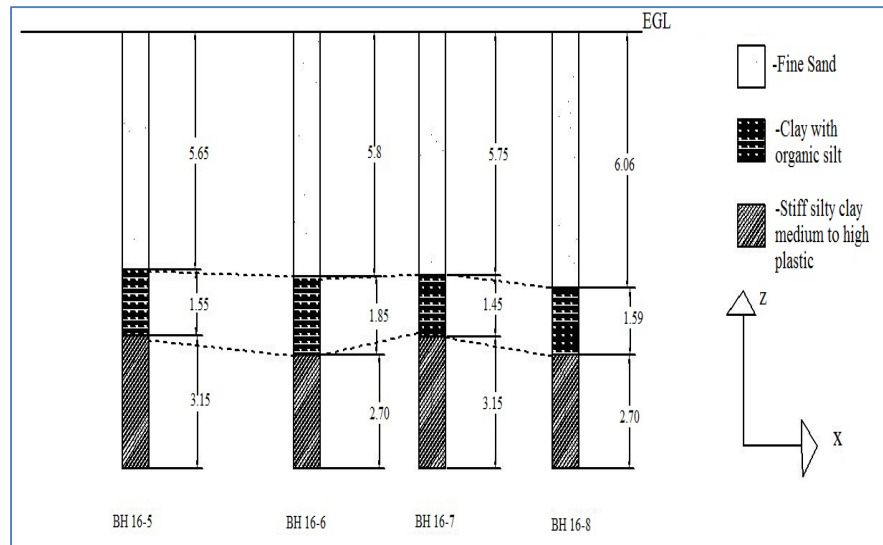


Figure 6.1. Study location (Uttara 3rd Phase)

The subsurface profile at study area can be divided into three strata based on the results of the subsurface explorations. The soil within the test area is largely comprised of fine sand and silt clay particles. The top layer consists of light grey to grey medium to loose fine sand trace

mica with a total thickness approximately 4.75 m to 7.5 m. Directly below this layer, a layer of dark grey silty clay with organic matter is situated to a depth varied from 7.65 m to 9.45 m. The bottom layer consists of high plastic grey medium stiff clay or medium plastic soft to medium stiff clay upto the depth of 10.35 m. Ground water table is located at 2.3-2.7 m below from EGL.

6 boreholes were investigated from which section profile of Bore Hole 16-6 is shown in figure 6.2 and 6.3.



**Figure 6.2 Cross sectional profile along X-axis of BH-16-6**

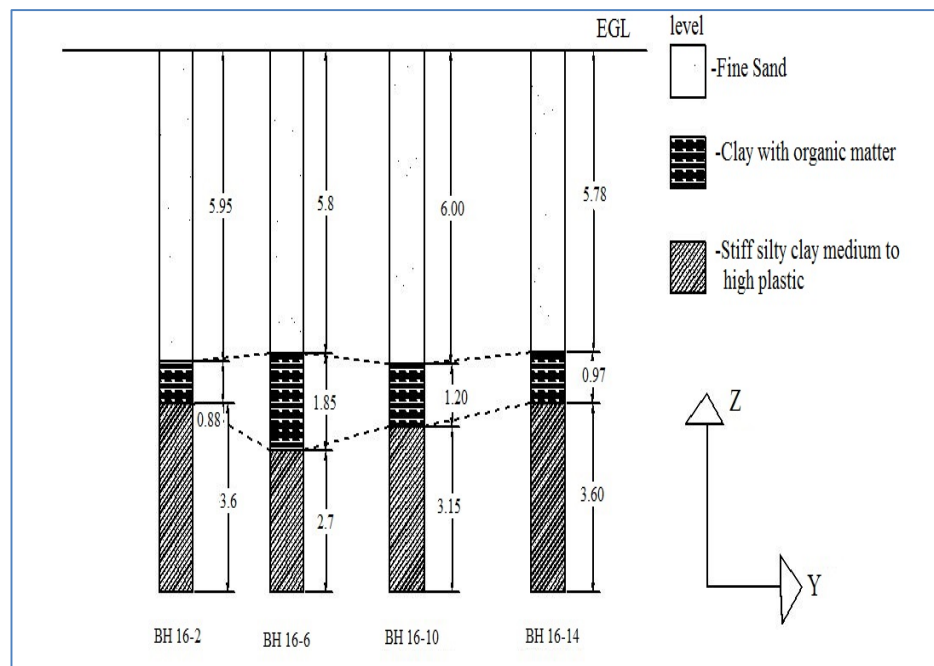


**Figure 6.3 Cross sectional profile along Y-axis of BH-16-6**

The corrected tip resistance ( $q_t$ ), corrected SPT value  $(N_1)_{60}$  values are presented in Figure 6.4

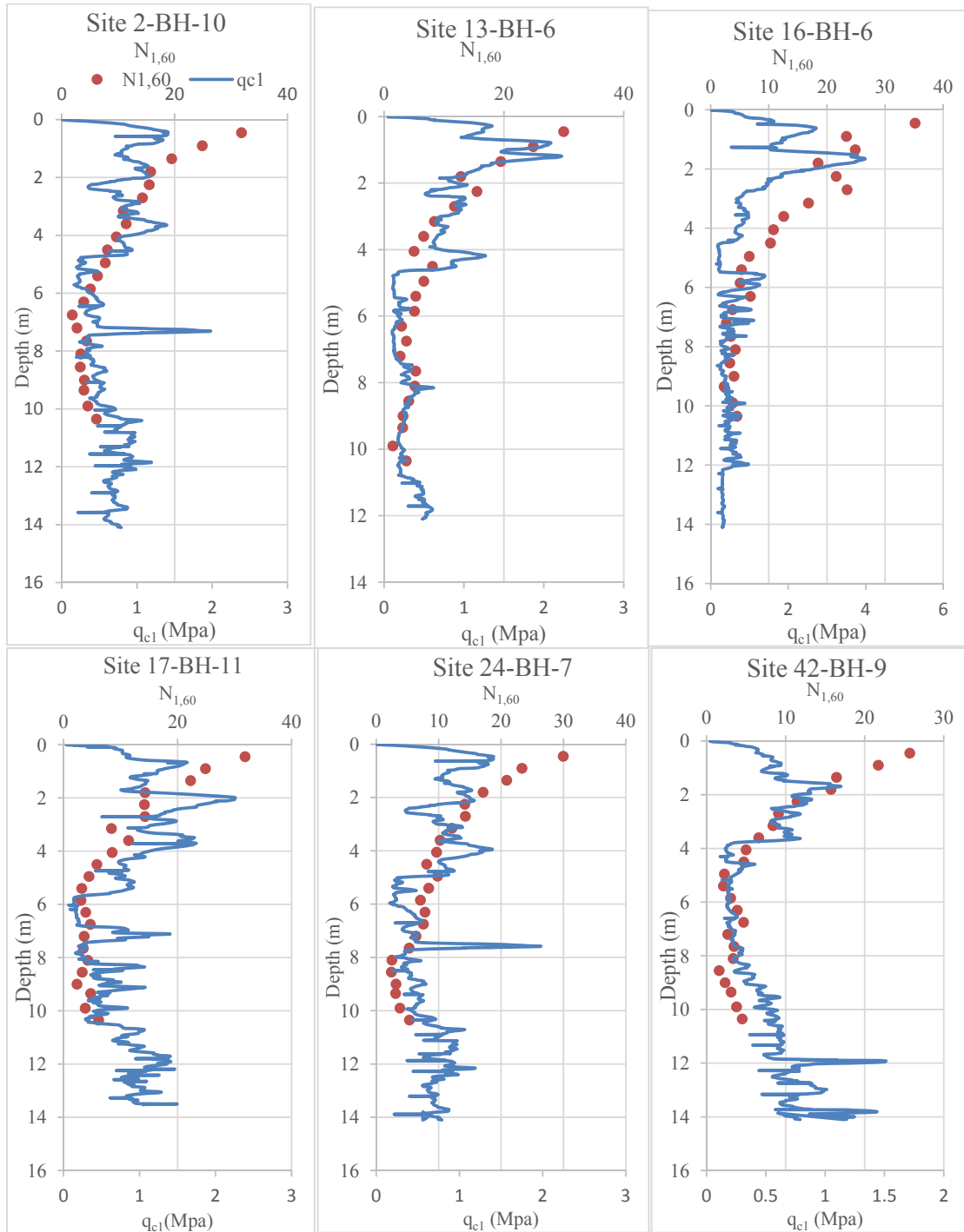


**Figure 6.4. Depth versus corrected cone tip resistance ( $q_t$ ), SPT  $N_{60}$  and  $(N_1)_{60}$  values for all borehole**

Note that, there was considerable variability in the measured SPT N-value indifferent boreholes at different depths ranging from 2 to 18 and maximum corrected cone tip resistance ( $q_t$ ) was close to 4 MPa consistency of the soils at different depth varies from stiff to loose.

### **Cone Penetration Test**

The cone penetration or cone penetrometer test (CPT) is a method used to determine the geotechnical engineering properties of soils and delineating soil stratigraphy. It was initially developed in the 1950s at the Dutch Laboratory for Soil Mechanics in Delft to investigate soft soils. Based on this history it has also been called the "Dutch cone test". Today, the CPT is one of the most used and accepted soil methods for soil investigation worldwide. In procedure Cone penetration testing two parameters is usually taken into account. One is pre- drilling and the other is verticality. In our test procedure a Hogentogler type piezocone penetrometer with a cross sectional area of 10 cm<sup>2</sup> was used as pre-drilling which can measure the pore water pressure ( $u_2$ ), as well as the cone tip resistance ( $q_c$ ) and sleeve friction( $f_s$ ). In order to perform the test correctly the thrust machine should be set up vertically. The deviation of the initial thrust direction from vertical should not exceed 2 degrees and push rods should be checked for straightness. In our test procedure the cone was pushed vertically into the ground at a constant rate of approximately 11-12.5m/min. During the procedure, measurements of dynamic pore water pressure, tip resistance and sleeve friction were recorded continuously at 10 mm depth increments. The typical penetration depth for this study was approximately 12-14 m below from ground surface. For soil exploration, a modern and expedient approach is offered by cone penetration testing (CPT) which involves pushing an instrumented electronic penetrometer into the soil and recording multiple measurements continuously with depth (e.g., Schmertmann, 1978; Campanella & Robertson, 1988; Briaud & Miran, 1992). Per ASTM and international standards, three separate measurements of tip resistance ( $q_c$ ), sleeve friction ( $f_s$ ), and porewater pressure ( $u$ ) are obtained with depth as depicted in figure 6.5

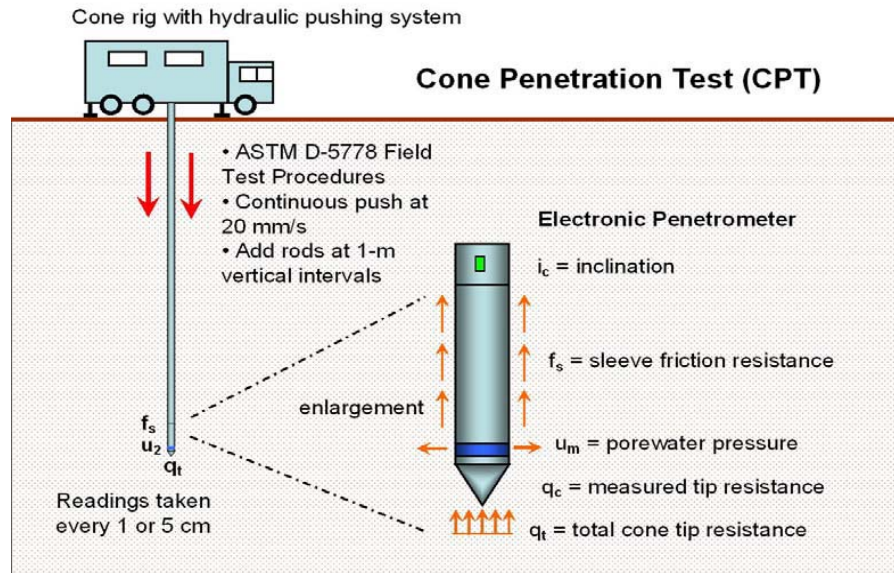
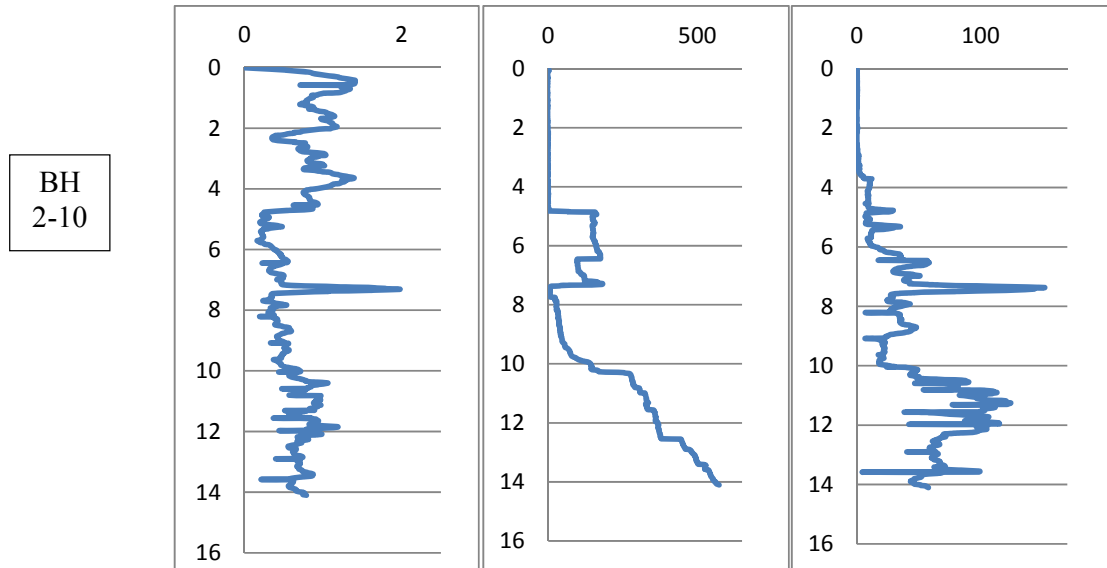
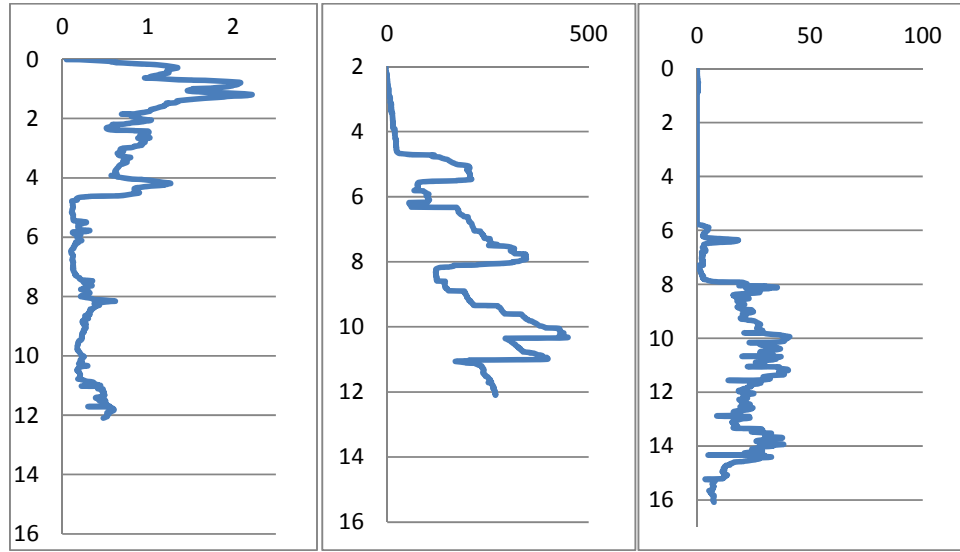


**Figure 6.5. Overview of the Cone Penetration Test (CPT) Per ASTM D 5778 Procedures.**

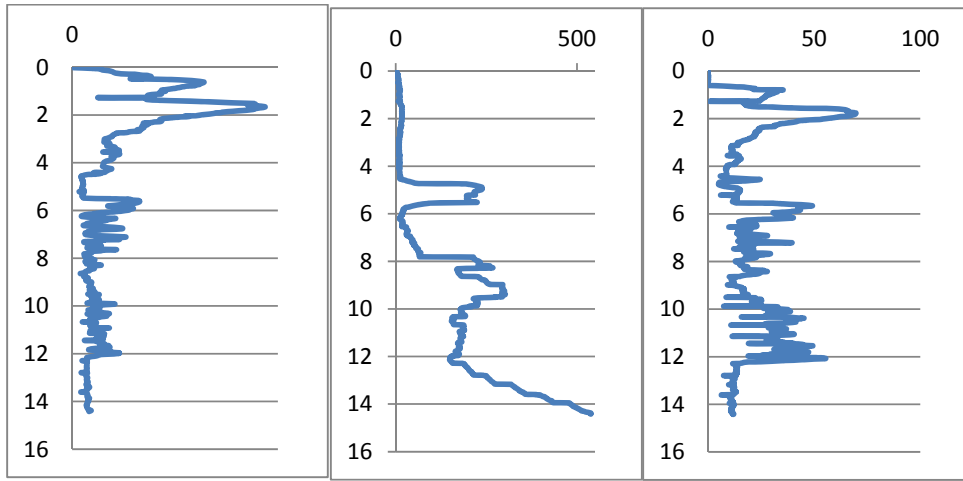
According to this we also obtained a relationship of Cone Resistance ( $q_t$ ), Sleeve friction ( $f_s$ ) and Pore pressure ( $u_2$ ) with Depth for the six bore holes. They are given below in figure 3.7.



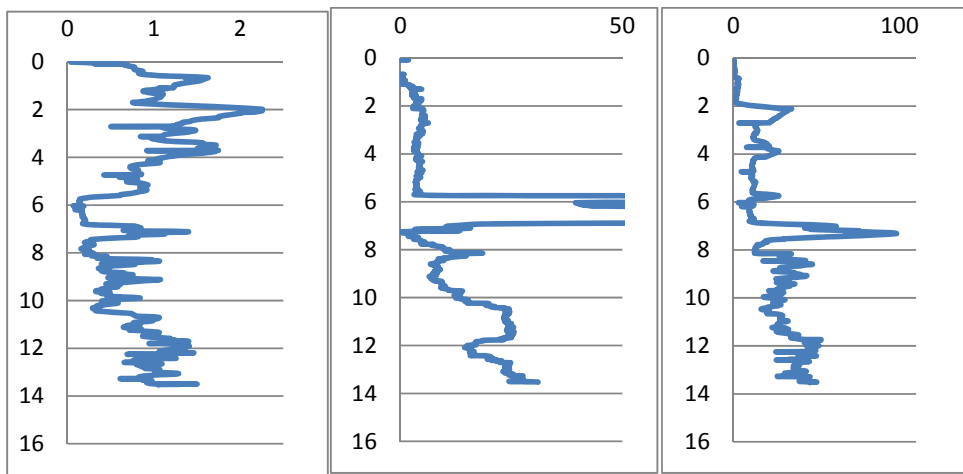
BH  
13-6



BH  
16-6



BH  
17-  
11



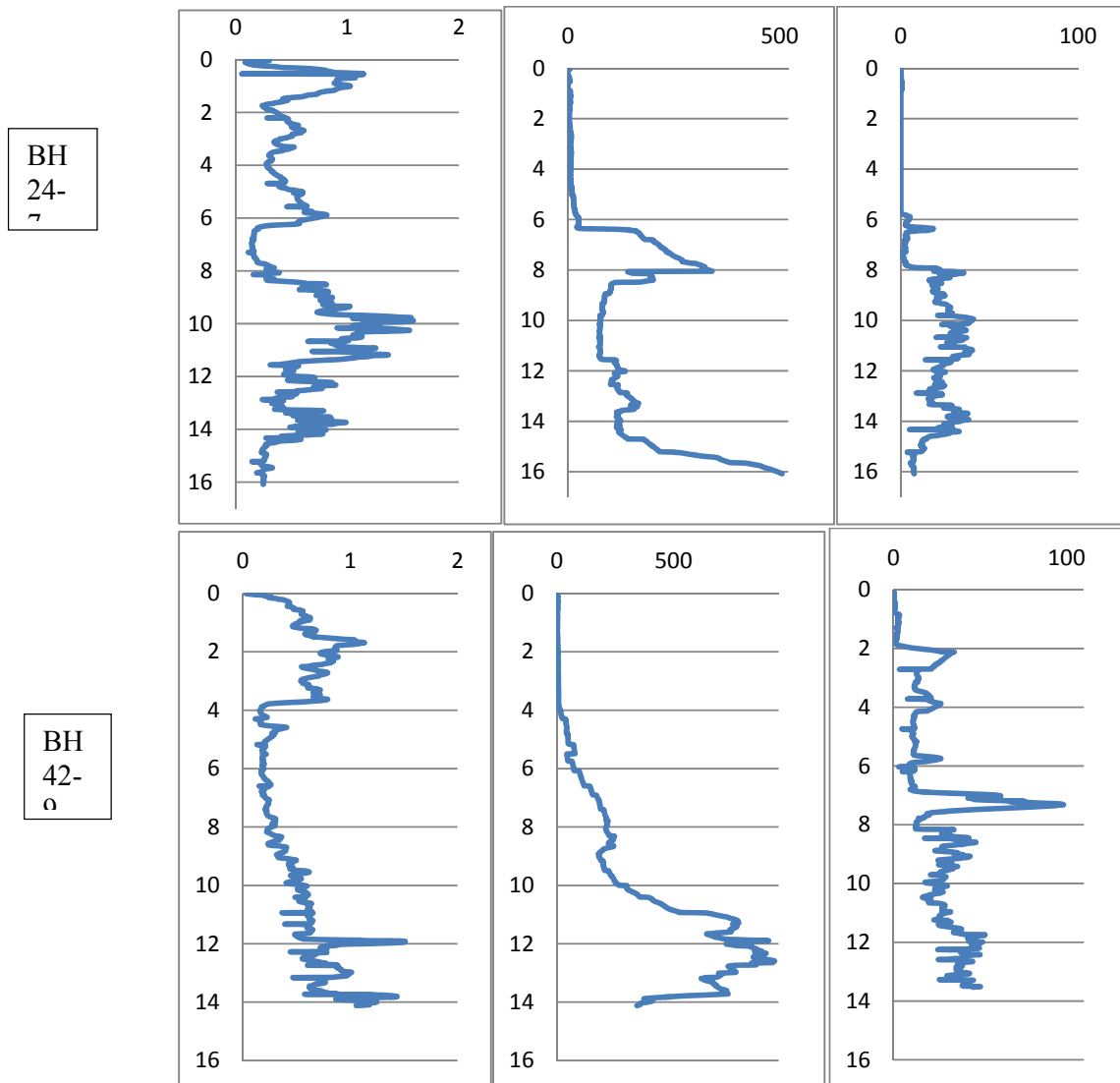


**Figure 6.6. Representative Soil profile for Cone resistance, Pore Pressure and friction ratio along Depth for Uttara 3rd phase**

## 7 Laboratory Test

The sand samples recovered in the sampler during the Standard Penetration Tests were used for laboratory test for determination of grain size distribution, unit weight relative density and effective friction angle.

### Sieve Analysis

A Sieve analysis is a practice or procedure used to assess the particle size distribution of a granular material. Sieve analysis was performed on each soil sample according to ASTM C136. Soil samples which were recovered from six bore holes were individually

assessed and classified based on dry sieve analysis for sieve analysis testing. These soils contained significant amounts of fines ( $f_c$ ) which ranged from 2.3 to 96.4. Fineness modulus is an empirical figure which was obtained by adding the total percentage of the sample of an aggregate retained on each of a specified series of sieves, and dividing the sum by 100. Range of fineness modulus was 0.02 to 1.02 and mean grain size ( $d_{50}$ ) was ranging from 0.12 to 0.19. Based on the sieve analysis results, the soils are generally classified into two groups; Well graded sands with little silt and Poorly graded sands with silt. According to the unified soil classification system, the soils can be symbolized as SW and SP-SM, respectively. The mean grain size ( $d_{50}$ ), percent finer than 0.074 mm ( $f_c$ ) and fineness modulus (F.M) for six boreholes are given in table 3.2.

Table 7.1. Grain Size Distribution

Depth m	bore hole 2-10			borehole 13-16			borehole 16-6			borehole 17-11			borehole 24-7			borehole 42-9		
	$d_{50}$	$f_c$	F.M.	$d_{50}$	$f_c$	F.M.	$d_{50}$	$f_c$	F.M.	$d_{50}$	$f_c$	F.M.	$d_{50}$	$f_c$	F.M.	$d_{50}$	$f_c$	F.M.
0.45	0.14	5.3	0.4	0.15	10	0.6	0.17	7.1	0.67	0.15	4.8	0.6	0.2	5.6	0.72	0.16	14	0.57
0.9	0.14	10	0.51	0.16	8.1	0.6	0.18	12.7	0.78	0.17	3.4	0.7	0.2	5.6	0.72	0.16	15	0.58
1.35	0.14	7.3	0.49	0.16	8.8	0.6	0.17	13.3	0.68	0.17	6	0.7	0.2	4.1	0.79	0.14	15	0.47
1.8	0.14	10	0.5	0.17	8.6	0.7	0.17	9.8	0.7	0.16	8.6	0.6	0.2	3.4	0.77	0.15	9.5	0.53
2.25	0.14	6.8	0.49	0.19	5.6	0.8	0.15	14.6	0.56	0.17	10	0.7	0.2	3.7	0.78	0.14	7.1	0.47
2.7	0.15	7.2	0.54	0.18	6.9	0.8	0.14	18.4	0.51	0.17	9.9	0.6	0.2	2.9	0.8	0.14	16	0.48
3.15	0.14	7	0.48	0.18	7.1	0.8	0.13	17.4	0.44	0.17	9.8	0.7	0.2	3.4	0.79	0.14	9.2	0.51
3.6	0.15	4.2	0.52	0.19	7.6	0.8	0.14	16.6	0.48	0.17	8	0.6	0.2	3.4	0.79	0.14	8.2	0.49
4.05	0.15	6.3	0.51	0.18	6.8	0.8	0.15	15.2	0.6	0.17	8.2	0.6	0.2	3.9	0.79	0.15	7.1	0.54
4.5	0.15	3.1	0.55	0.19	6.4	0.8	0.14	19.9	0.49	0.16	8.9	0.6	0.2	7.2	0.71	0.16	16	0.57
4.95	0.14	8.1	0.45	0.18	6	0.7	0.17	8.7	0.7	0.17	8.6	0.6	0.2	3.6	0.8	ND*	53	1
5.4	0.17	10	0.4	0.18	6.9	0.8	0.17	6.3	0.63	0.15	11	0.6	0.2	3.4	0.79	ND*	79	0.15
5.85	0.12	2.3	0.62	0.18	6.8	0.8	0.17	5.3	0.64	0.13	14	0.4	0.2	3.9	0.78	ND*	79	0.15
6.3	ND*	13	0.35	ND*	29	0.9	ND*	8.3	0.34	ND*	53	1	0.2	4	0.79	ND*	79	0.15
6.75	ND*	91	0.06	ND*	29	0.3	ND*	69.1	0.69	ND*	96	0	0.2	11	0.75	ND*	79	0.15
7.2	ND*	ND*	ND*	ND*	ND*	ND*	ND*	ND*	ND*	ND*	96	0	0.2	8.8	0.65	ND*	79	0.15

ND\*=Not-Determined

$d_{50}$  in mm

## Relative Density Test

Relative density or density index is the ratio of the difference between the void ratios of a cohesion less soil in its loosest state and existing natural state to the difference between its void ratio in the loosest and densest states. Porosity of a soil depends on the shape of grain, uniformity of grain size and condition of sedimentation. Hence porosity itself does not indicate whether a soil is in loose or dense state. This information can only be obtained by comparing the porosity or void ratio of the given soil with that of the same soil in its loosest and densest possible state and hence the term, relative density is introduced.

According to ASTM D2167 Relative Density Test was done which was done which is described below.

### Calibration of mould :

1. At first the inside diameter of mould was measured at different depths using a bore gauge and the average was taken.
2. Then the mould on a flat surface or flat plate was kept. The height at different positions was measured and the average was taken. (accuracy = 0.025 mm).
3. For loose state soil sample was poured in the container and the weight was taken.
4. For Dense state soil sample was poured in three layers by tamping two times in which the blowing was done 25 times each.



**Figure 7.1. Pouring soil sample in the container.**

### Minimum Density:

The mould was weighed accurately (W). The dry pulverized soil into the mould was poured through a funnel in a steady stream. The spout was adjusted so that the free fall of soil particle was always 25 mm. While pouring soil the spout must have a spiral motion from the rim to the centre. The process was continued to fill up the mold with soil upto about 25mm above the top. It was then leveled, with the soil and weight was recorded (W<sub>1</sub>).

**Volume of mould V cc**

**Mass of dry soil M<sub>s</sub> = (W<sub>1</sub> - W) gm**

**(γ<sub>d</sub>)<sub>min</sub> = M<sub>s</sub> / V g/cc**

**e<sub>max</sub> = Gγ<sub>s</sub> / (γ<sub>d</sub>)<sub>min</sub> - 1**

### Maximum Density:

The empty mould (W) was weighted. The collar on top of the mould was put and it was clamped. The mould was filled with the oven dried soil sample till 1 / 2 or 2 / 3 of the collar is filled. The mould was placed on the vibrating deck and fix it with nuts and bolts. Then the surcharge weight was on it. The vibrator was allowed to run for 8 minutes. Then mould was weighed with the soil and weight is recorded (W<sub>2</sub>).

**Volume of mould V cc**

**Mass of dry soil M<sub>s</sub> = (W<sub>2</sub> - W) gm**

**(γ<sub>d</sub>)<sub>max</sub> = M<sub>s</sub> / V g/cc**

**e<sub>min</sub> = Gγ<sub>s</sub> / (γ<sub>d</sub>)<sub>max</sub> - 1**

### Natural Density:

The mould with dry soil was weighted. Knowing the volume of the mould and weight of dry soil natural density can be calculated.

**e = Gγ<sub>s</sub> / (γ<sub>d</sub>) - 1**

**Relative Density =  $\frac{e_{max} - e}{e_{max} - e_{min}}$**

### Direct Shear Test

A direct shear test is a laboratory or field test used by geotechnical engineers to measure the shear strength properties of soil or rock material, or of discontinuities in soil or rock masses.

The Test has been conducted according to ASTM.

1. At first the inner dimension of the soil container has been checked.
2. Then the parts of the soil container have been put together.
3. After that the volume of the container has been calculated and the container has been weighted.
4. At first the soil was placed in loose state. Then it was placed in medium dense state by tamping 1 time by 40 blows. After that the soil sample was placed in dense state by tamping 2 times in which number of blow was around 40 each time.
5. Then the soil container was weighted, the difference of these two is the weight of the soil. It was observed that in loose state, weight of soil was around 100-110 gm. In medium dense state the weight was between 110-120 gm. And in dense state the weight of soil was more than 120 gm. Then the density of the soil has been calculated.
6. For the purpose of the test the surface of the soil was made plane.
7. Then the upper grating was put on stone and loading block was put on top of soil.
8. After that the thickness of soil specimen was measured and it was one inch.
9. Then load of 5 kg, 10 kg and 20 kg were applied for each bore hole for three different states that was loose, medium dense and dense.
10. Removing the shear pin was a must.
11. Then the dial gauge was attached which measured the change of volume.
12. After that the initial reading of the dial gauge was recorded and calibration values was also recorded.



**Figure 7.2. Equipment of Direct Shear Test.**

13. Before proceeding to test all adjustments were checked to see that there is no connection between two parts except sand.

14. Then the motor was started. The reading of the shear force was taken and the reading was recorded also. The dial gauges was set to zero, before starting the experiment.

Thus, Test program and procedure of Sieve Analysis Test, Relative Density Test and Direct Shear Test as well as relevant images of equipment has been discussed in this chapter.

## **8 TEST RESULT, COMPARISON AND DISCUSSION**

This chapter contains the interpretation of the establishment of correlations of a suite of geotechnical engineering parameters with the measured data from CPTu and SPT by using a variety of theoretical, analytical and statistical methods. The soil parameters those are included in this study are mean grain size( $D_{50}$ ), fines content ( $f_c$ ), unit weight ( $\gamma$ ), relative density ( $D_r$ ), effective friction angle ( $\phi'$ ). Correlations are established through multiple regression analysis which may be used for further study for the local soil of Bangladesh.

### **Cone Penetration Test**

Vertical readings of cone tip resistance ( $q_t$ ) and sleeve friction ( $f_s$ ) are used either separately or together to evaluate soil engineering parameters. The tip resistance is corrected ( $q_c$ ) for pore water effects on the back of the cone tip (Lunne et al., 1997). A calibration factor of 0.32 is used to perform the calibrations on recorded cone tip resistance data as provided by the cone manufacturer to get corrected cone tip resistance  $q_c$ . Furthermore, the cone tip resistance was normalized ( $q_{t1}$ ) to an overburden stress level of 100 kPa.

### **Standard Penetration Test**

The relationships between corrected SPT number  $(N_1)_{60}$  and soil parameters have been discussed to make sure the applicability of this relations for local soil. Corrected SPT number  $(N_1)_{60}$  is obtained by The SPT energy corrections and overburden pressure corrections applied to the recorded field N-values based on field SPT N values soil is profiled into medium dense( $N=10-30$ ), loose( $N=4-10$ ) and very loose( $N\leq 4$ ).

## Laboratory Tests

Results from sieve analysis, relative density test and direct shear test are used to obtain the CPT-SPT based correlations for soils of a selected area of Uttara, Dhaka city. From the subsurface explorations it was observed that the soil within the test area is primarily comprised of fine sand and silt clay particles. The sand layer contain appreciable amounts of fines ( $f_c$ ) ranging from 2.3 to 96.4, fineness modulus (an empirical figure obtained by adding the total percentage of the sample of an aggregate retained on each of a specified series of sieves, and dividing the sum by 100) ranging from 0.02 to 1.02 and mean grain size ( $D_{50}$ ) ranging from 0.12 to 0.19. Based on the sieve analysis results, the soils are generally classified into two groups: - either well graded sands with little silt or poorly graded sands with silt.

Results obtained from the relative density shows that the average density of sand for loosest state is ranged between  $12.31 \text{ KN/m}^3$ - $12.91 \text{ KN/m}^3$  whereas average density for densest state ranging from  $15.5 \text{ KN/m}^3$ - $16.6 \text{ KN/m}^3$ . Field density was about the average of density of maximum and minimum state.

Effective friction angle for the sand layer has been determined for very loose, loose and medium dense condition from direct shear test. Shear stress vs normal stress graph for the sands of five boreholes for very loose, loose and medium dense state shows a small amount of cohesion are present though the test has been conducted for sandy layer because the layer of sand was not pure, silt was considerably present in sand.

## Statistical Analysis:

To determine the correlation between CPT and SPT and soil parameters we executed a statistical analysis. This analysis was performed in various states including all obtained data and filtered data. The filtering procedure which is defined as  $\bar{X} \pm 2\sigma$  ( $\bar{X}$  is mean value of 'n' and  $\sigma$  is the standard deviation of the mean value of n were disregarded by using 95% of the data is still allowed in the investigation range) aimed to remove data situated far from the general trend. After data filtering and elimination, the same trend should be confirmed to be maintained in plot. Then, to determine the correlation functions using the least square method, linear and power regression were implemented.

## **CPT-SPT based correlations:**

### Mean Grain Size ( $D_{50}$ )

Correlations based on Mean grain size ( $D_{50}$ ) and  $q_c/N_{60}$  illustrated by Robertson et al. for north American soil (1983), Burland and Burbidge for London soils (1985), Kulhawy & Mayne for soils of California (1990), Canadian foundation engineering manual (Canadian Geotechnical Society 1992) and Anagnostopoulos for Greek soils (2003) are shown in Figure 4.1. The data sets selected for this study are then plotted on the same figure to evaluate the applicability of these correlations to the local soils. Results of CPT readings are averaged over 0.45m intervals for cone tip resistance values and compared with the SPT N-value situated over the same depth range. When choosing the level, the first thing considered was the depth of the SPT blow count accomplished. Then, the cone resistance values were averaged over 0.45 m at the same level. A total of 75 data points for the sand deposits from the 6 boreholes presented in Table 1 were selected for this study to perform comparative analysis with mean grain size ( $D_{50}$ ).

$q_c/N_{60}$  ratio of selected data set are less scattered and varies from 1-11 for a variation of  $D_{50}$  from .14-.19 mm and surprisingly 71.4% of the data fall within the range of existing correlations. The upper and lower range for study soil was provided using regression analysis. Linear correlation with zero intercept is preferred although the linear correlation with intercept and power correlation also give the acceptable range of correlation coefficient.

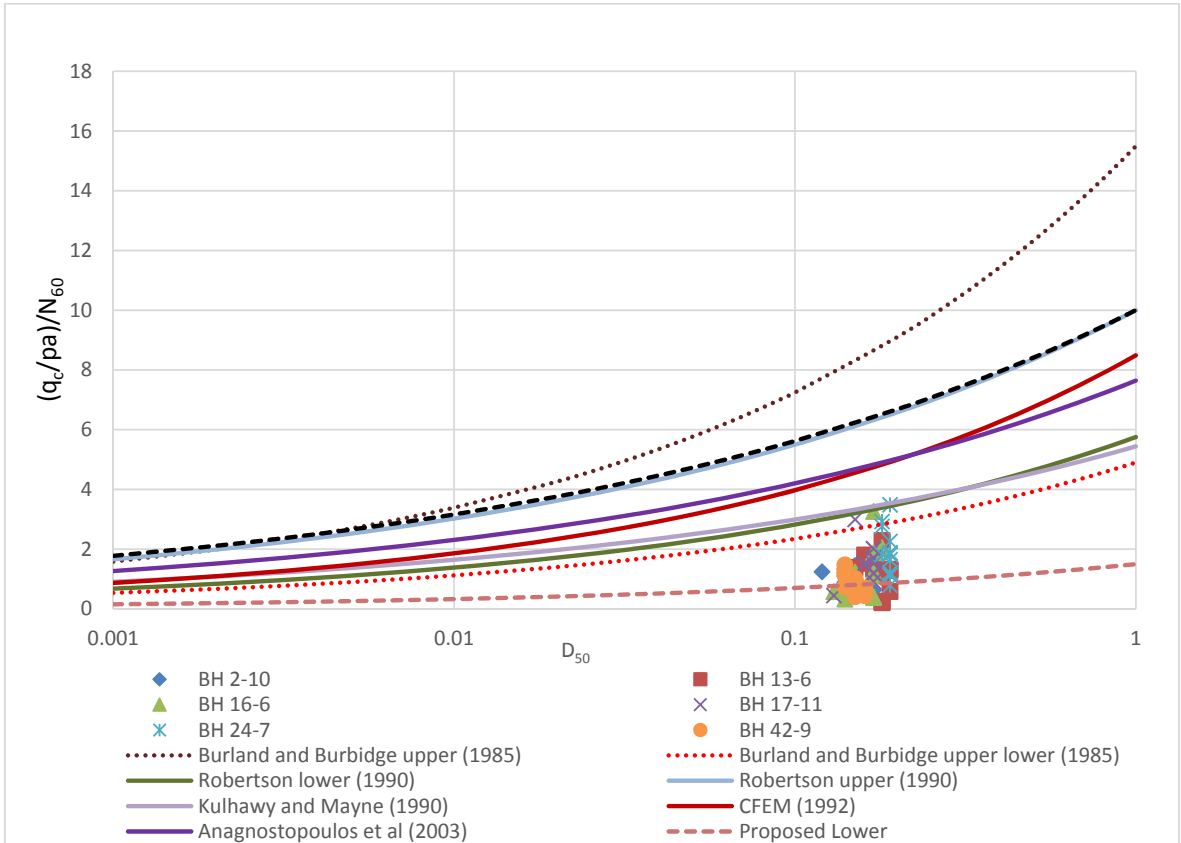


**Figure 8.1. Variation of ratio  $(q_c/pa)/N_{60}$  with mean grain size,  $D_{50}$  comparison**

**The proposed upper range nearly coincides with the upper range of Robertson et al.**

$$\text{Proposed Upper : } (q_c/pa)/N_{60} = 10 * D_{50}^{0.25}$$

$$\text{Proposed Lower } (q_c/pa)/N_{60} = 1.5 * D_{50}^{0.3}$$

### **Percent of fine content**

The fine content based correlations proposed by Jamiolkowski(1986) for undisturbed soil, Chin et al. (1988) and Kulhawy & Mayne (1990) for dubai soil are presented in Figure 8.2 along with collected data sets of this study.

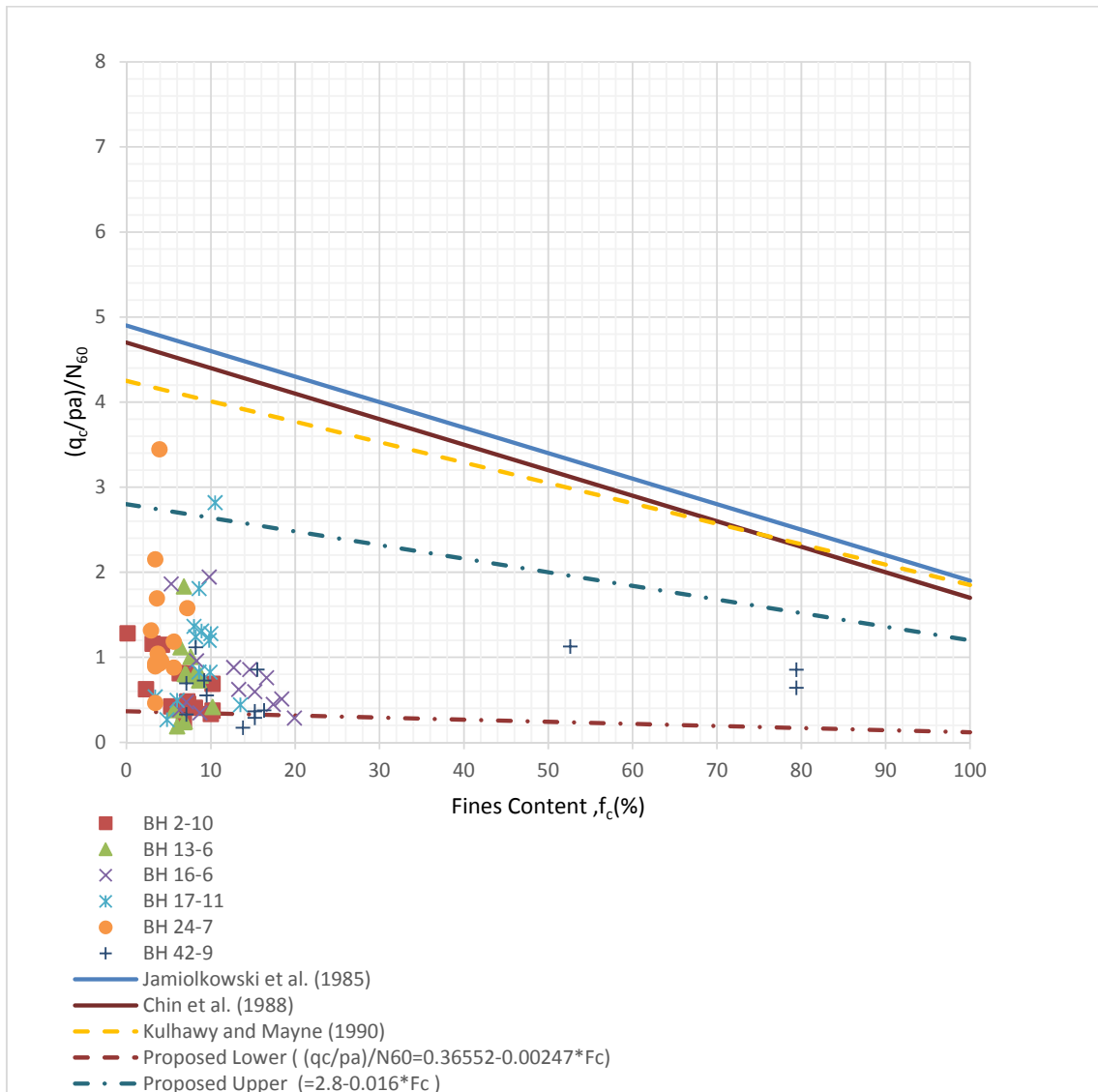


**Figure 8.2. Variation of ratio  $(q_c/p_a)/N_{60}$  with fine content ( $f_c$ ) comparison**

But, from the plotted data it can be noted that the amount of fines content for the soil of Uttara 3<sup>rd</sup> phase is ranged mainly between 2-20 %. The upper and lower range for study soil was provided using regression analysis, linear correlation with intercept. Proposed upper range (for  $q_c/N \geq 3$ )  $(q_c/p_a)/N_{60} = 2.8 - 0.016 * f_c$ , the  $q_c/N$  ratio decreased with increasing fine content which is somewhat similar to the existing correlations but for the proposed lower range for  $q_c/N < 3$   $(q_c/p_a)/N_{60} = 0.365 - 0.00247 * f_c$ , the  $q_c/N$  ratio increased with increasing fine content.

## Unit weight ( $\gamma$ )

A direct unit weight relationship with the CTP sleeve friction proposed by Mayne and Peuchen (2012) is presented in Figure 4.3. where the specific units include:  $\gamma$  (kN/m<sup>3</sup>) and  $f_s$  (kPa). A simpler expression is also represented in Fig 2 by Mayne (2014) for the sandy soil of the eastern suburbs of New Orleans.

The data sets selected for this study are then plotted on the same figure to evaluate the applicability of these correlations to the local soils. Results of CPT readings for five boreholes are averaged over the sand layer for sleeve friction values .5 data point is achieved for unit weight by Laboratory Investigation for comparison with sleeve friction. it is evident that 60% of the data are less scattered and falls in the existing correlation

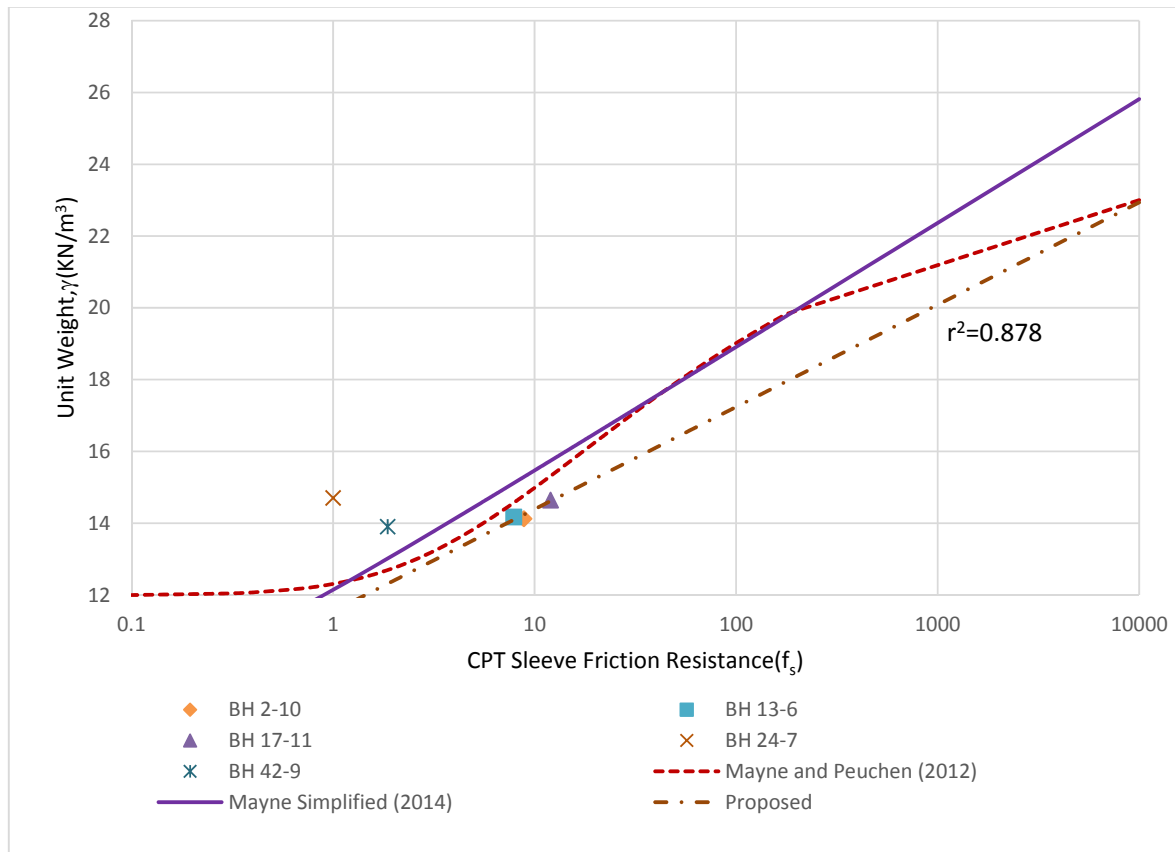


**Figure 8.3. Trend of soil unit weight with CPT sleeve friction reading.**

So, based on existing correlation regression analysis is done and new correlation is proposed for which coefficient of correlation is quite satisfactory ( $r^2=.878$ ).

Proposed Correlation:  $\gamma = 11.54285 + 1.236825 * \ln(f_s)$  ( $r^2=0.848$ )

## Relative Density( $D_r$ )

Correlation based on relative density with SPT ( $N_1$ )<sub>60</sub> values given by Terzaghi and Peck (1948) for undisturbed sandy soil is illustrated in Fig.4.4. To make the comparison with existing correlation with the results from SPT blow count and relative density test is also plotted in the same Fig. Relative density of a respective borehole is plotted against the average ( $N_1$ )<sub>60</sub> values for the whole sand layer.

Figure 8.4 indicates that actual values of  $D_r$  for the sand of Uttara 3<sup>rd</sup> phase are higher than the values predicted from the existing correlation. So, a new equation is needed for determining  $D_r$  from SPT ( $N_1$ )<sub>60</sub> for the soil of Uttara 3<sup>rd</sup> phase.

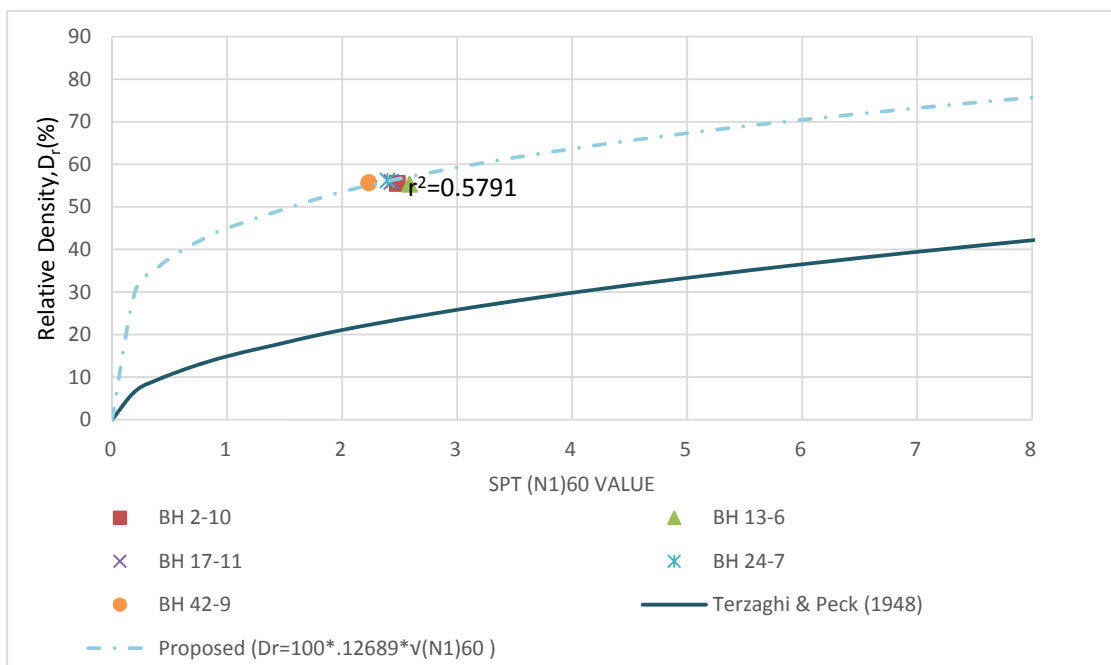


Figure 8.4. Relative Density of sands from Standard Penetration Test Data.

The proposed correlation :  $D_r = 100 * 0.12689\sqrt{(N_1)_{60}}$  ( $r^2=0.5791$ )

**Relation expressed by Robertson and Campanella (1983) for normally-consolidated clean quartz sands are illustrated in Figure 4.5. Results from CPT and laboratory relative density test of sand of respective boreholes are plotted in same Fig and are used to compare with the existing correlation. Values of normalized cone tip resistance are averaged for the sand layer for a certain borehole.**

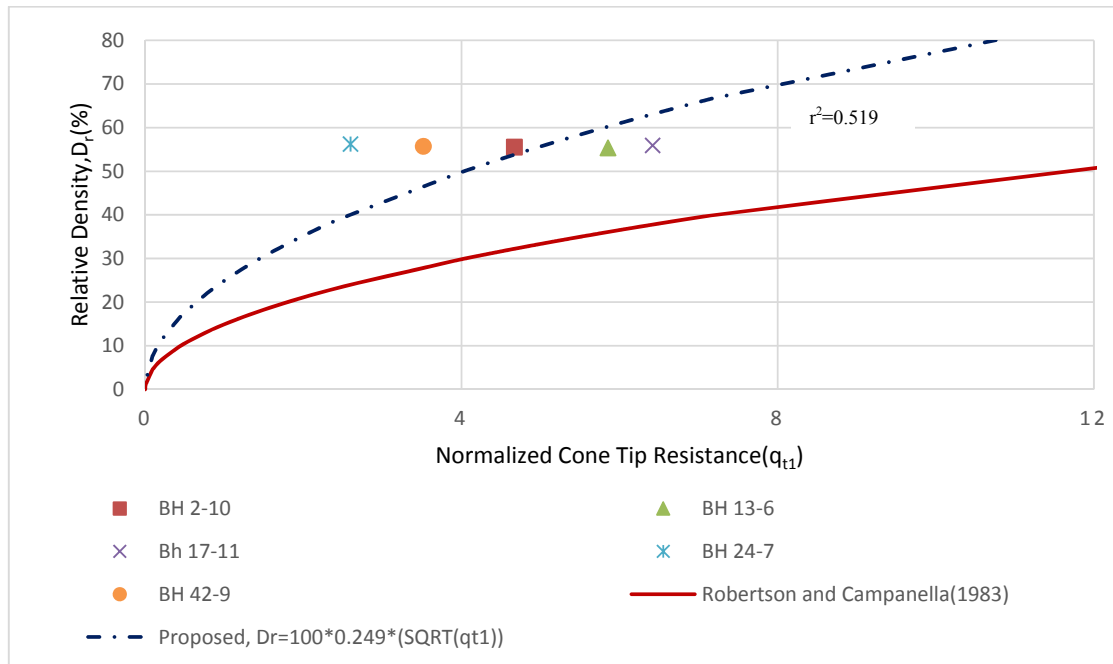


Figure 8.5. Relative Density Evaluations of NC sands from normalized cone tip resistance

All set of data from relative density test have fallen in the higher range than predicted value from correlation given by Robertson and Campanella(1983). So, a new correlation is established by regression analysis in by following the same trend for which coefficient of correlation is quite satisfactory.

Proposed correlation:  $D_r = 100 * 0.249\sqrt{q_{t1}}$  ( $r^2=0.519$ )

### Effective Friction Angle( $\phi'$ )

Correlations based on effective friction angle and SPT ( $N_1$ )<sub>60</sub> values illustrated by Hatanaka and Uchida (1996) for Japanese soil (1983) and specification for highway bridge shown in Figure 4.6. Result from SPT are plotted in the same Fig to compare the relationship with Friction angle for very loose, loose and Medium Dense condition. While taking ( $N_1$ )<sub>60</sub> for these three condition average of ( $N_1$ )<sub>60</sub> values are taken for certain layer for 5 boreholes. For Bore Hole 24/7 and 42/9 there is no layer of medium Dense sand and for BH 13/6 there is no layer of very loose sand. So, those data point are eliminated from plotting and comparing with existing correlations. From the relationship between effective friction angle,  $\phi'$  and corrected standard penetration blow number for sands the effective friction angle for very loose state <30 for loose state 30-35, for medium Dense 35-40 (Meyerhof 1956, Foundation Engineering Handbook). Almost same relationship given by Peck (1974) and Bowels (1971)

Figure 4.6 shows that though for very loose state effective friction angle is little higher; for loose and medium dense state values of friction angle follows the range given by Meherhoff (1956) It is also evident that for each density state, values of effective friction angle are higher than the proposed Hatanaka and Uchida(1996) and specifications for highway bridge.

For Very Loose:  $\phi' = 25.4749 + 4.89816 * (N_1)_{60}^{0.3}$  ( $r^2=0.37$ )

For Loose:  $\phi' = 29.23022 + 2.03656 * (N_1)_{60}^{0.6}$  ( $r^2=0.442$ )

For medium Dense:  $\phi' = 29.47 + 5.66584 * (N_1)_{60}^{0.1}$  ( $r^2=0.319$ )

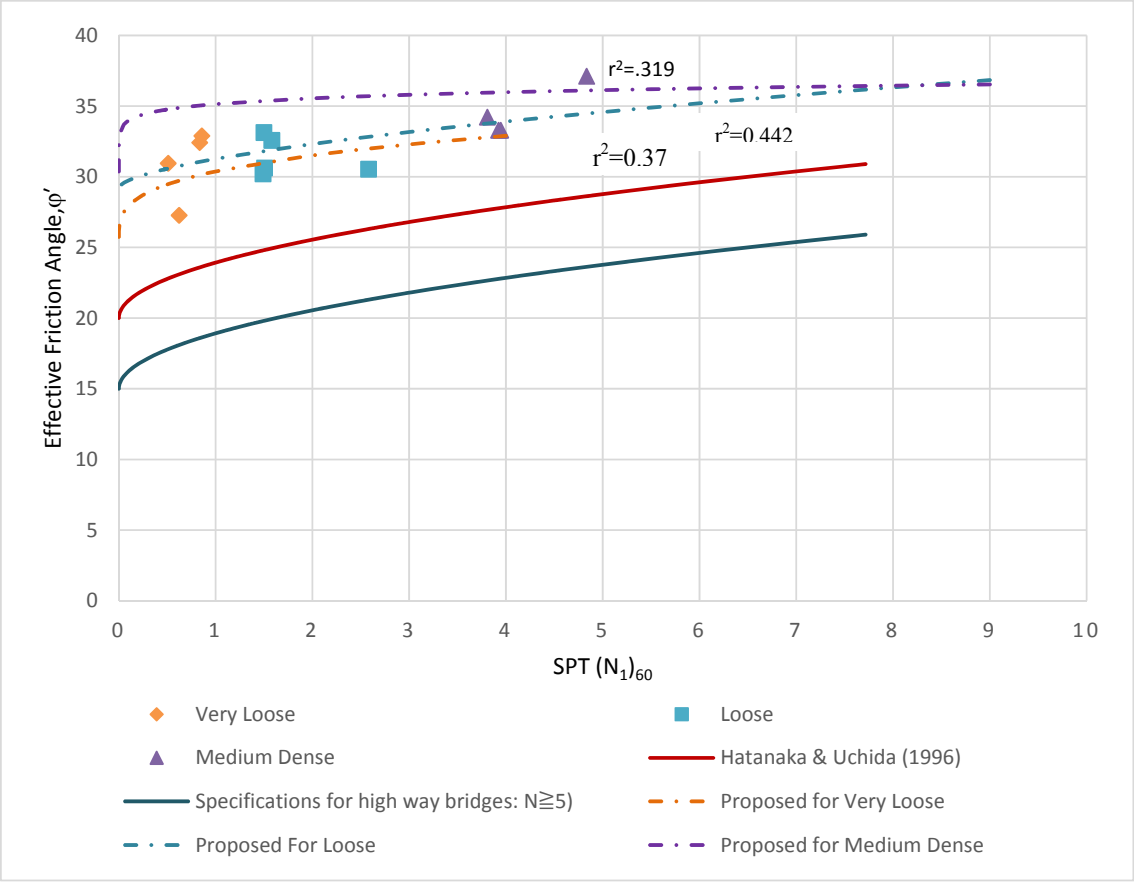


Figure 8.6. Peak friction angle of sands from SPT data

The expression derived by Kulhawy & Mayne (1990) for soil of California for quartz-silica sands, Robertson and Campanella(1983) for Okland soil and Uzeilli et al (2013) to correlate effective friction angle with normalized cone tip resistance are illustrated in Figure. 4.7. Result obtained from direct shear test for three different density state for five boreholes and from CPT are also plotted in the same Fig to compare with the reference expressions. Results from CPT for cohesionless layer are averaged for very loose, loose and Medium Dense sands.

Figure 4.7 Shows that value of Effective Friction for all density condition for normalized Cone tip resistance are higher than values obtained from predicted correlation for effective friction angle, which explains the necessity for new correlation for local soil.

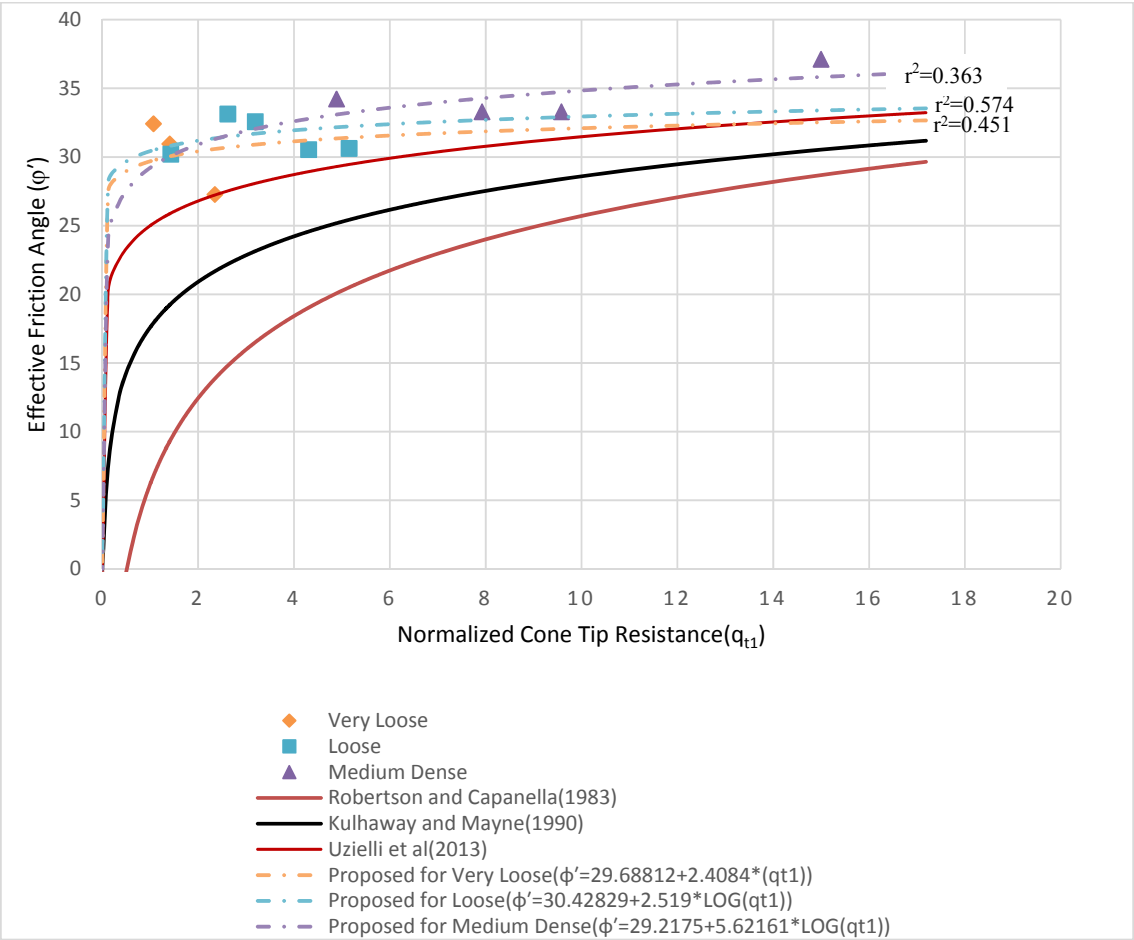


Figure 8.7. Direct relationships between peak friction angle and normalized cone resistance

Multiple regression analysis is performed in the similar way to obtain new correlation for effective friction angle with cone tip resistance as test results are following almost same trend line and coefficient of correlation obtained is quite satisfactory.

For Very loose :  $\phi' = 29.68812 + 2.4084 * \log (q_{t1})$  ( $r^2=0.451$ )

For Loose:  $\phi' = 30.42829 + 2.519 * \log (q_{t1})$  ( $r^2=0.574$ )

For Medium dense:  $\phi' = 29.2175 + 5.62161 * \log (q_{t1})$  ( $r^2=0.363$ )

## Correlation for cone tip resistance and SPT blow

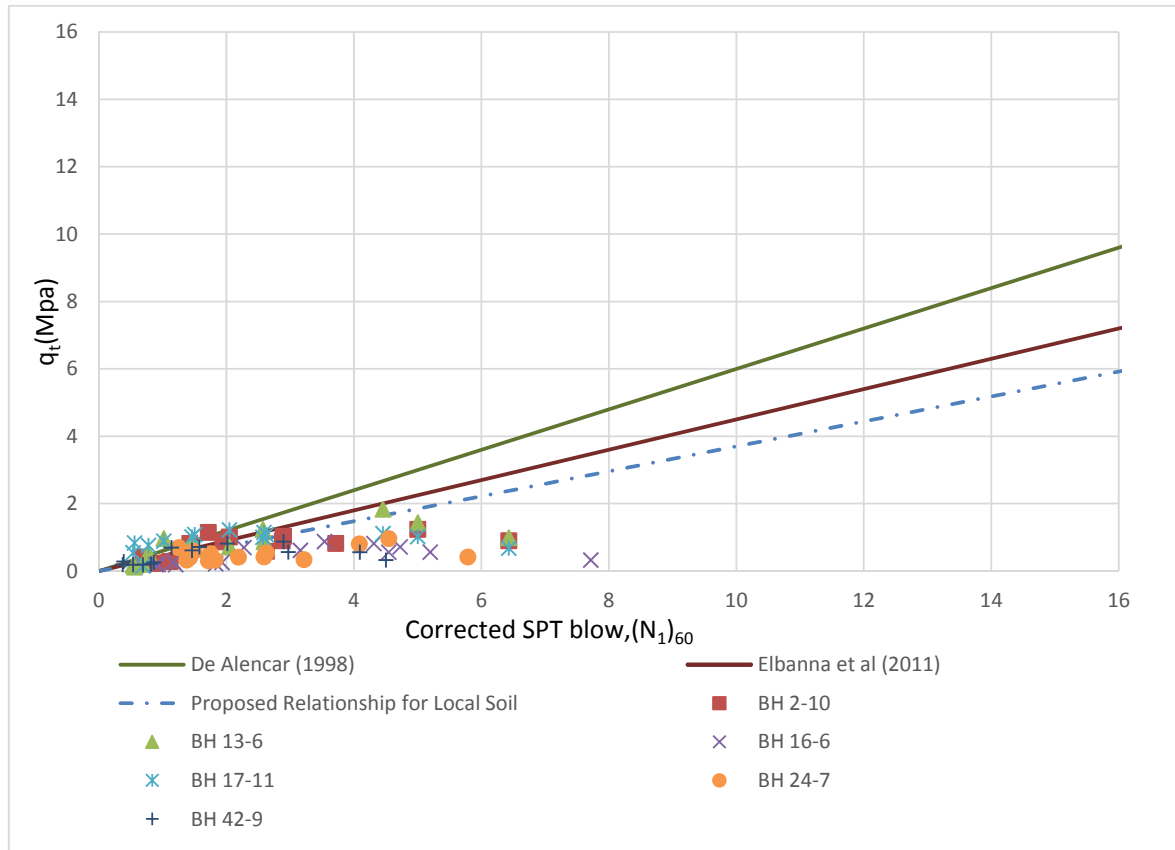


Figure 8.8. Variation of normalized cone tip resistance ( $q_t$ ) with normalized SPT blow count

Fig. 8.8 compares the measured data with the single value of  $q_t/(N_1)_{60}$  ratio of 0.45 suggested by de Alancer (1995) Elbanna et al. (2011).

The plotted data shows surprisingly are within the range of values with the average value of 0.45 though the study soil was not pure sand, but they show a similar linear relationship and nearly maintains a  $q_t/(N_1)_{60}$  ratio of 0.35. It is believed that the proposed correlation between normalized cone tip resistance and normalized SPT ( $N_1)_{60}$  can serve as a better relationship for the local soils. The main advantage of this relationship is that it can be used in the absence of gradation results. Therefore, it is a need to collect additional high quality CPT and SPT data to develop a better relationship.

## 9 CONCLUSIONS

This research has assessed the correlation based on CPT and SPT for Dhaka sand from the selected area. The existing SPT-CPT correlations were reviewed considering:-

- a) the historical evolution of the need for SPT-CPT correlations,
- b) the factors that influence the correlation;

c) sources of scatter in the correlations, and

d) the existing correlations

Based on data from laboratory investigation of undisturbed samples and measured SPT and CPT resistance, an empirical correlation between the SPT blow count and CPT cone tip resistance and sleeve friction of sandy soils is established. The results obtained in the research work is summarized below :

- It has been observed that rather than available relationships between  $q_c/N_{60}$  and Fine content for cohesionless soil, the developed correlations for  $q_c/N_{60}$  with  $D_{50}$  show good applicability to local soils. New correlation ranges to  $(q_c/p_a)/N_{60}=10 \cdot D_{50}^{0.25}$  to  $(q_c/p_a)/N_{60}=1.5 \cdot D_{50}^{0.3}$  and  $(q_c/p_a)/N_{60} = 2.8 - 0.0016 \cdot f_c$  (for  $q_c/N_{60} \geq 3$ ) and  $(q_c/p_a)/N_{60} = 0.36552 - 0.00247 \cdot f_c$  (for  $q_c/N_{60} < 3$ ) have been proposed.
- Compared with the correlation for unit weight with CPT sleeve friction given by Mayne and Peuchen (2012) and the simplified correlation by Mayne (2014) , a new correlation developed for local sand. In the developed relationship the unit weight is increasing by a factor of 2.3 ( $10 \text{ kN/m}^3 \leq \gamma \leq 23 \text{ kN/m}^3$ ) while the sleeve friction is spanning three orders of magnitude ( $0.5 \text{ kPa} \leq f_s \leq 1000 \text{ kPa}$ ), thus an accurate  $f_s$  is not necessary given that the expected variance is on the order of  $\pm 1.236 \text{ kN/m}^3$  in the estimated value of unit weight. Correlation for relative density with SPT blow count and CPT normalized cone tip resistance is established separately. The determined relation between relative density with corrected SPT  $(N_1)_{60}$  values ,  $D_r = 100 \cdot 0.12689 \cdot \sqrt{(N_1)_{60}}$  matches better than the existing relation expressed by Terzaghi and Peck (1948) for local sands. In case of correlation between relative density with normalized cone tip resistance , rather than the existing correlation by Robertson and Campanella (1983) the determined relationship  $D_r = 100 \cdot 0.249 \cdot \sqrt{q_{t1}}$  fits better with a quite satisfactory correlation coefficient. Separate correlations are also developed for CPT and SPT with effective friction angle. Values of effective friction angle for loose and medium dense state are matched satisfactorily within the range of values for effective friction angle given by Mayerhoff(1956) and Peck (1974) while the values for very loose state are deviated from the range. Thus, a set of new correlations are developed for effective friction angle using CPT and SPT data separately for each of density state of sand from Uttara 3<sup>rd</sup> phase. A correlation is also established between CPT  $q_c$  and SPT  $N_{60}$  for sandy soil of the selected

area in which the CPT and SPT data used for this study better suit with  $(q_t/(N_1)_{60})$  ratio of 0.35 instead of 0.45 proposed by Elbanna (2011).

- Results that are found from the statistical approach give almost similar results with literature value. Using regression analysis correlations are developed for which higher correlation coefficient is obtained.
- Generally speaking, available established correlations provide a good framework to start with, but the direct application of the average curve in engineering practice may lead to deviation, so proper relationships should be developed for local soils. Unfortunately, the available data sets which exist for the study area falls within a relatively narrow range for developing good correlations. It is needed to further investigate by accumulating large amount of high quality data from various sands from different places.

## References

- Agaiby S, Abdel-Rahman A, Ahmed S, Baghdady A.  $q_c/N$  Ratio for recently deposited crushable soils. In: Singapore, Phoon K, Chua T, Yang H, Cham W, editors. International symposium on advances in foundation engineering (ISAFE 2013) 5–6 December 2013; in press.
- Ahmed S.M, Agaiby S.W, Abdel-Rahman A.H. (2013) , A unified CPT–SPT correlation for non-crushable and crushable cohesionless soils Geotechnical Engineering, Ain Shams University, Cairo, Egypt, Geotechnical & Heavy Civil Eng Dept., Dar Al-Handasah (Shair and Partners), Cairo, Egypt, Geotechnical Engineering, National Research Center, Cairo, Egypt.
- Akca N. Correlation of SPT–CPT data from the United Arab Emirates. Eng Geol 2003;67:219–31.
- Anagnostopoulos M, Jamiolkowski M, Peterson R. Preliminary result of CPT tests in calcareous Quiou sand. In: Proceedings of the international symposium on calibration chamber testing, Potsdam, New York; 2003. p. 41–53
- Banglapedia, National Encyclopedia of Bangladesh
- Burland R, Burbidge S, Fretti C, Ghionna VN, Pedroni S. Compressibility and crushability of sands at high stresses. In: Proceedings of the international symposium on calibration chamber testing, Potsdam, New York; 1985. p. 79–90.

- Chin C, Duann S, Kao T. SPT–CPT correlations for granular soils. In: Proceedings of the 1st international symposium on penetration testing (ISOPT-1), vol. 1; 1988. p. 335–9.
- CPT guide 2015 by GREGG
- Cubrinovski M., Ishihara K.( 2014) Correlation between penetration resistance and relative density of sandy soils, Science University of Tokyo, Tokyo, Japan
- De Alencar F, Politano C, Danziger B, Robertson P, Mayne P.CPT–SPT correlations for some Brazilian residual soils. In:Geotechnical site characterization, Proceedings of the firstinternational conference on site characterization-ISC'98 vol. 2. Atlanta, Georgia, USA, AA Balkema; 1998. p.907–12.
- Elbanna T.M.,Ain Shams University, Cairo, Egypt/ Sogreah Gulf, Dubai, UAE, Ali H.E, AinShams University, Cairo, Egypt/ COWI, Dubai, UAE (2011) CPT-SPT correlations for calcareous sand in the PersianGulf area.
- Elkateb T, Ali H. CPT–SPT correlations for calcareous sand inthe Persian Gulf area. In: 2nd International symposium on cone penetration testing, 9–11, California, USA; 2010.
- Hatanaka O, Uchida M. Japan 1996, Analysis for correlation of SPT and other geotechnical parameters for soil of Japan.
- Jefferies M, Davies M. Use of CPTU to estimate equivalent SPTN60. Geotech Test J ASTM 1993;16(4):458–68.
- Kara O, Gu" ndu" z Z. Correlation between CPT and SPT inAdapazari, Turkey. In: International symposium on cone penetration testing, 9–11, California, USA; 2010.
- Kulhawy F, Mayne P. Manual on estimating soil properties for foundation design. Report no. EPRI-EL-6800, Electric PowerResearch Institute, EPRI; 1990.
- Lambe T.W, Soil Testing for Engineers (1951)
- Lee J, Guimaraes M, Santamarina J. Micaceous sands: microscale mechanisms and macroscale response. ASCE J Geotech Geoenviron Eng 2007;133(9):1136–43.
- Lunne T, Robertson P, Powell J. Cone penetration testing ingeotechnical practice. New York (USA): Blackie Academic, EFSpon/Routledge Publ; 1997.
- Mayne, P.W. (2014). KN2: Interpretation of geotechnical parameters from seismic piezocone tests.Proceedings, 3rd International Symposium on Cone Penetration Testing(CPT'14, Las Vegas), ISSMGETechnical Committee TC 102, Edited by P.K. Robertson and K.I. Cabal: p 47-73.
- Mominul H.M, Ansary M.A, Abedin M.J. (2016) Applicability of existing CPT, SPT and soil parameter correlations for Bangladesh,Bangladesh University of Engineering and Technology, Dhaka, Bangladesh

- Moore C. Effect of mica on  $K_0$  compressibility of two soils. ASCEJ Soil Mech Found Eng Div 1971;97(SM9):1251–91.
- Ozan C. Estimation of grain characteristics of soils by using cone penetration test (CPT) data. M.Sc. Thesis, The Dept. of Civil Engineering, The Middle East Technical University, Turkey; 2003. 60p.
- Paul W. Mayne, (2007), Cone Penetration Testing State-of-Practice
- Peck R.B, Hanson W.E, Thornburn T.H, Foundation Engineering (2<sup>nd</sup> edition, 1974)
- Robertson P. In-situ testing of soil with emphasis on its application to liquefaction assessment. Ph.D. thesis. Department of Civil Engineering, University of British Columbia, Vancouver, Canada; 1982. 395p.
- Robertson P. Interpretation of in-situ tests – some insights. Mitchell Lecture-ISC'4 Brazil; 2012.
- Robertson P, Campanella R, Wightman A. SPT-CPT correlations. ASCE J Geotech Eng 1983;109(11):1449–59.
- Robertson P, Cabal K. Guide to cone penetration testing for geotechnical engineering, 5th ed. Gregg Drilling & Testing; 2012.
- Robertson P. Soil classification using the cone penetration test. Can Geotech J 1990;27(1):151–8.
- Robertson P, Campanella R. Interpretation of cone penetration tests. Part I: Sand. Can Geotech J 1983;20(4):718–33.
- Salehzadeh H, Hozouri A, Golestani A. Correlation between cone and standard penetration tests. In: 5th Symposium on advances in science and technology (SASTech 2011), Khavaran Higher Education Institute, Mashhad, Iran. May 12–14; 2011.
- Terzaghi K, Peck R.B. (1948) The Influence of Modern Soil Studies on the Design and Constructions of Foundations.
- Uzeilli K.R, Hozouri A, Robertson P. Interpretation of CPT on Geotechnical Parameters. Sand. Geotech Gate J 2011;20(4):718–33.



**BANGLADESH NETWORK  
OFFICE FOR URBAN SAFETY**



## **PART-XIII**

# **THE UTILIZATION OF CPT AND SPT TO OBTAIN SOIL PARAMETERS FOR C- $\phi$ SOIL AT UTTARA 3<sup>RD</sup> PHASE, DHAKA, BANGLADESH**

**BANGLADESH NETWORK OFFICE FOR URBAN  
SAFETY (BNUS), BUET, DHAKA**

**Prepared By: Zinan A. Urmi**

**Mehedi Ahmed Ansary**

# 1 INTRODUCTION

Soil sampling combined with laboratory testing is the most reliable method to determine soil properties. Sometimes due to limited budgets, tight schedules, or lack of concern projects do not receive proper laboratory recommendation. However in many cases subsoil investigation data like SPT blow count or CPT cone resistance and sleeve friction along with soil type and depth of water table are available to judge the subsurface soil characteristics. Therefore when laboratory data are not available it is a common practice to estimate the soil properties from the SPT-CPT results. Many empirical correlations have been created between the SPT N-value and CPT cone resistance with other engineering properties of soils. But due to variability of soil properties for same type of soil from place to place it is very difficult to predict the outcome of those relations without justifying them for local soil. The local soil may follow previous correlations with slight deviation or may not follow the trend at all. For the latter case new correlations for local soil must be provided to fulfill the above mentioned purpose.

The Standard Penetration Test (SPT) is the most common in situ test for site investigations in Bangladesh and most of foundation designs have been based on SPT-N values and physical properties of soils recovered in the SPT sampler. The SPT has some disadvantages such as potential variability of measured resistances depending on operator variability and possibility of missing delicate changes of soil properties owing to the inevitable discrete record. Around the world the Cone Penetration Test (CPT) is becoming increasingly popular as an in situ test for site investigation and geotechnical design especially in deltaic areas since it provides a continuous record which is free from operator variability. For economic consideration it is unlikely that both CPT and SPT are done for investigation. So it is important to establish correlation between soil parameters individually with CPT and SPT along with interrelation between these investigation methods.

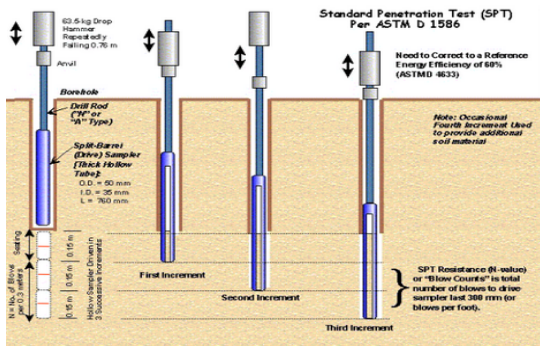


Fig. 1.1: Standard Penetration Test

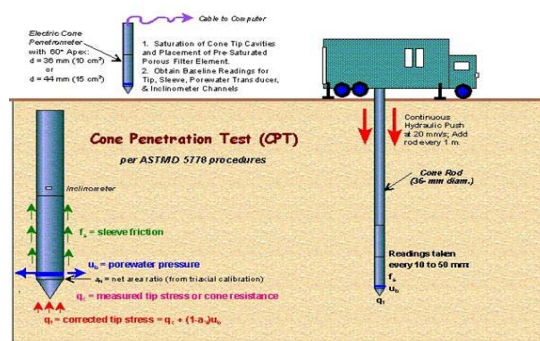


Fig. 1.2: Cone Penetration Test

## **2 BACKGROUND**

During the last few decades, many researches have been carried out to obtain soil parameters directly from soil investigation reports for different soils by different researchers around the world. But most of these researches have been done on clean sand or quartz or pure clay. Unfortunately for Bangladeshi soil there is hardly researches in this area. Ansary et al (2014) has worked with alluvial sandy soil in Bangladesh. But no researches regarding silty clay has been done for local soils till now which indicates the need for justification of existing correlation for local soils and appropriate correlations that may serve good results.

## **3 OBJECTIVE OF THE RESEARCH**

The present study was aimed to investigate the justification of existing correlation between CPT-SPT with soil parameters for local silty clay to meet the following objectives.

- i. To determine soil behavior index  $I_c$  from CPT
- ii. To interrelate CPT and SPT based on soil behavior index  $I_c$
- iii. To compare the shear strength parameter ( $C_u$ ) obtained from unconfined compression test and direct shear test with shear strength parameter ( $C_u$ ) obtained from SPT blow count ( $N_{60}$ ) using existing correlations.
- iv. To compare the shear strength parameter ( $C_u$ ) obtained from unconfined compression test and direct shear test with shear strength parameter ( $C_u$ ) obtained from CPT cone resistance ( $q_c$ ) using existing correlations.
- v. To compare the Friction angle ( $\phi$ ) obtained from direct shear test with Friction angle ( $\phi$ ) obtained from SPT blow count ( $N_{60}$ ) using existing correlations.
- vi. To compare the Friction angle ( $\phi$ ) obtained direct shear test with Friction angle ( $\phi$ ) obtained from CPT cone resistance ( $q_c$ ) using existing correlations.
- vii. To compare the OCR obtained from consolidation test with OCR obtained from CPT test data using existing correlations.
- viii. To compare the 50% consolidation time  $t_{50}$  from consolidation test data with  $t_{50}$  obtained from CPT<sub>u</sub> dissipation test and to establish correlation among them.
- ix. To establish correlation between Plasticity Index with SPT
- x. To justify existing correlations used for comparison and propose new correlation for local soil where necessary.

## **5 FIELD AND LABORATORY INVESTIGATIONS**

This chapter presents the details of field and laboratory investigations, equipment used, methodology and investigation results. For convenience, the chapter is divided into two parts i) Field Investigation

and ii) Laboratory investigation. Research location, site geology, sub soil profile and details of SPT and CPT tests are discussed in the first part. Laboratory test methods and test results are described in the last part.

### FIELD INVESTIGATION

Field investigations were carried out mainly through the application of cone penetration testing (CPT) and standard penetration testing (SPT). A total of six pairs of CPT and SPT were performed in different locations within the study area and each pair of CPT and SPT was carried out as close as possible, maximum horizontal distance was not greater than 1m. In this research, field investigations were carried out in Uttara Residential Model Town (3<sup>rd</sup> Phase), Dhaka, Bangladesh as shown in Figure 3.1.

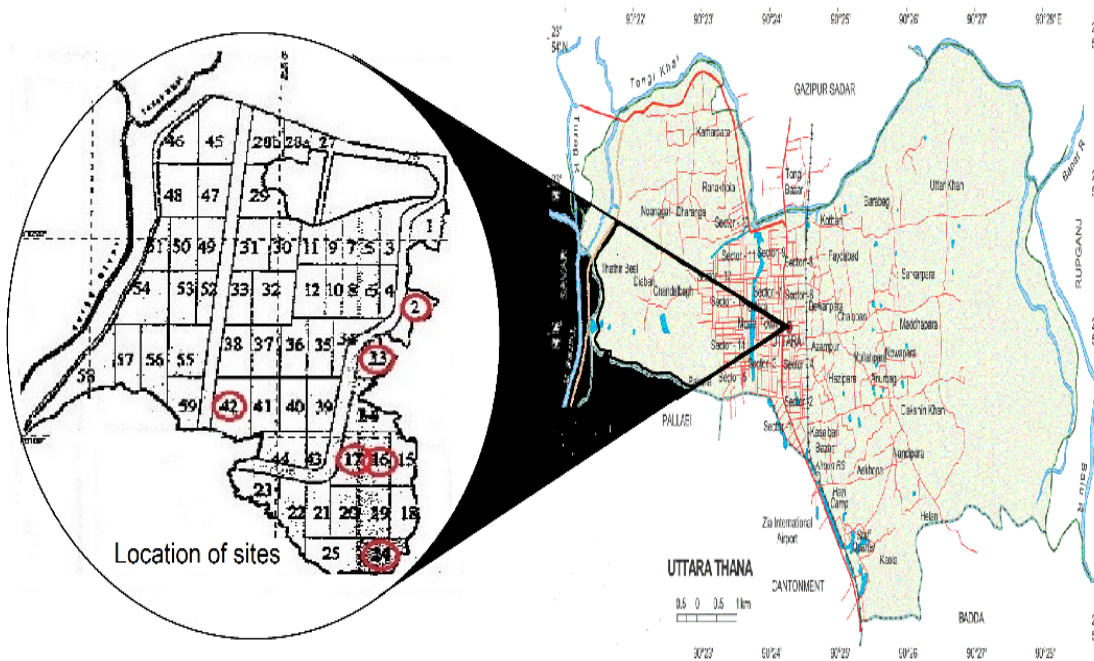


Figure 5.1: Study location

### Geologic formation of research site

The geologic formations of the research site are mainly consisting of alluvial silt and clay. The alluvial silt and clay part has medium to dark grey silt; color is darker as amount of organic material increases. A combination of alluvial and paludal deposits has been observed there including flood-basin, back swamp silty clay, and organic rich clay in sag ponds and large depressions. Some depressions contain peat. Large areas underlain by this unit are dry only a few months of the year; the deeper part of depressions and bils contain water throughout the year.

### Cone penetration test

CPT soundings were advanced using a Hogentogler type piezocone penetrometer with a cross sectional area of 10 cm<sup>2</sup> and which can measure the pore water pressure ( $u_2$ ), as well as the cone tip resistance ( $q_c$ ) and sleeve friction( $f_s$ ). To perform the test, the cone was pushed vertically into the ground at a constant rate of approximately 20mm/sec. During the advancement, measurements of dynamic pore water pressure, tip resistance and sleeve friction were recorded continuously at 10 mm depth increments. The typical penetration depth for this study was approximately 12-14 m below from ground surface. CPTu dissipation test were done for each borehole.



Fig 5.2 : Carrying out CPT on site no 16 bore hole 1

### Standard penetration test

SPT were conducted per ASTM D1586. Boreholes for the SPT were advanced by wash boring. The split spoon sampling method was used to obtain soil samples from boreholes and disturbed representative samples were collected. Samples recovered from boreholes were stored in plastic bags which were used for laboratory testing. Potential source of uncertainty which may affect SPT N-value has been carefully considered. Borehole drilling, soil sampling and SPT N-value recording procedures were observed by experienced geologist during the entire test program and this individual provided visual descriptions of the collected samples. The SPT N-value and samples were every .45 m intervals. Rope and cathead SPT hammer-release was used and the efficiency of hammer was 60%.

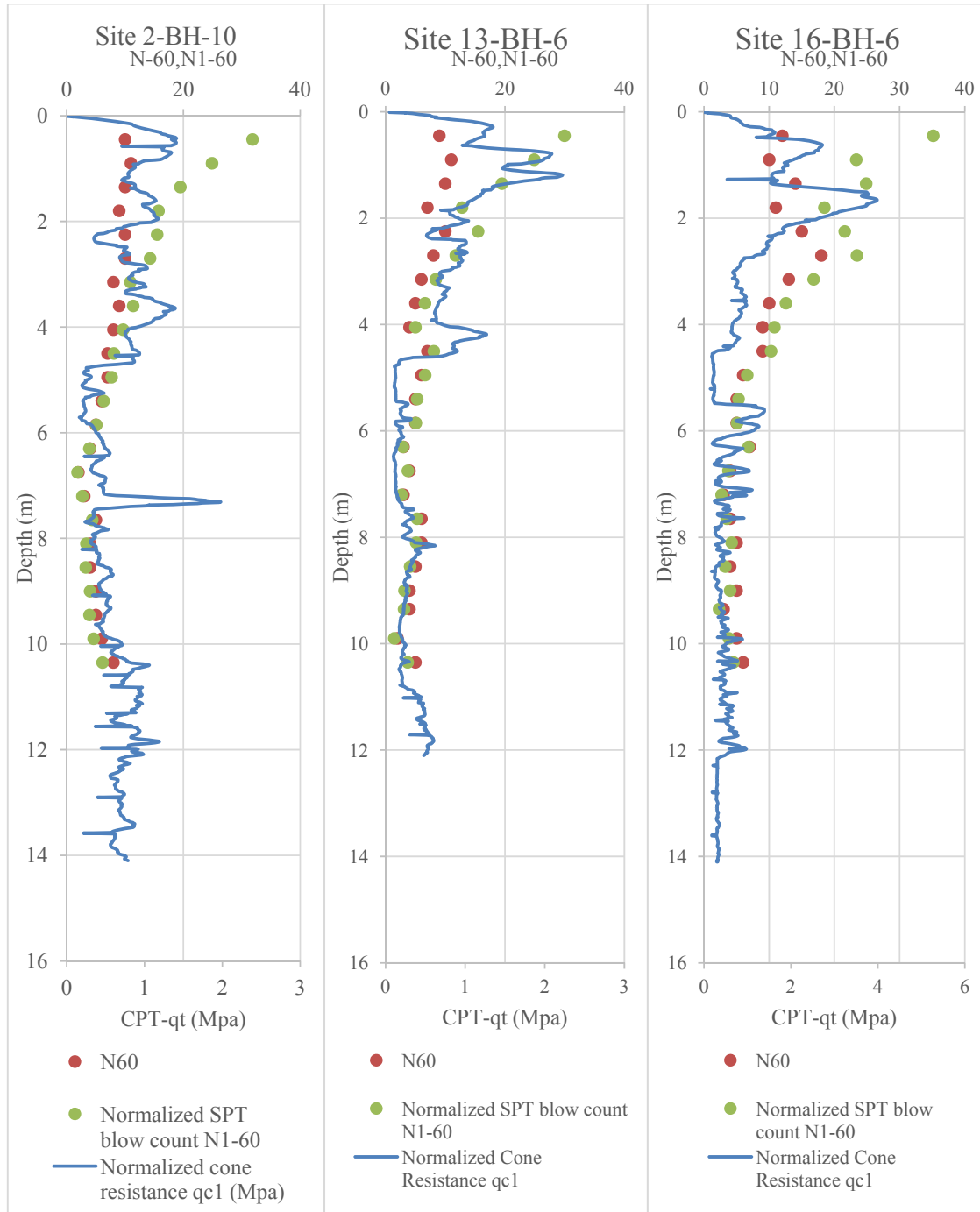


Fig

5.3(a):Carrying out of SPT by rope hammer (b) Sample collection by split spoon sample

### Subsoil Profile

The corrected tip resistance ( $q_{c1}$ ), corrected SPT value  $N_{1,60}$  values are presented in Figure 5.4



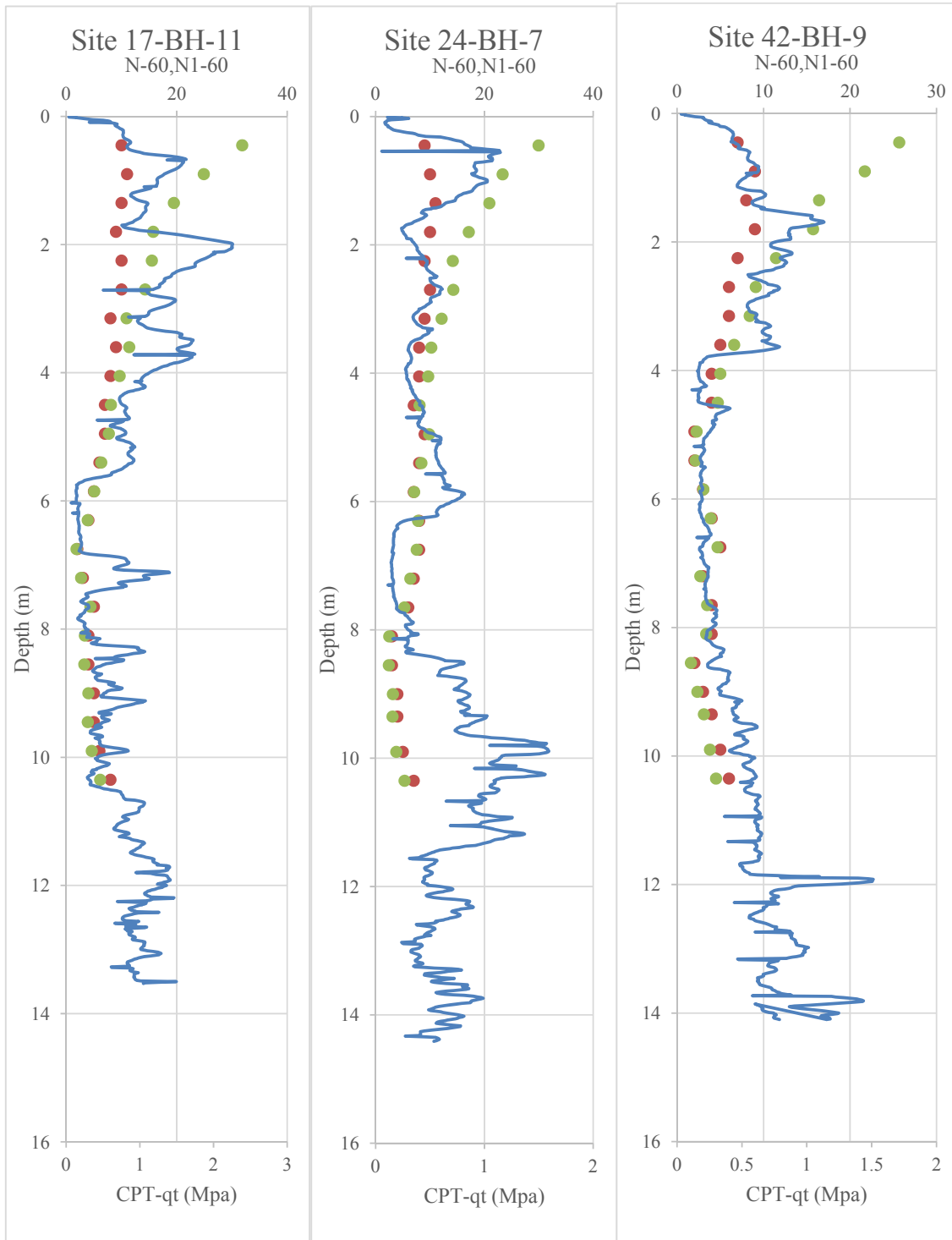
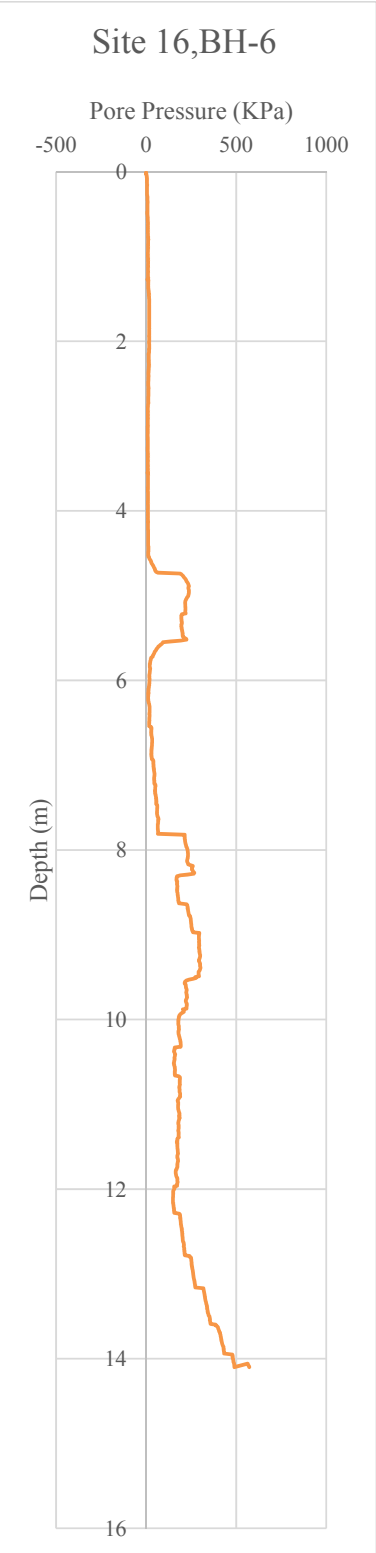
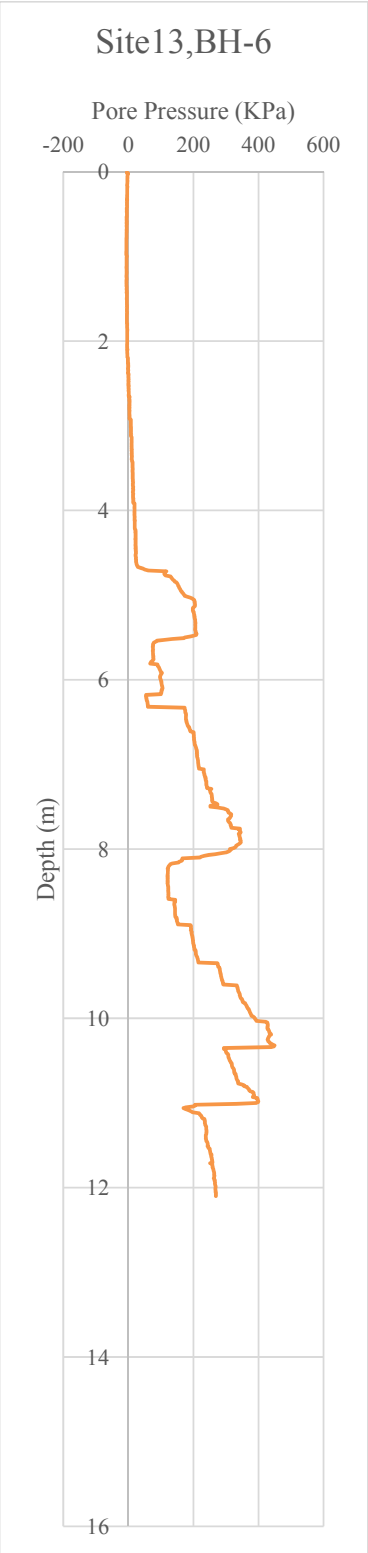
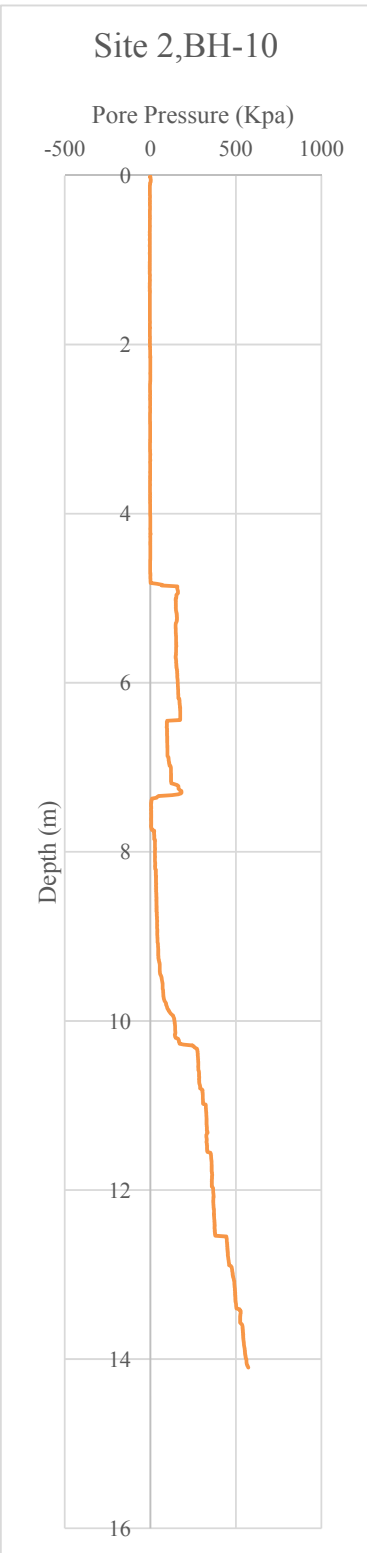


Figure 5.4. Depth versus corrected cone tip resistance ( $q_{c1}$ ), SPT  $N_{60}$  and  $N_{1,60}$  values for all boreholes

shown in fig. 3.1

The variation of pore pressure with respect to depth for all the boreholes are shown in figure 5.5



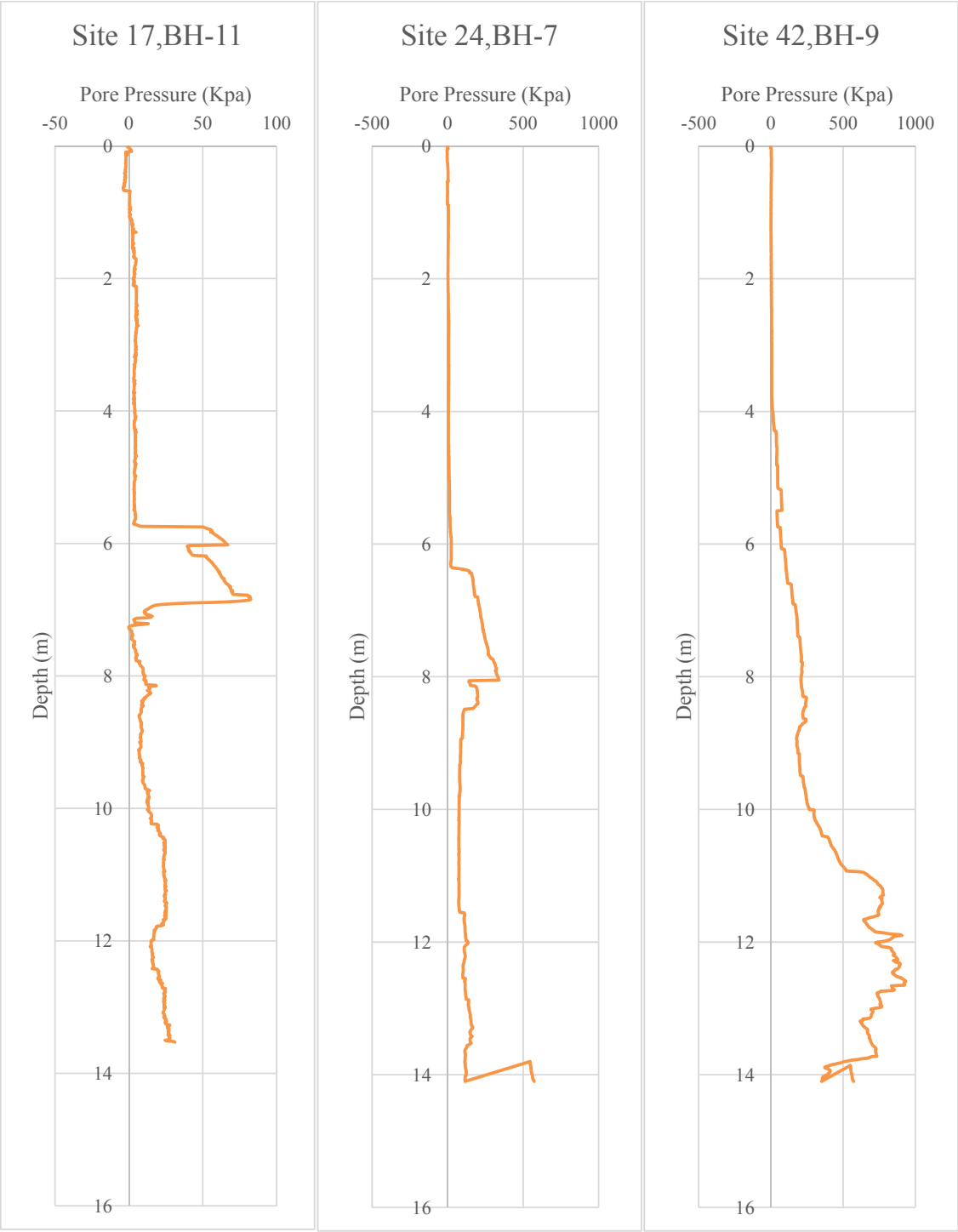
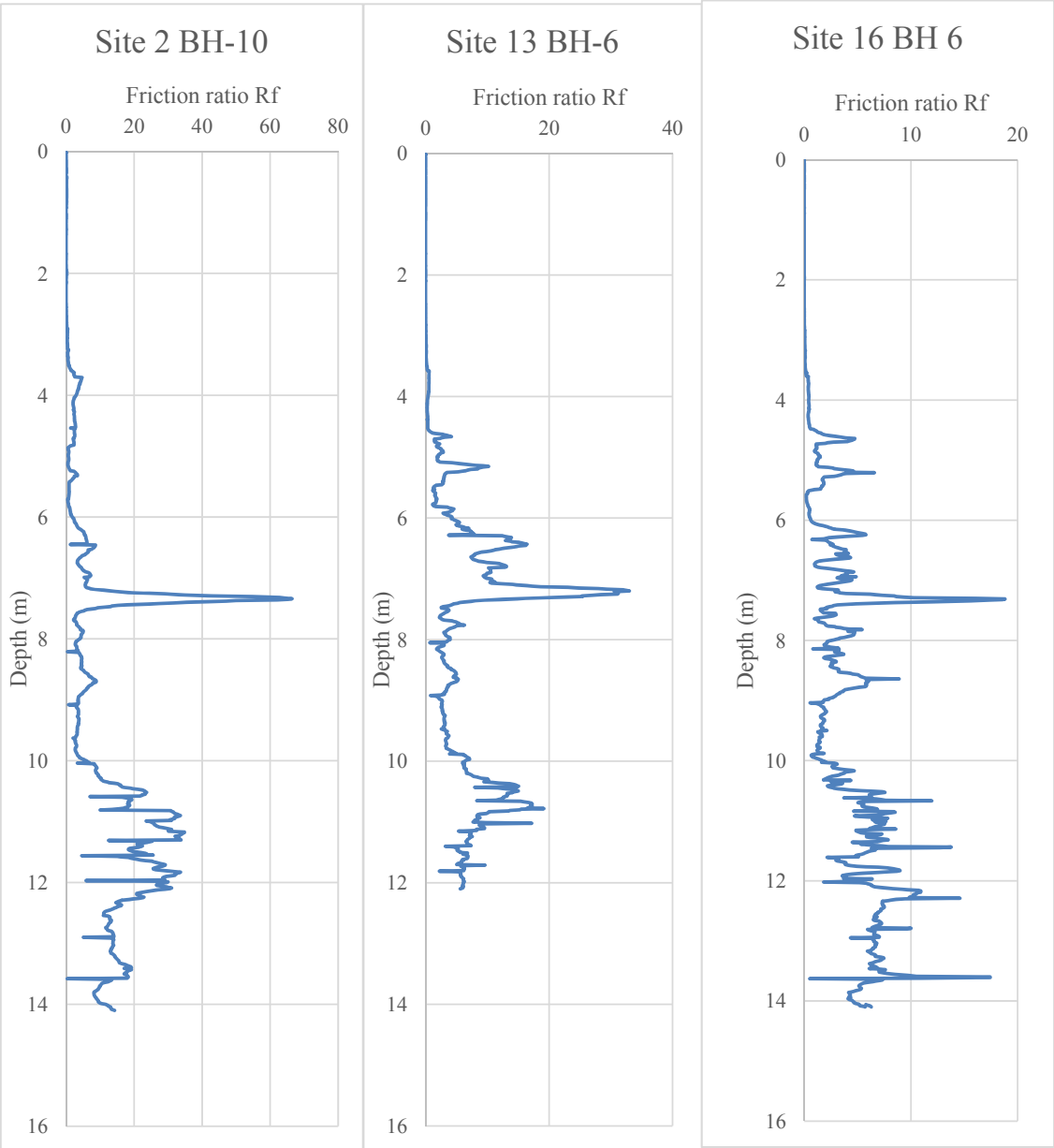


Fig 5.5: Variation of pore water pressure (u) with respect to depth (m) for all the boreholes

Friction ratio ( $R_f$  or  $f_r$ ) is defined as the ratio of sleeve friction ( $f_s$ ) to cone tip resistance ( $q_t$  or  $q_c$ )  
 $R_f \% = 100 * f_s / q_c$

Variation of friction ratio with respect to depth for all the boreholes are shown in figure 5.6



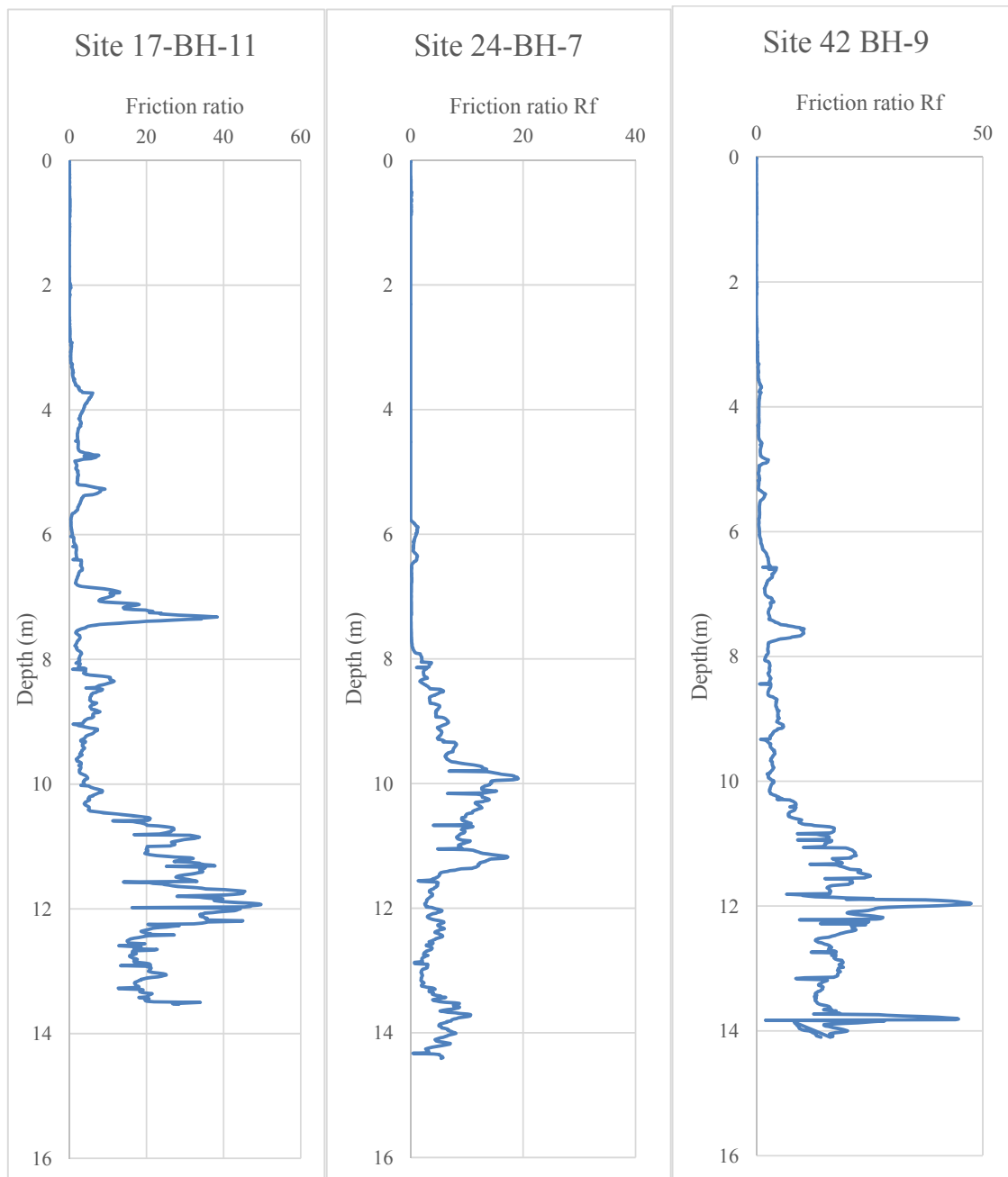
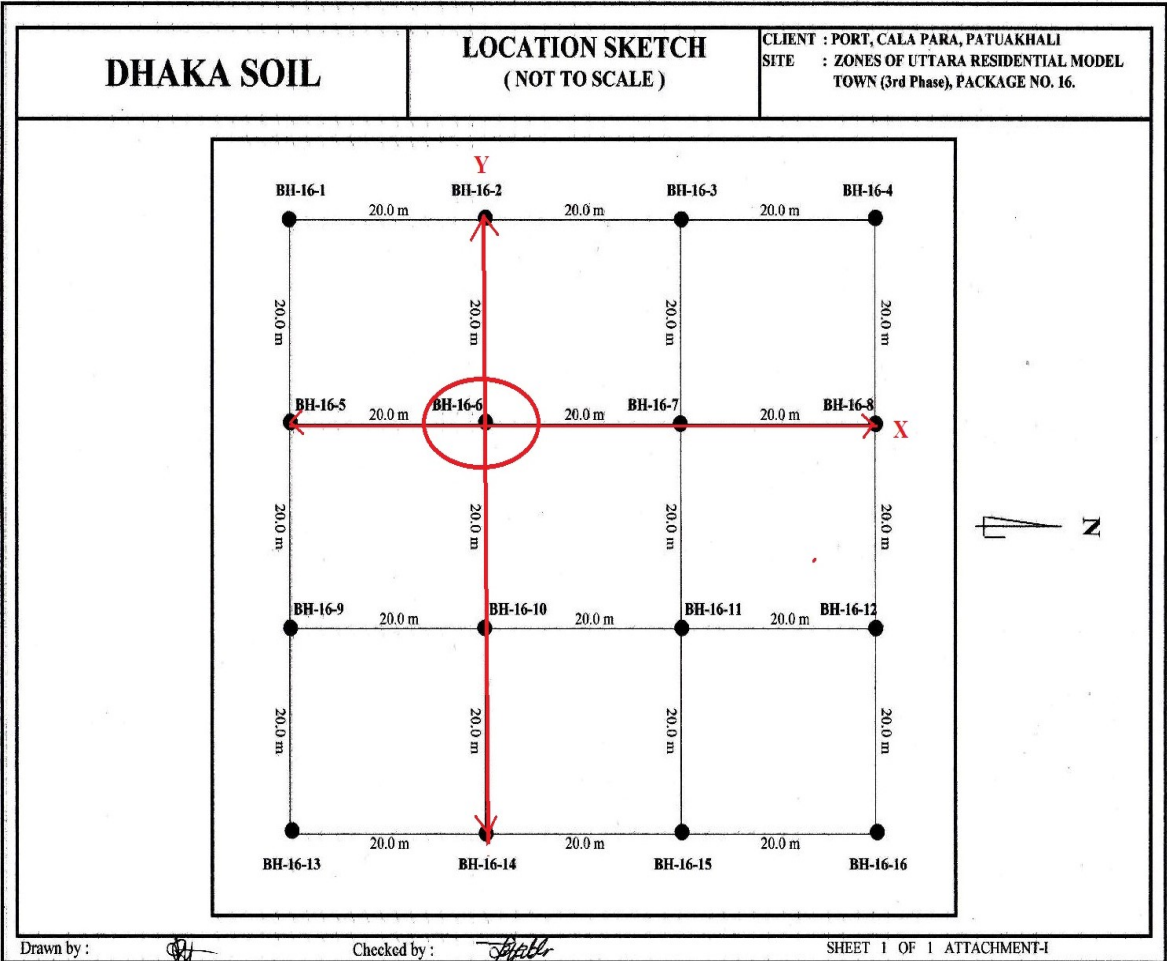


Fig 5.6: Variation of friction ratio (Fr) with depth for all the boreholes.

Based on the results of the subsurface explorations, the subsoil profile at study area can be divided into three strata. The soil within the test area is primarily comprised of fine sand and silt clay particles. The top layer consists of light grey to grey medium to loose fine sand trace mica with a total thickness approximately varied from 4.75 m to 7.5 m. Immediately below this layer, a layer of dark grey silty clay with organic matter is extended to a depth varied from 7.65 m to 9.45 m. The bottom layer consists of high plastic grey medium stiff clay or medium plastic soft to medium stiff clay up to the depth of 10.35 m. Ground water table is located at 2.3-2.7 m below from EGL. Note

that, there was considerable variability in the measured SPT N-value indifferent boreholes at different depths ranging from 2 to 18 and maximum corrected cone tip resistance ( $q_{c1}$ ) was close to 4 MPa. The pore pressure varies from 0-1000 kpa. The piezometric profile is approximately hydrostatic with groundwater at a depth of about 3m. Four out of six boreholes have maximum pore water pressure close to 500kpa, one bore hole has higher pore pressure which has a maximum value about 1000kpa and other one has lower pore water pressure having a maximum value about 100kpa. Friction ratio is nearly 0 upto 4m depth and has a peak value about 50% in between 7m to 14m depth. Consistency of the soils at different depth varies from stiff to loose. For the same location subsoil profile is found to be almost similar for different boreholes. For better understanding ross sectional profile for all the bore holes in X and Y direction keeping borehole 16-6 as origin is given bellow



Fig

5.7: Location sketch of site 16

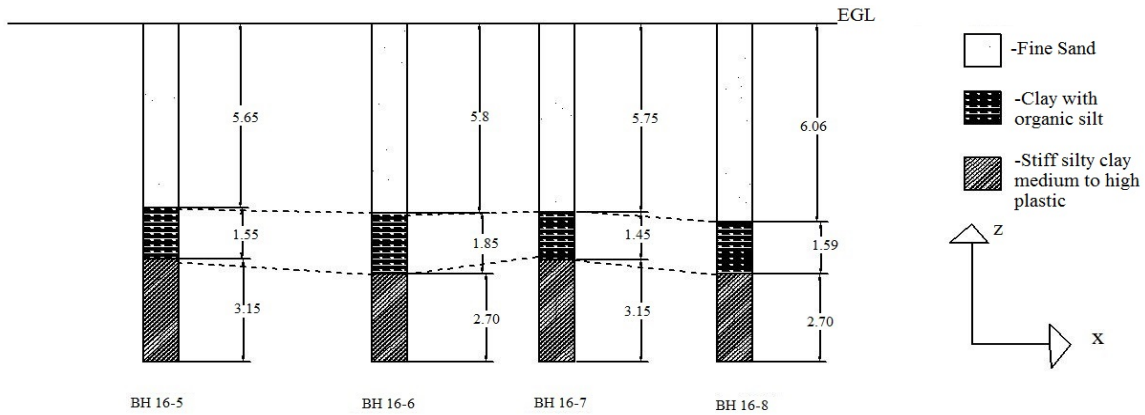


Fig 5.8: Cross sectional Profile in X direction

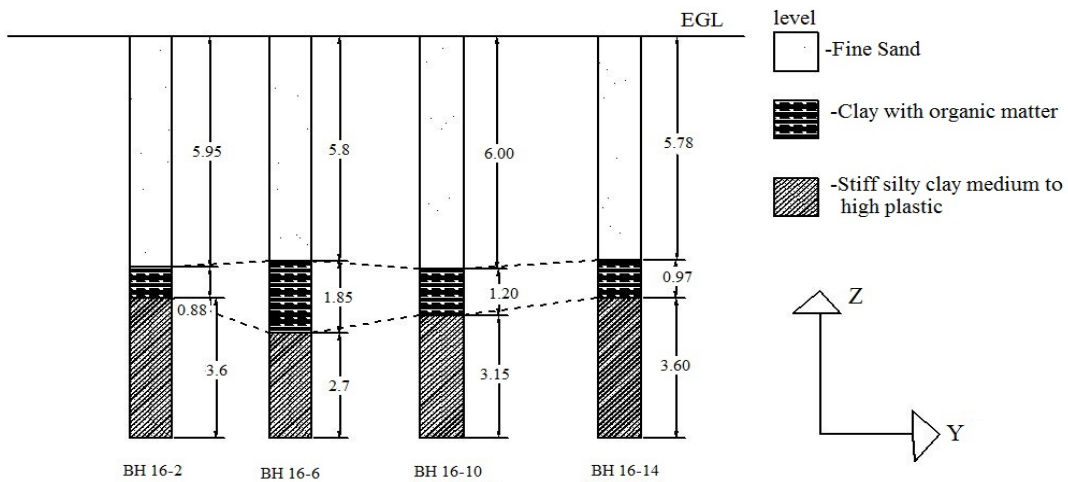


Fig 5.9: Cross sectional Profile in Y direction

## LABORATORY INVESTIGATION

As part of laboratory investigation Atterberg limit test for liquid and plastic limit was done with four samples as per ASTM Standard D 4318, direct shear test was done with five remolded samples ASTM standard D-3080, "Standard Method for Direct Shear Test on Soils under Consolidated Drained Conditions", unconfined compression test was done with four remolded sample according to ASTM D2166-06 "Standard Test Method for Unconfined Compressive Strength of Cohesive Soil" and consolidation test was done with six undisturbed clay sample as per ASTM D 2435 – "Standard Test Method for One-Dimensional Consolidation Properties of Soils."

### Sample Remolding

For remolded samples compaction test was done first per ASTM D 698 "Test Method for Laboratory Compaction Characteristics of Soil Using Standard Effort". About 2-2.5kg sample passing #4 sieve

was taken and compacted with different moisture content in a 4-inch-diameter (100 mm) mold which holds 1/30 cubic foot of soil, and compaction was done by three separate lifts of soil using 25 blows by a 5.5 lb hammer falling 12 inches, for a compactive effort of 12,400 ft-lbf/ft<sup>3</sup>. Then moisture content was plotted against dry density. 95% moisture content at the wet side was taken which was determined 28.5% was the moisture content for sample remolding and all the samples were remolded with this moisture content by compaction as the same manner described above.

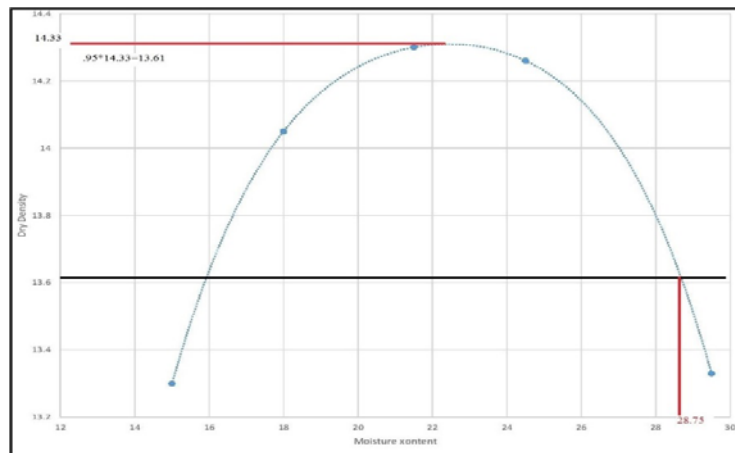


Fig 5.10: Compaction test to determine remolding moisture content

### Atterberg limits

The Atterberg limits are a basic measure of the critical water contents of a fine-grained soil: its shrinkage limit, plastic limit, and liquid limit. As a dry, clayey soil takes on increasing amounts of water, it undergoes distinct changes in behavior and consistency. Depending on the water content of the soil, it may appear in four states: solid, semi-solid, plastic and liquid. In each state, the consistency and behavior of a soil is different and consequently so are its engineering properties. Thus, the boundary between each state can be defined based on a change in the soil's behavior.

### Plastic Limits

The plastic limit (PL) is determined by rolling out a thread of the fine portion of a soil on a flat, non-porous surface. The procedure is defined in ASTM Standard D 4318. If the soil is at a moisture content where its behavior is plastic, this thread will retain its shape down to a very narrow diameter. The sample can then be remolded and the test repeated. As the moisture content falls due to evaporation, the thread will begin to break apart at larger diameters. The plastic limit is defined as the moisture content where the thread breaks apart at a diameter of 3.2 mm (about 1/8 inch). A soil is considered non-plastic if a thread cannot be rolled out down to 3.2 mm at any moisture possible.



Fig 5.11 : Plastic Limit test

Plastic limits for different boreholes is given in table 5.1

Table 5.1: Plastic limits of different boreholes

Bore Hole No	BH 2-10	BH 13-6	BH 17-11	BH 24-7
Plastic Limit	29.35	21.7	31.94	30.62

### Liquid Limits

The Liquid Limit test is being done as per ASTM standard test method D 4318 with Casagrande apparatus. Soil is placed into the metal cup portion of the device and a groove is made down its center with a standardized tool of 13.5 millimeters (0.53 in) width. The cup is repeatedly dropped 10 mm onto a hard rubber base at a rate of 120 blows per minute, during which the groove closes gradually because of the impact. The number of blows for the groove to close is recorded. The moisture content at which it takes 25 drops of the cup to cause the groove to close over a distance of 13.5 millimeters (0.53 in) is defined as the liquid limit.



Fig 5.12: Liquid limit test with casagrande apparatus

Liquid limits for different boreholes are as follows

Table 5.2: Liquid limits of different boreholes

Bore Hole No	BH 2-10	BH 13-6	BH 17-11	BH 24-7
Liquid Limit	35.8	39.6	46	40.8

### Plasticity Index

The plasticity index (PI) is a measure of the plasticity of a soil. The plasticity index is the size of the range of water contents where the soil exhibits plastic properties. The PI is the difference between the liquid limit and the plastic limit ( $PI = LL - PL$ ). Soils with a high PI tend to be clay, those with a

lower PI tend to be silt, and those with a PI of 0 (non-plastic) tend to have little or no silt or clay. Soil descriptions based on PI

Table 5.3: Soil classification based on Plasticity Index

Plasticity Index	0 to 3	3 to 15	15 to 30	>30
Soil Type	Non-plastic	Slightly plastic	Medium plastic	Highly plastic

Plasticity Index for different boreholes was calculated as follows

Table 5.4: Plasticity Index of different boreholes

Bore Hole No	BH 2-10	BH 13-6	BH 17-11	BH 24-7
Plasticity Index	6.45	17.91	14.06	10.18

The results suggest that three out of four samples were medium plastic and one sample was slightly plastic.

Soil can be classified based on Atterberg limits as per Unified Soil Classification System (USCS)

Example of 2 Group Symbol: SM

Primary Component (Sand = S) and Secondary Description (M = Silty)

Primary Components: G = Gravel, S = Sand, M = Silt, C = Clay, O = Organic

Secondary Components:

M = Silty: > 12% fines,  $PI < 4$  or plots below "A" Line

C = Clayey: > 12% fines,  $PI > 7$  and plots on or above "A" line

L = Low Plasticity (Lean for Clay) ( $LL < 50\%$ )

H = High Plasticity (Fat for Clay, Elastic for Silt) ( $LL \geq 50\%$ ) (e.g. high quality pottery clay)

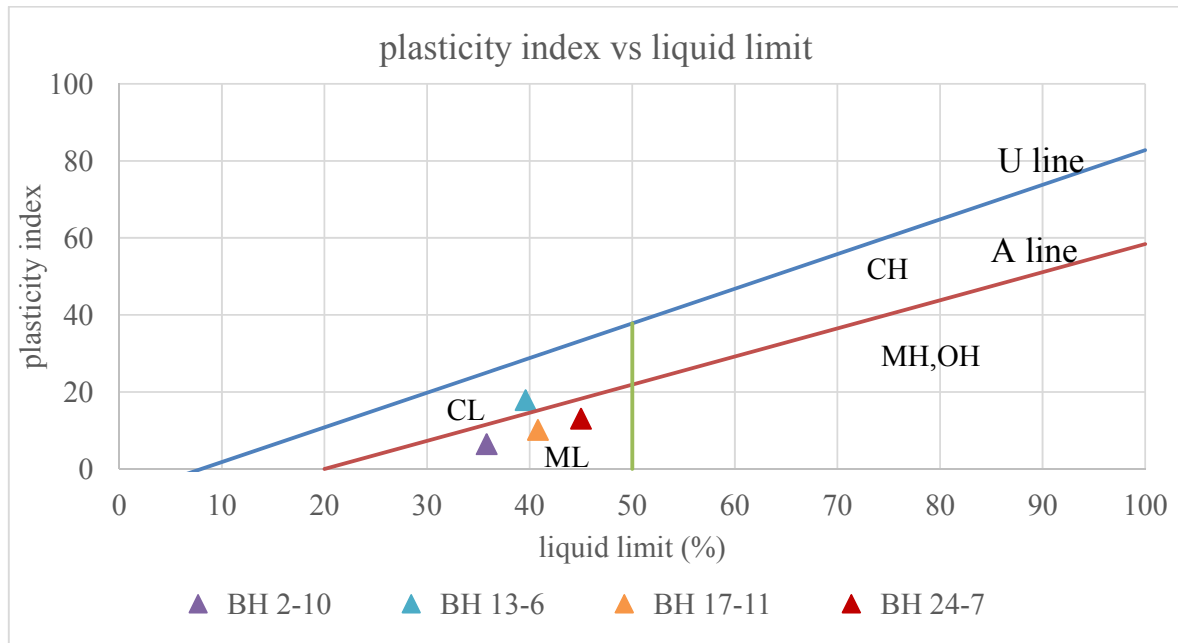


Fig 5.13: Soil classification based on Atterberg limits

Three out of four samples were found to be low plastic silt and one sample was low plastic clay per USCS

### Unconfined Compression Test

Unconfined compression test on four remolded sample was done as per ASTM D 2166 - Standard Test Method for Unconfined Compressive Strength of Cohesive Soil.



Fig 5.14 : Preparation of samples for unconfined compression test from compacted mold

In the unconfined compression test, each sample was placed in the loading machine between the lower and upper plates. Before starting the loading, the upper plate was adjusted to be in contact with the sample and the deformation was set as zero. The test then started by applying a constant axial strain of about 0.5 to 2% per minute. The load and deformation values were recorded as needed for obtaining a reasonably complete load-deformation curve. The loading was continued until the load

values decrease or remain constant with increasing strain, or until reaching 15% axial strain. At this state, the sample was at failure. The sample was then removed for measurement of the water content.



Fig 5.15: (a) Recording data for unconfined compression test (b) Failure of sample

As for the results, the axial stress was plotted versus the axial displacement ( Appendix B7-B10). The maximum axial stress, or the axial stress at 15% axial strain if it occurs earlier, was reported as the unconfined compressive strength  $\sigma_c$ . The undrained shear strength was obtained

$$Su = \sigma_c / 2$$

Undrained shear strength obtained for different bore holes are summarized below

Table 5.5: Undrained shear strength obtained for different bore holes

Sample No	BH 2-10	BH 17-11	BH 24-7	BH 42-9
Shear strength	27.58	39.4394	28.75215	23.1672

### Direct Shear Test

Direct shear testing was done per ASTM standard D-3080, "Standard Method for Direct Shear Test on Soils under Consolidated Drained Conditions" with direct shear apparatus.



Fig 5.16: Direct shear apparatus with shear box

The inside of the shear box was lightly greased to minimize side friction. The lower porous stone was placed in the shear box. Spacer disks were placed below this stone to adjust the elevation of its top to accommodate soil samples of different thicknesses. The trimming ring is then carefully

aligned with the top of the shear box. The trimming ring and top shear box have been machined so the ring fits into the shallow slot in the top of the shear box, to provide proper alignment. The sample was then slowly extruded into the shear box by pressing on its top surface, using the top porous stone or a suitable disk. The upper porous stone and loading cap were placed in the shear box, and the system to apply the normal-load was brought into place and a small normal load (seating load) was applied. The normal load was applied through a simple hanger system. The lateral load was applied using a screw jack which was activated using an electric motor and a variable-speed transmission. The transmission is usually geared to apply about 0.25 inch (typical deformation to cause failure) in a time ranging from five minutes to a week. The load transmitted to the top of the sample was measured using a proving ring. Readings were taken of horizontal displacement, vertical movement of the top cap, and shearing force, as a function of time. Stress conditions in the sample become increasingly uncertain as deformation continues so the test is usually stopped when shearing stress reached a peak value. The procedure was repeated thrice for each sample with three different normal stresses of 25kN/m<sup>2</sup>, 50kN/m<sup>2</sup> and 100kN/m<sup>2</sup>. Peak shear stress for each normal stress was obtained by plotting shear stress against displacement. Peak shear stresses were then plotted against normal stress. The slope angle of this curve represents the friction angle ( $\phi$ ) and the vertical intercept represents the shear strength ( $S_u$ ).

The internal friction angle and shear strength for different bore holes are summarized below in the table

Table 5.6: The internal friction angle and shear strength for different bore holes

Sample No	BH 2-10	BH 13-6	BH 17-11	BH 24-7	BH 42-9
Shear strength ( $S_u$ )	14.8	20.1	25	41	22
Internal friction angle ( $\phi$ )	11	30	32	20	19

### Consolidation Test

Consolidation test was done with six undisturbed clay sample as per ASTM D 2435 – “Standard Test Method for One-Dimensional Consolidation Properties of Soils.” It was the most time-consuming laboratory investigation.



Fig 5.17: Consolidation test Apparatus

The change in height of soil sample for loading and unloading stage were recorded with respect to time. At first load was increased incrementally from 0 to 5,25,100,200,400 and 800 kPa , then decremented from 800 to 400,100 and 10kPa. Load increments were done at one day interval. Time vs vertical dial reading was plotted to obtain 50% consolidation time  $t_{50}$  and 90% consolidation time  $t_{90}$  (Appendix B1-B6)

For each sample e-logP (void ratio vs pressure) curve and  $C_v$  (co-efficient of volume compressibility) against Pressure curve was obtained. Pre-consolidation pressure was obtained using e-logP curve (Appendix B1-B6)

Calculation of each borehole to form e-logP curve and  $C_v$  against Pressure curve are discussed separately below.

### BH 13-12 depth 6.3m

Table 5.7: Calculation for co efficient of volume compressibility ( $C_v$ ) and compression index ( $C_c$ ) for BH 13-12

	P	FDR	$\Delta H$	Ht	Hv	e	Ht(av)	time	min	$c_v$ from		$C_c$
	(kpa)	(in)	(in)	(in)	(in)		(in)	t50	t90	t50	t90	
Loading	0	0.089		1	0.528	1.119						
			0.007				1					
	5	0.096		0.99	0.521	1.105						0.1
			0.033				0.98					
	25	0.129		0.96	0.488	1.035		1.7	4	0.0276	0.0506	0.155
			0.022				0.95					
	50	0.151		0.94	0.466	0.988		4.5	1.44	0.0099	0.1327	0.296

			0.042				0.92					
	100	0.193		0.9	0.424	0.899		7.7	16	0.0054	0.0112	0.493
			0.07				0.86					
	200	0.263		0.83	0.354	0.751		12.5	17.2	0.0029	0.0091	0.742
			0.105				0.77					
	400	0.368		0.72	0.249	0.528		17	14	0.0017	0.0091	0.714
			0.102				0.67					
Unloading	800	0.47		0.62	0.148	0.313		16	24.1	0.0014	0.004	
			-0.02									
	400	0.448		0.64	0.169	0.359						
			-0.08									
	100	0.372		0.72	0.245	0.52						
		-0.14			0							
	10	0.23		0.86	0.286	0.607						

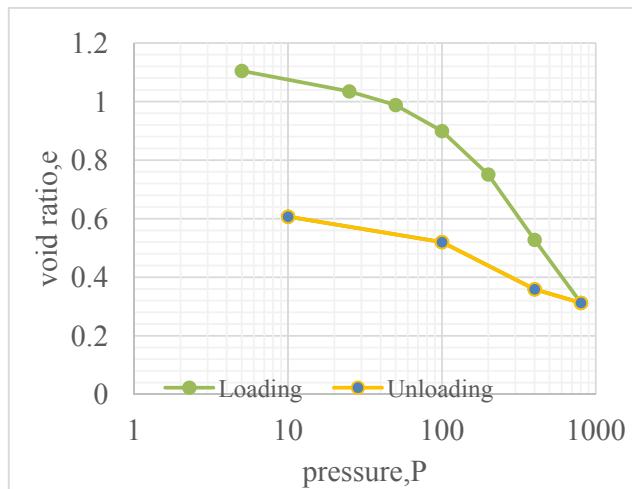


Fig 5.18: e-logP curve for BH 13-12

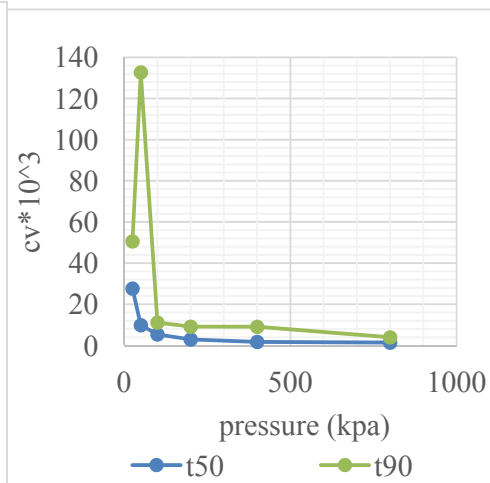


Fig 5.19: Cv Vs Pressure curve for BH 13-12

12

### BH 16-3 depth 6.3m

Table 5.8: Calculation for co efficient of volume compressibility (Cv) and compression index (Cc) for BH 16-3

	P	FDR	$\Delta H$	Ht	Hv	e	Ht(av)	time	min	cv from		Cc
	(kpa)	(in)	(in)	(in)	(in)		(in)	t50	t90	t50	t90	
Loading	0	0.0894		1	0.4499	0.81785						
			0.0066				0.9967					
	5	0.096		0.9934	0.4433	0.80585						0.0369
			0.0142				0.9863					
	25	0.1102		0.9792	0.4291	0.78004		3.8	1	0.0126	0.206	0.0773
			0.0128				0.9728					

	50	0.123		0.9664	0.4163	0.75677		6.5	4.84	0.0072	0.041	0.128
			0.0212				0.9558					
	100	0.1442		0.9452	0.3951	0.71823		7.5	10.24	0.006	0.019	0.3515
			0.0582				0.9161					
	200	0.2024		0.887	0.3369	0.61243		8	4	0.0052	0.044	0.305
			0.0505				0.86175					
	400	0.2529		0.8365	0.2864	0.52063		14	4	0.0026	0.039	0.465
			0.077				0.798					
	800	0.3299		0.7595	0.2094	0.38066		16	33.64	0.002	0.004	
		-										
		0.0044										
Unloading	400	0.3255		0.7639	0.2138	0.38866						
			-									
			0.0208									
	100	0.3047		0.7847	0.2346	0.42647						
			-									
		0.0525										
	10	0.2522		0.8372	0.2871	0.52191						

P= Pressure, FDR=Final Dial Reading,  $\Delta H$ = Change in specimen height, Ht= Final Specimen height,  
Hv=Height of void  
e=Void ratio

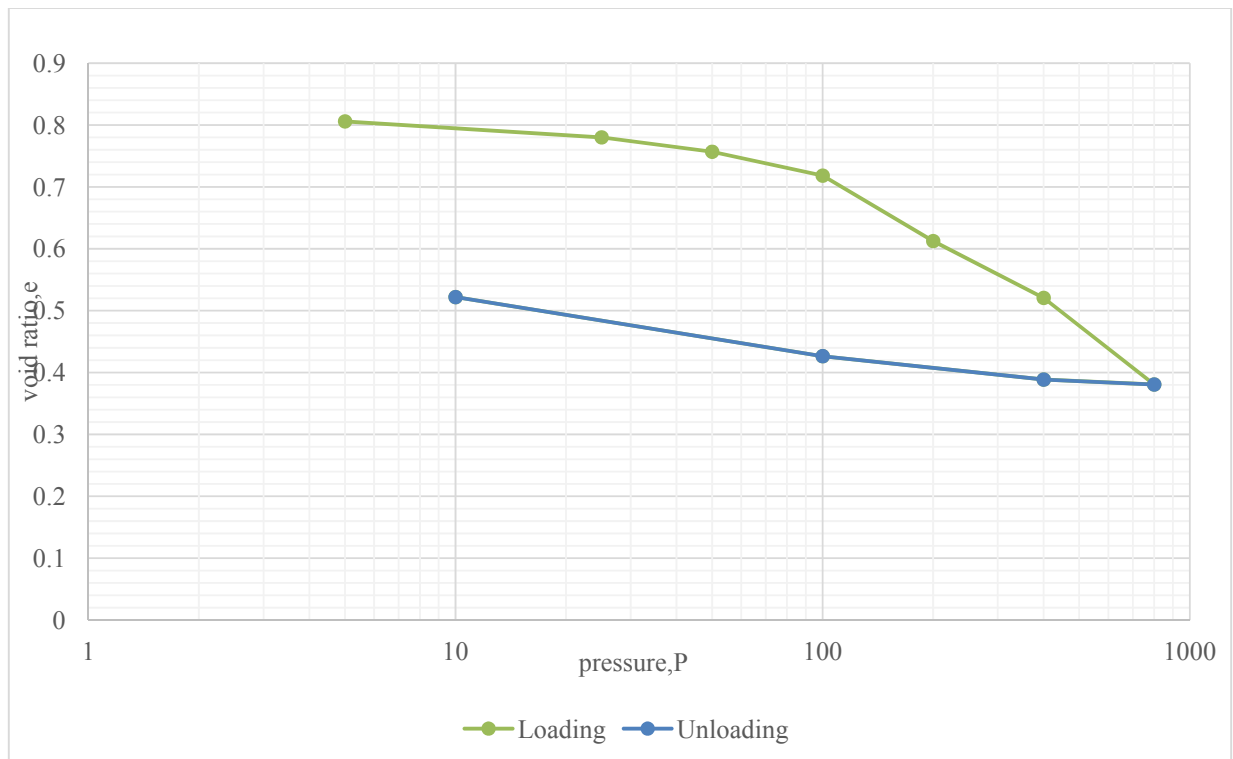


Fig 5.20: e-logP curve for BH 16-3

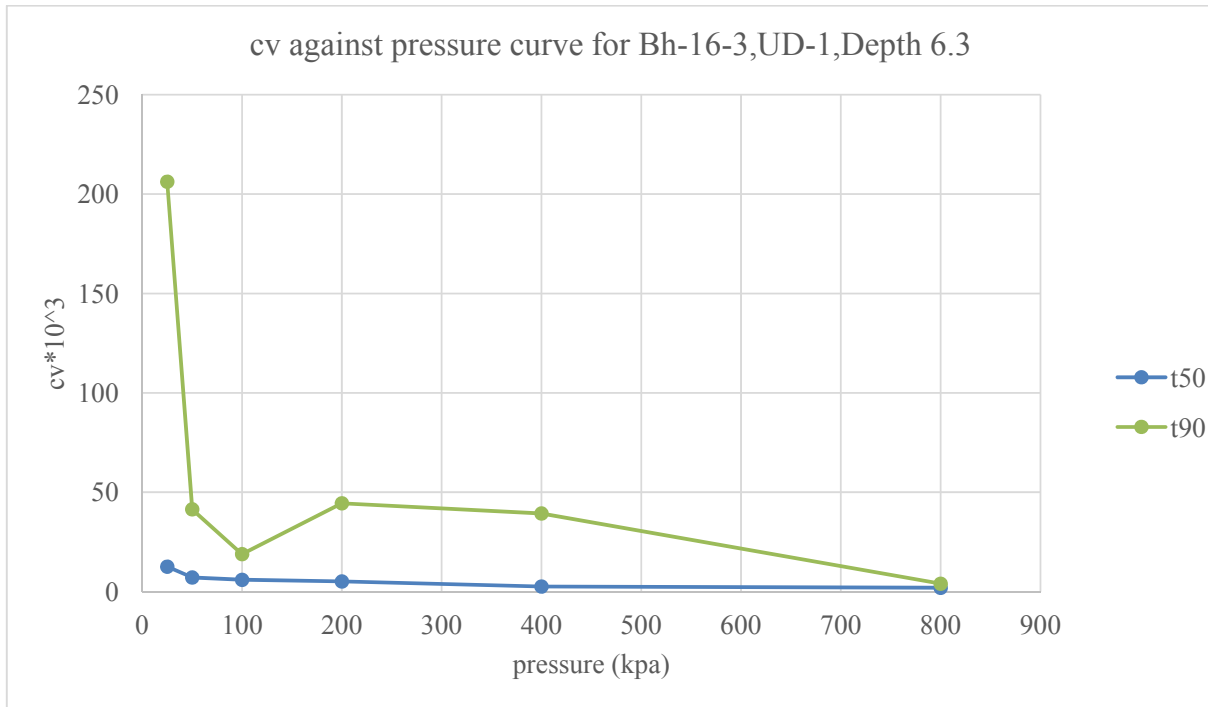


Fig 5.21: Cv Vs Pressure curve for BH 16

**BH 17-16 depth 8.1m**

Table 5.9: Calculation for co efficient of volume compressibility (Cv) and compression index (Cc) for BH 17-16

	P	FDR	ΔH	Ht	Hv	e	Ht(av)	time	min	cv from		Cc
	(kpa)	(in)	(in)	(in)	(in)		(in)	t50	t90	t50	t90	
Loading	0	0.0852		1	0.4499	0.8179						
			0.0076				0.9962					
	5	0.0928		0.9924	0.4423	0.804						0.05
			0.0206				0.9821					
	25	0.1134		0.9718	0.4217	0.7666		6.2	18.1	0.0077	0.01	0.14
			0.0238				0.9599					
	50	0.1372		0.948	0.3979	0.7233		6.5	9.61	0.007	0.02	0.23
			0.0388				0.9286					
	100	0.176		0.9092	0.3591	0.6528		12	20.3	0.0035	0.01	0.35

			0.0586				0.879 9					
	200	0.2346		0.850 6	0.3005	0.546 3		14	10. 2	0.002 7	0.0 2	0.4 3
			0.071				0.815 1					
	400	0.3056		0.779 6	0.2295	0.417 2		14	13. 9	0.002 3	0.0 1	0.4 7
			0.078				0.740 6					
	800	0.3836		0.701 6	0.1515	0.275 4		13	11. 6	0.002 1	0.0 1	
		- 0.0048										
<b>Unloading</b>	400	0.3788		0.706 4	0.1563	0.284 1						
			- 0.0206									
	100	0.3582		0.727	0.1769	0.321 6						
			- 0.0496									
	10	0.3086		0.776 6	0.2265	0.411 7						

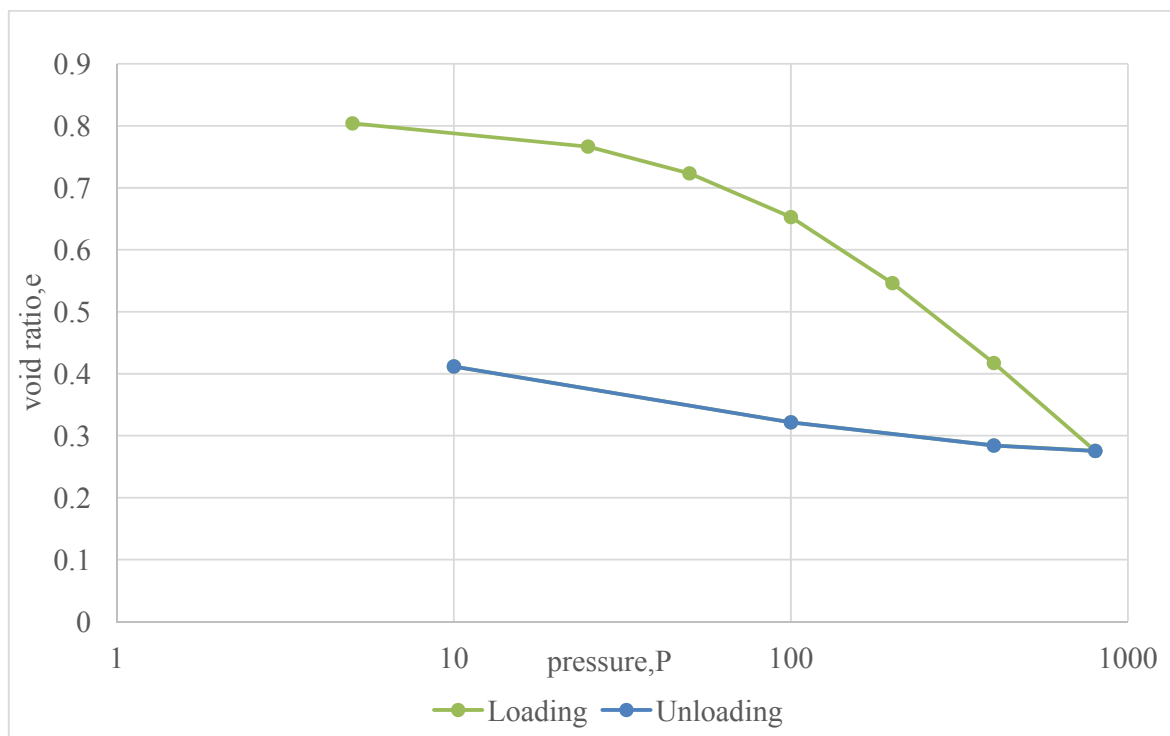


Fig 5.22: e-logP curve for BH 17-16

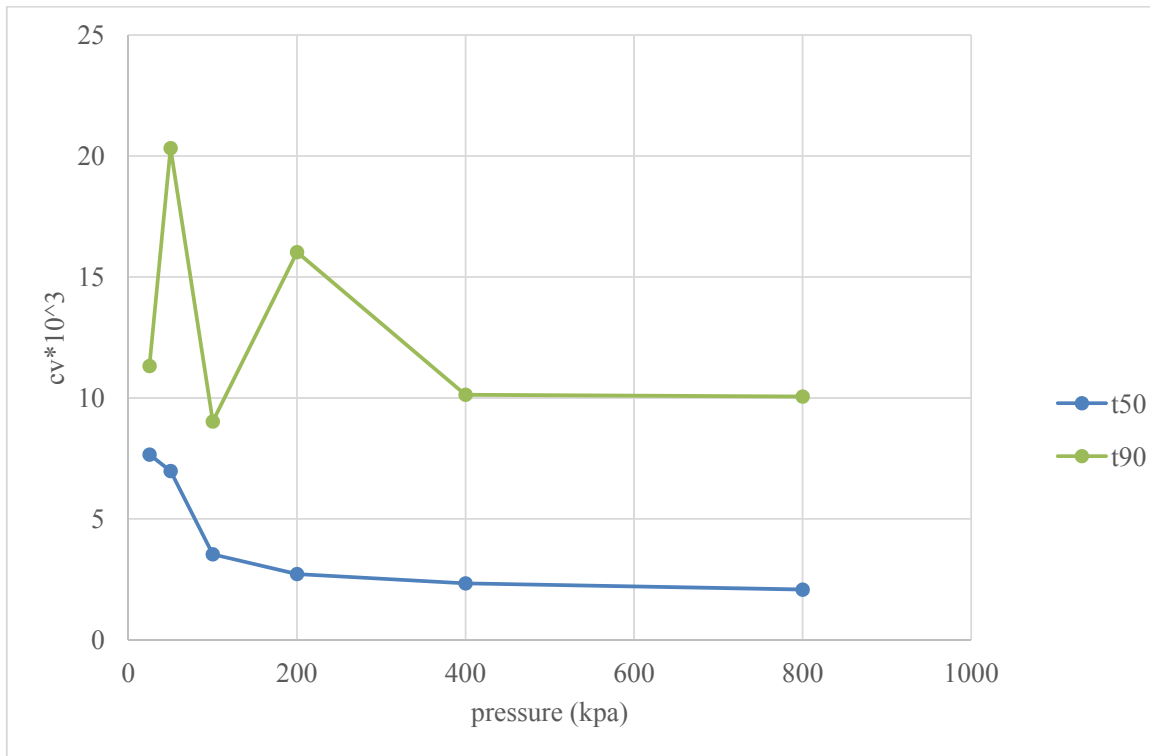


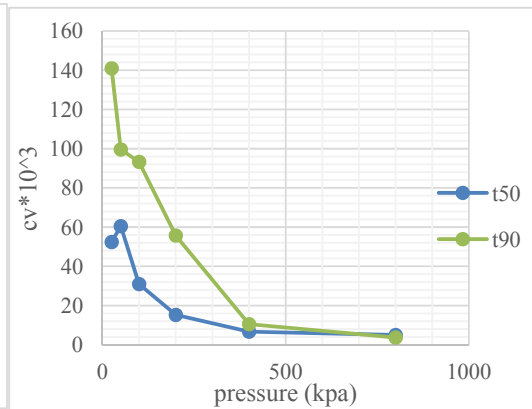
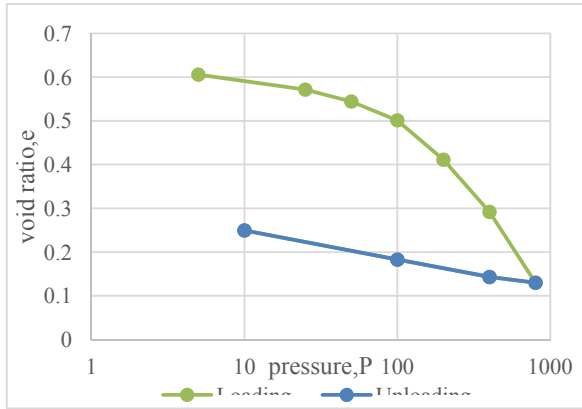
Fig 5.23: Cv Vs Pressure curve for BH 17-11

**BH 24-2 depth 8.55**

Table 5.10: Calculation for co efficient of volume compressibility (Cv) and compression index (Cc) for BH 24-2

	P	FDR	ΔH	Ht	Hv	e	Ht(av)	time	min	cv from		Cc
	(kpa)	(in)	(in)	(in)	(in)		(in)	t50	t90	t50	t90	
<b>Loading</b>	0	0.058		1	0.384	0.62						
			0.01				0.995					
	5	0.069		0.99	0.373	0.61						0.05
			0.02				0.979					
	25	0.09		0.97	0.352	0.57		0.9	1.44	0.0524	0.14	0.09
			0.02				0.96					
	50	0.107		0.95	0.335	0.54		0.75	1.96	0.0605	0.1	0.14
			0.03				0.938					
	100	0.134		0.92	0.309	0.5		1.4	2	0.031	0.09	0.3
			0.06				0.897					
	200	0.189		0.87	0.253	0.41		2.6	3.063	0.0152	0.06	0.4
			0.07				0.833					
	400	0.262		0.8	0.18	0.29		5.1	14	0.0067	0.01	0.54
			0.1				0.746					
	800	0.362		0.7	0.08	0.13		5.5	32	0.005	0	
		-0.01										
<b>Unloading</b>	400	0.354		0.7	0.088	0.14						
			-0.02									

	100	0.33		0.73	0.113	0.18						
			-0.04									
	10	0.289		0.77	0.154	0.25						



Fig

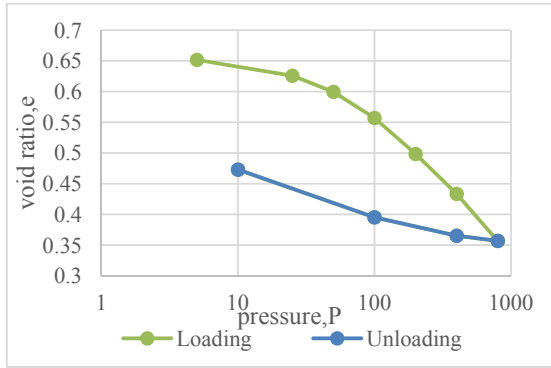
5.24: e-logP curve for BH 24-2

Fig 5.25: Cv Vs Pressure curve for BH 24-2

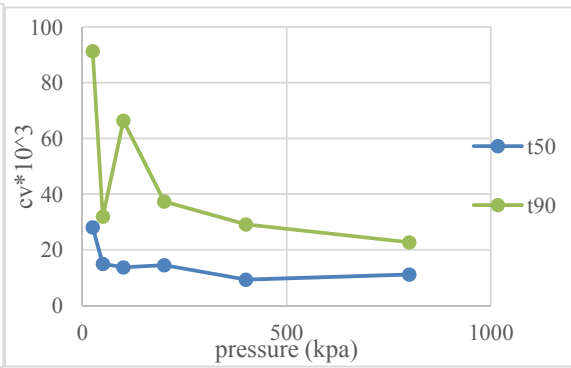
**BH 2-1 depth 7.65m**

Table 5.11: Calculation for co efficient of volume compressibility (Cv) and compression index (Cc) for BH 2-1

	P	FDR	ΔH	Ht	Hv	e	Ht(av)	time	min	cv from	Cc	
	(kpa)	(in)	(in)	(in)	(in)		(in)	t50	t90	t50		t90
<b>Loading</b>	0	0.0652		1	0.367	0.667151						
			0.0086				0.9957					
	5	0.0738		0.9914	0.3584	0.651518					0.0369	
			0.0142				0.9843					
	25	0.088		0.9772	0.3442	0.625704		1.7	2.25	0.0281	0.0913	0.087
			0.0143				0.97005					
	50	0.1023		0.9629	0.3298	0.599527		3.1	6.25	0.0149	0.0319	0.1413
			0.0235				0.95115					
	100	0.1258		0.9394	0.3064	0.55699		3.25	2.89	0.0137	0.0664	0.1951
			0.0323				0.92325					
	200	0.1581		0.9071	0.2741	0.498273		2.9	4.84	0.0145	0.0373	0.2156
		0.0357				0.88925						
	400	0.1938		0.8714	0.2384	0.433376		4.2	5.76	0.0093	0.0291	0.2542
		0.0421				0.85035						
	800	0.2359		0.8293	0.1963	0.356844		3.2	6.76	0.0111	0.0227	
		-										
		0.0046										
<b>Unloading</b>	400	0.2313		0.8339	0.2009	0.365206						
			-									
			0.0165									
	100	0.2148		0.8504	0.2174	0.395201						
		-										
		0.0427										
	10	0.1721		0.8931	0.2601	0.472823						



5.26: e-logP curve for BH 2-1



Fig

Fig 5.27: Cv Vs Pressure curve for BH 2-1

**BH 17-5 depth 5.85m**

Table 5.12: Calculation for co efficient of volume compressibility (Cv) and compression index (Cc) for BH 17-5

	P	FDR	ΔH	Ht	Hv	e	Ht(av)	time	min	cv from		Cc
	(kpa)	(in)	(in)	(in)	(in)		(in)	t50	t90	t50	t90	
<b>Loading</b>	0	0.0557		1	0.531	1.132						
			0.0017				0.99915					
	5	0.0574		0.9983	0.5293	1.129						0.0903
			0.0296				0.9835					
	25	0.087		0.9687	0.4997	1.065		1	3.24	0.0476	0.063	0.0694
			0.0098				0.9638					
	50	0.0968		0.9589	0.4899	1.045		8	2.89	0.0057	0.068	0.1112
			0.0157				0.95105					
	100	0.1125		0.9432	0.4742	1.011		5.1	4.84	0.0087	0.04	0.1834
			0.0259				0.93025					
	200	0.1384		0.9173	0.4483	0.956		6.5	14.82	0.0066	0.012	0.3032
			0.0428				0.8959					
	400	0.1812		0.8745	0.4055	0.865		4.1	15.21	0.0096	0.011	0.4257
			0.0601				0.84445					
		800	0.2413		0.8144	0.3454	0.736		3	12.25	0.0117	0.012
		-										
		0.0042										
<b>Unloading</b>	400	0.2371		0.8186	0.3496	0.745						
			-									
		0.0153										
	10	0.198		0.8577	0.3887	0.829						

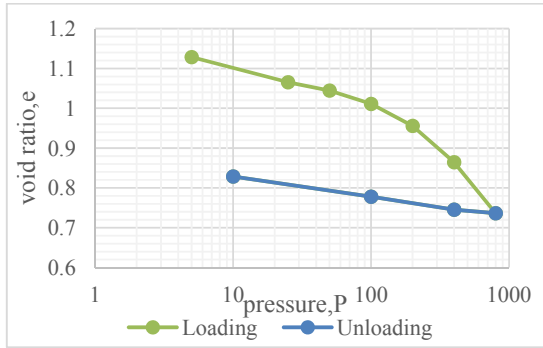


Fig 5.28: e-logP curve for BH 17-5

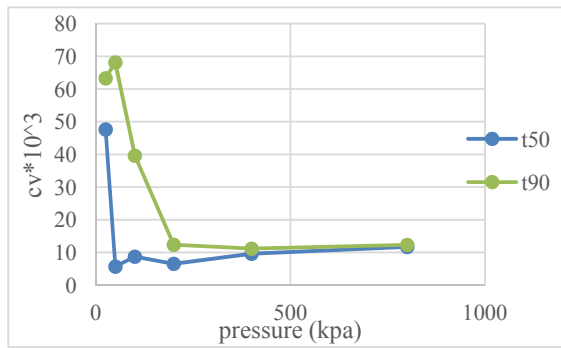


Fig 5.29: Cv Vs Pressure curve for BH 17-5

### Calculation of Over Consolidation Ratio (OCR)

Table 5.13: Calculation of OCR for different boreholes

Borehole no	$\sigma_p'$ (kpa)	depth (m)	$\sigma_v$ (kpa)	$\sigma_v'$ (kpa)	OCR= $\sigma_p' / \sigma_v'$
13-12	93	6.3	83.19	38.997	2.133241
16-3	130	6.3	120.19	38.997	3.082032
17-16	88	8.1	78.19	50.139	1.559465
17-5	121	5.85	111.19	36.2115	3.070572
2--1	91	7.65	81.19	47.3535	1.714551
24-2	140	8.55	130.19	52.9245	2.459919

Here,

$\sigma_p'$ =Pre-consolidation pressure,  $\sigma_v$ = Overburden stress and  $\sigma_v'$ =Effective overburden stress

## 6 RESULTS COMPARISON AND DISCUSSIONS

### Correlation of CPT and SPT based on soil behavior index

Soil Behavior index  $I_c$  was determined for all the boreholes using the equation 2.1 provided by Robertson (1990)

$$I_{SBT} = [(3.47 - \log(qc/pa))^2 + (\log Rf + 1.22)2]^{0.5} \text{ ----- (2.1)}$$

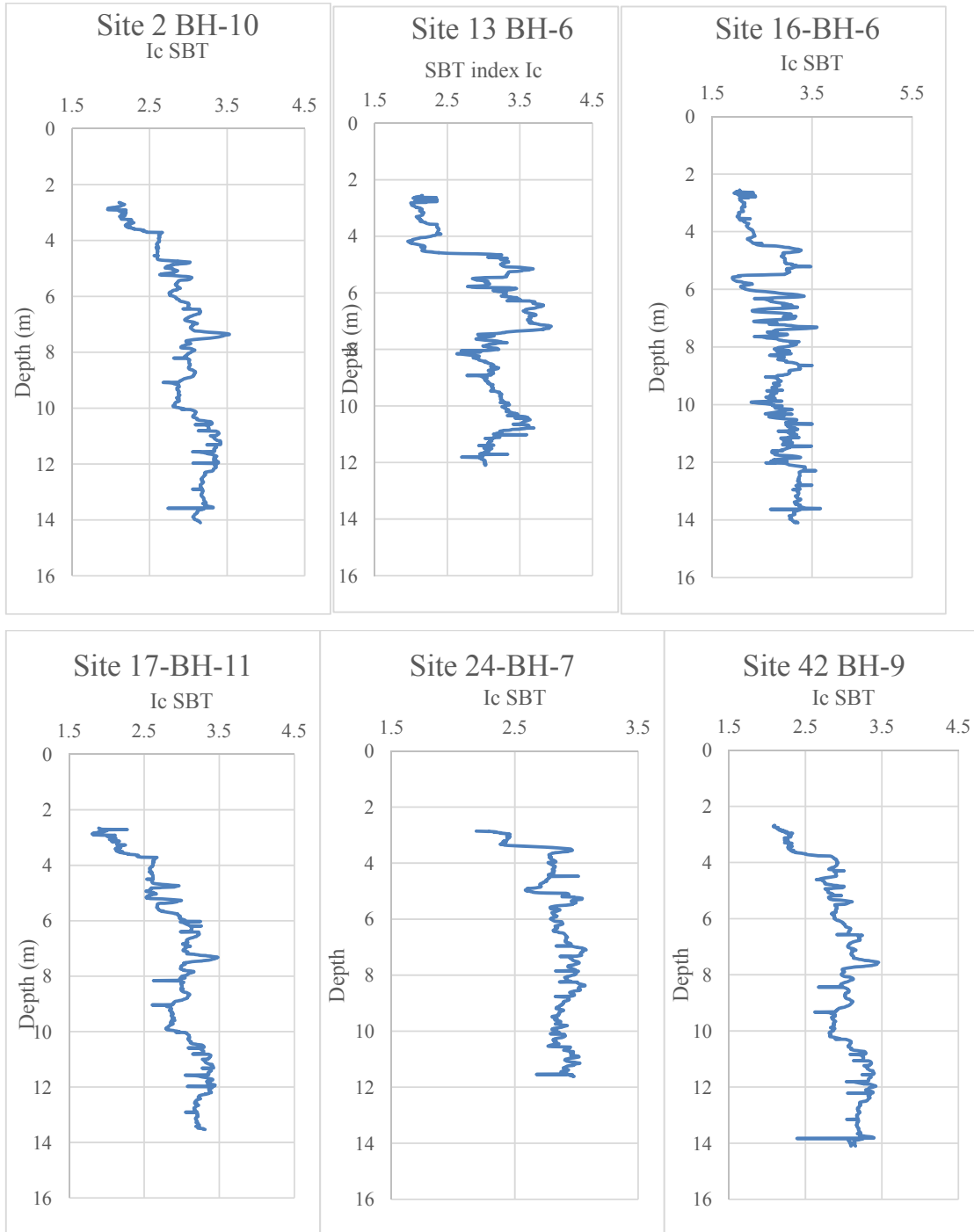


Fig 6.1: SBT profile for all the bore holes

All the bore hole has similar type of variation in behavior index( $I_c$ ) and it reached a peak value about 3.5 to 4 in all the bore holes at a depth greater than 5m.

Calculated CPT based  $I_c$  was plotted against the ratio of CPT cone resistance  $q_t$  to SPT blow count  $N_{60}$  ( $q_t/N$ ) and compared to the existing correlation between  $q_t/N$  and  $I_c$  provided by Jefferies & Davies (1993) which was modified by Robertson and wide in (1998) and Robertson(2012) as per equation 4.2 and 4.3 discussed in section 4.

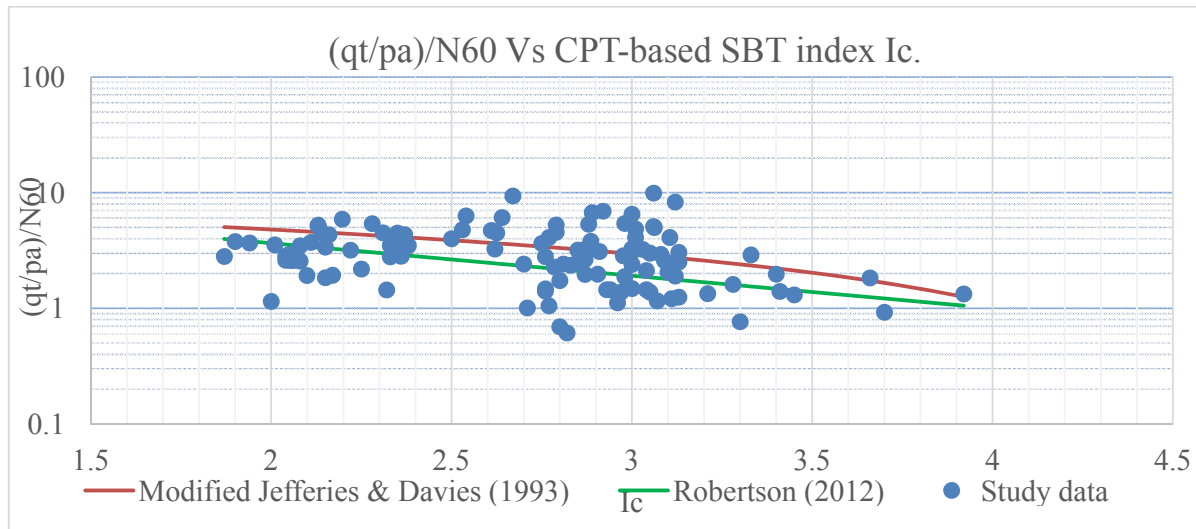


Fig 6.2 :  $(qt/pa)/N_{60}$  Vs CPT-based SBT index  $I_c$  comparison with existing correlations

Fig 6.2 shows that  $qt/N$  ratio for local soil shows the same pattern as existing correlations.  $qt/N$  ratio for selected data points varies from 0.6 to 10 with a variation of SBT index from 1.9 to 3.9 whereas existing correlations suggest that with similar variation of SBT index  $qt/N$  has a range of 1 to 5. From the graph, we can see the number of data points showing deviation is very less and about 85% of the data points falls within the range of existing correlations. So, we can conclude that CPT data are reliable to calculate SBT index and also, SBT index based CPT-SPT correlations are fairly applicable for local soil.

### Correlation of SPT with undrained shear strength $S_u$ or $C_u$

Shear strength obtained from direct shear test and unconfined compression test were compared with shear strength obtained from SPT based correlation provided by Kulhawy and Mayne (1990) as per equation 4.7 mentioned in section 4.

Table 6.1: Comparison of shear strength from laboratory test results with SPT based shear strength

Sample No	Observed UC (kpa)	Direct shear (kpa)	SPT $N_{60}$	$C_u$ (Kulhawy Mayne 1990) (kpa)
BH 2-10	27.58	14.8	5	30.3975
BH 13-6		20.1	4.375	26.5978125
BH 17-11	39.4394	25	5	30.3975
BH 24-7	28.75215	41	4.57	27.783315
BH 42-9	23.1672	22	3.87	23.527665

Three out of four unconfined compression test results coincide with SPT derived shear strength but direct shear test results show deviation. This is mainly because Kulhawy and Mayne established the

empirical correlation between SPT and undrained shear strength for pure clay sample based on unconfined compression test results. Besides direct shear test is suitable for fine grained soil not pure clay. A slight variation in moisture content can significantly affect direct shear test. Only a single compaction test was done to determine optimum moisture content for all the sample remolding. Thus, some samples may have moisture content more than necessary which may cause the deviations.

Both of the laboratory test results were plotted against SPT on the same graph with relationship provided by Kulhawy-Mayne (1990)

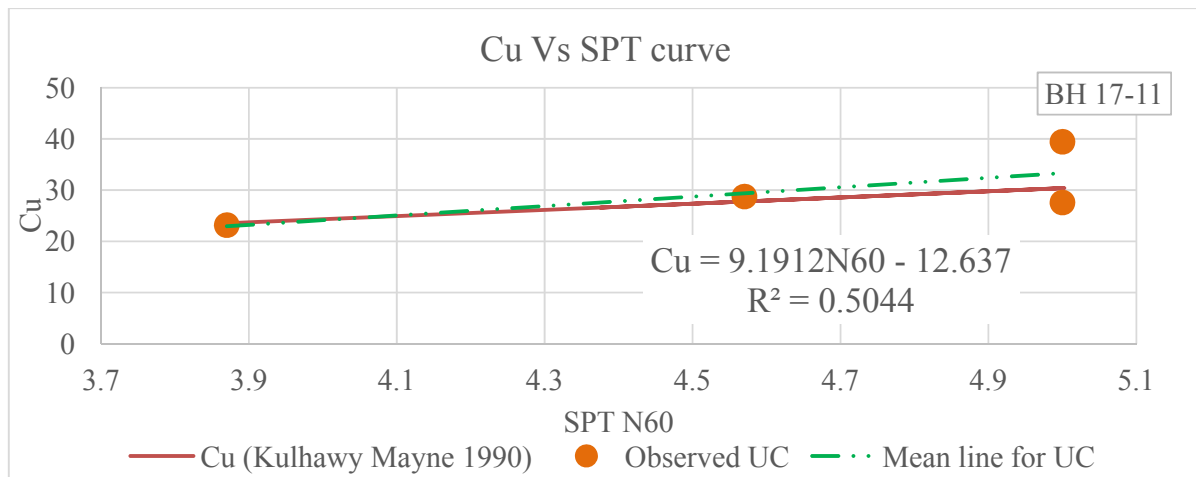


Fig 6.3: Cu Vs SPT blow count  $N_{60}$  curve for comparison of unconfined compression test results. From fig 6.3 we see that only Shear strength obtained from the sample of BH 17-11 shows deviation, yet the mean line of unconfined compressive results was very close to that of Kulhawy and Mayne and has a  $R^2 > 0.3$  which ensures good applicability of this correlation for local soil.

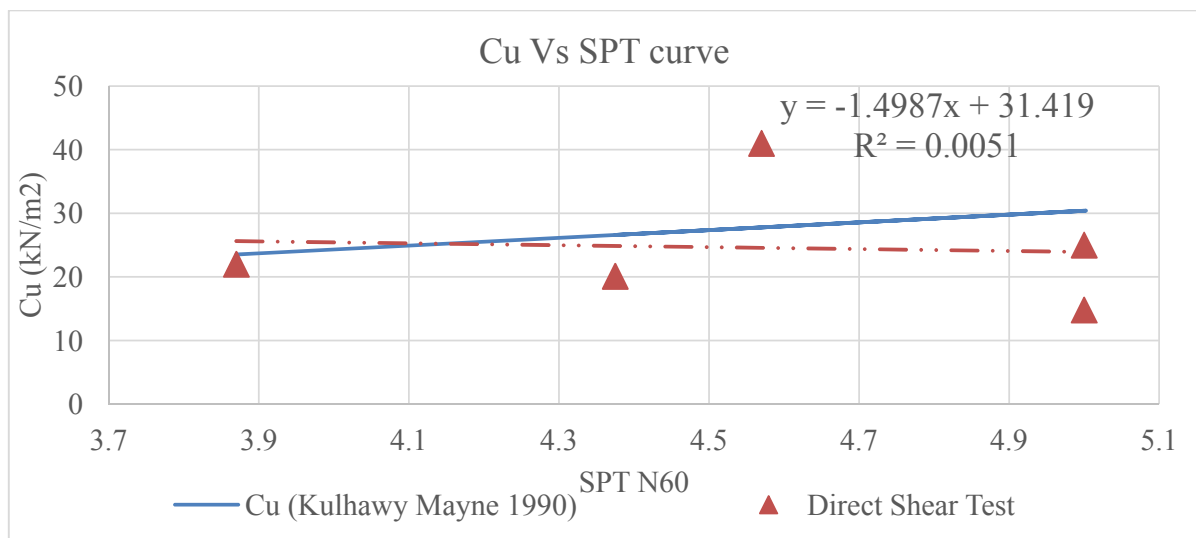


Fig 6.4: Cu Vs SPT blow count  $N_{60}$  curve for comparison direct shear test results. Fig 6.4 shows the poor applicability of existing correlation and the study data points do not maintain any different correlation with SPT as the mean line has a  $R^2 \ll 0.3$ .

### Correlation of CPT with undrained shear strength $S_u$ or $C_u$

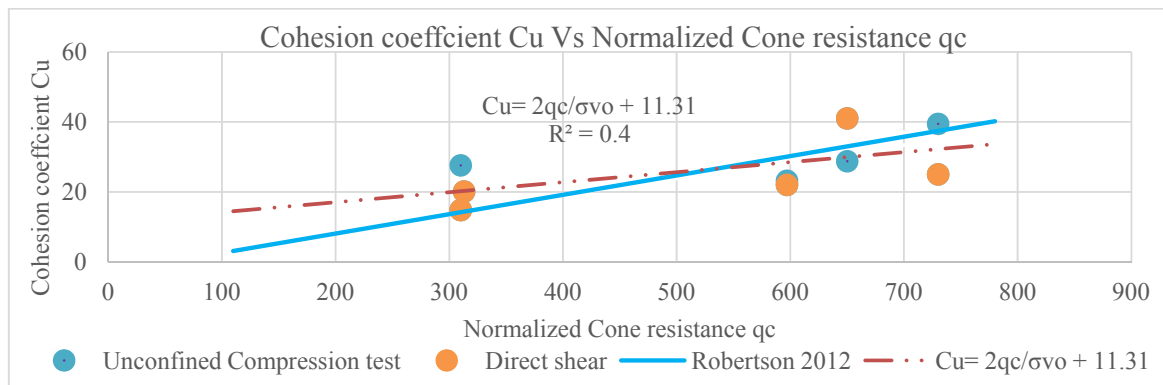
Shear strength obtained from direct shear test and unconfined compression test were compared with shear strength obtained from CPT based correlation as per equation 2.14 with modified  $N_{kt}$  value provided by Robertson (2012) in equation 2.15 mentioned in chapter 2.

Table 6.2: Comparison of shear strength from laboratory test results with CPT based shear strength

Sample No	Observed UC(kN/m <sup>2</sup> )	Direct shear(kN/m <sup>2</sup> )	Fr	$N_{kt} = 10.5 + 7 \log(Fr)$	$q_c$ (kpa)	$C_u = (q_c - \sigma_{vo})/N_{kt}$ (Robertson 2012) (kpa)
BH 2-10	27.58	14.8	13.71	18.45926218	310	13.00431174
BH 13-6		20.1	6.41	16.14800621	313	15.05139377
BH 17-11	39.4394	25	15.65	18.86160039	730	34.99437939
BH 24-7	28.75215	41	5.85	15.87009106	650	36.54988479
BH 42-9	23.1672	22	11.7	17.97730103	597	29.31752653

We observe from table 6.2 that with a variation of  $q_c$  from 310kpa to 730kpa the existing correlation gives a  $C_u$  range of 13 to 29 where laboratory test results give a  $C_u$  range of 23.17 to 39 for Unconfined compression test and 14.8 to 41 for direct shear test.

Both laboratory test results were plotted against SPT on the same graph with relationship provided by Robertson (2012) to justify the applicability this correlation to local soils.



Fig

4.5:  $C_u$  Vs CPT cone resistance  $q_c$  curve for comparison laboratory test results

The study data points follows a similar linear pattern as correlation established by Robertson (2012) but better suits with  $C_u = 2q_c/\sigma_{vo} + 11.31$  rather than  $C_u = (q_c - \sigma_{vo})/N_{kt}$ . The proposed correlation has  $R^2 > 0.3$  and has a scope of development when large amount of data points are available.

### Correlation of SPT with internal friction angle $\phi$

Friction angle obtained from direct shear test was compared with SPT based friction angle with equation 2.4, 2.5 and 2.6 provided by Wolff (1989), Kulhawy and Mayne (1990) and Hatanaka and Uchida (1996) respectively.

Table 6.3: Comparison of friction angle from direct shear test results with SPT based friction angle

Sample No	SPT N60(avg)	From direct shear test (in degree)	kulhawy and mayne 1990,( $\phi$ ) (degree)	Hatanaka and uchida 1996 (degree)	wolff 1989 (degree)
BH 13-6	4.38	30	24.89	28.49956106	28.40
BH 17-11	5	32	25.88	29.08641298	28.59
BH 24-7	4.57	20	25.17	28.68691495	28.46
BH 42-9	3.87	19	23.75	27.99397806	28.25

We can see from Table 6.3 that for a variation of SPT from 3.87 to 5 angle of internal friction remains within the range of 24-29 in the existing correlations whereas results obtained from direct shear test shows a variation of  $\phi$  has a range of 19 to 30 which is close to the existing correlations. For better understanding friction angle from direct shear test has been plotted against SPT blow count  $N_{60}$  in the same graph where existing correlations have been illustrated.

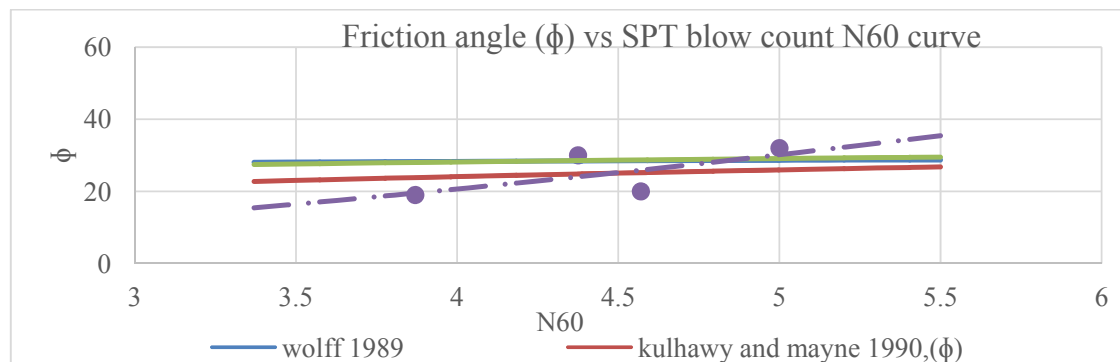


Fig 6.6 : Friction angle ( $\phi$ ) vs SPT blow count N60 curve

From figure 6.6 we see the plotted study data points has a steeper curve than existing correlations. So the study points were plotted separately to obtain a new correlation for local soil.

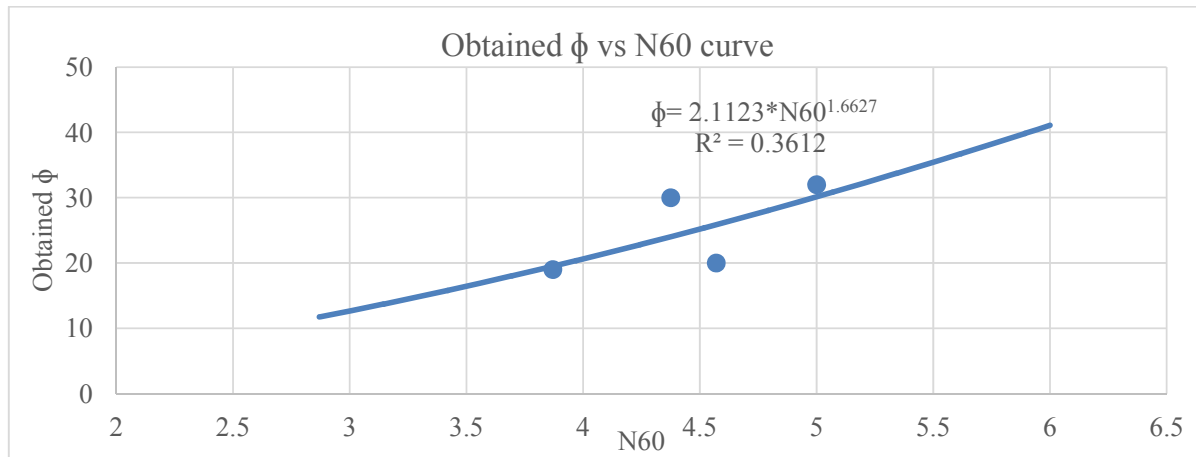


Fig 6.7: Friction angle ( $\phi$ ) vs SPT blow count N60 curve for selected data points

The above figure suggests a new correlation of  $\phi = 2.1123 * N60^{1.6627}$  for local soil. This correlation gives a scope for obtaining internal friction angle directly from SPT data but more data points are required to establish a reliable correlation for local soil.

#### Correlation of CPT with internal friction angle $\phi$

Friction angle obtained from direct shear test was compared with CPT based friction angle with equation 2.9, 2.10(a) and 2.10(b) provided by Robertson and Campanella (1983), Kulhawy and Mayne (1990) and Minmura (2003) respectively as discussed in chapter 2.

Table 6.4: Comparison of friction angle from direct shear test results with CPT based friction angle

Sample No	From direct shear test ( $\phi$ )	cpt qc(MPa)	Robertson & Campanella (1983) (degree)	Kulhawy & Mayne (1990) (degree)	Mimura (2003) (deg)
BH 13-6	30	0.313	13.04	16.730	22.23
BH 17-11	32	0.73	20.3	20.78	26.28
BH 24-7	20	0.65	19.29	20.22	25.72
BH 42-9	19	0.597	18.67	19.82	25.32
BH 2-10	11	0.31	13	16.68	22.18

From above table we observe that for a variation of cone resistance from .31Mpa to .73 Mpa existing correlations provides a range of 13-26 ° whereas friction angle from direct shear test varies from 11 to 32°.

Data points BH 13-6 and BH 17-11 shows larger deviation it may be because of the selection of optimum moisture content for remolding as explained before. For better understanding friction angle from direct shear test has been plotted against CPT cone resistance  $q_c$  in the same graph where existing correlations have been illustrated.

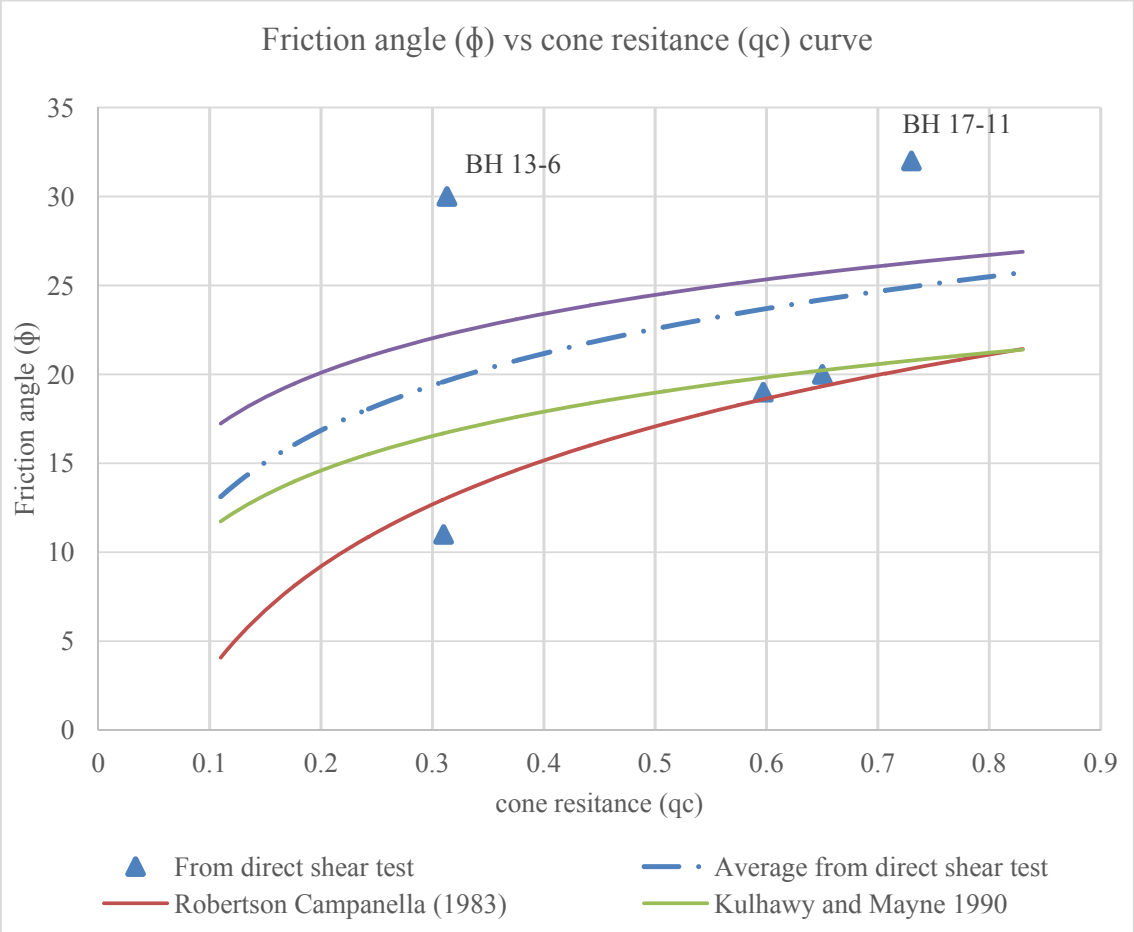


Fig 6.8: friction angle Vs CPT cone resistance  $q_c$

Above graph shows that three out of four data points falls on the Robertson Campanella (1983) curve. Two samples show greater deviation yet the mean curve obtained from direct shear test falls within the range of the existing correlations and follows a similar pattern.

To establish correlation between CPT cone resistance and internal friction angle for local soil, data points of BH 13-6 and BH 17-11 (larger deviation) was neglected.

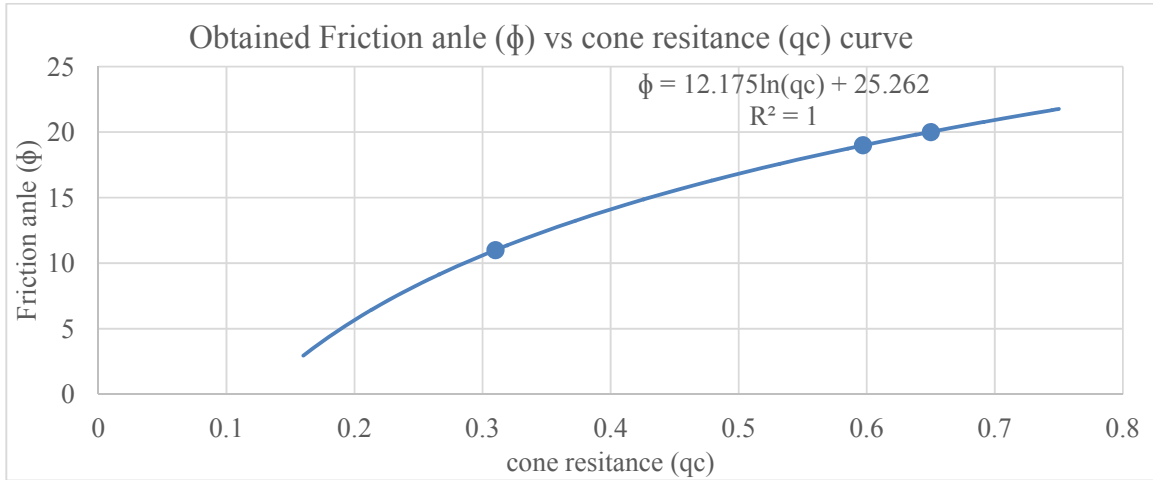


Fig 6.9 : New correlation between friction angle( $\phi$ ) and cone resistance( $q_c$ ) for local soil

Fig 6.9 shows a strong correlation between friction angle and CPT having a  $R^2=1$ . So the proposed new correlation for local soil is  $\phi = 12.175\ln(q_c) + 25.262$

#### Comparison of $t_{50}$ from consolidation test and CPTu dissipation test

CPTu dissipation test was done on different depths on different bore holes (details appendix C Test No F7). These depths range from 6-8m having a overburden pressure about 100kpa. So  $t_{50}$  obtained from dissipation tests were compared to  $t_{50}$  obtained for 100kpa loading during consolidation test. The bore hole number of consolidation samples were different from the bore hole numbers of CPTu dissipation tests. But as discussed in chapter 3 and illustrated in fig 3.7 and 3.8 that the cross sectional profile of boreholes of the same site is uniform so the effect of borehole numbers being different is neglected.

Table 4.5: Comparison of  $t_{50}$  from consolidation test and  $t_{50}$  CPTu dissipation test

Site No	Site 13	Site 24	Site 16	Site 17
$t_{50}$ obtained from consolidation test(min)	7.7	1.4	7.5	12
$t_{50}$ Obtained from cptu dissipation test (min)	2.8	4	4	8

The table shows lower  $t_{50}$  values for CPTu dissipation test than consolidation test other than site 24. To determine whether  $t_{50}$  values obtained from laboratory and field data maintains any correlation,  $t_{50}$  obtained from field data was plotted against  $t_{50}$  obtained from consolidation test and a correlation has been proposed between these two as follows

$$t'_{50} = 1.0346 * t_{50} - 4.4466$$

where  $t'_{50}$  = 50% consolidation time from CPTu dissipation

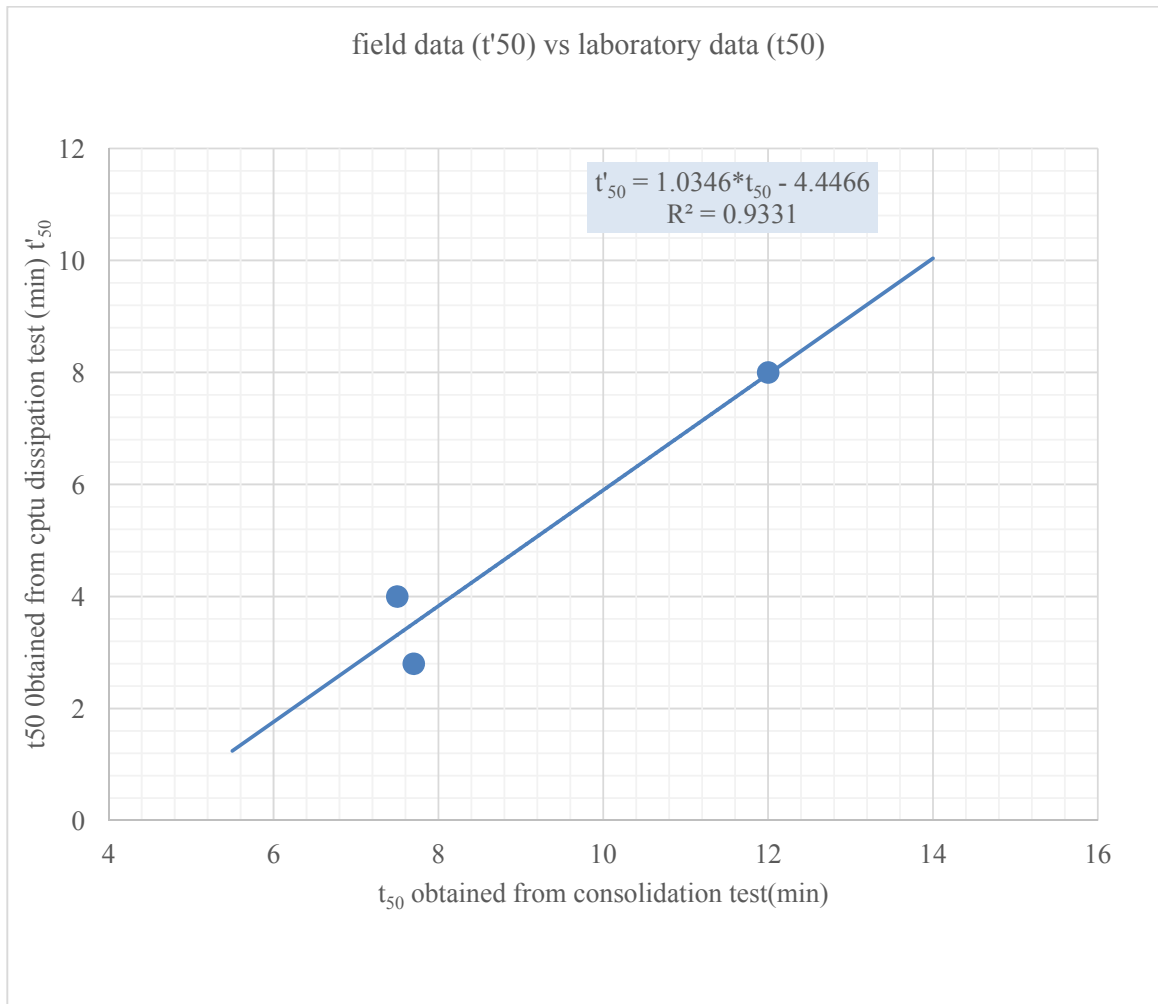


Fig 4.10: 50% consolidation time from field data (t'50) vs laboratory data (t50)

**Correlation of Over Consolidation Ratio (OCR) with CPT cone resistance**

OCR obtained from consolidation tests were compared to OCR obtained from the empirical correlations with CPT cone resistance using equation 2.19, 2.25 and 2.26 provided by Kulhawy and Mayne (1990), Karlshud et al (2005) and Been et al. (2010) as discussed in chapter 2.

Table 4.6 : Comparison of laboratory obtained OCR with CPT based OCR

B H N o.	From Consolidation test					Kulhawy & Mayne (1990)				Karlshrud et al (2005)	Been et al. (2010)				
	$\sigma'_p$ (kpa)	dept h (m)	$\sigma_v$ (kpa)	$\sigma'_v$ (kpa)	OC R	K	$\sigma_v$ (kpa)	q(t) kpa	OC R	$OCR = .25 * Qt^{1.2}$	fr kpa	N(K t)	s u	Q(t l)	OC R
13-12	93	6.3	83.19	38.997	2.13	0.33	100.8	142.4	0.5	1.182808829	12.7	18.22	8	3.7	0.8
16-3	130	6.3	120.2	38.997	3.08	0.33	100.8	654.4	4.52	7.374193329	1.85	12.37	53	17	8.3

17-16	88	8.1	78.19	50.139	1.56	0.33	129.6	300.8	1.47	2.146162517	0.44	8.004	38	6	3.9
17-5	121	5.85	111.2	36.212	3.07	0.33	93.6	132.8	0.2	1.188945317	2.54	13.33	10	3.7	1.1
2--1	91	7.65	81.19	47.354	1.71	0.33	122.4	304	1.55	2.327907974	5.47	15.67	19	6.4	1.9
24-2	140	8.55	130.2	52.925	2.46	0.33	136.8	752	3.88	6.039671264	5.02	15.41	49	14	5.1

From above table we see that for a variation of qc value from 132.8 kpa to 752kpa CPT based OCR varies from 1 to 4.5 (Kulhaway and Mayne 1990), 1-7.37 (Karlshrud et al 2005), 1-8.3 (Been et al 2010) whereas laboratory test results provide OCR range 1.56 to 3.08. Empirical OCR <1 was ignored as OCR cannot be less than 1.

Obtained OCR from consolidation tests show least deviation with OCR obtained as per Kulhaway and Mayne (1990) but other correlations show significant deviation with laboratory results. All the OCR values were plotted against CPT cone resistance for better understanding.

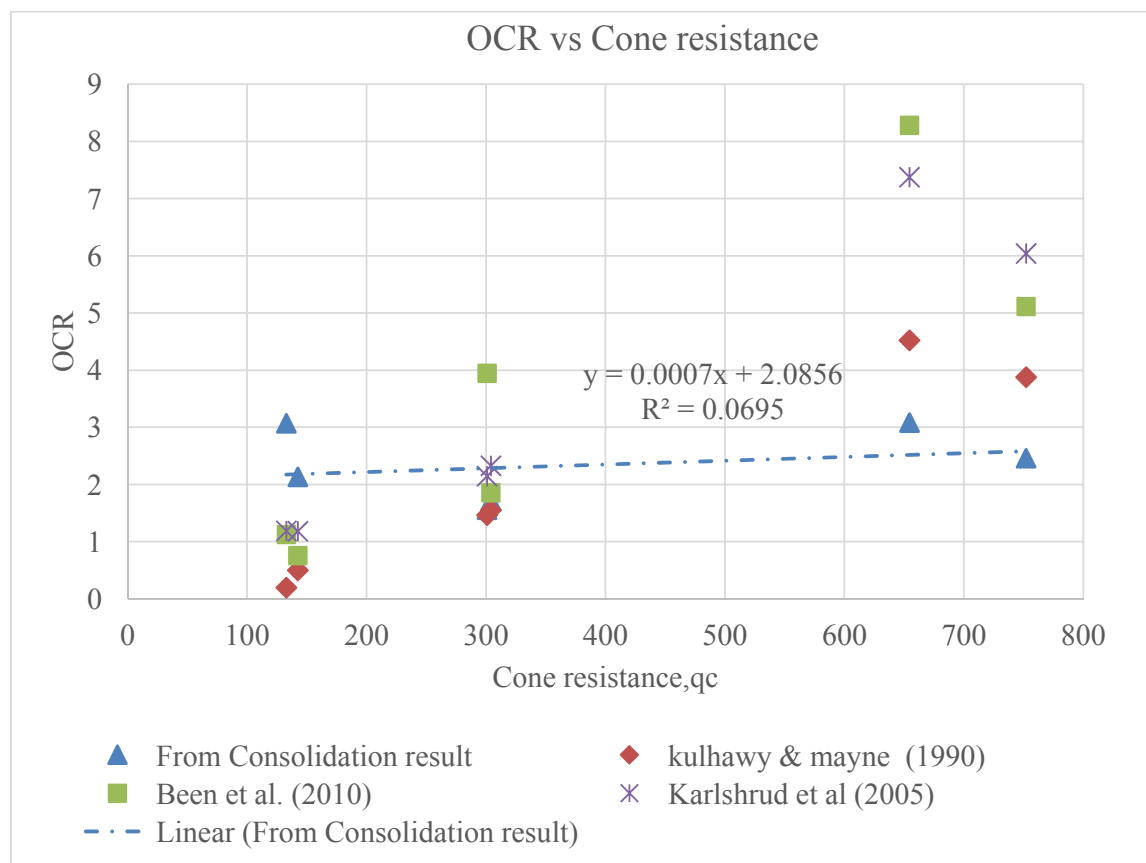


Fig 6.11: Over consolidation ratio vs CPT cone resistance curve for Laboratory test results and CPT based correlations

From Fig 6.11 we see the mean line for OCR obtained from consolidation test has a very low  $R^2$  value which implies CPT value doesn't affect the over consolidation ratio for local soil.

**Correlation of Atterberg Limits with Normalized SPT blow count**

There is no available correlation that directly relates Atterberg limits with SPT blow count. An approach to such correlation was made by Mostafa Abdou Abdel Naiem Mahmoud (2013) but the study failed to establish any correlation between LL, PL or PI with normalized SPT. Such approach has been taken here with the hope of a better result for local soil.

Firstly Liquid limit and Plastic Limit were plotted against normalized SPT blow count ( $N_{1,60}$ ).  $N_{1,60}$  is corrected N value for overburden pressure using the formula of Boulanger (2003) which is a modification of Liao and Whitman (1986)

$$N_{1,60} = C_N * N_{60}$$

$$\text{Where } C_N = (pa/\sigma'_v)^m \leq 1.7 \text{ and } m = .784 - .0768 * N_{60}^{0.5}$$

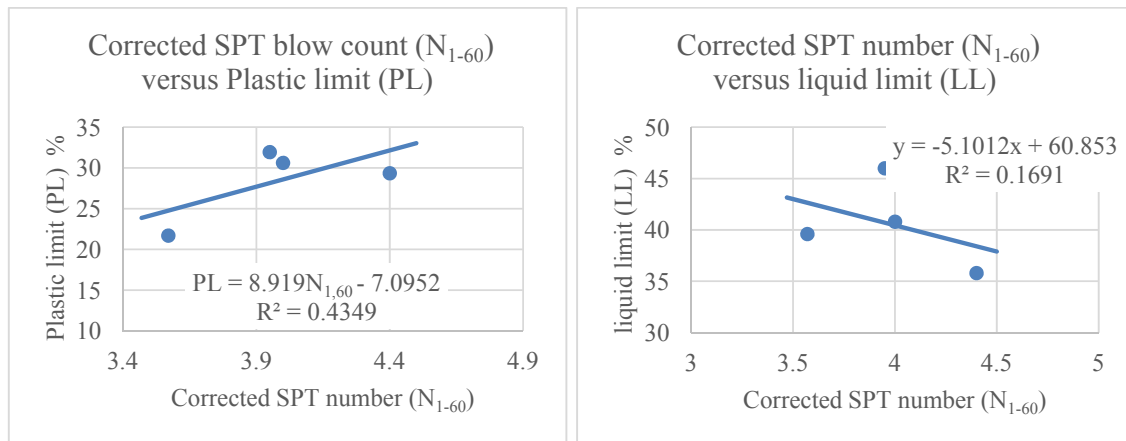


Fig 6.12: Corrected SPT blow count ( $N_{1,60}$ ) versus Plastic limit (PL) and Liquid limit (LL)

Above figure shows Plastic limit shows a correlation to normalized SPT blow count with  $R^2 = .43$  whereas plots regarding Liquid limit was found to be scattered indicating no noticeable effect on SPT blow count.

To correlate plasticity index with SPT value a similar approach like Stroud (1974) was taken and the ratio of shear strength to SPT blow count ( $f_1$ ) was plotted against PI and compared to the pattern of Stroud (1974)

Table 6.7: Calculation of  $f_1$

site	SPT blow count, $N_{60}$	Cu from DS	$f=Cu/N60$
BH 2-10	4.4	14.8	3.363636364
BH 13-6	3.57	20.1	5.630252101
BH 17-11	3.95	25	6.329113924
BH 24-7	4	41	10.25

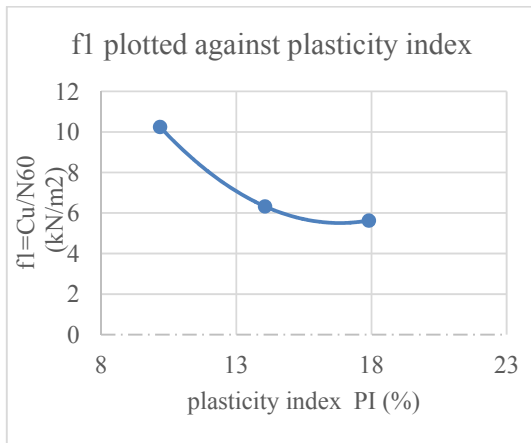


Fig 6.13: Variation of  $f_1$  with PI for study data Stroud (1974)

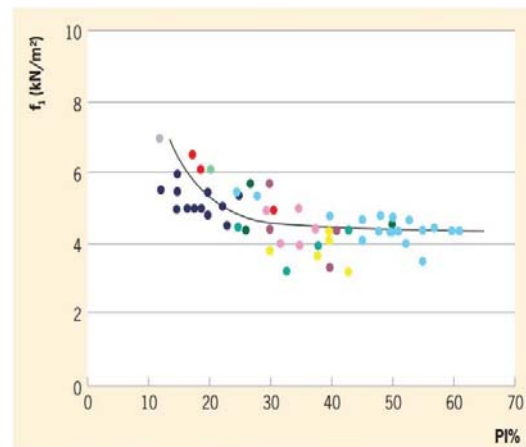


Fig 6.14: Variation of  $f_1$  with PI as per

In above figures for both of the curves Plasticity index decreases with increasing  $f_1$  maintaining similar pattern, so it can be concluded that plasticity index can be correlated with SPT blow counts.

To correlate Plasticity index with SPT blow counts Plasticity Index was plotted against  $N_{60}$

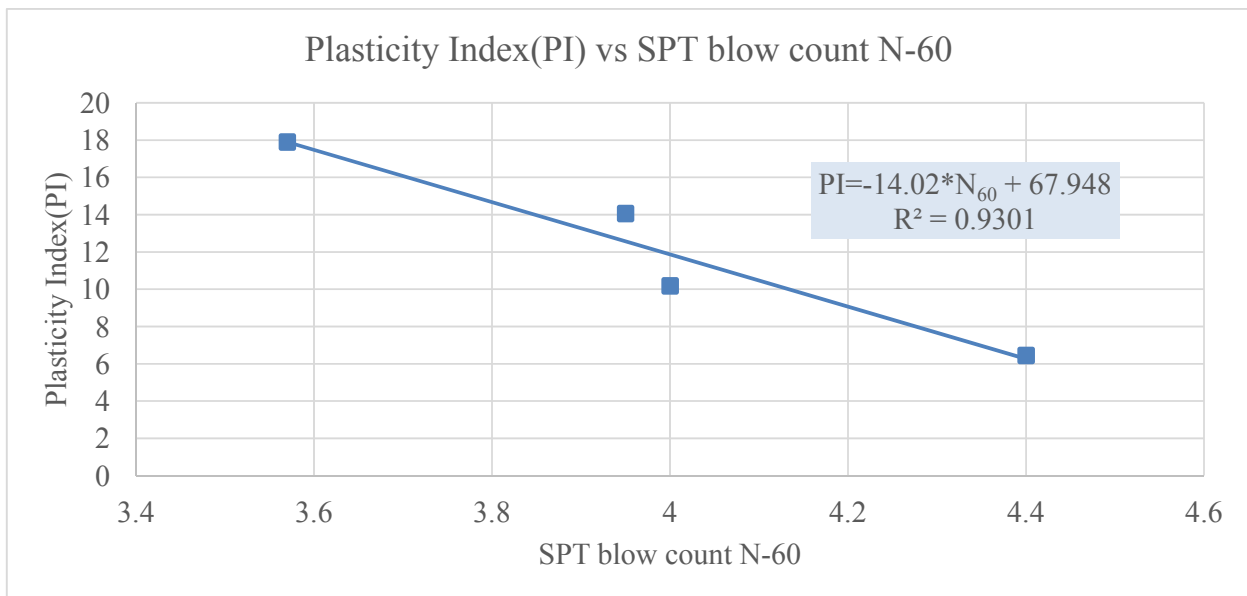


Fig 6.14: Correlation of Plasticity index (PI) with SPT blow count  $N_{60}$

Above figure illustrates a linear relationship between PI and  $N_{60}$  and Plasticity index decreases with increasing SPT blow count. The correlation can be given as

$$PI = -14.02 \cdot N_{60} + 67.948$$

## 7 CONCLUSIONS

The following conclusion can be drawn from present study

- a) CPT data are reliable to calculate SBT index from the equation provided by Robertson (2012)

$$ISBT = [(3.47 - \log(qc/pa))^2 + (\log Rf + 1.22)2]^{0.5}$$

- b) SBT index based CPT-SPT correlations provided by Robertson and Wride (1998) and Robertson (2012) are fairly applicable for local soil.

- c) SPT based correlation to obtain undrained shear strength (Su) by Kulhawy and Mayne (1990) ensures good applicability of this correlation for local soil.

- d) Correlation between shear strength (Su) and CPT cone tip resistance shows similar pattern but not exactly the same as Robertson (2012). So a new correlation was proposed as follows

$$Cu = 2qc/\sigma_{vo} + 11.31 \text{-----}(5.1)$$

- e) A new correlation for SPT blow count and internal friction angle( $\phi$ ) for local soil was given by

$$\phi = 2.1123 * N_{60}^{1.6627} \text{-----}(5.2)$$

- f) Study soil follows the correlation between friction angle and CPT cone resistance provided by Robertson and Campanula (1983) with slight deviation. A better correlation was proposed for local soils as

$$\phi = 12.175 \ln(qc) + 25.262 \text{-----}(5.3)$$

- g) A new correlation between 50% consolidation time obtained from consolidation test ( $t_{50}$ ) and

CPTu dissipation test ( $t'_{50}$ ) has been proposed as follows

$$t'_{50} = 1.0346 * t_{50} - 4.4466 \text{-----}(5.4)$$

- h) CPT value doesn't affect the over consolidation ratio for local soil.

- i) A correlation between Plastic Limit and SPT blow count is proposed as given bellow

$$PL = 8.919 N_{1,60} - 7.0952 \text{-----}(5.5)$$

- j) Plasticity index decreases with increasing SPT blow count. The correlation can be given as

$$PI = -14.02 * N_{60} + 67.948 \text{-----} (5.6)$$

## References

- Alam et al, J.W. 1990. Geological Map of Bangladesh. Dhaka: Geological Survey of Bangladesh.
- Ameratunga et al, C.2016. Correlations of Soil and Rock Properties in Geotechnical Engineering. P.144
- Alan Reid and Dr John Taylor, geotechnical engineers, South Lanark shire Council, The misuse of SPTs in fine soils and the implications of Eurocode 7.
- Douglas, B.J., and Olsen, R.S., 1981. Soil classification using electric cone penetrometer. In Proceedings of Symposium on Cone Penetration Testing and Experience, Geotechnical Engineering Division, ASCE. St. Louis, Missouri, October 1981, pp. 209-227.
- Hiroshan Hettiarachchi, Timothy Brown, "Use of SPT Blow Counts to Estimate Shear Strength Properties of Soils: Energy Balance Approach" Article in Journal of Geotechnical and Geoenvironmental Engineering · June 2009
- H.M. Mominul, M.A. Ansary & M.J. Abedin. Bangladesh University of Engineering and Technology, Dhaka, Bangladesh, "Applicability of existing CPT, SPT and soil parameter correlations for Bangladesh" in 3rd International Symposium on Cone Penetration Testing, Las Vegas, Nevada, USA – 2014
- Jefferies, M.G., and Davies, M.P., 1993. Use of CPTU to estimate equivalent SPT N60. Geotechnical Testing Journal, ASTM, 16(4): 458-468.
- Kasim, A.Chu, M. & Jensen, C. 1986. Field Correlation of Cone and Standard Penetration Tests. J. Geotech. Engrg., 112(3):368–372.
- Kulhawy, F.H. & Mayne, P.W. 1990. Manual on estimating soil properties for foundation design. New York: Electric Power Research Inst., Geotechnical Engineering Group, (EPRI-EL-6800): 2-36 to 2-28.
- Long, M., 2008. Design parameters from in situ tests in soft ground – recent developments. Proceedings of Geotechnical and Geophysical Site Characterization. Taylor & Francis Group, 89-116
- Lunne, T., Robertson, P.K., and Powell, J.J.M., 1997. Cone penetration testing in geotechnical practice. Blackie Academic, EF Spon/Taylor & Francis Publ., New York, 1997, 312 pp.

Molle, J., 2005. The accuracy of the interpretation of CPT-based soil classification methods in soft soils. MSc Thesis, Section for Engineering Geology, Department of Applied Earth Sciences, Delft University of Technology, Report No. 242, Report AES/IG/05-25, December.

McNulty, G. & Harney, M. D. 2010. Comparison of CPT-and DMT-correlated effective friction angle in clayey and silty sands. 2nd international symposium on cone penetration testing, CPT'10, California, USA, Paper ID 2-53.

Meyerhof, G.G. 1956. Penetration tests and bearing capacity of cohesion less soils. Proc. SM1, (82): 1-19

M.D. Boone, Bechtel, San Francisco, CA, USA, W.P. Duffy, Bechtel, London, UK, M.R. Lewis, Bechtel, Augusta, GA, USA 3rd International Symposium on Cone Penetration Testing, Las Vegas, Nevada, USA - 2014, The use of the CPT in deltaic deposits in Northern Africa

Mostafa Abdou Abdel Naiem Mahmoud, "Reliability of using standard penetration test (SPT) in predicting properties of silty clay with sand soil "INTERNATIONAL JOURNAL OF CIVIL AND STRUCTURAL ENGINEERING, Volume 3, No 3, 2013."

Paul W. Mayne, U.S.A." Enhanced geotechnical site characterization by seismic piezocone penetration tests" Invited Lecture, Fourth International Geotechnical Conference, Cairo University, January 2000, pp. 95-120.

Robertson, P.K. and K.L. Cabal 2010, "Guide to Cone Penetration Testing for Geotechnical Engineering".

Robertson, P.K 2012. Cone penetration test (CPT)-based soil behavior type (SBT) classification system an update.

Robertson, P.K. Campanella, R.G. & Wightman, A. 1983. SPT □ CPT Correlations. J. Geotech. Engrg., 109(11): 1449-1459.

Robertson, P.K. & Campanella, R.G. 1985. Liquefaction Potential of Sands Using the CPT. J. Geotech. Engrg., 111(3): 384-403.

Robertson, P.K. & Campanella, R. G. 1983. Interpretation of cone penetration tests. Part I: Sand. Canadian Geotechnical Journal. 20(4): 718-733.

Robertson, P.K., 1990. Soil classification using the cone penetration test. Canadian Geotechnical Journal, 27(1): 151-158.

Robertson, P.K., 2009. CPT interpretation – a unified approach, Canadian Geotechnical Journal, 46: 1-19

Robertson, P.K., Campanella, R.G., Gillespie, D., and Greig, J., 1986. Use of Piezometer Cone data. In-Situ'86 Use of In-situ testing in Geotechnical Engineering, GSP 6 , ASCE, Reston, VA, Specialty Publication, pp 1263-1280.

Schmertmann, J.H. 1975. Measurement of in-situ shear strength. In ASCE Specialty Conference on In-Situ Measurement of Soil Properties. (2): 57-138



**BANGLADESH NETWORK  
OFFICE FOR URBAN SAFETY**



## **PART-XIV**

# **EARTHQUAKE IN TRIPURA, 3 JANUARY 2017**

**BANGLADESH NETWORK OFFICE FOR URBAN  
SAFETY (BNUS), BUET, DHAKA**

**Prepared By: Tasnim Tarannum Isaba**

**Mehedi Ahmed Ansary**

## 1. Introduction

Bangladesh lies in a seismically active zone making it extremely vulnerable to major earthquakes. Two major fault lines run through Bangladesh, one 144 km and the other 370 km from Dhaka. Bangladesh has experienced several fairly mild earthquakes in the last two decades and two major ones in the past 100 years. Most of the deadliest earthquakes have happened in the Asian belt in the past 30 years and thousands of lives have been lost and countries damaged, especially in Iran, Pakistan, China, Indonesia, Japan, Haiti and Turkey. At present, due to the recent disaster in Nepal, Bangladesh is highly susceptible to the risk of an earthquake.

On January 3 (Tuesday), 2017, a moderate intensity earthquake measuring 5.5 on the Richter scale occurred in the North-East and adjoining districts of Bangladesh. According to the Central Seismological Observatory (CSO) in Shillong, the epicenter of the earthquake is located in Dhalai district of Tripura, close to Mizoram and the Chittagong Hill Tracts of Bangladesh. The earthquake was felt for about five to six seconds and tremor was strongly felt across Bangladesh and India. According to USGS, there were 13 839 866 people living within 100 km (50 miles) and 2 million were living within 50 km (31 miles).

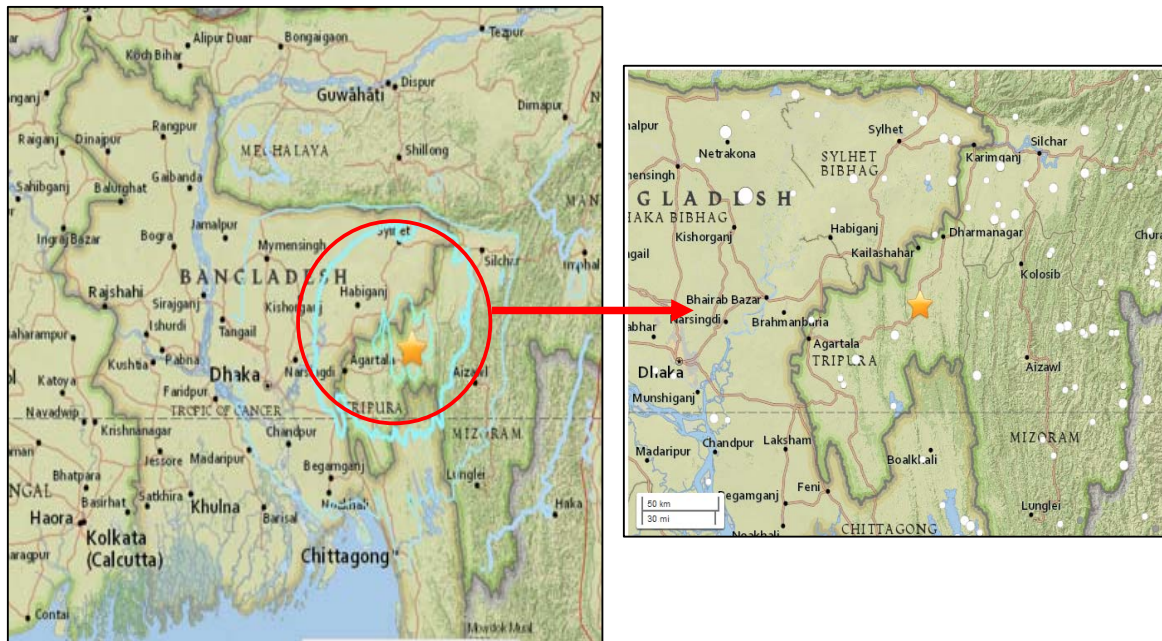


**Figure 1:** Map showing the affected areas of earthquake in Tripura on January 3, 2017

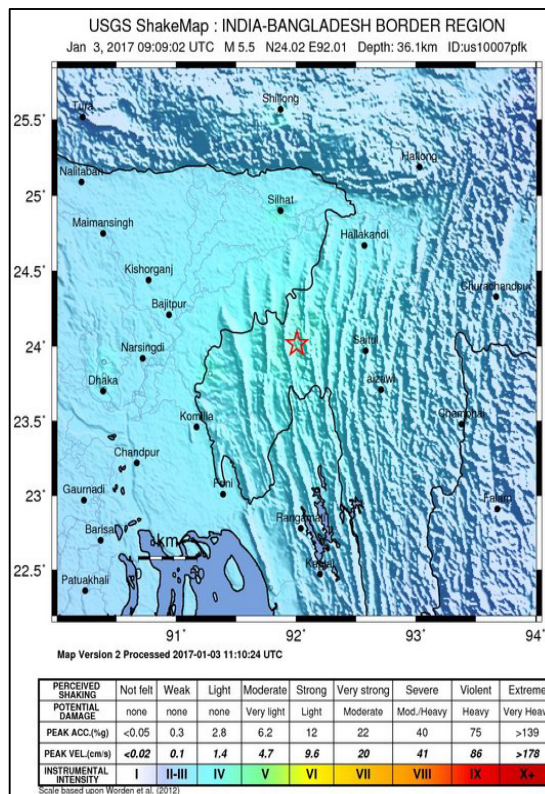
**Table 1: General information of e**

Region	India-Bangladesh Border Region
Geographic coordinates	24.016N, 92.006E
Magnitude	5.5
Depth	36 km
Universal Time (UTC)	3 Jan 2017 (09:09:03)
Time near the Epicenter	3 Jan 2017 (14:39:03)
Local standard time in Bangladesh	3 Jan 2017 (01:09:03)
<b>Location with respect to nearby cities:</b>	
19 km (11 miles) NE of Ambasa, India 35 km (21 miles) S of Kailashahar, India 39 km (24 miles) ESE of Khowai, India 42 km (26 miles) SSW of Dharmanagar, India 166 km (102 miles) ENE of Dhaka, Bangladesh	

**Intensity and fatalities:**

ShakeMap is a product of the USGS Earthquake Hazards Program which provides real-time maps of ground motion and shaking intensity following significant earthquakes. These maps are used by federal, and local organizations, both public and private, for post-earthquake response and recovery, public and scientific information, well as for preparedness exercises and disaster planning.

For the earthquake on January 3, USGS issued a green alert for shaking-related fatalities and economic losses. There is a low likelihood of casualties and damage.



near-  
state  
as

**Figure 2: USGS ShakeMap generated for India-Bangladesh border region after**

**Population exposure to earthquake shaking:**

According to USGS, 79,286 thousand people were exposed to weak shaking (MMI scale of II to III) and 29,352 thousand people were exposed to light shaking (MMI scale of IV).

Figure 2 shows the estimated population exposure to Tripura earthquake, January 3, 2017. The population exposure is higher on the Bangladesh side, particularly on Sunamganj and Moulvibazar districts. Table 2 shows the list of exposed cities of this earthquake.

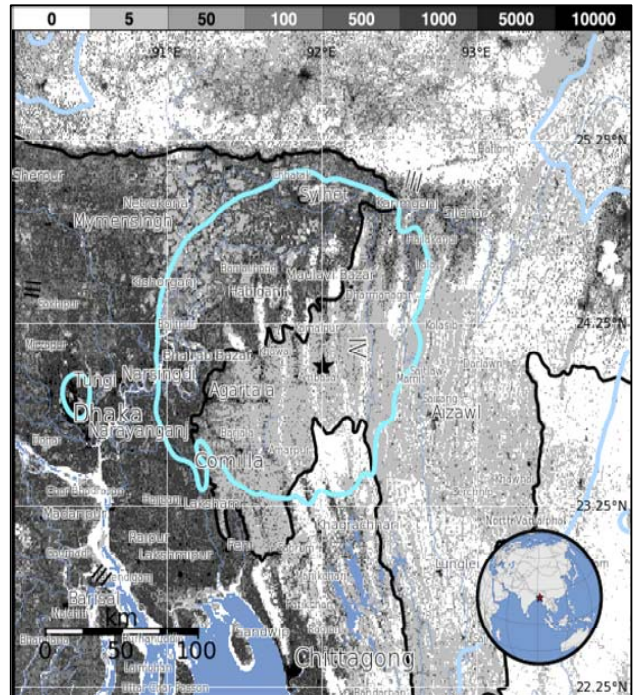


**Table 2:** Selected cities exposed to earthquake in Tripura on January 3, 2017

**Figure 3:** Estimated population exposure to earthquake shaking

Modified Mercalli Intensity (MMI) Scale	City	Population (in thousands)
IV	Ranir Bazar	12
IV	Kamlapur	6
IV	Agartala	203
IV	Ambasa	6
IV	Kaliashahar	22
IV	Sylhet	237
III	Dhaka	10,357
III	Aizawl	265
III	Chittagong	3,920
III	Imphal	224
III	Barisal	202

## 2. Impact of the Earthquake

### 2.1. Primary Hazards

As a result of the earthquake, separate cracks have been appeared on the ground in some places across the country including Kamalganj of Moulvibazar. According to the local people of the area, water and sand were seen coming out of the cracks triggering panic among the villagers. Cracks were developed in at least 50 places including paddy fields of Kamalganj, playground of Kamalganj High School, land near upazila land office and Adampur Herengabazar ground. The cracks range from 10 to 50 feet.



**Figure 4:** Cracks appeared in the cropland and playground of Moulvibazar

### 2.2. Secondary Hazards

According to the upazila chairman of Kamalganj in Moulvibazar district, soil liquefaction occurred in some places to some extent after the earthquake event. Walls and electric poles collapsed in Moulvibazar. Also, a fire was reported in a mobile phone tower in Moulvibazar after the earthquake.

As the earthquake occurred in both Bangladesh and India, some secondary hazards have also been seen in Tripura. Landslides occurred in a number of places on the remote Chhamanu-Gobindabari Road of Dhalai district. According to the officer-in-charge of state fire service department in Dhalai and Unakoti districts, landslides occurred in a number of places in a five-km radius along the Chhamanu-Gobindabari road. A portion of the boundary wall of the fire service office at Unakoti district had collapsed due to the earthquake.



**Figure 5:** Fire in a mobile phone tower's control in Moulvibazar town

### **2.3. Human Casualties**

The earthquake was reported to cause 3 deaths and several injuries in both Bangladesh and India. All the deaths were caused by panic and heart attack. An elderly person died of shock at Jagannathpur upazila in Sunamganj district. According to the doctor of Jagannathpur Upazila Health Complex, the victim had a cardiac arrest at home after being frightened by the earthquake. The second victim was a student studying at 8<sup>th</sup> grade in Chhatak Cement Factory School. She suffered lethal injuries after falling from stairs when the quake hit. According to Indian Express, a panic-stricken woman, identified as 50-year-old Kamalini Kanda of Mayachari village under Kamalpur police station died due to a heart attack.

Due to the collapse of walls and electric poles in Moulvibazar, at least 115 persons were injured as walls collapsed on them. Four people were seriously injured as they were hit by bricks and brickbats of walls and by electric poles when they collapsed during the earthquake. The injured were undergoing treatment at Moulvibazar Sadar hospital.

### **2.4. Impact on Infrastructure**

According to the local people, the earthquake caused damages to the land, roads and buildings of both Sunamganj and Moulvibazar district. Many roads of the Kamalganj upazila including Kumrakapon area were broken and cracks have been spotted in roads of Ranirbazar area. According to Kamalganj Municipality Mayor, there were cracks in more than 150 buildings, including the municipality office. Cracks were also observed in the newly constructed upazila auditorium, a three-storied restaurant building at Shamshernagar and a state-run orphanage at Sreemangal. Some parts of walls and ceiling collapsed as well while the front veranda caved in by about 1.5 feet. The building of Grand Sultan Tea Resort and Golf Plaza were mildly damaged. According to Kamalganj upazila executive officer, the cracks developed were as long as 40 feet at some points. Public Work

Department officials have already visited the building and reported that the buildings are fine right now but further damage cannot be ruled out if another earthquake occurs. Reports from Moulvibazar said that many half-brick houses were damaged in the tremor and cracks were developed in more than two hundred buildings. In Tripura, one bridge also developed cracks in Dhalai district.



**Figure 6:** Cracks developed in buildings of Kamalganj upazila in Moulvibazar after the earthquake

### **2.5. Impact on Properties**

Cracks appeared in the house of many people. Traders have suffered losses as well due to the earthquake. Glass and tiles stored in a shop at Bhanugachh Bazar broke into pieces during the tremor. According to the General Secretary of Bhanugachh Poura Bazar Banik Samity, around 20 businesses in that market have incurred losses. While the tremor was felt strongly in Tripura, reports of the quake being felt have also come in from Meghalaya, Manipur, Mizoram and southern Assam. Sources in Agartala said that as many as 60 houses were reportedly damaged in Dhalai and the number of properties damaged is likely to increase.

### **2.6. Impact on Power Supply and Telecommunication**

Power connections remained suspended for hours in more than one hundred villages as the quake caused a glitch on the Sreemangal grid. According to the Moulvibazar Palli Bidyut Samity DGM (technical), a jumper got disconnected at the Sreemangal Power Grid during the earthquake. As a

result, power connection was suspended in several areas. However, it resumed after the glitch was repaired.

### **2.7. Impact on Human Life**

Many of the city dwellers came outside in the streets as there was panic when buildings were shaking by the earthquake. At least five people, including a Shahjalal University of Science and Technology student, were injured as they tried to come out of multi-storey buildings in Sylhet during the tremor. New Age correspondent in Chittagong reported that many people of the port city came out of houses as they felt the quake. In Sylhet metropolis, at least three people sustained minor injuries during stampede in different parts of city when the earthquake began.

### **3. Lessons Learned**

According to the scientists, Bangladesh is highly vulnerable to earthquake due to its geographical location. Bangladesh is positioned at the juncture of several active tectonic plate boundaries and is one of the most tectonically active regions in the world. It sits where three tectonic plates meet: the Indian Plate, the Eurasian Plate, and the Burmese Plate. Moreover, it sits at the top the world's largest river delta at close to sea level, facing both the risk posed by an earthquake and secondary risks of tsunamis and flooding in the quake's aftermath. Although Bangladesh has achieved considerable success in managing natural disasters like cyclone and flood, researchers have indicated that earthquake preparedness in Bangladesh is still inadequate. Unplanned development, high population density, lack of education and safety training as well as poorly constructed buildings in major cities have alleviated the earthquake risk in Bangladesh. The collapse of Rana Plaza in 2013 caused the loss of 1,136 lives. Although no major earthquake has occurred in the recent years, the collapse of Rana Plaza has provided a glimpse of what could happen in the event of a major earthquake.

The news reports for the earthquake event in Sylhet and Tripura revealed that most of the injuries of the earthquake were caused by panic attack and building collapse. People got injured when they were trying to escape from the building. The response of people in Bangladesh to the earthquake indicates that there is a lack of education and preparation about what to do if such an event occurs or how to be safe during an earthquake. One news report highlighted the fact that people came out of high-rise buildings using the stairs during the shaking of the earthquake. This is incorrect, instead they should find a safe corner of a room or building.

Earthquake damages can be more severe when it is accompanied with poorly constructed buildings. The news reports indicated that more than 200 buildings were cracked during and after earthquake. The tilting and cracking of many of these buildings indicated to their weak construction. According

to experts, Bangladesh is urbanizing rapidly and almost no building conform to the building codes. Many buildings are constructed by encroaching roads and covering natural waterbodies. Poorly constructed buildings are also common that are partly built with concrete, bamboo and tin. Earthquake resistant building construction is not yet considered with proper importance in Bangladesh. A regular survey should be undertaken to audit integrity of older buildings, major public highways and bridges to identify vulnerabilities and prevent future damage.

In addition to educating the public, an appropriate gas leakage management system, power supply control, firefighting, alternative power generation, wireless communication system, heavy equipment for removing debris and emergency medical facilities are needed to help deal with the aftermath of an earthquake.